

University of Kentucky

UKnowledge

Theses and Dissertations--Earth and
Environmental Sciences

Earth and Environmental Sciences


2020

TRACING SOURCE CONTRIBUTIONS TO ASSESS SPATIAL PATTERNS OF EROSION IN A MIXED LAND USE ENVIRONMENT: OTTER CREEK CATCHMENT, FORT KNOX, KENTUCKY

Cara Peterman

University of Kentucky, cara.peterman@uky.edu

Author ORCID Identifier:

 <https://orcid.org/0000-0003-1822-2552>

Digital Object Identifier: <https://doi.org/10.13023/etd.2020.062>

[Right click to open a feedback form in a new tab to let us know how this document benefits you.](#)

Recommended Citation

Peterman, Cara, "TRACING SOURCE CONTRIBUTIONS TO ASSESS SPATIAL PATTERNS OF EROSION IN A MIXED LAND USE ENVIRONMENT: OTTER CREEK CATCHMENT, FORT KNOX, KENTUCKY" (2020). *Theses and Dissertations--Earth and Environmental Sciences*. 80.

https://uknowledge.uky.edu/ees_etds/80

This Doctoral Dissertation is brought to you for free and open access by the Earth and Environmental Sciences at UKnowledge. It has been accepted for inclusion in Theses and Dissertations--Earth and Environmental Sciences by an authorized administrator of UKnowledge. For more information, please contact UKnowledge@lsv.uky.edu.

STUDENT AGREEMENT:

I represent that my thesis or dissertation and abstract are my original work. Proper attribution has been given to all outside sources. I understand that I am solely responsible for obtaining any needed copyright permissions. I have obtained needed written permission statement(s) from the owner(s) of each third-party copyrighted matter to be included in my work, allowing electronic distribution (if such use is not permitted by the fair use doctrine) which will be submitted to UKnowledge as Additional File.

I hereby grant to The University of Kentucky and its agents the irrevocable, non-exclusive, and royalty-free license to archive and make accessible my work in whole or in part in all forms of media, now or hereafter known. I agree that the document mentioned above may be made available immediately for worldwide access unless an embargo applies.

I retain all other ownership rights to the copyright of my work. I also retain the right to use in future works (such as articles or books) all or part of my work. I understand that I am free to register the copyright to my work.

REVIEW, APPROVAL AND ACCEPTANCE

The document mentioned above has been reviewed and accepted by the student's advisor, on behalf of the advisory committee, and by the Director of Graduate Studies (DGS), on behalf of the program; we verify that this is the final, approved version of the student's thesis including all changes required by the advisory committee. The undersigned agree to abide by the statements above.

Cara Peterman, Student

Dr. Alan E. Fryar, Major Professor

Dr. Edward Woolery, Director of Graduate Studies

TRACING SOURCE CONTRIBUTIONS TO ASSESS SPATIAL PATTERNS OF
EROSION IN A MIXED LAND USE ENVIRONMENT: OTTER CREEK
CATCHMENT, FORT KNOX, KENTUCKY

DISSERTATION

A dissertation submitted in partial fulfillment of the
requirements for the degree of Doctor of Philosophy in the
College of Arts and Sciences
at the University of Kentucky

By

Cara Leigh Peterman

Lexington, Kentucky

Co- Directors: Dr. Alan E. Fryar, Professor of Earth and Environmental Sciences
and Dr. Dwayne R. Edwards, Professor of Biosystems and Agricultural
Engineering

Lexington, Kentucky

2020

Copyright © Cara Leigh Peterman 2020
[<https://orcid.org/0000-0003-1822-2552>]

ABSTRACT OF DISSERTATION

TRACING SOURCE CONTRIBUTIONS TO ASSESS SPATIAL PATTERNS OF EROSION IN A MIXED LAND USE ENVIRONMENT: OTTER CREEK CATCHMENT, FORT KNOX, KENTUCKY

There is an inherent difficulty in predicting source contributions of fine-grained fluvial sediment in mixed land-use watersheds. Over a 56-week period, the spatial and temporal variability in sediment-source contributions and water quality was monitored at three sites along Otter Creek in Hardin and Meade counties, Kentucky (USA). The 203-km² study area drains rural and agricultural lands and includes Fort Knox Army Post's tracked-vehicle training areas. The main objectives for sediment source apportionment were to 1) identify and differentiate characteristics of civilian and military source soils to Otter Creek and 2) to apportion sediment at locations along Otter Creek to different source-soil categories. We hypothesized that the primary sources of fine-grained sediment to Otter Creek were derived from Fort Knox's tracked-vehicle training areas within the watershed. The water-quality objectives were to 1) draw inferences about spatial and temporal controls on water chemistry in Otter Creek and 2) compare measurements obtained during the study with historical data obtained from the U.S. Geological Survey (USGS) and the National Oceanic and Atmospheric Administration.

In civilian lands, which occupy 81.6% of the study area, primary land use/land cover is cropland (57.1%), with the remainder allocated to forest (29.6%), developed area (12.2%) and other (1.1%). Only 18.4% of the study area is composed of military training lands, of which forest is 63.6%, cropland is 0%, 23.8% is developed and 12.1% is other. The greatest proportion of military lands is located in the farthest downstream subcatchment, which had the largest amount of forested land (74.5%) and least amount of cropland (5.3%). Between summer (March–September) and winter (October–February) and between base- and stormflow, differences in sediment yield and composition were observed. The farthest downstream sampling site had the greatest sediment yield for summer, winter, baseflow and stormflow. The USGS program Sed_SAT identified Cu, Zn, Co, Ni, Al and Mg as conservative tracers that could distinguish between source-soil groups during the unmixing model process. Sed_SAT allocated target sediment to five source-soil groups: civilian near-

stream, military near-stream, military forest, military average erosion and military extreme erosion. Because of geochemical similarities, those groups were combined into two simplified categories in two different scenarios. Sediment sources were dominated by streambank/forest soils (63-67%) in the first scenario and by military upland soils (57-66%) in the second scenario.

Water-quality monitoring included water pressure, electrical conductivity and specific conductance (EC and SC), water temperature, dissolved oxygen (DO) and pH, in addition to chloride (Cl^-), nitrate (NO_3^-), phosphate (PO_4^{3-}) and sulfate (SO_4^{2-}) over a 6-month period. Seasonality was observed in fluid-pressure responses, with higher peaks in wetter seasons (December–mid-May) and lower peaks during drier months (mid-May–November). During storm events, a temporary EC decrease in response to dilution from runoff and corresponding increase in fluid pressure were observed at the two upstream sites. The downstream increase in pH between the first and last sampling sites corresponds to dissolution of carbonate bedrock that underlies the area. A significant positive relationship was observed at all three sites for Cl^- and SO_4^{2-} , which suggests a common source for both anions. During winter, elevated concentrations of Cl^- were likely to result from deicer washing off roadways. The increases in NO_3^- observed from late fall through winter may be a result of higher-than-average precipitation and slow nitrification and leaching from soils. A comparison of historical water quality data (1994-98) to the study period (2015-16) shows there was a significant increase in SC, a significant decrease in DO, and a marginally significant increase in pH at the farthest downstream site.

KEYWORDS: Fingerprinting, Sediment, Erosion, Water-quality, Multi Land-use

Cara Leigh Peterman

February 28, 2020

TRACING SOURCE CONTRIBUTIONS TO ASSESS SPATIAL PATTERNS OF
EROSION IN A MIXED LAND-USE ENVIRONMENT: OTTER CREEK
CATCHMENT, FORT KNOX, KENTUCKY

By
Cara Leigh Peterman

Dr. Alan E. Fryar

Co-Director of Dissertation

Dr. Dwayne R. Edwards

Co-Director of Dissertation

Dr. Michael M. McGlue

Director of Graduate Studies

February 28, 2020

Date

DEDICATION

This is dedicated to the following people. To my mother, Pamela Petkoff who was there in the beginning of my journey but was not able to be there to see the end. She was the reason the sun shown the day I walked for graduation. To my undergraduate and graduate advisor at the University of Michigan-Dearborn, Dr. Kent Murray. Thank you for seeing something in me that I had not seen in myself, for the countless hours of encouragement, patience and push to reach beyond what I thought possible. To my Special Olympics family, the Lexington Torpedoes and Lexington Dazzlers; Thank you all for making me your family, for the countless hours of fun, the endless hugs, the unconditional love and for being my biggest cheering section that this world has ever seen. There are no words to express how much I appreciate and love each of you. You are my family, you will always be my family, no matter where I am in this world! Lastly, to William D. Phipps, though you were not here at the beginning of my doctoral program, you were here at the end. It is said that the people you know in high school will be shadows in your life one-day, that who you are and what you want in life changes, and so our lives diverged for nearly 26-years. I cannot imagine a better ending of this chapter than to have you come back into my life, and we can open a new chapter together. You are my best friend, my confidant, my trusted adviser, my fellow-weirdo and explorer, you are whom I choose to partner my life with, from now till the end of time. Thank you for your calm steady demeanor and rock-solid support, it has provided a cornerstone on which to stand so that I could navigate my way to the finish line.

ACKNOWLEDGMENTS

The following dissertation, while an individual work, benefited from the insights and direction of several people. First, my Co-Directors, Alan E. Fryar and Dwayne R. Edwards, they exemplify the high-quality scholarship to which I aspire. Next, I wish to thank the complete Dissertation Committee, and outside reader, respectively: Michael M. McGlue, Steve Greb, Jonathan Phillips and Joseph Sottile. In addition, Fort Knox Environmental and Natural Resource Divisions for allowing me access to my research area. The individuals involved played a crucial role to this project's success, substantially improving the finished project.

In addition to the technical and instrumental assistance above, I received equally important assistance from my family. They stood beside me and cheered me on, and on my darkest days encouraged me to look beyond the immediate struggle at the bright future that laid ahead of me; Malinda (Sally Mae) Chuvala, Estelle Peterman, Sandra Lynd, Charles Kemp, Shelby Farrell, Clay Farrell, B.B. Farrell, William Farrell, John and Josanne Billcheck, Doug and Jennifer Mynear, Sherry Anderson and the Gilley Family (Matt, Adrienne, Emma and Maya)

TABLE OF CONTENTS

ACKNOWLEDGMENTS	iii
LIST OF TABLES	vii
LIST OF FIGURES	viii
LIST OF ADDITIONAL FILES	xi
CHAPTER 1. INTRODUCTION	1
1.1 Overview and Objectives.....	1
1.2 Land Use.....	3
1.3 Climate.....	5
1.4 Geology.....	6
1.5 Soils and Vegetation	7
1.6 Hydrology	9
1.7 Literature Review.....	10
1.7.1 Soil Erosion.....	10
1.7.2 Sediment Fingerprinting	12
1.7.3 Hydrochemical Aspects of Water Quality	14
CHAPTER 2. FINGERPRINTING SOURCE CONTRIBUTIONS TO ASSESS SPATIAL PATTERNS OF EROSION IN A MIXED LAND USE ENVIRONMENT: OTTER CREEK, FORT KNOX, KENTUCKY.....	25
2.1 Introduction.....	26
2.2 Study Area	29
2.2.1 Land Use / Land Cover and Geologic Setting	29
2.2.2 Soils and Vegetation	31
2.3 Background.....	32
2.3.1 Sediment Transport in Karst Terrain	32
2.3.2 Sediment Fingerprinting	34
2.4 Materials and Methods.....	35
2.4.1 Source Soil Samples	35
2.4.2 Stream Sediment Samples.....	37
2.4.3 Tracer Analysis	39
2.4.4 Isotopic Analysis.....	40

2.4.5	Grain Size Analysis.....	41
2.4.6	Statistical Analysis and Modeling	42
2.5	Results.....	44
2.5.1	Particle Size, Sediment Yields and Tracer Statistics	44
2.5.2	Principal Component Analysis	46
2.5.3	Apportionment of Source Soils to Sediment Samples.....	49
2.6	Discussion.....	51
2.7	Conclusions.....	58
CHAPTER 3.	SPATIAL AND TEMPORAL VARIABILITY IN STREAM WATER QUALITY IN A MIXED LAND-USE WATERSHED: OTTER CREEK, KENTUCKY.....	103
3.1	Introduction.....	104
3.2	Regional Setting.....	105
3.3	Materials and Methods.....	108
3.4	Results.....	111
3.4.1	Stage and Discharge.....	111
3.4.2	Field Parameters.....	112
3.4.3	Solutes.....	114
3.5	Discussion.....	115
3.5.1	Streamflow and Field Parameters	115
3.5.2	Solutes.....	117
3.5.3	Statistical Analyses	119
3.5.4	Comparisons with Historical Data	120
3.5.5	Limitations of Results.....	122
3.6	Conclusions.....	123
CHAPTER 4.	CONCLUSIONS.....	153
4.1	Purpose and Objectives.....	153
4.2	Major Findings.....	154
4.2.1	Sediment Fingerprinting	154
4.2.2	Stream-Water Quality	156
4.3	Study Limitations and Recommendations for Future Research	158
APPENDICES	161
APPENDIX 2.1	Site 1 Percent Sediment Classified Correctly Sed_SAT.....	161
APPENDIX 2.2	Site 2 Percent Sediment Classified Correctly Sed_SAT.....	163
APPENDIX 2.3	Site 3 Percent Sediment Classified Correctly Sed_SAT.....	165

APPENDIX 2.4 Source Soil Geochemical Data.....	167
APPENDIX 2.5 Target Sediment Geochemical Data.....	169
APPENDIX 3.1 Basic Statistics for Solutes and Field Parameters.	171
APPENDIX 3.2 Site 1 Water Quality Results and Field Parameter Readings.....	172
APPENDIX 3.3 Site 2 Water Quality Results and Field Parameter Readings.....	173
APPENDIX 3.4 Site 3 Water Quality Results and Field Parameter Readings.....	174
APPENDIX 3.5 Basic Statistics for Solutes and Field Parameters.	175
REFERENCES	176
VITA.....	197

LIST OF TABLES

Table 2.1 Percent contribution of land use/land cover categories per subcatchment, Hardin and Meade counties, Kentucky	61
Table 2.2 Pearson correlation between sediments collected between sampling sites for zinc and strontium.....	62
Table 2.3 Descriptive statistics for TOC and $\delta^{13}\text{C}$ for all source soils and source soil groups.....	63
Table 2.4 Descriptive statistics for TOC and $\delta^{13}\text{C}$ for all sediment and sediment sampling locations and for base-and stormflow.	64
Table 2.5 Pearson correlation between source soil groups for TOC and for $\delta^{13}\text{C}$	65
Table 2.6 Pearson correlation between sediment sampling sites for base- and stormflow and for all sediment combined for TOC and for $\delta^{13}\text{C}$	66
Table 2.7 Principal component analysis (PCA) for all source soils and target sediments: first two principal component factor loadings (PC1 and PC2) with proportion of variation.	67
Table 2.8 Principal component analysis (PCA) for source soil groups: first two principal component factor loadings (PC1 and PC2) with proportion of variation and associated tracers.	68
Table 2.9 Principal component analysis (PCA) for each sediment sampling site: first two principal component factor loadings (PC1 and PC2) with proportion of variation.....	69
Table 2.10 Shapiro-Wilks normality test for source soils and target sediment.	70
Table 2.11 Amount of sediment collected (g) and descriptive statistics for each of the three sediment sampling locations along Otter Creek, Fort Knox, Kentucky..	71
Table 2.12 Percent of contributions of sediment during summer and winter months with percent precipitation. Hardin and Meade counties, Kentucky.....	72
Table 2.13 Source soil group percentages combined for comparison, Hardin and Meade counties, Kentucky.....	73
Table 3.1 Predominant crops grown in Hardin and Meade counties, Kentucky	126
Table 3.2 Pearson correlation between water quality parameters.....	127
Table 3.3 Principal component analysis for solutes with first and second factor loadings, proportion of variance and variables.....	128
Table 3.4 Historical water-quality data from the U.S. Geological Survey.....	129
Table 3.5 Kruskal-Wallis H-test, historical vs. study period parameters. Otter Creek, Hardin and Meade counties, Kentucky	130
Table 3.6 Percent land use / land cover for 1992 and 2011, Hardin and Meade counties, Kentucky	130

LIST OF FIGURES

Figure 1.1 Location of study area, Hardin and Meade counties, Kentucky.....	17
Figure 1.2 Images of Fort Knox restoration efforts.	18
Figure 1.3 Physiographic region map of Kentucky with yellow highlighted area representing the study area.....	19
Figure 1.4 Ecoregion map of Kentucky with red marking the study area.	20
Figure 1.5 Geologic map of the study area with karst features displayed, Hardin and Meade counties, Kentucky.....	21
Figure 1.6 Study area geologic map with well types displayed, Hardin and Meade counties, Kentucky.....	22
Figure 1.7 Soil map with percent slope for the study area, Hardin and Meade counties, Kentucky.	23
Figure 1.8 Hjulström-Sundborg diagram, sediment transport and movement as it relates to particle size and flow velocity.	24
Figure 2.1 Images of training lands that show some erosion with sparse vegetation and well developed gullies with little to no vegetation: Fort Knox, Kentucky.	74
Figure 2.2 Location of study area in Hardin and Meade counties, Otter Creek, Kentucky.	75
Figure 2.3 Land use/land cover for the study area, Hardin and Meade counties, Kentucky	76
Figure 2.4 Image of agricultural field along Otter Creek showing slumping and erosion, Hardin County, Kentucky.	77
Figure 2.5 Physiographic regions of Kentucky.....	78
Figure 2.6 Geology of the study area with karst features depicted, Hardin and Meade counties, Kentucky.....	79
Figure 2.7 Images of Otter Creek sinking into the karst conduit and re-emerging out of fractured bedrock.	80
Figure 2.8 Soil and percent slope in the study area, Hardin and Meade counties, Kentucky.	81
Figure 2.9 Percent sand in the study area, Hardin and Meade counties, Kentucky.....	82
Figure 2.10 Percent silt in the study area, Hardin and Meade counties, Kentucky.	83
Figure 2.11 Percent clay in the study area, Hardin and Meade counties, Kentucky.	84
Figure 2.12 Ecoregions of Kentucky	85
Figure 2.13 Source soil sampling locations, Hardin and Meade counties, Kentucky	86
Figure 2.14 Cross-section of time-integrated suspended sediment samplers..	87
Figure 2.15 Images of the time-integrated sediment samplers in situ at site 1.....	87
Figure 2.16 Ternary diagram for selected soils, Hardin and Meade counties, Kentucky. 88	88
Figure 2.17 Fines analysis of selected sediment samples, Otter Creek, Hardin and Meade counties, Kentucky.....	89
Figure 2.18 Box and whisker plots with error bars for source soil groups and sediment sampling locations by tracer. Tracers: TOC, $\delta^{13}C$, Zn, Sr, Rb and Co.....	90

Figure 2.19 Box and whisker plots with error bars for source soil groups and sediment sampling locations by tracer. Tracers: Ni, Al, Na, Mg, Si and P.....	91
Figure 2.20 Box and whisker plots with error bars for source soil groups and sediment sampling locations by tracer. Tracers: K, Ca, Mn, Fe and Cu.....	92
Figure 2.21 $\delta^{13}\text{C}$ and TOC for all source soil groups, all target sediment and base- and stormflow by monitoring location along Otter Creek.....	93
Figure 2.22 Source soil $\delta^{13}\text{C}$ (‰) values overlaid onto the LU/LC map, Hardin and Meade counties, Kentucky.....	94
Figure 2.23 Source soil $\delta^{15}\text{N}$ versus $\delta^{13}\text{C}$ for civilian and three military source soil groups.....	95
Figure 2.24 Plot of second vs. first principal factor loadings and proportion of variation for all source soils and target sediments.	96
Figure 2.25 Plot of second vs. first principal factor loadings and proportion of variance for each of the five source soil categories.....	97
Figure 2.26 Plot of second vs. first principal factor loadings and proportion of variation for all target sediments.....	98
Figure 2.27 Percentages of target sediment apportioned to source soil groups by Sed_SAT for baseflow at each of the sediment sampling sites.	99
Figure 2.28 Percentages of target sediment apportioned to source soil groups by Sed_SAT for stormflow at each of the sediment sampling sites	100
Figure 2.29 Tukey test on XRF data (post-hoc analysis completed after ANOVA) showing that mean concentrations of Ni, Co, Rb, Sr, Zn and Cu were statistically significant ($p < 0.0001$) in differentiating civilian from military source soils, Hardin and Meade counties, Kentucky.....	101
Figure 2.30 Conterminous United States karst map, with different types of karst formations and identified military installations.	102
Figure 3.1 Land use and land cover for Hardin and Meade counties, Kentucky.....	131
Figure 3.2 Study area, Hardin and Meade counties, Kentucky.	132
Figure 3.3 Images of Otter Creek sinking into the karst conduit and re-emerging out of fractured bedrock	133
Figure 3.4 Minimum and maximum air temperature and precipitation throughout the study period, Hardin and Meade counties, Kentucky.	134
Figure 3.5 Kentucky geology with karst overlay, Hardin and Meade counties, Kentucky.	135
Figure 3.6 Soils and percent slope within Hardin and Meade counties, Kentucky	136
Figure 3.7 Image of Xylem YSI InSitu® datalogger and stilling well, and stage gage at site 2.....	137
Figure 3.8 Precipitation (cm) versus pressure (kPa) at sites 1 and 2	138
Figure 3.9 Comparison of the study period monthly total precipitation from October 2015 through October 2016 with average monthly precipitation for 1986 through 2016, Otter Creek, Kentucky	139
Figure 3.10 Pressure (kPa) and stage (cm) versus precipitation (cm) at sites 1 and 2....	140
Figure 3.11 Stream profiles for site 1, 2 and 3 completed on July 18, 2016.	141

Figure 3.12 Measured discharge on July 18 at ~ 1200 hr from 1999 to 2010, and 2016, Otter Creek, Kentucky	142
Figure 3.13 Continuously monitored water temperature (sites 1 and 2) and weekly manual water temperature readings for sites 1, 2 and 3 versus precipitation (cm).....	143
Figure 3.14 Continuous water-quality monitoring of electrical conductivity ($\mu\text{S}/\text{cm}$) versus precipitation (cm) sites 1 and 2.....	144
Figure 3.15 Weekly manual readings of specific conductivity (uS/cm) for all three sampling sites versus continuously monitored electrical conductance (uS/cm) at sites 1 and 2.....	145
Figure 3.16 Weekly manual readings of dissolved oxygen (mg/L) for all three sampling sites, Otter Creek, Kentucky	146
Figure 3.17 Weekly readings for pH for all three sampling sites, Otter Creek, Kentucky.	147
Figure 3.18 Weekly water samples for chloride (mg/L) for all three sampling sites, Otter Creek, Kentucky	148
Figure 3.19 Weekly water samples for sulfate, phosphate and nitrate (mg/L) for all three sampling sites, Otter Creek, Kentucky	149
Figure 3.20 Baseflow index for the Commonwealth of Kentucky	150
Figure 3.21 Historical discharge for Otter Creek from the discontinued USGS gaging station (03302110) from 1999 through 2010.....	151
Figure 3.22 Site 2 regression analysis between manual stage measurements and InSitu datalogger continuous monitoring of pressure, Otter Creek, Kentucky	152
Figure 3.23 Site 1 regression analysis between manual stage measurements and InSitu datalogger continuous monitoring of pressure, Otter Creek, Kentucky.	152

LIST OF ADDITIONAL FILES

Supplemental Site 1 InSitu Continuous Monitor Data..... [PDF 687 KB]
Supplemental Site 2 InSitu Continuous Monitor Data.....[PDF 687 KB]

CHAPTER 1. INTRODUCTION

1.1 Overview and Objectives

The U.S. Environmental Protection Agency (EPA) lists sediment as the most common pollutant found in rivers, streams, lakes and reservoirs (USEPA 2016). From 1974 to 2012, urban areas in the conterminous United States increased by almost 50% (202,342 km²) and crop production increased 114% while cropland area increased only 23%, which reflects the vast growth in agricultural productivity (Falcone et al. 2018). Understanding how anthropogenic land use and land management changes affect an area is vital in determining where sources of sediment originate from. Although erosion is a natural process that occurs when surface soils experience heavy rainfall, wind, freezing and thawing, areas that are heavily disturbed by anthropogenic activities can see an increase in sedimentation to waterways. Land use practices that can increase erosion rates can be observed in construction areas, deforested regions, vehicle recreational areas, military vehicle-track training lands and farm fields when the land is being plowed or vegetation is removed. Agriculture and urban land management practices have the potential to either degrade or improve water quality (Deacon et al. 2005; Sullivan et al. 2009; Hribar 2010; Bryant and Carlisle 2012; Anning and Flynn 2014; Stone et al. 2014; Ryberg and Gilliom 2015; Garcia et al. 2016; Shoda et al. 2016; Ryberg et al. 2017; Stets et al. 2017; Falcone et al. 2018). However, in watersheds that have multiple ongoing land use practices it is inherently difficult to identify specific sources of excess sedimentation to waterways.

The attempt to relate sediment to its origin can be a complicated and costly endeavor and a number of different approaches have been used, all with advantages and disadvantages. Studies that use erosional pins and troughs to estimate sediment loads and relative

contributions provide discrete data but are constrained by spatial and temporal limitations, are labor intensive as they rely on field measurements and manpower, and are better suited to smaller catchments (<50 km²) (Peart and Walling 1988; Foster et al. 1990; Collins et al. 1998). GIS (Geographical Information Systems), DEMs (Digital Elevation Models), LiDAR (Light Detection and Ranging) and UAVs (Unmanned Aerial Vehicles) have become popular in soil erosion investigations and sediment source tracking (d'Oleire-Oltmanns et al. 2012; Wirtz et al. 2012; Peter et al. 2014; Neugirg et al. 2015). Although less intensive with respects to manpower and time they may produce a wide range of results that require validation through the collection of discrete samples taken from the field (Gellis and Sanisaca 2018). Sediment fingerprinting entails the identification of specific source soil groups through unique physical and or chemical properties, allowing for relative contributions of suspended sediment to be apportioned to predetermined source groups.

Despite advances in sediment fingerprinting and studies of nonpoint-source impacts on water quality at the catchment scale, more research is needed regarding tracer conservatism and source discrimination. In particular, there is a lack of published studies on sediment contributions and water-quality impacts in watersheds that include both military and civilian land uses. This study has two primary parts, presented as two separate papers. The main objectives of the sediment sourcing study (chapter 2) were to: 1) identify and differentiate unique characteristics of civilian and military source soils transported to a 3rd-order stream (Otter Creek, Kentucky); 2) apportion source contributions of fine-grained sediment to each of five source categories (civilian lands; military lands with scrub/grasses but no visible soil; military forest; military average erosion; and military extreme erosion); and 3) characterize specific stormflow contributions in relation to samples collected weekly

from sediment traps. We hypothesized that the primary sources of fine-grained sediment to Otter Creek were derived from areas of average and extreme erosion, which were tracked-vehicle training areas for the military installation (Fort Knox) within the watershed. Samples have been analyzed for 18 chemical tracers and an optimal tracer fingerprint composite has been identified utilizing multivariate statistics. The purpose of the second paper (chapter 3) is a water-quality study to explain hydrochemical variations at three points along Otter Creek. We examined weekly variability in field parameters (dissolved oxygen, specific conductance, water temperature, and pH) over a 1-year period, anions (chloride, phosphate, sulfate and nitrate) over a concurrent 6-month period and continuous in-stream monitoring of pressure, electrical conductivity, and water temperature for over 10 months at the first two sites. We investigated whether significant relationships exist between analytes and, using historical discharge, water-quality, and weather data from the region, we have drawn inferences about temporal and spatial controls on water chemistry.

1.2 Land Use

The Commonwealth of Kentucky has an area of 102,896 km² (39,728 mi²) and as of the 2010 U.S. Census a population of 4.3 million people. The study area (Figure 1.1) lies within the watershed of Otter Creek, a tributary of the Ohio River, in Hardin and Meade counties in north-central Kentucky. The 203-km² area is dominated by rural and agricultural land uses; as of 2011, almost half (46.5%, or 94.6 km²) of the area consisted of cropland and pasture (NLCD 2011). In Hardin and Meade counties, the predominant row-crop agricultural crops are burley tobacco and wheat, followed by hay, corn and soybeans (KYFB 2015). Sheep and goats are the primary pasture animals; other livestock includes cattle, poultry and horses (KYFB 2015). The largest community within the study area is Vine Grove with a

population of roughly 4,520 residents as of 2010 (U.S. Census 2010). Part of the study area (18.4%, or 37.3 km²) is occupied by Fort Knox Army Post. Fort Knox constitutes the 17th largest urban community by area in the Commonwealth. It has a workweek population of roughly 23,000 and supports a population of about 160,000 active and reserve component members, retirees, military dependents, Department of Defense civilians and contractors in the region covering roughly 441 km² (170 mi²) within Bullitt, Hardin, and Meade counties (IMCOM Fort Knox 2016).

In the 2016 Integrated Report to Congress on the condition of water resources in Kentucky, Otter Creek was classified as impaired (2016IR-305b), with the primary sources of pollutants being unspecified urban stormwater, municipal point-source discharges, and livestock grazing and or feeding operations (KEEC 2018). The diversity of land uses in the study area, including row-crop and pasture agriculture, small urban areas, and military training activities, makes identification of pollutant sources challenging. An improved understanding of sediment and solute contributions in multi-land use catchments is essential for developing a sustainable management plan that balances civilian and military interests with protection of aquatic ecosystems.

Fort Knox was established in 1918 as Camp Knox when the Army was looking to create a new artillery training center due to the U.S. involvement in World War I (Fort Knox 2019). Within the study area on the western portion of the installation, training areas (TAs) were designated to train service members on armor tactics, tank gunnery, communications and armored vehicle maintenance (Fort Knox 2019). For nearly 71 years Fort Knox was the primary location for armored-vehicle training until 2011, when the Base Realignment and Closure (BRAC) commission began its assessment of installation activities and efficiencies.

Within a few years of BRAC the Armor Center and School was relocated to Fort Benning, Georgia (Fort Knox 2019). However, the restructuring led the U.S. Army Cadet Command (USACC), U.S. Human Resources Command, the 84th Training Command, 3rd Sustainment Command (Expeditionary), 11th Aviation Command, 100th Division and 83rd Army Reserve Readiness Training Center to relocate to Fort Knox (IMCOM Fort Knox 2016). The TAs no longer experience the heavy traffic associated with the Armor Center and School training so restoration efforts are being implemented (Figure 1.2). However, Fort Knox still offers a wide variety of training and services to military personnel year-round, which can contribute to soil erosion and sedimentation of Otter Creek.

1.3 Climate

Climate in the study area can be highly variable given its mid-latitude position on the continent; prevailing surface winds are southerly and light, while upper-level westerly winds steer frontal systems across the state (KYCC 2017). The Köppen-Geiger climate classification, which uses averaged monthly temperature and precipitation data over long periods of time, classifies the study area as mild temperate, full humid (Cf) with hot summers ($T_{\max} \geq +22^{\circ}\text{C}$) (Chen et al. 2013). During the months of June, July and August, the region experiences average summer temperatures of 25.4°C, with average maximum and minimum temperatures of 30.8°C and 20.1°C, respectively, and an average rainfall of 24.3 cm (NOAA n.d.). During the winter months of January and February, the average temperature is 2.8°C, with average maximum and minimum temperatures of 7.5°C and -1.7°C, respectively, average rainfall of 26.0 cm and average snowfall of 27.4 cm (NOAA n.d.).

1.4 Geology

The research area lies within two physiographic regions, Muldraugh Hill and the Pennyroyal (Figure 1.3), and is part of the Mitchell Plain (Level IV-71b) ecoregion (Figure 1.4). Based on the Kentucky Geological Survey's (KGS) online mapping information service (KGS n.d.) and an environmental impact study performed for Fort Knox (Hill 1981; Rawson 2008), the Otter Creek watershed is underlain by gently dipping Mississippian sedimentary rocks, largely karst limestones and shales of the Meramec Group. Within the study area a linear sand body (Figure 1.5, in yellow on the map) is part of the Mooretown Formation which runs southwest–northeast, intersecting the northwestern corner of the Fort Knox cantonment area. The upper portion of Muldraugh Hill consists of siltstone, dolomite and limestone with the lower part consisting of mostly shale (KGS n.d.). Extensive karst topography is developed on the St. Louis Limestone and Ste. Genevieve Limestone, which have a combined total thickness of more than 53 m and underlie most of the study area in Hardin and Meade counties (Rawson 2008; KGS n.d.). Fort Knox's tracked vehicle TAs in Meade County contain karst uplands (Figure 1.5) with more than 20 sinkholes in each TA, as well as steep hills and flood plains, from just upslope of the armored vehicle TA downstream to the confluence with the Ohio River (Crim et al. 2011).

The Kentucky Geologic Mapping Information Service (KGS n.d.) shows one abandoned limestone mine in Hardin County, but no other bulk mineral resources (including coal ore mineral points) are listed. There are several wells within the study area used for gas production, gas storage, gas injections, with several having been abandoned (Figure 1.6). Most of these are located within Meade County and range in depth from 22.8 to 305 meters with the majority seen abandoned in Hardin County. The wells are scattered across both civilian and commercial properties with ownership rights varying; some are still maintained

by the original owners, others are held by leasing companies and some are currently held and operated by the Louisville Gas & Electric Company.

1.5 Soils and Vegetation

The Kentucky Soil Atlas (Karathanasis 2018) and the U.S. Department of Agriculture Web Soil Survey (USDA-WSS) describe the majority of the soil units in the area as Baxter, Bedford, Caneyville, Crider, Fredonia, Hammack, Nolin, Pembroke and Vertrees (Figure 1.7), which are formed in a residuum of limestones. Baxter and Hammack soils have slopes ranging from 2 to 40% with the rock outcrop areas between 20-60%. Baxter soils are found along hillsides and ridge tops and areas that have karst topography. Hammack soils are formed in a 50- to 100-cm loess mantle underlain by cherty limestone. Both the Baxter and Hammack soils can be found on ridgetops and side slopes of rolling to hilly areas. Bedford and Crider soils have 0 to 12% slopes; Bedford soils are moderately well drained with a fragipan (altered subsurface soil layer that inhibits water flow and root penetration) and Crider soils form in a thin silty mantle over fine-textured residuum of limestone. Bedford soils are on summits, shoulders and to a lesser extent backslopes of hills, while Crider soils are on nearly level to moderately steep upland areas. Fredonia and Vertrees soils have slopes ranging from 2 to 30%. Fredonia soils are formed in residuum from massive gray limestone and are found mostly on rolling uplands. Vertrees soils are formed in residuum of limestone interbedded with siltstone and shale and are found in a range of areas from gently sloping hills to steep ridges and in most karst areas. The Nolin soils are formed in alluvium derived from limestone, sandstone, siltstone, shale and loess and found in flood plain areas, concave depressions or on natural levees of major streams and rivers and have slopes ranging from 0

to 25%. Pembroke soils formed in thin silty mantle and are underlain by older alluvium or limestone residuum or both, and have slopes ranging from 0 to 12%.

The region is dominated by several species (spp.) of hardwood trees, native shrubs, herbaceous flowering plants, warm season grasses and non-native tall fescue (Cranfill 1991; White and Palmer-Ball 1994; Schoonover et al. 2015). The composition and diversity of the forested areas is similar to the mesophytic forests described by Braun (1950) and Homoya et al. (1985) in southern Indiana and Ohio, specifically those found in lower sloped areas (Cranfill 1991). Vegetation in the Mitchell Plain ecoregion can include bluestem prairie grasses, oak-hickory forests and on steep slopes a mix of oak species (Sprandel 1999). The most abundant hardwood trees in the research area are black maple (*Acer nigrum*), buckeye (*Aesculus* spp.), hickory (*Carya* spp.), white ash (*Fraxinus americana*), oak (*Quercus* spp.), eastern red cedar (*Juniperus virginiana*) and American elm (*Ulmus americana*). Understory trees, shrubs and vines include flowering dogwood (*Cornus florida*), American hornbeam (*Carpinus caroliniana*), paw paw (*Asimina trilobal*), Virginia creeper (*Parthenocissus quinquefolia*), grape vines (*Vitis* spp.) and poison ivy (*Toxicodendron radicans*) (Cranfill 1991; NRCS 2019). Some native warm season grasses found in the area are switchgrass (*Panicum virgatum*), big bluestem (*Andropogon gerardi*), Indian grass (*Sorghastrum nutans*), eastern gamagrass (*Tripsacum dactyloides*), little bluestem (*Schizachyrium scoparium*) and sideoats grama (*Bouteloua curtipendula*) (Smith et al. 2009). Non-native tall fescue (*Festuca arundinacea*) is located in the study area as well (White and Palmer-Ball 1994; Schoonover et al. 2015).

1.6 Hydrology

Surface water within the study area is drained by Otter Creek, with its headwaters located approximately 1.6 km south of the City of Vine Grove. Otter Creek flows south to north through residential and agriculture areas, passing on the west side of Vine Grove before entering Fort Knox. After Otter Creek exits Fort Knox it flows through Otter Creek Recreational Park where it drains into the Ohio River. Between source and sink there are multiple sinkholes and depressions formed from the extensive limestone bedrock that underlies the area and influences the surface water drainage of Otter Creek (Figure 1.5). The stream at baseflow conditions disappears into a karst conduit, reappearing ~ 1.6 km downstream (Figure 1.1).

The majority of the source drinking water for Hardin and Meade counties comes from public water treatment plants (WTPs), private wells, creeks, springs or cisterns (Rawson 2008). The three WTPs that service Hardin County civilians, Fort Knox and 70% of Meade County are Pirtle Spring (PSWTP), Fort Knox Central (FKCWTP) and Muldraugh (MWTP). There are two source waters for PSWTP, Pirtle Spring which is located at the WTP and the Head of Rough Spring about 2.4 km from the plant, which is considered groundwater under the influence of surface water (Rawson 2008; Hardin County Water District No. 1 2018). The MWTP and FKCWTP are both owned by Fort Knox and supply the installation, the City of Muldraugh and surrounding area. The MWTP obtains its water from 15 deep water wells located in the West Point aquifer near the Ohio River. The FKCWTP is supplied by McCracken Spring in addition to some of the wells from MWTP (Rawson 2008; Muldraugh 2018). McCracken Spring originates from the St. Louis Limestone and eventually flows into Otter Creek. The water in Otter Creek is generally hard due to dissolved calcium from the limestone bedrock and is mostly clear, but discolors

during flooding, and bicarbonate, hardness and pH levels are usually higher in Otter Creek than those in the surrounding streams (IMCOM Fort Knox 2016).

1.7 Literature Review

1.7.1 Soil Erosion

Surface soil erosion takes place in three stages: dislodgement, transportation and sedimentation (Ffolliott 2013). Although erosion of surface soils is a naturally occurring process, the impact of human activities such as agriculture, logging, industrialization, construction and military training can increase erosion and degradation processes. Biogeochemical and physical changes in soil often take place during erosion and transport. Biological properties can be difficult to quantify and measure; chemical properties can be offset with fertilizer and pH-modifying inputs (Arriaga and Lowery 2003); and the breakdown of soil structures from physical processes alters particle size. How far eroded soil, now referred to as sediment, is transported depends on its particle size, type and the velocity of water. The Hjulström (1938) diagram (Figure 1.8; Earle 2015) shows that silt and clay can remain in suspension longer and travel farther under low flow conditions than larger size fractions. Eroded soil, including both organic and inorganic components, can be transported in streams as solid material and in solution (Owens et al. 2005). The competence and transport capacity of a stream are related to its velocity and discharge. The solid material is divided into two categories, bedload and suspended load. Their relationship is determined by the flow conditions and the structure, density and size of the material, with the suspended load composed primarily of particles $< 63 \mu\text{m}$ (silt and clay) and/or less dense material (Owens et al. 2005). For the purpose of this study, bedload is not considered.

In many cases sediment is considered to be silt and clay (Walling and Moorehead 1989). Excessive mobile sediment in a waterbody degrades the quality of the water for drinking, increases the potential for flooding, harms the habitat for aquatic species (including clogging fish gills, increasing the growth of algae, and inhibiting light penetration), and affects navigational and recreational use (USEPA 2012; Williamson et al. 2014). Sediment < 63 µm can also transport nonpoint-source (NPS) contaminants, including nutrients and heavy metals, that have been mobilized into the water column (Davis and Fox 2009). It is imperative to answer several important questions when trying to identify sediment source locations and targeting restoration efforts. First, are there areas within the watershed that experience anthropogenic activities such as construction or tilled agriculture which could potentially increase sedimentation to waterways? What are routes and where are the sinks associated with the mobilization of sediment within the watershed (Gellis and Walling 2011)? Answering these questions is important for pinpointing the locations of active source soil erosion by identifying the links between source and sink, ultimately providing crucial information for the implementation of best management practices.

In an effective land management strategy, pinpointing the provenance of sediment is integral to mitigation and remediation of erosion. Understanding fluvial processes is especially useful for determining the relative magnitude of sources from upland soil erosion compared to fluvial erosion and river-related mass wasting (USEPA 2016). Sediment fingerprinting has become a tool with which land managers and scientists can quantitatively determine the sources and movement of sediment. In the process of identifying the magnitude of the problem and the specific sources of sediment, the results can be used to develop an implementation plan based on the proximity of active sediment sources to

important areas within a river system, such as spawning beds for fish, water intakes and drinking water resources (USEPA 1999, 2016).

1.7.2 *Sediment Fingerprinting*

The provenance of sediment contributions to streams has been studied for more than 60 years. Glymph (1957) collected and measured the amount of sediment produced from various outlets, then estimated the amounts delivered to the main channel (Klages and Hsieh 1975). Early fingerprinting studies used mineralogy (Klages and Hsieh 1975; Wall and Wilding 1976) and magnetism (Oldfield et al. 1979) to relate suspended sediment back to its geologic source. Certain biological properties were introduced as tracers, which included pollen (Brown 1985) and soil enzymes (Nosrati et al. 2011). Over the decades, scientists began working on improving source discrimination through the introduction of additional tracers and advanced mathematical and statistical techniques. Additional tracers such as color (Krein et al. 2003; Martinez-Carreras et al. 2010), major and trace metals (Evrard et al. 2011; Navratil et al. 2012), fallout radionuclides (Olley et al. 2013; Belmont et al. 2014), carbon and nitrogen isotopes, and organic and inorganic carbon (Blake et al. 2012; Hancock and Reville 2013; Fox and Martin 2015) were introduced. It became clear that a composite set of tracers would be needed to discriminate source contributions with any degree of certainty. However, cost and time can render some tracers undesirable. For example, fallout radionuclides decline rapidly with depth and soil below a depth of about 30 cm is unlikely to yield enough cesium-137 or lead-210 to be useful; in addition, the analytical cost could prohibit their use as a sediment fingerprinting tracer (Gellis and Walling 2011).

The application of multivariate statistics has increasingly been used to improve source discrimination, and the development of unmixing models has been helpful in allocating source contributions quantitatively (Walling and Woodard 1995; Collins et al. 1997; Fox and Papanicolaou 2008). Even with the addition of multivariate statistics, some tracers have a propensity to change from source to sink and/or over long periods of time, which can potentially influence findings (Collins 2017). Phosphorus used in agricultural fertilizers may vary in concentration when used over long periods of time, as may lead and other heavy metals where atmospheric releases relating to industrial practices have changed over time with increasing or decreasing regulations (Foster and Charlesworth 1996; Collins et al. 2017). Changes in grain size and the alteration of organic content happen routinely during sediment transport. The effects of those factors on many of the geochemical properties commonly used as sediment source tracers have been recognized (Goldberg 1954; Rex and Goldberg 1958; Goldberg and Arrhenius 1958; Kononova 1966; Jones and Browser 1978; Horowitz 1991; Collins et al. 2017) and need to be carefully considered with regard to selecting tracer properties for the particular environment in which the tracer is found. The fundamental assumption in sediment fingerprinting is that the selected tracer properties behave in a conservative fashion during transport and delivery and that the source sample properties are proportional and can be compared directly to the collected target sediment sample.

Reviewing the spatial distribution of potential sediment sources within the watershed or catchment unit and then distinguishing between source types (e.g. cropland, pasture, forest, stream bed, channel bank) is an essential step before sampling can occur. There are two general ways of determining source groups; one largely depends on geology and the

other land-use patterns. Geology can be a major controlling factor within a watershed, especially if the geology of the drainage basin is diverse, which can assist in source group classification. In smaller watersheds or those with homogeneous bedrock, classification by geology may provide less useful information for the identification of source groupings, in which case an alternative source group classification would need to be implemented (Collins et al. 2017). A different approach is to create the source grouping classification first, commonly performed *a priori*, to align source apportionment estimates with land-use patterns and corresponding management goals (Peart and Walling 1986; Walling and Woodard 1995; Collins et al. 1997; Owens et al., 1999; Porto et al., 2005; Collins et al. 2010a, b, c, d; Smith and Blake 2014; Lamba et al. 2015; Foucher et al. 2015; Collins et al. 2017). For example, van der Waal et al. (2015) used aerial photography to identify areas where erosion was taking place, such as gullies and then collected source soil samples. Another way is through a method of objective sediment source grouping. This method is based on pre-selected tracers from a cluster analysis in order to minimize uncertainty associated with quantitative source apportionment estimates (Walling et al. 1993; Pulley et al. 2017; Collins et al. 2017). Performing either *a priori* classification or objective sediment source grouping method assures that all source materials are represented. Whatever method is used to classify source groupings, it is imperative to have a clear understanding of the geology and land-use patterns within the study watershed.

1.7.3 *Hydrochemical Aspects of Water Quality*

Early studies of water quality at the catchment scale focused on physical properties (Kuehne 1962, 1966; Harrel and Dorris 1968; Johnson et al. 1997) and the influence of geomorphic characteristics such as drainage area, gradient, and stream order on turbidity,

dissolved oxygen concentration and stream temperature (Johnson et al. 1997). Over time, the focus evolved to include hydrochemical aspects of water quality (Hynes 1960; Johnson et al. 1997; Morgan and Good 1988) and relationships with different (e.g., urban or agricultural) land-use/land-cover types (Johnson et al. 1997; Basnyat et al. 1999; Zampella et al. 2007). Distinct relationships between hydrochemical water quality and watershed characteristics can be seen at various temporal and spatial scales. The chemistry of streams, rivers, lakes and reservoirs varies with lithology, seasons, climate and land-use activities. Watershed- or landscape-level processes define the overall supply of solutes to a stream and provide the framework within which other processes operate on smaller spatial and shorter temporal scales to regulate supply and availability (Meyer et al. 1988; Johnson et al. 1997).

As water percolates through the soil, it attacks the mineral constituents physically and chemically, leaching the more soluble fractions, which ultimately end up in rivers (Livingstone 1963). Aquatic organisms may take up dissolved material, particularly nutrients such as phosphate, nitrate and silica (Lund 1950) that tend to be in short supply, thus drastically reducing their aqueous concentrations. When large numbers of those organisms die suddenly, they release these nutrients into the surrounding water (Livingstone 1963).

The major-ion composition of river water can vary greatly and can reveal the type of weathering and a variety of other natural and anthropogenic processes on a basin-wide scale (Mohamed et al. 2015). Accordingly, the geochemical processes that control the chemistry of freshwater bodies are closely coupled to microbiological activity, climate forcing, atmospheric inputs and transport processes (Zhu and Schwartz 2010). For example, in karst terrain, the dissolution of limestone by carbonic acid (which forms via dissolution of CO₂ from the atmosphere and/or from soil respiration) results in calcium-bicarbonate dominated

water with a neutral to slightly alkaline pH (Hem 1985). Anthropogenic influences include, but are not limited to, agriculture, industrial practices, wastewater treatment plants, septic systems, and nonpoint urban runoff. More specifically, agriculture tends to introduce nutrients and sediments, whereas runoff from impervious surfaces can introduce heavy metals in addition to sodium and sulfate from road deicers (Tong and Chen 2002).

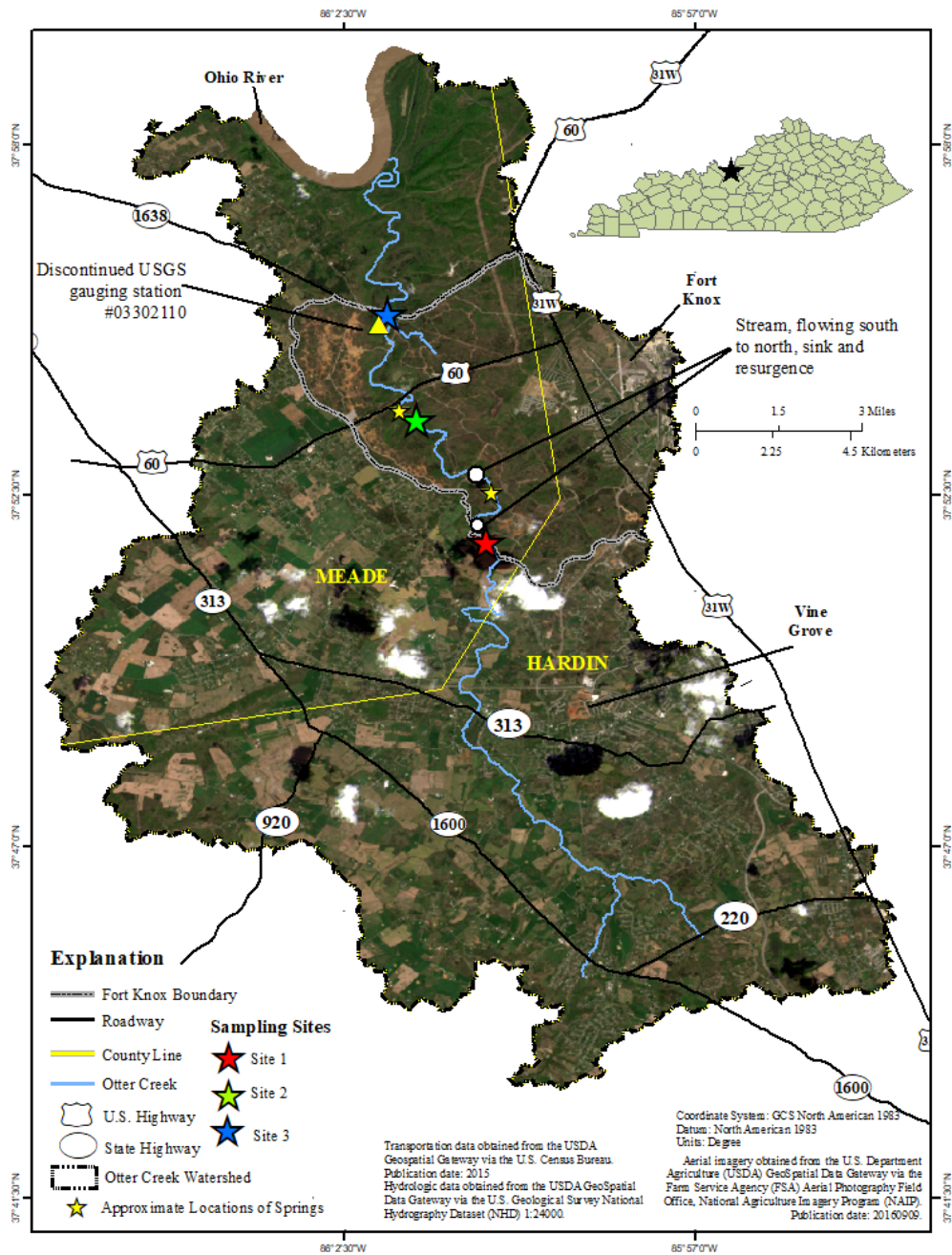


Figure 1.1 Location of study area, Hardin and Meade counties, Kentucky.



Figure 1.2 Fort Knox restoration efforts, images taken by Cara Peterman. Images from left to right: Fort Knox Training area, restoration using native grasses. Fort Knox erosion control method, using riprap to slow soil erosion and transport, newly installed. Fort Knox older erosion control riprap with some erosion present. Fort Knox, Kentucky.

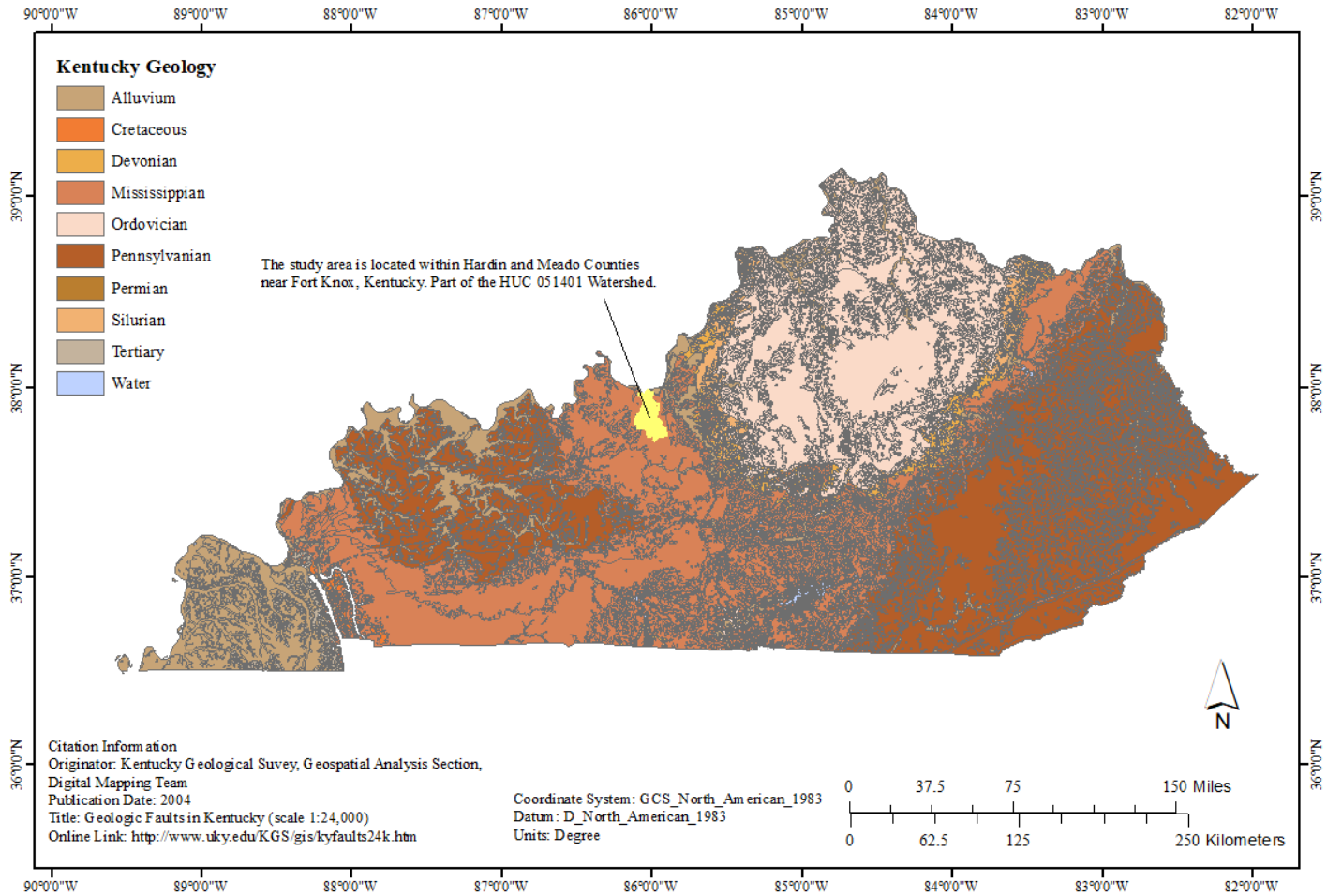


Figure 1.3 Physiographic region map of Kentucky with yellow highlighted area representing the study area.

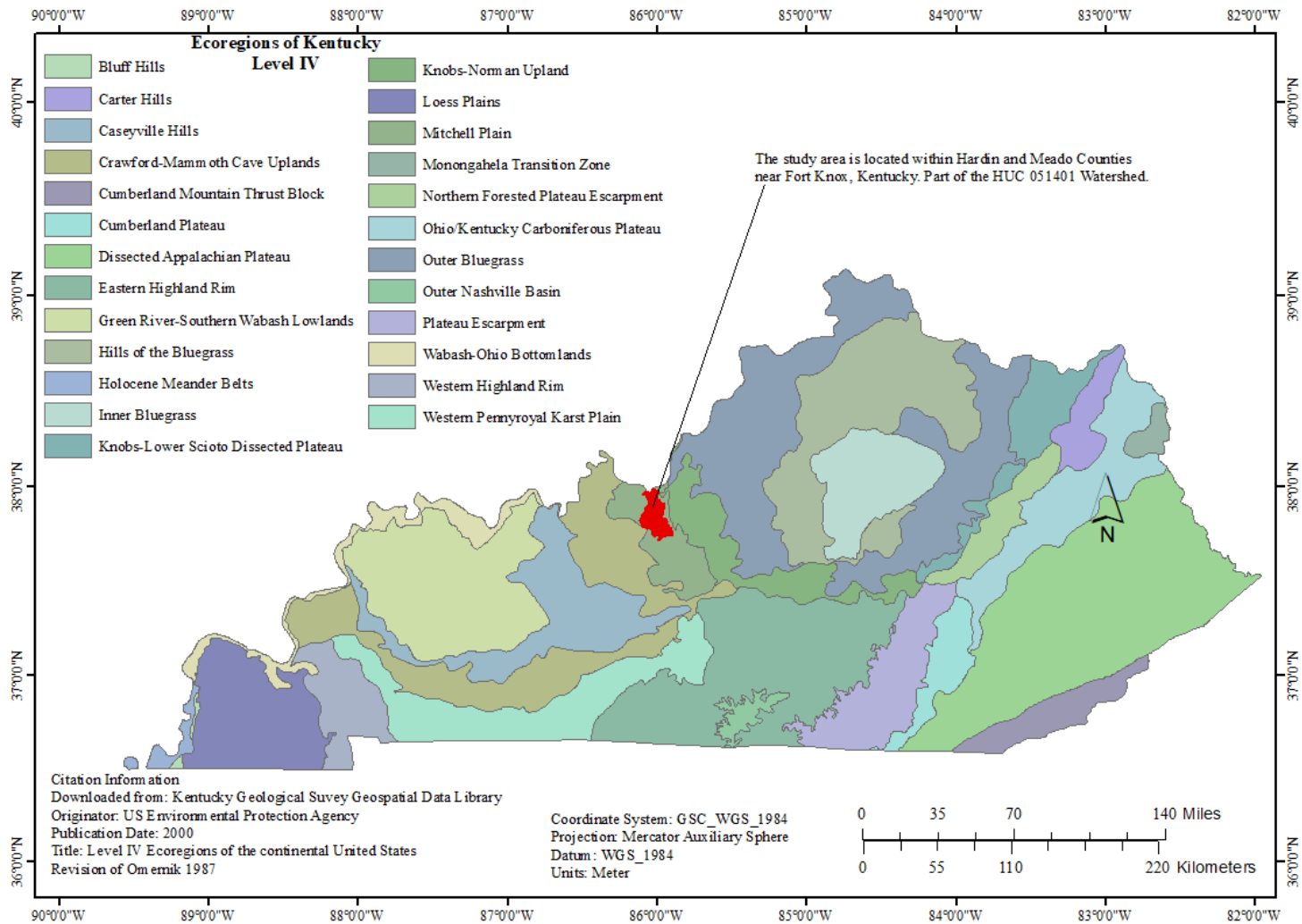


Figure 1.4 Ecoregion map of Kentucky with red marking the study area.

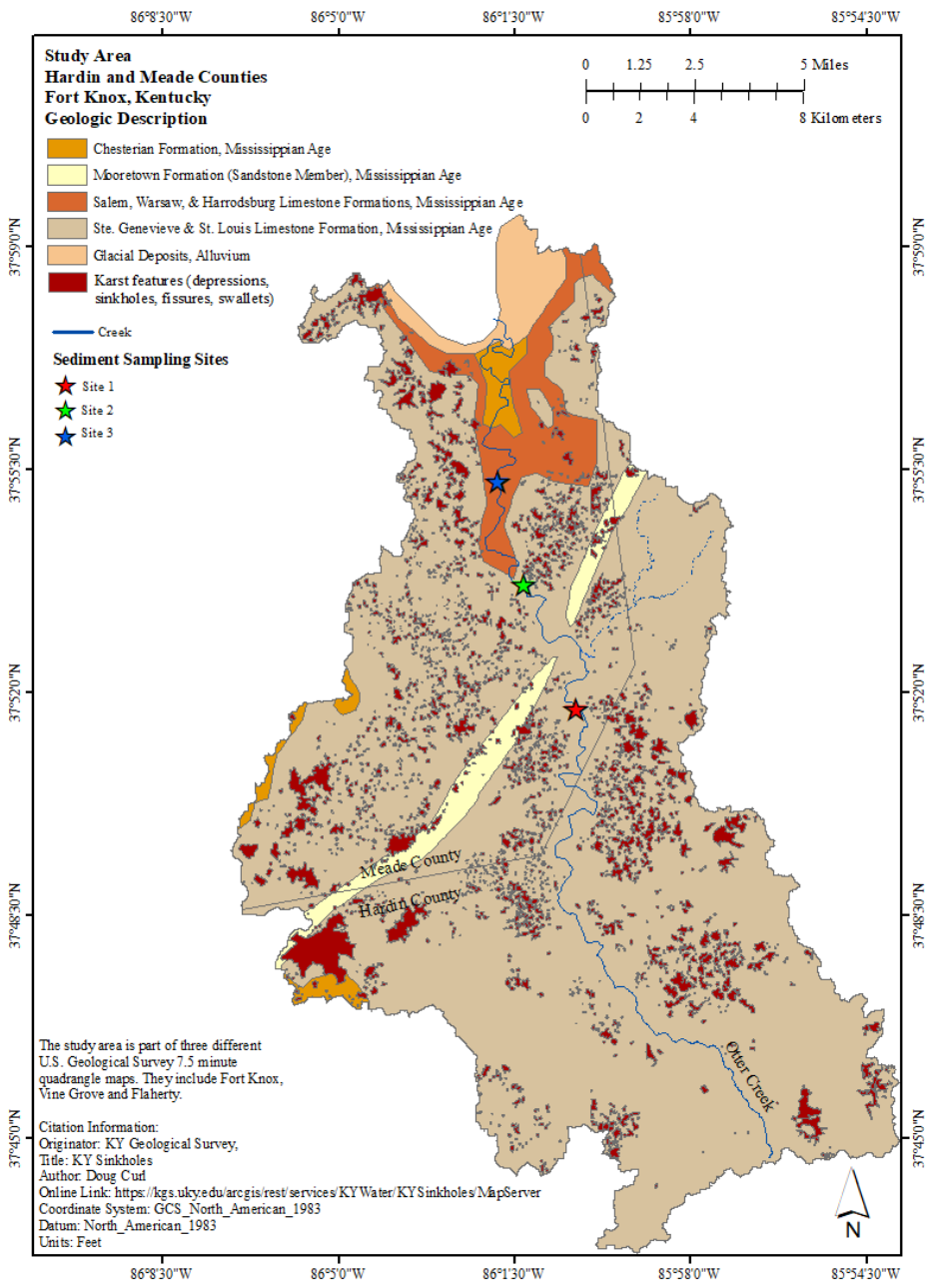


Figure 1.5 Geologic map of the study area with karst features displayed, Hardin and Meade counties, Kentucky.

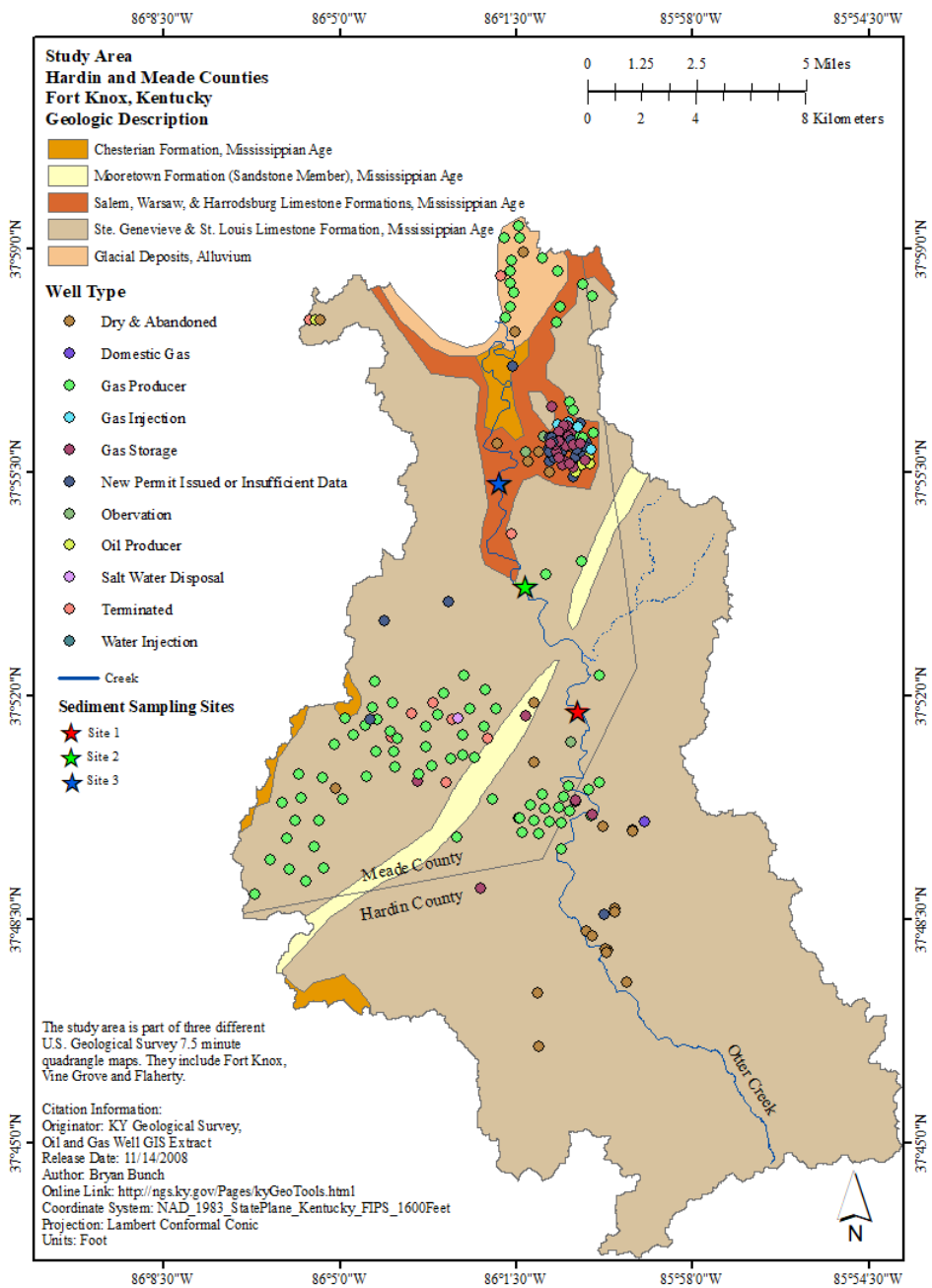


Figure 1.6 Study area geologic map with well types displayed, Hardin and Meade counties, Kentucky.

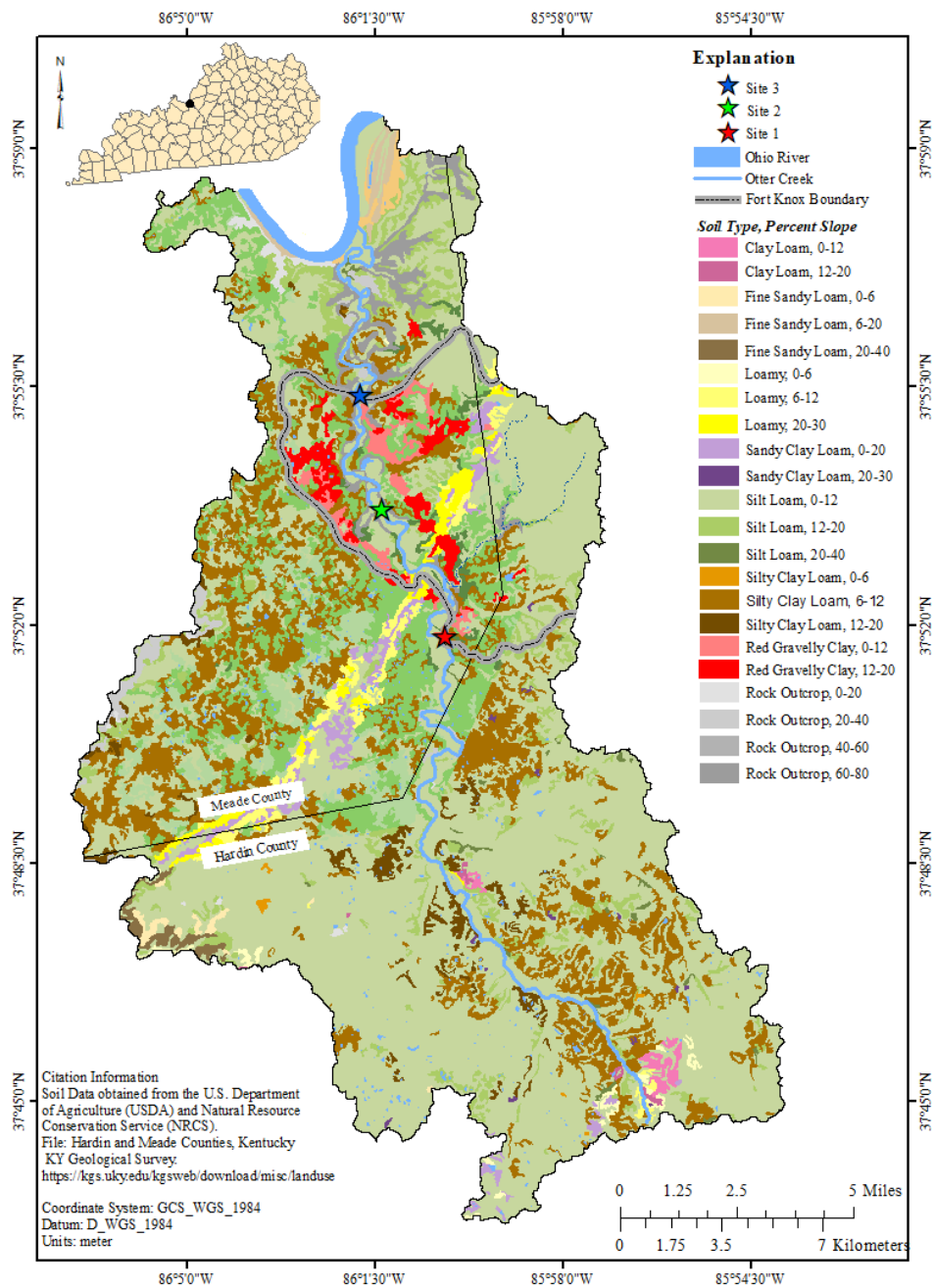
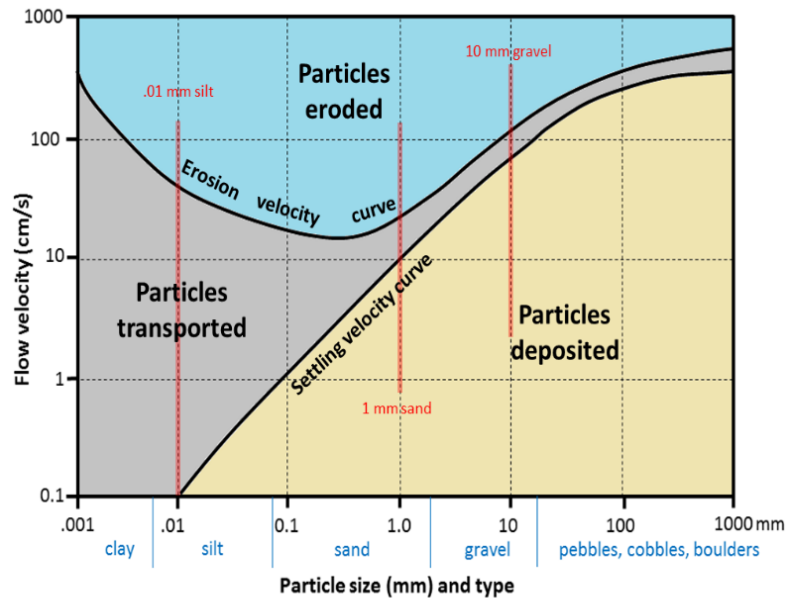


Figure 1.7 Soil map with percent slope for the study area, Hardin and Meade counties, Kentucky.



S. Earle, 2014

Figure 1.8 Hjulström-Sundborg diagram, sediment transport and movement as it relates to particle size and flow velocity, by Steven Earle and is licensed under a Creative Commons Attribution 4.0 International License.

CHAPTER 2. FINGERPRINTING SOURCE CONTRIBUTIONS TO ASSESS SPATIAL PATTERNS OF EROSION IN A MIXED LAND USE ENVIRONMENT: OTTER CREEK, FORT KNOX, KENTUCKY.

Peterman, C.^{a*}, D. Edwards^b, A. Fryar^a, L. Gorman Sanisaca^c, A. Gellis^c

^a University of Kentucky, Department of Earth and Environmental Sciences, 121 Washington Avenue, 101 Slone Research Building, Lexington, KY 40506

^b University of Kentucky, Department of Biosystems and Agricultural Engineering, 128 C.E. Barnhart Building, Lexington, KY 40546

^c U.S. Geological Survey MD-DE-DC-WSC, 5522 Research Park Drive, Catonsville, MD 21228

* Corresponding Author.

Email address: cara.peterman@uky.edu; (859) 257-3758; ORCID No.: 0000-0003-1822-2552

Keywords: Source tracing, sediment fingerprinting, unmixing model, stable isotopes, X-ray fluorescence, mixed land use

Abstract

While catchments that contain rural agriculture are common, fewer catchments include military installations. Identifying the contributions of military training activities to soil erosion and fluvial sediment transport is challenging in catchments with multiple land uses and relatively homogeneous lithology. In this study, sediment fingerprinting was conducted in the 203-km² catchment of Otter Creek (north-central Kentucky). This catchment is dominated by cropland and forest, including the tracked-vehicle training areas of Fort Knox Army Post, and is developed on karst terrain. Five source-soil groups were delineated and sampled: civilian and military near-stream (C-RB and M-RB), military forest

(M-FS), and military average and extreme erosion (M-AE and M-XE). Weekly suspended sediment samples were collected at three sites along Otter Creek for a 12-month period. Major and trace elements, total organic carbon, and carbon and nitrogen stable isotopes were analyzed. Using statistical analyses with the U.S. Geological Survey program Sed_SAT, six metals (Cu, Zn, Co, Ni, Al and Mg) were selected as conservative tracers for unmixing models. At each site, sediment yield was greater in summer than in winter, which may reflect agricultural practices. The greatest proportion of sediment in summer was attributed to M-XE at two sites and M-FS at the other, whereas the greatest proportion of sediment in winter was attributed to M-AE at all three sites. Because of geochemical similarities between soil groups, misclassification of source soils may have affected sediment apportionment. Consequently, we combined soil groups into two simpler scenarios: streambank/forest and military erosion versus streambank and military upland (including forest). All sediment sampling sites were dominated by streambank/forest (63–69%) in scenario one and by military upland (57–66%) in scenario two. Comparison with an agricultural watershed with similar soils suggests that sediment contributions from military training are broadly analogous to those from crop cultivation.

2.1 Introduction

Water quality is a representation of natural processes and human perturbations. Over the last several decades there has been a growing concern about sediment contributions to catchments as a result of erosion from lands that experience excess grazing, row crop farming, and unpaved roads, which can include civilian off-roading (Megahan and King 2004; Macdonald et al. 2003; Anderson and Lockaby 2011) and military training areas (Schoonover et al. 2015). The delivery of sediment to water bodies increases turbidity and

reduces water clarity, leading to aquatic impairment (George et al. 2004). The question of where sediment originates in river basins is not only important from a water-quality perspective, but also to the study of erosion and the sediment delivery process (Caitcheon 1993). Reliable quantitative information on fine-grained sediment sources is required to help target remedial actions for mitigating the impacts of excessive fine sediment on aquatic ecosystems (Kemp et al. 2011; Jones et al. 2012; Collins et al. 2017).

Sediment fingerprinting has become increasingly popular for discriminating source contributions to watersheds. Fingerprinting relies on physical and biogeochemical properties of natural and artificial tracers as a means of distinguishing between target sediment and source soils (Davis and Fox 2009; Guzman et al. 2013; Abban et al. 2016). Throughout the last 50 years research has provided a wide range of properties that can be used as potential tracers in fingerprinting studies. These properties include mineral magnetism (Oldfield et al. 1979; Walling et al. 1979; Slattery et al. 2000; Russell et al. 2001), color (Krein et al. 2003; Martinez-Carreras et al. 2010), clay mineralogy (Eberl 2004; Gingele and De Deckker 2005), biological properties such as soil enzymes (Nosrati et al. 2011), major and trace metals (Evrard et al., 2011; Navratil et al., 2012), fallout radionuclides (Olley et al. 2013; Belmont et al. 2014), carbon and nitrogen isotopes (Blake et al. 2012; Hancock and Revill 2013) and organic and inorganic carbon (Fox 2009; Fox and Martin 2015). Fingerprinting is most often used in catchments dominated by agriculture (e.g., Peart and Walling 1986; Caitcheon 1993; Collins et al. 1996; Owens et al. 2000; Russell et al. 2001; Collins and Walling 2002; Minella et al. 2008; Walling et al. 2008), although some studies have been performed in urban and industrialized catchments (e.g., Charlesworth et al. 2000; Charlesworth and Lees 2001; Carter et al. 2003; Miguel et al. 2005, Charlesworth et al. 2011; Cashman et al. 2018).

None to date, however, have been performed in catchments that contain military training lands.

Fort Knox is one of the largest U.S. Army installations operating today, covering more than 441 km² of land in three Kentucky counties (Meade, Hardin and Bullitt). It hosts a workweek population of roughly 23,000 and supports a population of about 160,000 active and reserve component members, retirees, military dependents, Department of Defense civilians and contractors in the region (IMCOM Fort Knox 2016). Large military installations such as Fort Knox contain tracts of land that are designated for various training purposes, ranging from light dismounted infantry and mechanized forces to munitions detonation and use of heavy (tracked) and wheeled vehicles (Dale et al. 2002; Maloney et al. 2005). An unarmed M-1 Abrams tank weighs approximately 58 metric tons and applies roughly 9,200 kg-m⁻² of standing ground pressure (Fuchs et al. 2003). The constant skidding and turning of training vehicles can uproot and crush vegetation, causing exposure of surface soils to erosion. The results of this type of military training for an extended period in a designated area include loss of vegetative cover; collapsed pore structure of the soil, which reduces infiltration and increases runoff, leading to episodic erosional events; siltation of adjoining river bodies; and decrease in wildlife habitat (Anderson et al. 2005; Retta et al. 2014). The increased overland flow increases the hydrologic response to storm events and induces erosion of downslope surfaces and incision of the stream corridor, including the streambanks (Curtis 1978; Phillips and Walls 2004; Fox 2009).

Training areas at Fort Knox have experienced extensive activity for more than 40 years, with soil being deposited into the ephemeral stream networks and ultimately being transported into Otter Creek, which empties into the Ohio River. The Environmental

Management Division (EMD) of Fort Knox follows the Army's Sustainable Range Program (SRP) Army Regulation 350-19, which defines the responsibilities and policies for maintaining Army-controlled lands (Crim et al. 2011). The training areas are no longer being used for tracked-vehicle training but are still utilized for other types of military readiness activities. The EMD has been actively attempting to restore heavily eroded lands by the planting of native vegetation, installing erosion barriers in areas where gully erosion is prevalent and working with Range Control on rotating training activities. While much is being done to stop or slow erosion, there are still large swaths of exposed land (Figure 2.1).

2.2 *Study Area*

2.2.1 *Land Use / Land Cover and Geologic Setting*

The study area is bounded by Fort Knox cantonment area to the east, civilian farmland to the south and west, and the Ohio River to the north (Figure 2.2). Hardin County is located on the southern border of Fort Knox and consists of agricultural land with little development other than small clusters of residential structures and the City of Vine Grove. Fort Knox extends west into Meade County, which consists of mostly agricultural land with a scattering of residences. The Otter Creek Recreational Park, owned by the City of Louisville, consists of 982 hectares of land and is located on the northwestern edge of Fort Knox downstream of the study area (Rawson 2008). Land cover percentages in the study area were calculated using ESRI ArcMAP[®] v.10.7 with GIS data obtained from the U.S. Department of Agriculture and the Web Soil Survey Natural Resources Conservation Service (NRCS; Figure 2.3). Civilian land cover is composed of 30% forest, 57% cropland, 12% developed and 1% other. Some agricultural lands have shown deep erosional gullies and rills, which are associated with the high-impact traffic of farm animals (Figure 2.4). Military

land cover is composed of 64% forest, 24% developed, and 12% other, with no cropland.

The study area overlaps two physiographic regions, Muldraugh Hill and the Pennyroyal Plateau (Figure 2.5), which are characterized by well-developed karst, low relief and extensive agriculture with sinkholes, ponds, springs, sinkhole wetlands, subterranean drainage, and dry valleys (Sprandel 1999). The eastern Pennyroyal Plateau is underlain by gently dipping Mississippian sedimentary rocks, largely limestones and shales of the Meramec Group (Hill 1981; Rawson 2008; Kentucky Geological Survey [KGS] n.d.). Within the study area (Figure 2.6), a linear sand body that is part of the Mooretown Formation runs southwest–northeast, clipping the northwestern corner of the Fort Knox cantonment area. The Muldraugh Hill upper part consists of Mississippian siltstone, dolomite and limestone and the lower part consists mostly of shale (KGS n.d.). Extensive karst topography is developed on the St. Louis Limestone and Ste. Genevieve Limestone, which have a combined total thickness of more than 53 m and underlie most of the study area in Hardin and Meade counties (Rawson 2008; KGS n.d.). Fort Knox’s tracked vehicle training areas (TAs) in Meade County contain karst uplands with more than 20 sinkholes in each TA, as well as steep hills and flood plains, from just upslope of the armored vehicle TA downstream to the confluence with the Ohio River (Crim et al. 2011).

Otter Creek originates from a karst spring within a forest in Hardin County and flows north through rural residential and agricultural areas before entering Fort Knox (Figure 2.2). The stream at baseflow conditions disappears into a karst conduit, reappearing ~ 1.6 km downstream emerging out of fractured bedrock (Figure 2.7). The extensive karst drainage network within the study area (Figure 2.6) can contribute to the storage of target sediment, especially during baseflow conditions when discharge is low. Following intense rainfalls,

sediment is transported through the karst groundwater basins within the catchment because of enhanced permeability within conduits.

2.2.2. Soils and Vegetation

Soils found in Hardin and Meade counties (Figure 2.8) consist mostly of Alfisols, a taxonomic soil order that is clay-enriched and forms in semi-arid to humid environments (NRCS 2019). The Kentucky Soil Atlas (Karathanasis 2018) and the U.S. Department of Agriculture Web Soil Survey describe the soil units in the area as Baxter, Bedford, Caneyville, Crider, Fredonia, Hammack, Nolin, Pembroke and Vertrees, which are formed in a variety of residuum of limestones. Baxter and Hammack soils have slopes ranging from 2 to 40%. Baxter soils are found along hillsides and ridge tops and areas that have karst topography. Hammack soils are formed in a 50- to 100-cm loess mantle underlain by cherty limestone. Both the Baxter and Hammack soils can be found on ridgetops and sideslopes of rolling to hilly areas. Bedford and Crider soils have 0 to 12% slopes; Bedford soils are moderately well drained with a fragipan and Crider soils form in a thin silty mantle over fine-textured residuum of limestone. Bedford soils are on summits, shoulders and to a lesser extent backslopes of hills, while Crider soils are on nearly level to moderately steep upland areas. Fredonia and Vertrees soils have slopes ranging from 2 to 30%. Fredonia soils are formed in residuum from massive gray limestone and found mostly on rolling uplands. Vertrees soils are formed in residuum of limestone interbedded with siltstone and shale and are found in a range of areas from gently sloping hills to steep ridges and in most karst areas. The Nolin soils are formed in alluvium derived from limestone, sandstone, siltstone, shale and loess, and are found in floodplains, concave depressions or on natural levees of major streams and rivers, with slopes ranging from 0 to 25%. Pembroke soils formed in thin silty

mantle and are underlain by older alluvium or limestone residuum or both, with slopes ranging from 0 to 12%.

Data obtained from the Web Soil Survey (NRCS 2019) were integrated into ArcMap to generate maps depicting percent sand, silt and clay for the study area (Figures 2.9, 2.10 and 2.11, respectively). The study area is relatively low in sand (under 10%), with larger contributions seen mostly along the southwest-northeast sand wedge referenced earlier, which is part of the Mooretown Formation. The southern portion of the study area and the very tip near the confluence with the Ohio River have some areas with 20 to 40% sand. The majority of soils in the study area are dominated by silt (within the 62-80% range), while clay percentages are mostly between 16 to 25%.

The study area lies within the Mitchell Plain (Level IV-71b) ecoregion (Figure 2.12). This region is dominated by several species of hardwood trees, native shrubs, herbaceous flowering plants, warm season grasses and non-native tall fescue (Cranfill 1991; White and Palmer-Ball 1994; Schoonover et al. 2015). The composition and diversity of the forested areas are similar to the mesophytic forests described by Braun (1950) and Homoya et al. (1985) in southern Indiana and Ohio, specifically those found in lower sloped areas (Cranfill 1991).

2.3 *Background*

2.3.1 *Sediment Transport in Karst Terrain*

In the conterminous United States, karst terrain makes up nearly 15% of the land surface (Figure 2.2) (Davies and LeGrand 1972; Peterson and Wicks 2003). Karst systems add complexity when trying to apportion target suspended sediment to source soil groups. Karst networks are made up of soluble carbonate rock that features a fractured network of

openings that range from only a few centimeters to meters in size (Gale 1984; Peterson and Wick 2003). During high discharge (stormflow) events, water can transport sediment and other nonpoint source pollutants. Calculations have shown that the transport of suspended sediment can occur in fracture openings as small as 1 cm (White 1998; Vesper and White 2003). Ryan and Meiman (1996) tracked discharge events at Big Spring in Mammoth Cave National Park, Kentucky, and observed that there was a distinct lag in time between high-rainfall events and when Big Spring received the recharge waters. They noted that agricultural subcatchments were slower at delivering recharge water than forested subcatchments (Ryan and Meiman 1996).

Dogwiler and Wicks (2004) researched the sediment transport threshold for two karst systems, the Devils Icebox in central Missouri and Carter Caves in northeastern Kentucky, both of which are similar to Otter Creek, Kentucky. Both sites are considered to have mild winters and warm summers, a Cfa designation within the Köppen climate classification system (Lutgens and Tarbuck, 1995; Kottek et al. 2006). For both locations, precipitation is lowest in January and February; for central Missouri the maximum amount of precipitation is experienced in May and June, while in northeastern Kentucky it is seen in July (Dogwiler and Wicks 2004). In analyzing various precipitation and stage conditions in several reaches throughout both systems, it was noted that the overall transport rate of particles was low under baseflow conditions. When precipitation frequency and stage were high and bankfull (stormflow) conditions were attained, the stream's ability to transport its substrate increased. The basal shear stresses at bankfull conditions were sufficient to transport most particles (Dogwiler and Wicks 2004).

2.3.2 *Sediment Fingerprinting*

Classification of potential sediment sources within a watershed can be defined in terms of their spatial distribution (e.g., parts of the watershed underlain by different rock types or soil types), but in most situations, emphasis is placed on distinguishing what are commonly referred to as source types (Gellis and Walling 2011) and classification is performed *a priori* to align source soils with land use patterns and land management goals (Peart and Walling 1986; Walling and Woodward 1995; Collins et al. 1997; Owens et al. 1999; Porto et al. 2005; Collins et al. 2010a,b,c,d; Smith and Blake 2014; Lamba and Thompson 2015; Foucher et al. 2015; Collins et al. 2017). Source type classification can involve a simple distinction between sediment mobilized from areas located upslope (where source sediment comes from sheet and rill erosion) and from channel bank erosion. In many cases this classification is extended to include different land uses (e.g. cultivation, pasture, and forest), whereas channel erosion could be subdivided to include gully erosion, ditches, channel beds, tributaries, different stream orders and the main channel system, in addition to specific sources such as unpaved roads, construction area and mass movements (Nelson and Booth 2002; Gruszowski et al. 2003; Motha et al. 2003; Gellis and Walling 2011).

The sediment fingerprinting approach is based on characterizing each of the potential sediment sources within a watershed by composite fingerprints (tracers), defined by a number of physical (color and grain size), geochemical (clay mineralogy, geochemistry of source material, fallout and cosmogenic radionuclides, isotopes and trace and heavy metals) and/or biological properties (soil enzymes and pollen) of the source materials, and comparing the fingerprints of sampled suspended or bed sediment (target sediment) with the fingerprints of the potential sources. Using a statistical unmixing model, it is possible to estimate the relative contributions from different source types (Collins et al. 2010a;

Haddadchi et al. 2013; Gellis et al. 2014). Sediment fingerprinting assumes that the characteristics of the collected sediment samples directly reflect those of the source soils. This assumption is simplistic in part because the physical and biogeochemical properties of sediment can be altered from source to sink.

The steps required to apportion target sediment to characterize the types and locations of source soils can be quite involved and labor-intensive. The U.S. Geological Survey (USGS) created a Sediment Source Assessment Tool (Sed_SAT), which was written in the computational statistical software R (R Core Team 2016). It utilizes Microsoft Access[®] as a user-friendly platform (Gorman et al. 2017) and is available to the public for download and use (https://code.usgs.gov/water/sed_sat). Statistical computations performed in R allow Sed_SAT the ability to identify outliers, correct for differences in size and organic content of source samples relative to target samples, evaluate the conservative behavior of tracers used in fingerprinting by applying a “bracket test,” identify tracers with the highest discriminatory power, and provide a robust error analysis through a Monte Carlo simulation following the unmixing model (Gorman et al. 2017). The program allows the user the freedom to make changes in parameters, determine the fate of outliers, and decide how many iterations the Monte Carlo simulation performs. Several peer-reviewed studies have utilized Sed_SAT in apportioning sediment contributions to source soils (Cashman et al. 2018; Gellis and Gorman Sanisaca 2018; Patault 2019; Gellis et al. 2019; Russ et al. 2020).

2.4 Materials and Methods

2.4.1 Source Soil Samples

For the purpose of this study, source group classifications were done using aerial photography, visual geomorphic assessments and land use/land cover (LU/LC) data obtained

from the NRCS Soil Web Survey. Soil samples from five different source soil areas were collected from military training lands and adjoining rural residential and agricultural civilian lands for fingerprinting (Figure 2.13). The source soil categories identified were: 1) C-RB, civilian land; 2) M-RB, military land; 3) M-FS, military forest; 4) M-AE, military average erosion; and 5) M-XE, military extreme erosion. A total of 86 samples were collected but only 42 of these were analyzed. Source soils were collected by excavating soil from the top 5 cm, omitting the root mat if it was present and placing the samples in labeled zipper-lock bags, then storing them in a cooler until they reached the laboratory (Fox and Papanicolaou 2007).

In August 2016, C-RB soil samples (n = 20 collected, n = 11 analyzed) were collected starting from the headwaters of Otter Creek to where the creek enters the Fort Knox boundary. All but two samples were collected near rural residential or agricultural fields that showed visible signs of erosion, samples were taken 6–10 m from the creek to ensure they were not classified as bank samples. Because gaining access to civilian lands was more problematic than originally anticipated, the majority of samples had to be taken in areas where there was public access and source soils for civilian samples were grouped into one category.

Access to training lands that were actively being used near Otter Creek was granted for 2 days in August 2016 to collect source soil samples. Prior to sampling, visual inspection using Google Earth[®] and soil information from the NRCS Web Soil Survey website were used to devise a plan to maximize sampling time. Given the relatively homogeneous geology of the study area, creating the source soil groups based on geology was not practical, so soil groups were aligned with LU/LC patterns. Military land (M-RB) samples (n = 12 collected, n

= 5 analyzed) were collected in areas where scrub and grasses were plentiful with no visible soil, and any samples near the creek were at least 6–10 m from the edge to ensure they were not considered bank samples. Military forest (M-FS) samples (n = 12 collected, n = 5 analyzed) were taken in areas where tree canopy was present overhead and there was evidence of two tracks from vehicles moving through the forested areas for training. Military average erosion (M-AE) samples (n = 12 collected, n = 6 analyzed) were taken in areas where vegetation was present but thinning and soil was easily visible. Military extreme erosion (M-XE) samples (n = 30 collected, n = 15 analyzed) were taken from areas where little to no vegetation was present and extensive erosion was seen in well-developed rills and gullies. There were nearly double the M-XE samples taken given the extensive areas of erosion and ease of access.

2.4.2 *Stream Sediment Samples*

Sediment sampling locations (Figure 2.2) were selected to determine if there were any differences between the chemical signatures of civilian and military land-use contributions. Site 1, located where Otter Creek enters Fort Knox (37.862986° N, 86.004338° W), predominantly drains rural agricultural croplands (54.8%), forest (33.1%), developed lands (City of Vine Grove, roadways and a small portion of Fort Knox; 11.8%) and small patches of emergent wetlands (0.3%) (Table 2.1). The second sampling site was 0.2 km upstream from a small abandoned pump house with attached overflow structure located on Fort Knox (37.895191° N, 86.024041° W). The site 2 subcatchment drains mostly cropland (45.9%), forest (36.4%), developed areas that include Fort Knox and some roadways (16.5%) and wetlands (1.2%). The third sampling site was located where the creek leaves Fort Knox and enters Otter Creek Park (37.922364° N, 86.030081° W). Site 3 is

located within predominantly military training lands with minimal civilian areas present. The area is mostly forested (74.5%) with small areas of cropland (5.3%) and developed areas (8.3%) and a slightly higher percentage of wetlands (11.8%).

Time-integrated samplers (Figure 2.14) collecting fine-grained suspended sediment ($< 62.5 \mu\text{m}$; Phillips et al. 2000) were deployed at the three sites mentioned above. These traps have become standard for sediment tracer studies (Walling and Amos 1999; Phillips et al. 2000; Russell et al. 2001; Gruszowski et al. 2003; Fox 2005; Walling et al. 2006; Fox and Papanicolaou 2007; Fox 2009). Samplers were set into Otter Creek on 25 September 2015; the first set of samples was taken on 4 October 2015 and sampling continued every Friday until 14 October 2016. To provide consistency and sufficient sample mass (Gruszowski et al., 2003; Fox 2005), two sediment samplers (Figure 2.15) were deployed at each of the three sample locations. There were weeks when sediment samples were not collected due to weather, vehicle/equipment issues and/or inability to access field sites. The number of sediment samples not collected was 10 at site 1, 11 at site 2, and 10 at site 3 (Appendix 2.1, 2.2, and 2.3, respectively). During weeks when stream flow was too high to retrieve the sediment samplers, samples were taken using two clean 5-gallon (18-liter) buckets. Separately, the handle of each bucket was tied to ~ 8 meters of rope and the bucket was tossed into the middle of the stream near the center of flow and pulled in, capturing suspended sediment ($n = 6$). Stormflow samples ($n = 11$) were operationally classified as those collected after water levels had retreated following a precipitation event with ≥ 3.0 cm of rain within a 72-hour period sometime in the preceding week.

2.4.3 *Tracer Analysis*

Following Fox and Martin (2015), stream sediment samples were centrifuged with a high-volume rotor to concentrate the sediments, wet-sieved to retain the < 62.5- μm fraction, then freeze-dried and ground. The objective of sieving both source and sediment samples to < 62.5 μm is to ensure that the grain size distribution of the source material is similar to that of the sediment samples (Poulenard et al. 2009; Laceby et al. 2017) and represents the material that is transported as suspended sediment.

Total organic carbon in sediment and source soil samples was analyzed at the KGS. For total carbon, samples were dry-combusted under pure O_2 at approximately 1350°C in a LECO[®] SC-144DR instrument with an infrared detection method (LECO 2008). A UIC[®] CM5014 CO_2 coulometer was used to quantify inorganic carbon with a 99.95% CaCO_3 standard. Samples were placed into a hot block and slowly mixed with 5 mL of 10% phosphoric acid. CO_2 gas was quantitatively absorbed and reacted with ethanol amine solution (UIC 2017). Organic carbon values were determined by subtracting inorganic carbon from total carbon.

Target sediment and source soils were analyzed for trace elements using a Bruker[®] Tracer IV-SD X-ray fluorescence spectrometer, a non-destructive analysis which was performed on all source soils and sediments. Major elements include Na, Mg, Al, Si, P, S, K, Ca, Ti, Mn and Fe. Minor elements include V, Cr, Co, Ni, Cu, Zn, As, Rb, Sr, Y, Zr, Nb, Mo, Pb, Ba, Th and U. Although a large number of major and trace elements are available through this analysis, only Cu, Zn, Sr, Rb, Co, Ni, Al, Na, Mg, Si, P, K, Ca, Mn and Fe had detectable concentrations.

Prepared samples were placed into SpectroCertified XRF sample cups, filled two-thirds full and covered with a Mylar polyester film. The X-ray tube generates photons with enough energy to interact with the innermost electrons of an atom; the Tracer's detector can then identify the elements using Bruker's pre-programmed standard library (Bruker 2015). Major elements are lighter and were analyzed first using the vacuum pump with a set measurement duration time of 60 seconds, voltage setting of 40 kV and an anode current of 15 μ A. The vacuum removes the air between the samples and the device, allowing the maximum number of X-rays to be detected, thereby reducing detection limits (Bruker n.d.). Minor elements were measured without the vacuum pump with a maximum duration time of 60 seconds, voltage setting of 40 kV and an anode current of 35 μ A.

2.4.4 *Isotopic Analysis*

Carbon and nitrogen isotope analysis were performed on source soil and target sediment samples at the University of Kentucky's Stable Isotope Geochemistry Laboratory (KSIIGL) on a coupled elemental analyzer-isotope ratio mass spectrometer (IRMS) system. Samples were ground in a mortar and pestle to a powder and weighed into tin capsules where, following the U.C. Santa Cruz method for removal of inorganic carbon, samples were repeatedly acidified with 6% sulfurous acid (H_2SO_3) to remove carbonate material (Verado et al. 1990). After all traces of inorganic carbon were removed, which was signified by a reaction no longer taking place upon the addition of H_2SO_3 , samples were analyzed following methodology outlined by Coplen et al. (2006).

Isotopic results are reported in per mil (‰) relative to the Vienna Pee Dee Belemnite (V-PDB) standard for $\delta^{13}\text{C}$ and relative to air for $\delta^{15}\text{N}$. The isotopic signature is expressed in delta (δ) notation to indicate the differences between the isotopic ratio of the sample and

standards

as

$$\delta X (\text{‰}) = \left(\frac{R_{\text{sample}}}{R_{\text{standard}}} - 1 \right) \times 10^3$$

where X is ^{13}C or ^{15}N , R_{sample} is the isotope ratio ($^{13}\text{C}/^{12}\text{C}$ or $^{15}\text{N}/^{14}\text{N}$) of the sample and R_{standard} is the isotope ratio of the standard (Fox 2009).

2.4.5 Grain Size Analysis

Selected source soil samples (C-RB n = 12; M-RB n = 4; M-FS n = 4; M-AE n = 5; M-XE n = 4) were disaggregated and passed through a number 10 (2-mm) mesh sieve and dispersed overnight in a 4% sodium hexametaphosphate solution. Each dispersed sample was rinsed three times with deionized water and dried at 50°C overnight in aluminum pans. Sieve analysis was performed to determine the proportion of sand, silt and clay. Dried soil samples were placed on a shaker for 15 minutes and passed through stacked sieves (numbers 35 [0.5 mm], 60 [0.25 mm], 120 [0.125 mm], 140 [0.105 mm], 170 [0.088 mm] and 230 [0.0625 mm]). After shaking, each sieve was weighed to determine soil mass, which was plotted on a ternary diagram for sand, silt and clay percentages.

Selected sediment samples (n = 12) were placed in 50-mL plastic test tubes and a 30% hydrogen peroxide solution was continually added until all organic material was removed. Samples were rinsed three times in deionized water and dispersed in a 4% sodium hexametaphosphate solution overnight, then rinsed three times again in deionized water, placed in an aluminum tray and dried overnight at 50°C. Samples were sieved to retain the < 62- μm fraction and left in an aqueous solution for analysis in a Micrometrics SediGraph 5100 instrument. Analyses are based on Stokes' Law, which describes the force necessary to move a sphere through a given viscous fluid at a uniform velocity (Gibbs et al. 1971). Not all

sediment samples were analyzed but a representative amount from each month throughout the study period was chosen.

2.4.6 *Statistical Analysis and Modeling*

For this research, mean (\pm standard deviation) and median (standard error [SE]) are both used, depending on the nature of the analysis being performed, for the purpose of incorporating all the data and for representing the middle value in the result distribution. The differences in tracer concentrations between source soil groups, sediment sites and flow conditions reflect the geochemical and physical processes that take place. Using SigmaPlot v14.0 (Systat Software), a rank-based, nonparametric Kruskal-Wallis one-way ANOVA test ($p < 0.05$) was performed to assess the capability for individual tracers to identify and differentiate characteristics of civilian and military source soils to Otter Creek. A Shapiro-Wilks test was performed on all source soils and target sediment to detect all departures from normality, $p < 0.05$. The test for normality is vital and should be the first step performed after basic descriptive statistics, as many statistical analyses (e.g., correlation, regression, t-tests and analysis of variance) are based on the assumption of a normal distribution (Royston 1991; Altman and Bland 1995; Driscoll et al. 2000; Oztuna et al. 2006; Pallant 2007; Field 2009; Ghasemi and Zahediasl 2012). Principal component analysis (PCA) was performed using Excel (Microsoft Office 16) and SigmaPlot v14.0 on both source soils and target sediment datasets in an effort to reduce the dimensionality and assist in identifying the specific tracers that demonstrate the strongest influence on source discrimination, $p > 0.4$.

Sed_SAT executed necessary statistical steps regarding tracer discrimination and assignment of target sediment contributions to source soil groups. During transport and sample collection, target sediment must remain conservative from where it was eroded

(Gellis and Walling 2011). Because organic matter can influence tracer concentrations (Horowitz and Elrick 1987; Miller et al. 2015; Gellis and Gorman Sanisaca 2018), if there is a significant regression between TOC and the tracer's concentration (Collins et al. 2010a; Gellis and Noe 2013; Gellis and Gorman Sanisaca 2018), a correction needs to be applied in order to make the data comparable. If a relationship between TOC and tracer concentration is established, then each source soil tracer concentration is compared to the target sediment samples and corrected according to rules established by Gellis et al. (2016). Any source soil sample that had a tracer value greater or less than three times the standard deviation plus or minus the mean of that source group was removed. Because the outlier test requires that the univariate tracer concentration data are normally distributed, each source group is tested for normality using a Shapiro-Wilks test ($p < 0.05$) (Gellis and Gorman Sanisaca 2018).

Once Sed_SAT performed any necessary corrections on the data, a bracket test was done on each target sediment sample to test the tracer's ability to remain conservative. Each tracer must be within the source soil samples' tracer concentrations ($> 10\%$ of the minimum and $< 10\%$ of the maximum tracer concentration [Gorman Sanisaca et al. 2017]). A forward step-wise discriminate function analysis (DFA) is then performed on the conservative tracers to discern the ideal set of tracers needed to discriminate between target sediment and source soil samples. The default significance is 0.01. Tracer selection begins with the tracer that yields the greatest separation between source soil groups, then tracers are added using the Wilks' lambda criteria until there are no more significant tracers (Mardia et al. 1979; Gellis and Gorman Sanisaca 2018).

2.5 Results

2.5.1 Particle Size, Sediment Yields and Tracer Statistics

The ternary grain-size diagram (Figure 2.16) shows that clay and silt are predominant in all source soils. Source soil group C-RB had the highest mean percentage of sand (26.3%) and the lowest mean percentage of clay (35.6%) in comparison to the other four source soil groups. M-RB source soils had somewhat less sand (mean 19.1%) and somewhat more clay (mean 44.8%) than C-RB. In comparison to M-RB, source soil group M-FS had half as much sand (mean 9.6%) but more clay (mean 57.9%). M-AE source soils had less sand (mean 5.8%) than M-FS and the highest percentage of clay (mean 63.0%) of the source-soil groups. Source soil group M-XE had the smallest percentage of sand (mean 3.5%) and the percentage of clay (mean 58.7%) was similar to that of M-FS. Grain-size analysis for sediment samples (Figure 2.17) showed very little variation because the sediment traps collected only suspended load through a 4-mm opening.

The total amount of sediment collected during the study period was 2,760.22 g, of which 901.34 g was collected from site 1, 799.03 g was collected from site 2, and 1,059.85 g was collected from site 3. Sediment yield averaged 7.5 g/km² for the subcatchment upstream of site 1 (120.6 km²), 12.0 g/km² for the subcatchment between sites 1 and 2 (66.8 km²) and 67.0 g/km² for the subcatchment between sites 2 and 3 (15.8 km²).

Tables displaying all descriptive statistical values (minimum, maximum, mean, median, standard deviation and standard error) can be found in Appendix 2.4 for source soils and in Appendix 2.5 for target sediment. Box and whisker plots were generated with median quartile and 10th–90th percentile error bars showing all identified outliers for source soil groups and target sediment sites. Median values and outliers are shown for TOC, $\delta^{13}\text{C}$, Zn, Sr, Rb and Co on Figure 2.18; for Ni, Al, Na, Mg, Si and P on Figure 2.19; and for K, Ca,

Mn, Fe and Cu on Figure 2.20. Zn and Sr had the highest concentrations among trace elements in baseflow sediments. Zn concentrations were higher at sites 1 and 2 (134.41 and 135.76 ppm, respectively) than at site 3 (107.29 ppm), while Sr increased downstream from 91.06 to 101.36 to 155.91 ppm. A Pearson correlation showed a positive relationship for Zn between sites 1 and 3 ($p = 0.006$) and a positive relationship for Sr between sites 1 and 2 ($p = 0.001$) and sites 1 and 3 ($p = 0.005$; Table 2.2). No other elements show distinct differences between sampling locations during either baseflow or stormflow.

Figure 2.21 shows median concentration values for TOC and $\delta^{13}\text{C}$ between source soil groups, target sediments by site, and base- and stormflow sediments. Tables 2.3 and 2.4 provide basic statistics. Source soil groups M-RB, C-RB and M-AE were similar with respect to TOC concentrations (0.93%, 0.69% and 0.74%, respectively), while M-FS and M-XE source soil groups had the lowest concentrations (0.36% and 0.17%, respectively). TOC for source soils C-RB and M-XE and for M-FS and M-XE were positively correlated with each other ($p = 0.046$ and 0.005 , respectively; Table 2.5) indicating the variables that share similar tendencies to change. For source soil groups, $\delta^{13}\text{C}$ values ranged from -26.99‰ for M-RB to -24.37‰ for M-FS, but there was no statistically significant correlation between source soil groups for $\delta^{13}\text{C}$ (Table 2.5). Figure 2.22 shows $\delta^{13}\text{C}$ values for source soils mapped relative to LU/LC classifications. Median concentrations for TOC in sediment decreased downstream from 2.84% at site 1 to 2.55% at site 2 and 2.33% at site 3. However, $\delta^{13}\text{C}$ values were close, with site 3 being slightly more depleted (-27.48‰) than sites 2 (-27.35‰) and 1 (-27.39‰). There was no statistically significant correlation between sediment sampling sites for TOC or $\delta^{13}\text{C}$ (Table 2.6). Median baseflow TOC values (2.95%, site 1; 2.56%, site 2; 2.29%, site 3) were greater than median stormflow values (2.26%, site 1;

1.31‰, site 2; 1.93‰, site 3), while median baseflow $\delta^{13}\text{C}$ values (-27.42‰, site 1; -27.35‰, site 2; -27.63‰, site 3) were more depleted than median stormflow values (-26.87‰, site 1; -27.00‰, site 2; -27.02‰, site 3). As with all sediments combined, there was not statistically significant correlation between the sediment sampling sites at base- or stormflow for TOC or $\delta^{13}\text{C}$ (Table 2.6).

Out of 42 source soil samples, only 15 samples contained enough ^{15}N to be detectable during analysis (C-RB n = 5, M-RB n = 4, M-FS n = 3, and M-AE n = 3). None of the M-XE samples had sufficient ^{15}N . As shown on Figure 2.23, C-RB samples typically had higher $\delta^{15}\text{N}$ (3.45 to 4.77‰) than military samples (M-FS 0.41 to 3.41‰, M-AE 0.79 to 5.11‰, and M-RB -0.13 to 4.31‰).

2.5.2 *Principal Component Analysis*

Results of PCA (Table 2.7, Figure 2.24) for all source soils combined showed that the proportion of variation for the first factor loading (PC1) was 48.8%. Out of 17 tracer elements, 14 demonstrated strong correlations: 5 positive (Na, Mg, Si, P and Mn) and 9 negative (Cu, Zn, Sr, Rb, Co, Ni, Al, K and Fe). The second factor loading (PC2) for all source soils showed the proportion of variation to be 17.2%, with 2 positive correlations (Na and Mg) and 4 negative correlations (Sr, P, Ca and $\delta^{13}\text{C}$). The PCA analysis for all sediments (Table 2.7; Figure 2.24) showed the proportion of variation for the first factor loading to be 37.9%. Ten of 17 elements demonstrated strong correlations: one positive (Si) and nine negative (TOC, Cu, Zn, Rb, Co, Ni, Al, Mn and Fe). The proportion of variation for the second factor loading for target sediment was 20.5% with 3 positive correlations (Na, Mg and Si) and 2 negative correlations (Sr and Ca). The first principal component for both soils and sediment depicts factors with a stronger negative correlation (Cu, Zn, Rb, Co, Ni, Al and

Fe), which can be observed in the clustering of samples on the plot of PC2 versus PC1. Soil and sediment in PC1 only share one positive correlation (Si); the remaining positive correlations are seen in PC2 (Na and Mg).

Considering the five source soil categories (Table 2.8; Figure 2.25), the proportion of variation for the first factor loading for source soil group C-RB was 55.8%, with 9 positive correlations (Cu, Zn, Sr, Rb, Co, Ni, Al, K and Fe) and 4 negative correlations (Na, Mg, Si and P). The proportion of variation for the second factor loading was 15.0%, with only one positive correlation (Ca) and 3 negative correlations (TOC, K and Mn). For M-RB, the proportion of variation for the first factor loading was 51.2%, with 10 positive correlations (TOC, Cu, Zn, Sr, Rb, Co, Ni, Al, K and Fe) and 5 negative correlations (Na, Mg, Si, Ca and $\delta^{13}\text{C}$). The proportion of variation for the second factor loading was 30.0%, with 7 positive correlations (Zn, Ni, Al, Na, Mg, Fe and $\delta^{13}\text{C}$) and 4 negative correlations (TOC, Si, K and Mn). For M-FS, the proportion of variation for the first factor loading was 54.5%, with 9 positive correlations (Cu, Zn, Rb, Co, Ni, Al, Na, Mg, and Fe) and 5 negative correlations (TOC, Sr, P, Ca and $\delta^{13}\text{C}$). The proportion of variation for the second factor loading was 28.5%, with 6 positive correlations (Zn, Sr, Ni, Ca, Fe and $\delta^{13}\text{C}$) and 5 negative correlations (TOC, Na, Mg, Si and Mn). For M-AE, the proportion of variation for the first factor loading was 64.3%, with 9 positive correlations (Zn, Sr, Rb, Co, Ni, Al, K, Fe and $\delta^{13}\text{C}$) and 7 negative correlations (TOC, Na, Mg, Si, P, Ca and Mn). The proportion of variation for the second factor loading was 17.2%, with 6 positive correlations (Cu, Zn, Ni, Na, Mg and Mn) and one negative correlation (Sr). For M-XE, the proportion of variation for the first factor loading was 51.9%, with 9 positive correlations (Cu, Zn, Rb, Co, Ni, Al, K, Ca and Fe) and 5 negative correlations (Na, Mg, Si, P and Mn). The proportion of variation for the second

factor loading was 19.7%, with 5 positive correlations (TOC, Sr, Si, P and Mn) and 3 negative correlations (Al, Na and Mg).

For all five source soil groups, the proportion of variation was relatively close (51.2–64.3%) and each group shared a similar geochemical make-up. All five source soil groups shared a positive correlation in their first principal component with tracers Zn, Rb, Co, Ni and Al, while C-RB, M-AE and M-XE shared a negative correlation with tracers Na, Mg, Si and P.

For the first target sediment sampling location, site 1 (Table 2.9; Figure 2.26), the proportion of variation for the first factor loading was 47.3%, with 11 positive correlations (TOC, Cu, Zn, Sr, Rb, Co, Ni, Al, K, Mn and Fe) and 3 negative correlations (Na, Mg and Si). The proportion of variation for the second factor loading was 21.0%, with 4 positive correlations (Al, Si, K and $\delta^{13}\text{C}$) and 3 negative correlations (Sr, Ca and Mn). For site 2, the proportion of variation for the first factor loading was 49.4%, with 11 positive correlations (TOC, Cu, Zn, Sr, Rb, Co, Ni, Al, P, Ca, Mn and Fe) and 3 negative correlations (Na, Mg and Si). The proportion of variation for the second factor loading was 15.7% with 5 positive correlations (Rb, Co, Al, Si and $\delta^{13}\text{C}$) and 3 negative correlations (TOC, Sr and Ca). For site 3, the proportion of variation for the first factor loading was 47.5%, with 10 positive correlations (Cu, Zn, Rb, Co, Ni, Al, Na, K, Mn and Fe) and 3 negative correlations (Sr, P and Ca). The proportion of variation for the second factor loading was 26.7%, with 5 positive correlations (TOC, Zn, Sr, P and Ca) and 4 negative correlations (Na, Mg, Si and $\delta^{13}\text{C}$). All three sediment sampling sites had similar proportions of variation in PC1 (47.3–49.4%) and shared a positive correlation with tracers Cu, Zn, Rb, Co, Ni, Al, Mn and Fe.

2.5.3 *Apportionment of Source Soils to Sediment Samples*

The Shapiro-Wilks test (Table 2.10) performed using SigmaPlot and by Sed_SAT both identified the same tracers as deviating from normality except for Cu, Ni and Na, which were identified by SigmaPlot. Based on DFA, Sed_SAT found that the optimal tracers to use in the unmixing model are Cu, Zn, Co, Ni, Al and Mg; other tracers were considered to be nonconservative and eliminated from further consideration. Target sediment samples (n = 108) and source soil samples (n = 42) were input through Sed_SAT's unmixing model to apportion percent contributions to the five source soil groups. The full results of Sed_SAT's fingerprinting for each source soil group, with averaged percentages for each source soil group and percent error, can be found in Appendix 2.1 for site 1, Appendix 2.2 for site 2, and Appendix 2.3 for site 3.

Sediment fingerprinting results from the unmixing model showed that source soil samples varied between target sediment samples. There was a distinction between contributions of target sediment collected and apportioned between base- and stormflow events. Out of all sediment collected during the study period, 646.2g (23.4%) of the annual was collected during baseflow total 2114.0g (76.6%) was collected during stormflow. During baseflow (Table 2.11; Figure 2.27), 22.2% (199.7 g) of the sediment at site 1 was collected. Sed_SAT apportioned this sediment primarily to M-RB (36.3%), followed by M-XE (32.0%), M-FS (23.5%), C-RB (7.0%), and M-AE (1.3%). At site 2, 25.9% (206.6 g) of sediment for the study period was collected at baseflow. Sed_SAT apportioned this sediment to M-XE (32.8%), M-AE (30.3%), M-FS (17.0%), C-RB (10.4%), and M-RB (9.5%). At site 3, 22.6% (239.9 g) of sediment was collected during baseflow. Sed_SAT apportioned this sediment to M-FS (30.5%), M-AE (28.3%), M-XE (26.1%), M-RB (7.7%) and C-RB (7.4%).

As expected, most sediment was collected during stormflow events. At site 1 (Table 2.11; Figure 2.28), stormflow samples represented 76.6% (701.6 g) of sediment collected, which Sed-SAT apportioned to M-AE (43.4%), M-FS (31.2%), M-XE (25.4%), M-RB (0.02%) and C-RB (0.0%). At site 2, stormflow samples represented 74.1% (592.4g) of total sediment, which was apportioned to M-AE (44.7%), M-XE (33.0%), M-FS (22.3%), M-RB (0.0%) and C-RB (0.0%). Lastly, at site 3, 77.4% (820.0 g) of sediment was collected during stormflow, which was apportioned to M-AE (31.0%), M-XE (19.7%), M-FS (19.2%), C-RB (16.3%), and M-RB (13.9%).

Seasonal differences in contributions of source soils to sediment at various sites were also evident. For the purposes of data analysis and discussion, the dataset was broken into summer (March through September) and winter (October through February) (Table 2.12). During summer, the amount of sediment collected (1,940.16 g; 70.3% of the annual total) was disproportionate relative to the amount of precipitation during the period (51.5% of the annual total). At site 1, 73.0% (658.16 g) of the sediment was collected during summer. This sediment was apportioned primarily to M-XE (34.0%), then to M-AE (29.6%), M-FS (27.2%), C-RB (7.65%), and M-RB (1.60%). At site 2, 70.7% (564.72 g) of the sediment was collected during summer, and the dominant source soil group was M-XE (31.3%), followed by M-AE (28.9%), M-FS (16.4%), C-RB (14.9%), and M-RB (8.46%). At site 3, 67.7% (717.28 g) of the sediment was collected during summer, with the dominant source soil group being M-FS (30.4%), followed by M-AE (27.5%), M-XE (27.1%), C-RB (7.56%), and M-RB (7.45%).

During winter, the area received 48.5% of the precipitation and 29.7% (820.05 g) of the total sediment was collected. At site 1, 27.0% (243.18 g) of the sediment was collected

during winter. The dominant source soil group at site 1 during winter was M-AE (50.3%), followed by M-XE (26.2%), M-FS (19.8%), C-RB (3.26%), and M-RB (0.39%). At site 2, 30.3% (234.30 g) of the sediment was collected during winter, of which the dominant group was M-AE (37.0%), followed by M-XE (35.2%), M-FS (19.6%), and M-RB (8.27%); no sediment was attributed to C-RB. At site 3, 32.3% (342.57 g) of the sediment was collected during winter, with the dominant group being M-AE (30.7%), followed by M-FS (27.1%), M-XE (22.3%), M-RB (10.0%), and C-RB (9.89%).

2.6 Discussion

During erosion and transport, sediment undergoes a variety of biogeochemical transformations (Forstner and Salomans 1980; Foster and Lees 2000; Collins et al. 2017), which can affect concentrations of tracers and thereby confound distinctions between source soil groups. In addition, concentrations of some tracers may change over time as anthropogenic activities evolve (e.g., reduction in atmospheric releases of lead [Foster and Charlesworth 1996; Collin et al. 2017]). Examples of LU/LC changes include fields reverting to forested areas or being converted to pasture, crop rotation, urbanization, and the restoration of highly eroded lands.

Long periods of off-road vehicular training concentrated in one area can modify source soils through changes in chemistry as well as via erosion. Grinding of metal parts, leaking of fluids and wear of tires can contribute to higher concentrations of certain elements (Rodríguez-Eugenio et al. 2018), as can vehicle emissions, which include a variety of heavy metals (Zn, Co, Ni, Cr and Pb [Benson et al. 1986]). A Tukey test on XRF data (a post-hoc analysis completed after ANOVA; Figure 2.29) showed that mean concentrations of Ni, Co, Rb, Sr, Zn and Cu were statistically significant ($p < 0.0001$) in differentiating civilian from

military source soils. In contrast, TOC concentrations did not vary markedly between soil groups except for group M-XE, which contained very low TOC concentrations. Repeated military training activities that include high rates of travel and technical maneuvering of vehicles reduce the possibility to mitigate erosion (Warren et al. 1989; Fuchs et al. 2003) and sustain organic carbon inputs.

As a result of isotopic fractionation, the composition of carbon isotopes varies among plant tissues (O'Leary 1981; Marshall et al. 2007). Oelbermann and Voroney (2007) reported $\delta^{13}\text{C}$ values of -11.89‰ (shoots) and -11.76‰ (roots) for maize (corn), -26.62‰ (shoots) and -27.83‰ (roots) for soybean, and -30.34‰ (shoots) and -28.79‰ (roots) for wheat. Corn, soybean and wheat are rotated in the study area, and some C-RB samples had $\delta^{13}\text{C}$ values within the reported range for soybean. Incorporation of plant litter into soils is likely to average out short-term (diurnal-scale) variability in plant $\delta^{13}\text{C}$ values noted by Salmon et al. (2011). Median $\delta^{13}\text{C}$ values for C-RB, M-RB and M-FS (-26.24, -26.99, and -26.92‰, respectively) were similar to values for suspended sediment from streambank erosion in a surface-mined watershed in eastern Kentucky (-26.79‰ [Fox 2009]) and for soils under crop rotation (hay, winter wheat, lentils, peas, barley; mean -26.35‰) in the upper Palouse watershed in northwestern Idaho (Papanicolaou and Fox 2004). Nitrogen concentrations in most of the source soil samples (including all M-XE samples) were too low for isotopic analysis, but C-RB samples tended to have higher $\delta^{15}\text{N}$ values than military soils, consistent with the presence of vegetative cover (Fox and Papanicolaou 2007).

Differences observed in sediment yield and composition during summer (March-September) and winter (October-February) indicate seasonal shifts that may be related to precipitation and to anthropogenic activities. During summer the study area received 51.49%

of the total precipitation for the study period and collected 70.29% of the total sediment, whereas winter had 48.51% of the precipitation and collected 29.71% of the total sediment (Table 2.12). Gellis et al. (2014) noted that the lowest storm-weighted contributions of sediment to the Linganore Creek watershed (Frederick and Carroll counties, Maryland) from agriculture occurred during winter, when cover crops can reduce surface soil erosion in agricultural catchments and freezing temperatures can temporarily immobilize soil particles (Quinn et al. 2019). In the Otter Creek watershed, winter wheat (*Triticum aestivum*) is planted as a cover crop. However, the freeze-thaw action of a mild winter can also increase erosion in areas where surface soil is exposed and/or vegetation is not well-rooted (NRCS n.d.). The increased amount of sediment collected during May 2016 (Table 2.12) could be related to an increase in military training activity and to civilian farming practices, both of which would cause soil disturbance and increased erosion. In Kentucky the agricultural season typically begins in March as farmers start preparing soils for planting (Sudduth 2018).

The amount of sediment collected at each site does not necessarily represent recent erosion of upland areas. Gellis and Noe (2013) noted that a large percentage of sediment eroded from upland areas may not be delivered directly to the stream, but rather is stored for some amount of time. In the absence of sediment dating, we do not know when soil was eroded, and we do not know where sediment resides in storage (i.e. karst conduits, slopes, floodplains, channels) or for how long. Schoonover et al. (2015) estimated a total sediment flux to sinkholes at Fort Knox of 118.6 metric tons per year. Some of this sediment could be exported to Otter Creek during stormflow from springs located between sites 1 and 3.

The results from Sed_SAT's unmixing model for this study indicated unexpected contributions from military source soil groups, particularly M-AE, to sediment at site 1

(Figures 2.27–2.28; Appendices 2.1–2.3). Higher sediment contributions were expected from the C-RB source soil group given the predominance of civilian LU/LC upstream, although the part of Fort Knox bordering Otter Creek upstream of site 1 did experience active training maneuvers on a regular basis. For sites 2 and 3 at baseflow, there was a slight increase in source contributions attributed to C-RB, whereas the contributions from M-AE and M-XE were smaller than expected given the extent of exposed soil within the TAs, including well-defined rills and gullies. Compared to sites 1 and 2, site 3 had a greater proportion of sediment attributed to M-FS during baseflow, summer, and winter, which is consistent with the greater proportion of forest cover in the site 3 subcatchment. Site 3 during stormflow saw less of M-FS in comparison to sites 1 and 2 and higher percent contribution attributed to M-AE and M-XE which is consistent with high precipitation and subsequent erosion. At site 3, sediment traps were located under a highway bridge across Otter Creek in an area that is publicly accessible and popular for fishing. During baseflow periods, civilians wading upstream of the sediment traps could have contributed to artificially higher amounts of sediment collected.

In comparing all source soils to all target sediments (Table 2.7), the first principal component (PC1) had the largest variance (48.8%), which accounted for the majority of the variability in the source soils, with PC2 (17.2%) showing a much smaller variance. The positive correlations seen in Table 2.6 indicate better source discrimination, whereas the negative correlations indicate poorer discrimination ability. The majority of the factor loadings are in PC1 in all source soil groups (Table 2.8). Soil groups C-RB and M-RB showed similar positive and negative elements for PC1, which indicates that these two groups have a similar geochemical makeup, making it difficult to distinguish between them

during the unmixing model process. Likewise, M-FS has similar positive and negative elements to C-RB and M-RB, which indicates that some sediment samples could have been misclassified as C-RB and M-RB. Looking at target sediments by sampling site (Table 2.9), the majority of the factor loadings for all three sites are weighted toward PC1. Sediments from sites 1 and 2 have similar positive and negative correlations, indicating the sediments originated from similar source soils, in contrast to site 3. Therefore, the attribution of site 1 sediment to military lands may reflect misclassification of source soils to some extent.

Because of difficulties in distinguishing chemically between source soil groups for this study, soil groups were combined into two sets of categories for two different comparisons. In the first comparison (C1), soil groups C-RB, M-RB and M-FS were combined into a streambank/forest (STR-FS) category and M-AE and M-XE were combined into a military erosion (MIL-E) category (Table 2.13). In the second comparison (C2), C-RB and M-RB were combined into a streambank (STR) category and M-FS, M-AE and M-XE were combined into a military upland category (MIL-U). For C1, STR-FS had nearly double the percentage contributions at all three sediment sampling locations (63.39–68.66%) in comparison to the MIL-E category (31.97–36.61%). For C2, MIL-U had higher percentages (60.47% for site 1, 57.01% for site 2, and 65.58% for site 3) than STR. A student t-test with a 95% confidence interval indicated statistically significant differences in the mean values of the two groups for each set of comparisons, with the significance stronger for C1 ($p = 0.0001$) than for C2 ($p = 0.0033$).

Although the Sed_SAT program has only been available for public use since 2017, several studies have already utilized it. Cashman et al. (2018) studied the watershed of Difficult Run, a tributary to the Potomac River in Virginia, which is predominantly underlain

by gneiss and schist. Land cover went from forest to agriculture in the 18th and 19th centuries and today is mostly riparian secondary forest associated with urban sprawl. Three source group categories were defined and used in Sed_SAT: bank, forest and road. Cashman et al. (2018) found that suspended sediment was dominated by streambank-derived legacy sediment (87%), followed by roads (10%) and forest (2%). The Smith Creek watershed (Virginia) is located mostly on dolostone and limestone and drains to the Chesapeake Bay. The source soils were divided into four categories: cropland, pasture, forest and streambanks. Results showed that 70% of collected sediment was attributed to streambanks, 17% to pasture, 13% to forest and none to cropland (Gellis and Gorman Sanisaca 2018). The combined streambank and forest contributions for Difficult Run (87%) and Smith Creek (83%) are somewhat greater than those of the combined STR-FS source soil group along Otter Creek.

The Walnut Creek (Iowa) watershed has similar soils to the Otter Creek watershed (mostly silty clay loams, silt loams or clay loams) but much more agricultural LU/LC (65% cropland, 19% prairie, 8% pasture, 8% developed land/other). Source soil groups were defined as streambanks, cropland and other (prairie, pasture and unpaved roads). Sed_SAT calculated that cropland accounted for 62% of the sediment loads in Walnut Creek, with streambanks contributing 36% and the remaining $\leq 1\%$ attributed to the prairie, pasture and unpaved roads category (Gellis et al. 2019). The cropland and streambank percentages are similar to the MIL-U and STR contributions, respectively, in our C2 scenario, which suggests that sediment contributions from tracked-vehicle TAs are broadly analogous to those from tilled cropland in similar soils.

The approaches and findings of this study are potentially applicable to other catchments that include military tracked-vehicle training in karst terrain. More than 70 military installations within the United States besides Fort Knox are located on carbonate bedrock, which is prone to karst development (Vesper 2008; Figure 2.30). Many installations use karst waters as their primary drinking water supply, which can lead to a number of water quality and quantity issues, Figure 2.30. In particular, two installations with similar climatic, geologic, and LU/UC settings to Fort Knox share similar environmental concerns. Fort Campbell is located in southwest Kentucky and northwest Tennessee (IMCOM Fort Campbell 2016). Fort Campbell is underlain by limestones of the Mississippian St. Louis and Ste. Genevieve formations, and LU/LC around the installation is largely agriculture with some commercial and industrial activity (Vesper and White 2003). Sediment, soil, surface water and groundwater are listed as media of concern due to former and active military training activities (IMCOM Fort Campbell 2016). Fort Leonard Wood is located in south-central Missouri on bedrock that is predominantly Ordovician-age carbonate, and it lies within the Salem Plateau, part of the Ozark Plateau Physiographic Province (Albertson 2001). Overall climate is similar to that of Fort Knox and Fort Campbell, with warm, humid summers and cool, wet winters (Imes et al. 1996). Land use/land cover in the area includes hardwood forests and, due to a growing population, increased commercial and residential development (Richards et al. 2012). The resultant increase in construction has led to excess sediment delivered to local streams and has also potentially changed the overall hydrologic conditions (Richards et al. 2012).

2.7 Conclusions

Understanding sources of suspended sediment is imperative in creating and implementing successful strategies to limit soil erosion. Sediment fingerprinting can provide insight into potential sources of sediment. However, in many catchments no single geochemical tracer can apportion sediment to source soil groups, especially if the catchment lithology in the study area is relatively homogeneous. In this study, we examined sediment and soils in the Otter Creek (Kentucky) watershed, which drains farmland, forest, military training areas, and residential areas developed on limestone bedrock. We conducted weekly monitoring from September 2015 to October 2016 with time-integrated suspended-sediment samplers at three sites along the stream. We collected samples of five source-soil types: civilian and military near-stream (C-RB and M-RB), military forest (M-FS), and military average and extreme erosion (M-AE and M-XE). We used analyses of major and trace elements, TOC, and stable C and N isotopes in the program Sed_SAT, which identified Cu, Zn, Co, Ni, Al and Mg as conservative tracers for use in an unmixing model. Additional statistical tests were run independent of Sed_SAT to assess the capability of individual tracers to provide additional insight beyond the unmixing model results. A Tukey test showed that tracers were able to distinguish between civilian and military source soils. Principal component analysis was used to reduce dimensionality and assist in identifying tracers that might influence source discrimination.

Sediment yield varied between sampling sites, with season, and depending upon antecedent precipitation. Normalized by subcatchment area, site 3 (the farthest downstream) had the greatest yield. At each site, sediment yield was greater in summer than in winter, which may reflect agricultural practices, and was greater for stormflow (rainfall ≥ 3.0 cm within a 72-hour period sometime in the preceding week) than for baseflow. The greatest

proportion of sediment in summer was attributed to M-XE at sites 1 and 2 and M-FS at site 3, whereas the greatest proportion of sediment in winter was attributed to M-AE at all three sites. For baseflow, the greatest proportion of sediment was attributed to M-AE for site 1, M-XE for site 2 and M-FS for site 3, whereas for stormflow, the greatest proportion of sediment was attributed to M-AE for all three sites.

Because of geochemical similarities between soil groups C-RB, M-RB and M-FS, sediment apportionment may have been affected by misclassification of source soils. Consequently, we combined soil groups into simplified categories: streambank/forest (STR-FS = C-RB + M-RB + M-FS) and military erosion (MIL-E = M-AE + M-XE) in one scenario; streambank (STR = C-RB + M-RB) and military upland (MIL-U = M-FS + M-AE + M-XE) in a second scenario. All three sediment sampling sites were dominated by STR-FS (63.39–68.66%) in scenario one and by MIL-U (57.01–65.58%) in scenario two. Comparison with a watershed in Iowa developed on similar soils, but with cropland and grassland as primary LU/LC, suggests that sediment contributions from tracked-vehicle military training areas are broadly analogous to those from tilled cropland.

The approach taken in this study is particularly applicable to military training sites in similar geologic and climatic settings (e.g., Fort Campbell [Kentucky] and Fort Leonard Wood [Missouri]). Given the potential for karst features (e.g., sinkholes and conduit networks) to store sediment, legacy sediment is a concern when calculating sediment fluxes or trying to allocate target sediment to specific source soil groups. Further work at Fort Knox and similar sites should include deployment of sediment traps at major spring outlets, thorough delineation of flowpaths (such as by dye tracing), and sediment dating.

Acknowledgments

The authors gratefully acknowledge support from the Fort Knox Environmental Management Division, Natural Resource Division and Range Control for providing access to training lands. Funding for this project was provided by U.S. Geological Survey grant G16AP00055 through the Kentucky Water Resources Research Institute; by a Casner Fellowship from the University of Kentucky (UK) Tracy Farmer Institute for Sustainability and the Environment; and by University of Kentucky's Department of Earth and Environmental Sciences (UKEES) Farm Research Support Fund. We thank the KGS and Pioneer Lab at the UKEES for their laboratory support.

Table 2.1 Percent contribution of land use/land cover categories per subcatchment, Hardin and Meade counties, Kentucky.

Percent contribution per subcatchment			
	Site 1	Site 2	Site 3
Forest	33.1	36.4	74.5
Cropland	54.8	45.9	5.3
Developed	11.8	16.5	8.3
Other	0.3	1.2	11.8

Table 2.2 Pearson correlation between sediments collected between sampling sites for zinc and strontium. First line is the correlation coefficient and the second line is the p-value. Pink indicates statistically significant results.

Zinc			Strontium		
	Site 2	Site 3		Site 2	Site 3
Site 1	0.186	0.477	Site 1	0.586	0.488
	0.342	0.006		0.001	0.005
Site 2		-0.12	Site 2		0.236
		0.541			0.226

Table 2.3 Descriptive statistics for TOC and $\delta^{13}\text{C}$ for all source soils and source soil groups.

Total Organic Carbon (%)				
	Min	Max	Mean (SD)	Median (SE)
All Soil	<0.01	3.40	0.36 (0.86)	0.48 (0.06)
C-RB	0.37	3.21	0.95 (1.01)	0.69 (0.31)
M-RB	0.26	1.04	0.69 (0.30)	0.93 (0.14)
M-FS	0.22	3.40	0.65 (1.21)	0.36 (0.54)
M-AE	0.21	2.27	0.67 (0.66)	0.74 (0.27)
M-XE	<0.01	1.83	0.09 (0.44)	0.17 (0.11)
Carbon-13 (‰)				
	Min	Max	Mean (StdDev)	Median (SE)
All Soil	-28.76	-21.24	-25.41 (1.56)	-25.54 (3.92)
C-RB	-28.76	-22.51	-26.12 (1.52)	-26.24 (0.46)
M-RB	-28.10	-26.16	-26.91 (0.71)	-26.99 (0.32)
M-FS	-28.26	-23.68	-26.06 (1.74)	-26.92 (0.78)
M-AE	-26.07	-23.61	-25.01 (0.78)	-25.15 (0.32)
M-XE	-25.65	-21.24	-24.34 (1.11)	-24.37 (0.29)

Table 2.4 Descriptive statistics for TOC and $\delta^{13}\text{C}$ for all sediment and sediment sampling locations and for base-and stormflow.

Total Organic Carbon (%)				
	Min	Max	Mean (SD)	Median (SE)
All Sediment	0.19	4.41	2.36 (0.74)	2.51 (0.07)
Site 1	0.19	4.41	2.62 (0.83)	2.84 (0.14)
Site 2	0.97	3.61	2.28 (0.71)	2.55 (0.12)
Site 3	1.17	3.22	2.18 (0.50)	2.23 (0.08)
<i>Baseflow</i>				
Site 1	1.68	4.28	2.87 (0.63)	2.95 (0.11)
Site 2	1.25	3.61	2.42 (0.64)	2.56 (0.12)
Site 3	1.14	3.22	2.20 (0.49)	2.29 (0.09)
<i>Stormflow</i>				
Site 1	0.19	4.41	1.60 (1.38)	2.26 (0.56)
Site 2	0.97	2.86	1.64 (0.80)	1.31 (0.36)
Site 3	1.36	2.93	1.99 (0.53)	1.93 (0.22)
Carbon-13 (‰)				
	Min	Max	Mean (StdDev)	Median (SE)
All Sediment	-30.92	-25.45	-27.34 (1.73)	-27.42 (0.17)
Site 1	-28.05	-26.22	-27.26 (0.50)	-27.39 (0.08)
Site 2	-28.34	-26.63	-27.31 (0.62)	-27.35 (0.12)
Site 3	-30.92	-25.45	-27.47 (0.86)	-27.48 (0.14)
<i>Baseflow</i>				
Site 1	-28.05	-26.22	-27.31 (0.47)	-27.42 (0.08)
Site 2	-28.34	-25.47	-27.31 (0.62)	-27.35 (0.12)
Site 3	-30.92	-26.46	-27.62 (0.81)	-27.63 (0.15)
<i>Stormflow</i>				
Site 1	-27.99	-26.31	-26.98 (0.54)	-26.87 (0.22)
Site 2	-27.50	-26.63	-27.03 (0.36)	-27.00 (0.00)
Site 3	-27.45	-25.45	-26.71 (0.76)	-27.02 (0.31)

Table 2.5 Pearson correlation between source soil groups for TOC and for $\delta^{13}\text{C}$. First line is the correlation coefficient and second line is the p-value. Pink indicates statistically significant results.

Total Organic Carbon for Soils				
	M-AE	M-FS	M-RB	M-XE
C-RB	-0.335	0.347	0.319	0.610
	0.516	0.567	0.537	0.046
M-AE		0.347	-0.450	-0.216
		0.567	0.370	0.681
M-FS			0.440	0.973
			0.458	0.005
M-RB				0.632
				0.179

Carbon-13 for Soils				
	M-AE	M-FS	M-RB	M-XE
C-RB	-0.325	0.619	-0.046	0.340
	0.529	0.265	0.931	0.307
M-AE		-0.361	-0.147	-0.139
		0.550	0.781	0.793
M-FS			0.692	0.838
			0.196	0.076
M-RB				0.715
				0.111

Table 2.6 Pearson correlation between sediment sampling sites for base- and stormflow and for all sediment combined for TOC and for $\delta^{13}\text{C}$. First line is the correlation coefficient and second line is the p-value.

Total Organic Carbon

	Sediment, baseflow		Sediment, stormflow	
	Site 2	Site 3	Site 2	Site 3
	Site 1	0.092 0.642	0.037 0.845	0.868 0.132
Site 2		-0.025 0.900		0.775 0.225

All sediment

	Site 2	Site 3
Site 1	-0.013 0.945	0.023 0.892
Site 2		-0.085 0.645

Carbon-13

	Sediment, baseflow		Sediment, stormflow	
	Site 2	Site 3	Site 2	Site 3
	Site 1	-0.056 0.777	-0.050 0.794	-0.215 0.785
Site 2		0.344 0.073		0.388 0.612

All Sediment

	Site 2	Site 3
Site 1	-0.062 0.738	-0.107 0.530
Site 2		0.275 0.127

Table 2.7 Principal component analysis (PCA) for all source soils and target sediments: first two principal component factor loadings (PC1 and PC2) with proportion of variation. Blue (positive) and pink (negative) indicate variables that have a similar tendency to change in the same way.

	All Soils (n=42)		All Sediment (n=107)	
	48.8 PC1	17.2 PC2	37.9 PC1	20.5 PC2
TOC	0.302	-0.308	-0.603	-0.312
Cu	-0.598	0.169	-0.546	0.280
Zn	-0.825	0.205	-0.956	-0.072
Sr	-0.493	-0.513	0.034	-0.898
Rb	-0.906	0.008	-0.936	0.088
Co	-0.946	0.065	-0.912	0.058
Ni	-0.806	0.193	-0.892	0.072
Al	-0.867	0.375	-0.872	0.157
Na	0.683	0.578	0.218	0.672
Mg	0.774	0.496	0.289	0.740
Si	0.841	0.215	0.438	0.683
P	0.620	-0.612	-0.170	0.127
K	-0.516	-0.160	-0.093	-0.067
Ca	0.012	-0.877	0.193	-0.934
Mn	0.617	-0.114	-0.537	0.001
Fe	-0.960	0.129	-0.936	-0.045
δ¹³C	-0.291	-0.693	0.230	0.309

Table 2.8 Principal component analysis (PCA) for source soil groups: first two principal component factor loadings (PC1 and PC2) with proportion of variation and associated tracers. Blue (postive) and pink (negative) indicate variables that have a similar tendency to change in the same way.

	C-RB (n=10)		M-RB (n=6)		M-FS (n=5)		M-AE (n=6)		M-XE (n=15)	
	55.8	15.0	51.2	30.0	54.5	28.5	64.3	17.2	51.9	19.7
	PC1	PC2	PC 1	PC 2	PC 1	PC 2	PC 1	PC 2	PC 1	PC 2
TOC	0.090	-0.772	0.696	-0.591	-0.440	-0.699	-0.857	-0.137	-0.121	0.657
Cu	0.887	-0.199	0.864	0.166	0.897	0.393	0.381	0.556	0.892	-0.011
Zn	0.834	-0.215	0.841	0.499	0.726	0.543	0.619	0.684	0.852	-0.166
Sr	0.831	0.152	0.953	-0.080	-0.849	0.476	0.661	-0.716	0.375	0.633
Rb	0.938	-0.246	0.959	-0.165	0.883	0.048	0.961	0.201	0.885	0.330
Co	0.970	0.144	0.692	0.273	0.911	0.182	0.975	-0.208	0.984	0.082
Ni	0.833	0.001	0.746	0.625	0.614	0.575	0.563	0.692	0.857	-0.201
Al	0.941	0.181	0.845	0.413	0.947	0.301	0.944	0.259	0.794	-0.451
Na	-0.671	0.337	-0.701	0.680	0.833	-0.459	-0.797	0.444	-0.619	-0.666
Mg	-0.886	0.185	-0.722	0.643	0.736	-0.659	-0.738	0.492	-0.780	-0.523
Si	-0.863	-0.319	-0.574	-0.746	0.259	-0.914	-0.894	0.026	-0.826	0.469
P	-0.669	-0.353	-0.373	-0.702	-0.982	0.085	-0.796	-0.298	-0.404	0.747
K	0.651	-0.455	0.825	-0.329	0.203	-0.326	0.763	0.189	0.690	0.378
Ca	-0.130	0.631	-0.513	0.498	-0.833	0.548	-0.783	-0.322	0.715	-0.036
Mn	-0.282	-0.787	0.296	-0.606	-0.307	-0.883	-0.829	0.425	-0.472	0.601
Fe	0.944	0.191	0.592	0.783	0.894	0.439	0.984	-0.167	0.981	0.003
$\delta^{13}\text{C}$	0.244	0.297	-0.578	0.737	-0.756	0.597	0.828	-0.338	0.180	0.366

Table 2.9 Principal component analysis (PCA) for each sediment sampling site: first two principal component factor loadings (PC1 and PC2) with proportion of variation. Blue (postive) and pink (negative) indicate variables that have a similar tendency to change in the same.

	Site 1 - All (n=38)		Site 2 - All (n=32)		Site 3 - All (n=37)	
	47.3	21.0	49.4	15.7	47.5	26.7
	PC1	PC2	PC1	PC2	PC1	PC2
TOC	0.748	-0.322	0.626	-0.458	0.094	0.683
Cu	0.756	0.107	0.733	0.163	0.858	0.365
Zn	0.898	-0.030	0.909	0.058	0.819	0.529
Sr	0.522	-0.677	0.733	-0.465	-0.585	0.715
Rb	0.886	0.358	0.781	0.521	0.933	0.279
Co	0.856	0.284	0.828	0.474	0.894	0.314
Ni	0.848	0.257	0.856	0.372	0.812	0.246
Al	0.800	0.427	0.738	0.506	0.947	0.181
Na	-0.520	-0.051	-0.523	0.004	0.466	-0.697
Mg	-0.622	0.263	-0.659	-0.090	0.340	-0.746
Si	-0.580	0.563	-0.724	0.425	0.164	-0.836
P	0.146	-0.362	0.479	-0.083	-0.571	0.506
K	0.820	0.408	-0.259	0.246	0.927	-0.029
Ca	0.177	-0.938	0.631	-0.679	-0.754	0.623
Mn	0.600	-0.531	0.832	-0.292	0.438	-0.049
Fe	0.928	0.176	0.917	0.192	0.866	0.370
δ¹³C	-0.093	0.816	-0.266	0.697	0.172	-0.591

Table 2.10 Shapiro-Wilks normality test for source soils and target sediment.

	Source Soils		All Sediment	
	W-Statistic	p-value	W-Statistic	p-value
TOC	0.771	<0.001	0.995	0.976
Cu	0.418	<0.001	0.977	0.060
Zn	0.987	0.899	0.933	0.871
Sr	0.517	<0.001	0.825	<0.001
Rb	0.966	0.236	0.985	0.258
Co	0.996	0.067	0.980	0.113
Ni	0.793	<0.001	0.987	0.369
Al	0.956	0.109	0.986	0.299
Na	0.958	0.127	0.953	<0.001
Mg	0.953	0.085	0.980	0.095
Si	0.886	<0.001	0.990	0.620
P	0.948	0.045	0.593	<0.001
K	0.989	0.048	0.767	<0.001
Ca	0.618	<0.001	0.817	<0.001
Mn	0.844	<0.001	0.955	<0.001
Fe	0.944	0.069	0.981	0.114
$\delta^{13}\text{C}$	0.887	<0.001	0.365	<0.001

Shapiro-Wilks Normality Test for source soils and target sediment; values bolded have deviated from normality and varies significantly from the pattern expected.

Table 2.11 Amount of sediment collected (g) and descriptive statistics for each of the three sediment sampling locations along Otter Creek, Fort Knox, Kentucky. Precipitation (cm) throughout the study period and percent of contributions of sediment. Sediment samplers installed 25 September 2015; first sample taken 2 October 2016.

		Sediment Collected (g)				
		All	Site 1	Site 2	Site 3	PPT (cm)
2015	October	82.6	14.8	24.1	43.7	7.2
	November	430.7	125.4	101.4	203.8	7.2
	December	7.6	3.6	1.9	2.1	14.0
2016	January	90.0	35.4	47.2	7.3	2.1
	February	204.0	62.6	56.8	84.6	13.2
	March	174.8	130.7	13.7	30.5	5.4
	April	277.3	84.8	77.7	114.8	7.6
	May	922.1	264.3	292.9	364.9	8.0
	June	42.6	12.1	16.3	14.2	4.1
	July	188.0	82.3	49.1	56.6	7.8
	August	317.5	74.9	110.4	132.2	9.2
	September	17.9	9.1	4.6	4.2	4.6
	October	5.3	1.3	2.9	1.1	0.3
Total		<i>2760.2</i>	<i>901.3</i>	<i>799.0</i>	<i>1059.9</i>	<i>90.8</i>
Min		5.3	1.3	1.9	1.1	0.3
Max		922.1	264.3	292.9	364.9	14.0
Median		174.8	62.6	47.2	43.7	7.2
Std Dev		240.5	70.9	75.5	100.9	3.7
SE		23.0	11.5	13.0	16.6	0.2
Summer		70.3%	73.0%	70.7%	67.7%	51.5%
Winter		29.7%	27.0%	29.3%	32.3%	48.5%
<i>Summer includes March through September</i>						
<i>Winter includes October (2015 and 2016) through February</i>						
<i>Sediment Collected (g)</i>	Baseflow	646.2	199.7	206.6	239.9	
	Stormflow	2114.0	701.6	592.4	820.0	
	Total	<i>2760.2</i>	<i>901.3</i>	<i>799.0</i>	<i>1059.9</i>	
<i>Percent Contribution</i>	Baseflow	23.4%	22.2%	25.9%	22.6%	
	Stormflow	76.6%	77.8%	74.1%	77.4%	
<i>Baseflow is defined as < 3cm of rainfall within 72 hours of sampling</i>						

Table 2.12 Percent of contributions of sediment during summer and winter months with percent precipitation. Hardin and Meade counties, Kentucky.

<i>Summer (March through September) 51.49% Precipitation, 70.29% of total sediment</i>							
	C-RB (%)	M-RB (%)	M-FS (%)	M-AE (%)	M-XE (%)	Sediment Collected (g)	% Sed
Site 1	7.65	1.6	27.22	29.57	33.95	658.16	33.92
Site 2	14.87	8.46	16.41	28.92	31.34	564.72	29.11
Site 3	7.56	7.45	30.39	27.48	27.13	717.28	36.97
<i>Winter (October through February) 48.51% of Precipitation, 29.71 % of total sediment</i>							
Site 1	2.78	0.33	16.85	42.89	22.35	243.18	29.65
Site 2	0.00	7.01	16.6	31.31	29.81	234.3	28.57
Site 3	7.83	7.95	21.45	24.3	17.61	342.57	41.77

Table 2.13 Source soil group percentages combined for comparison, Hardin and Meade counties, Kentucky. Comparison one (C1) combines C-RB, M-RB and M-FS into a streambank-forest (STR-FS) category and M-AE and M-XE into a military erosion category (MIL-E). Comparison two (C2) combines C-RB and M-RB into a streambank (STR) category and M-AE, M-XE and M-FS into a military upland category (MIL-U).

Comparison One (C1)		
	STR-FS	MIL-E
Site 1	68.0	32.0
Site 2	63.4	36.6
Site 3	68.7	31.3
Comparison Two (C2)		
	STR	MIL-U
Site 1	39.5	60.5
Site 2	43.0	57.0
Site 3	34.4	65.6



Figure 2.1 Left image is of training lands that show some erosion with sparse vegetation. Right image shows well developed gullies with little to no vegetation present. Fort Knox, Kentucky. Image taken by C. Peterman, August 2016.

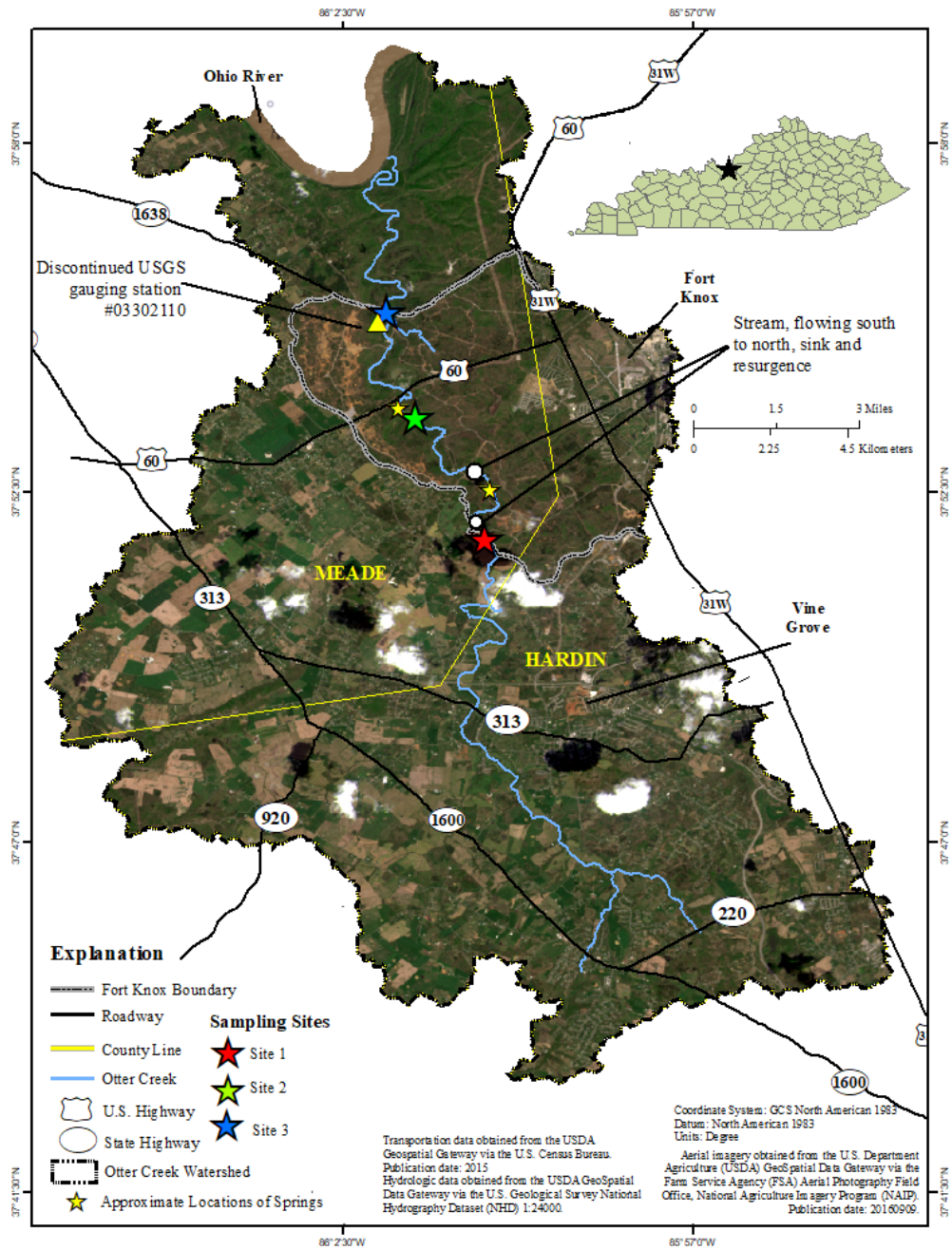


Figure 2.2 Location of study area in Hardin and Meade counties, Otter Creek,

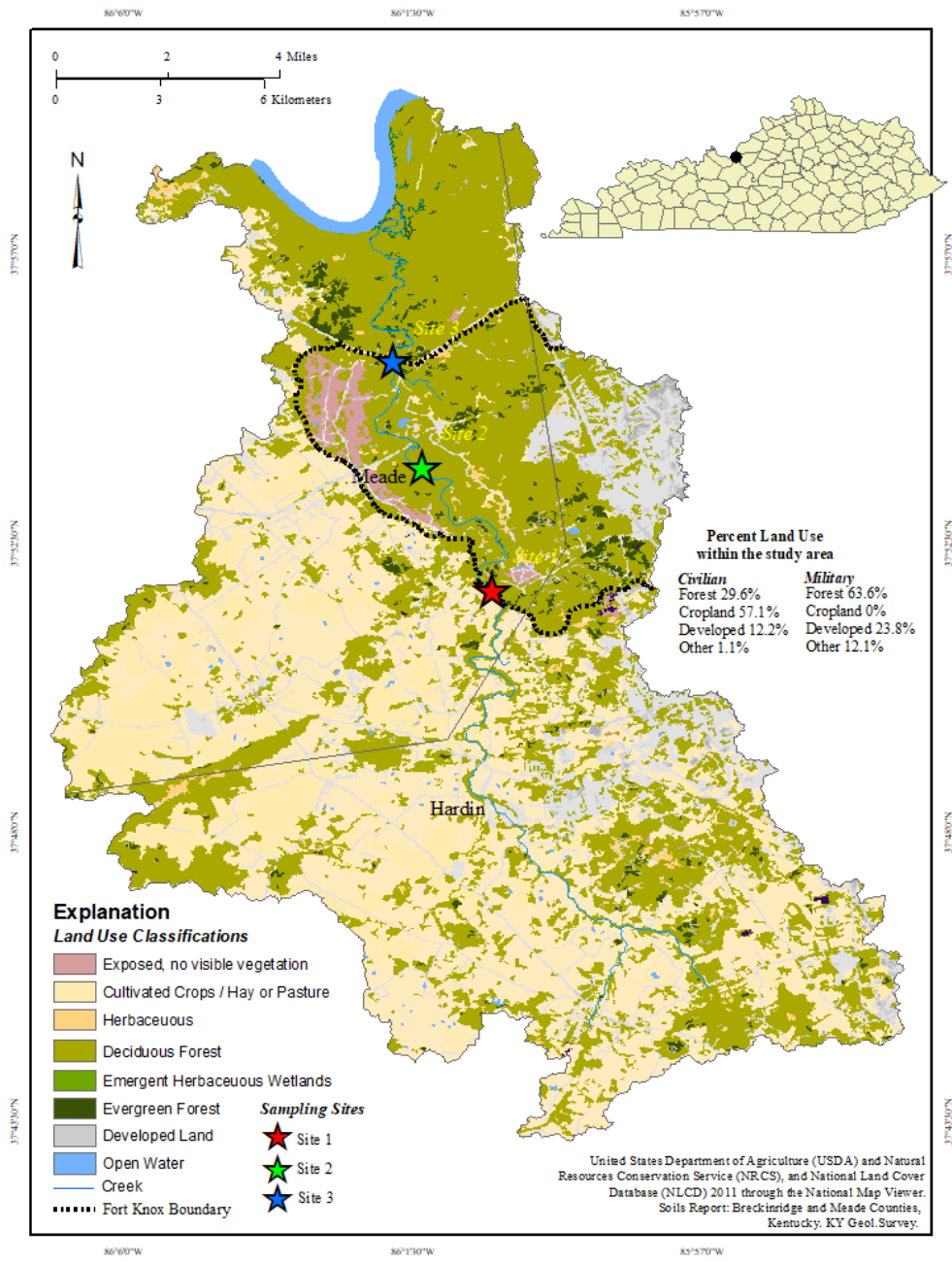


Figure 2.3 Land use/land cover for the study area, Hardin and Meade counties, Kentucky.



Figure 2.4 Agricultural field along Otter Creek showing slumping and erosion, Hardin County, Kentucky. Image taken by C. Peterman, Fall 2015.

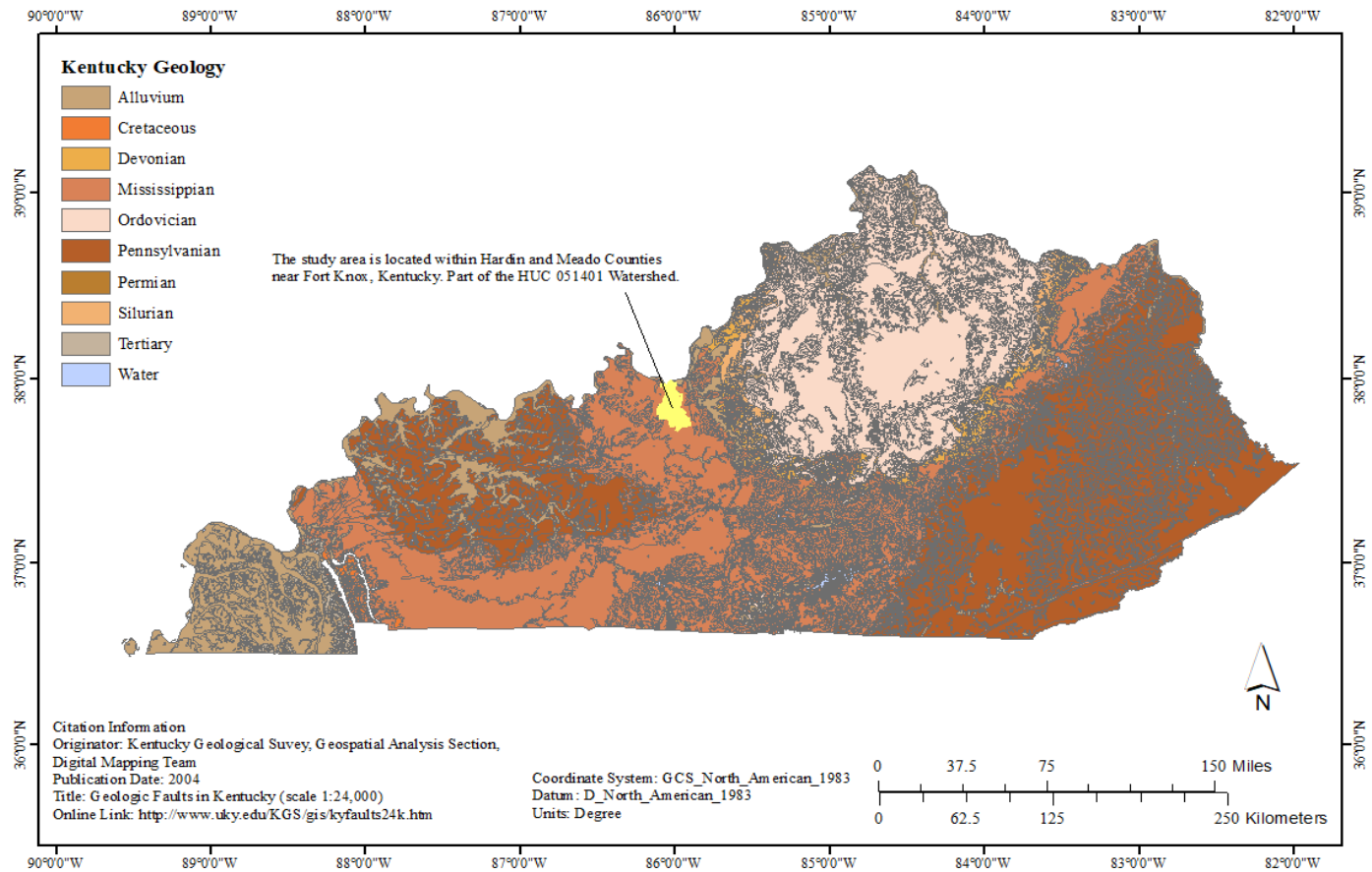


Figure 2.5 Physiographic regions of Kentucky; location of the study area is in yellow.

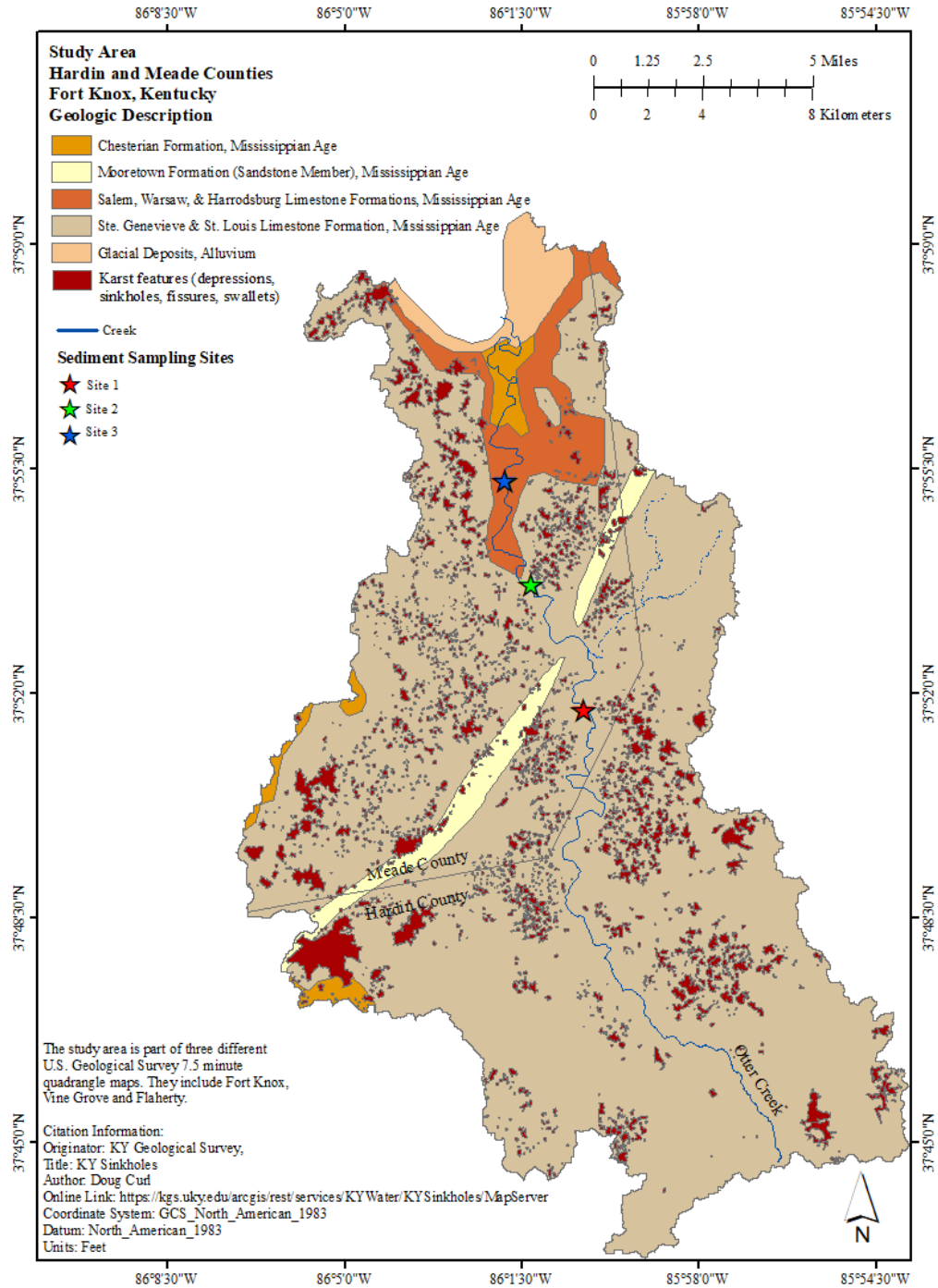


Figure 2.6 Geology of the study area with karst features depicted, Hardin and Meade counties, Kentucky.



Figure 2.7 Left: Otter Creek sinks into the karst conduit. Right: Otter Creek re-emerges out of fractured bedrock. Images taken by C. Peterman, July and September

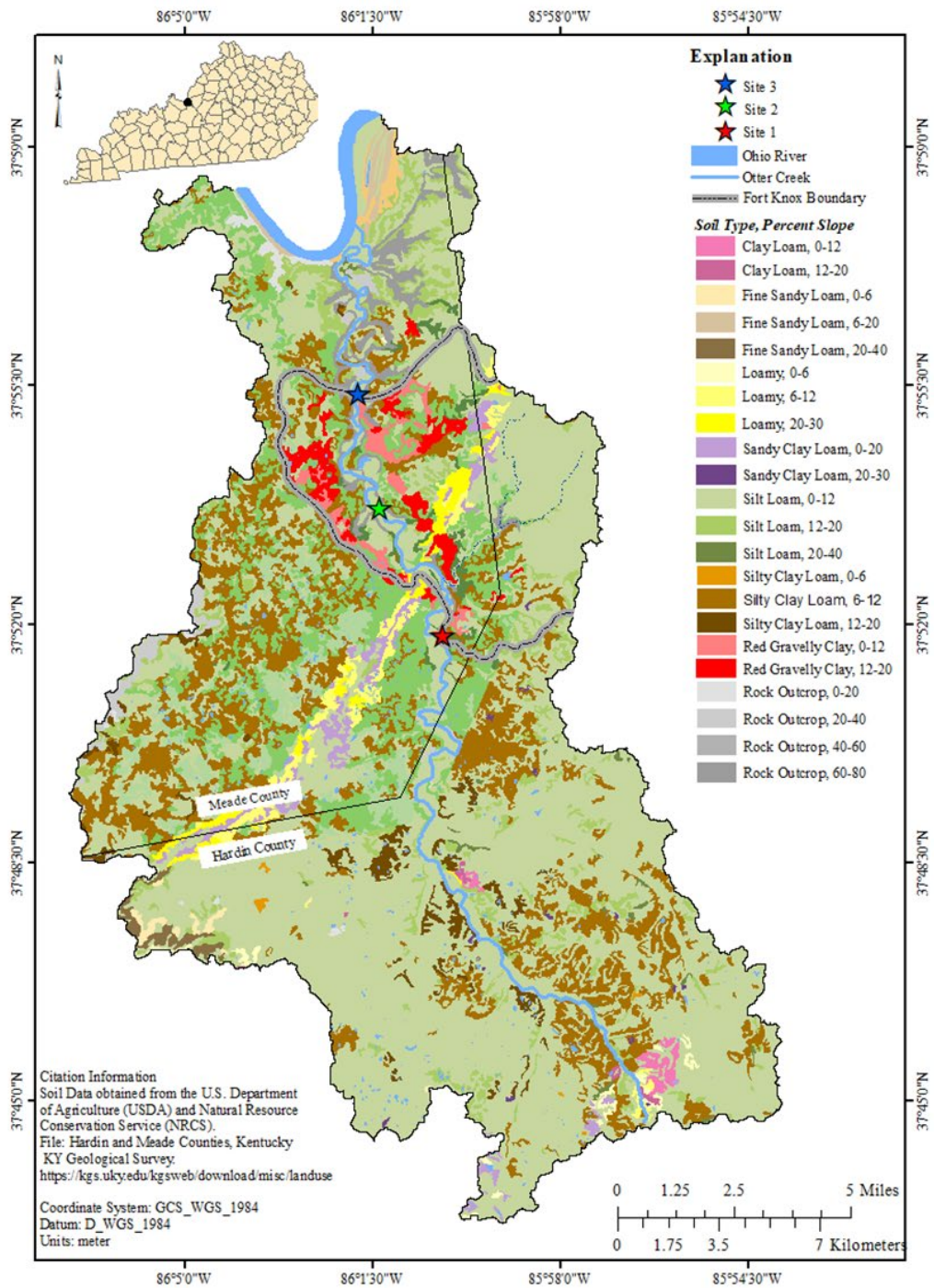


Figure 2.8 Soil and percent slope in the study area, Hardin and Meade counties, Kentucky.

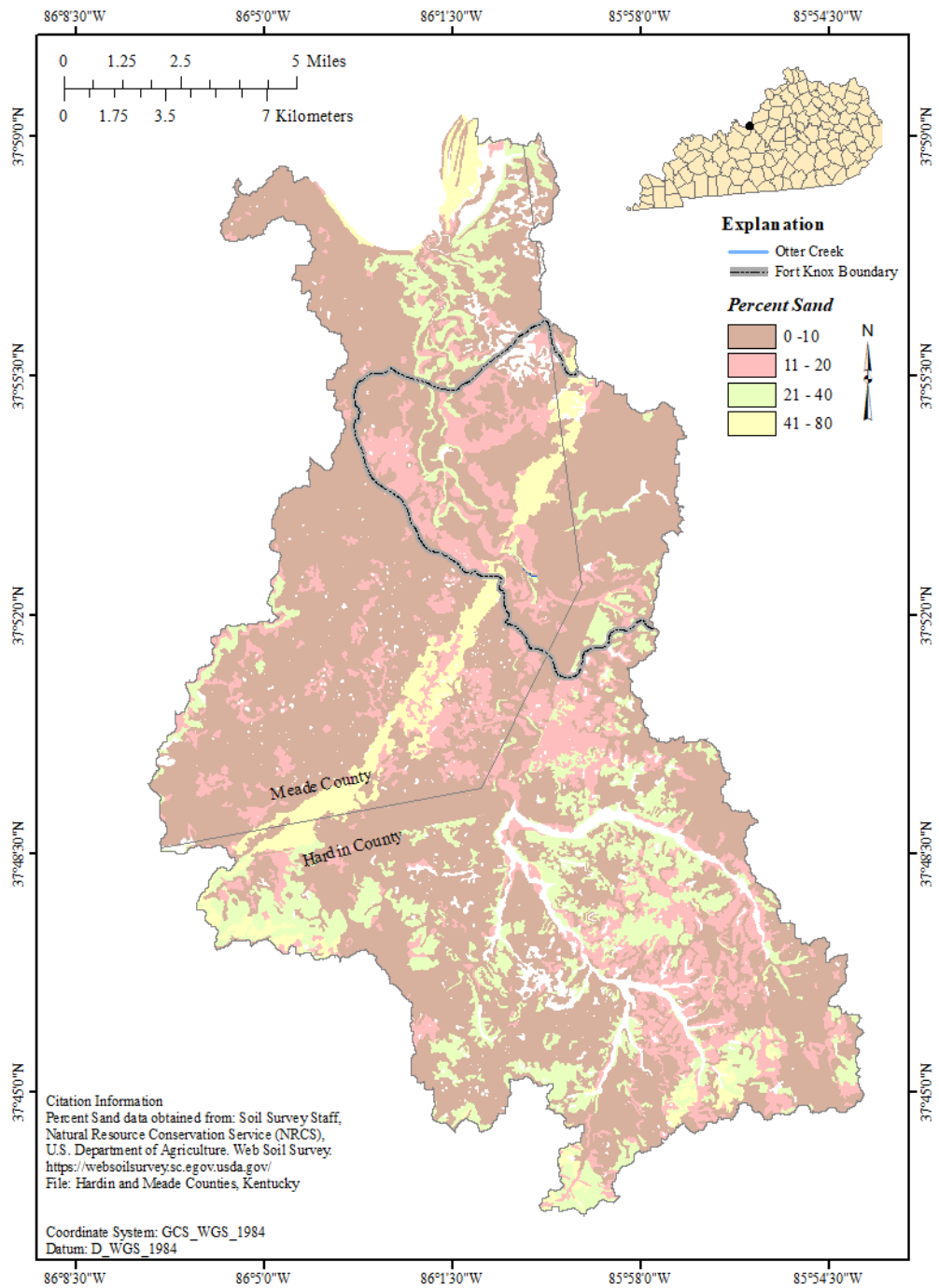


Figure 2.9 Percent sand in the study area, Hardin and Meade counties, Kentucky.

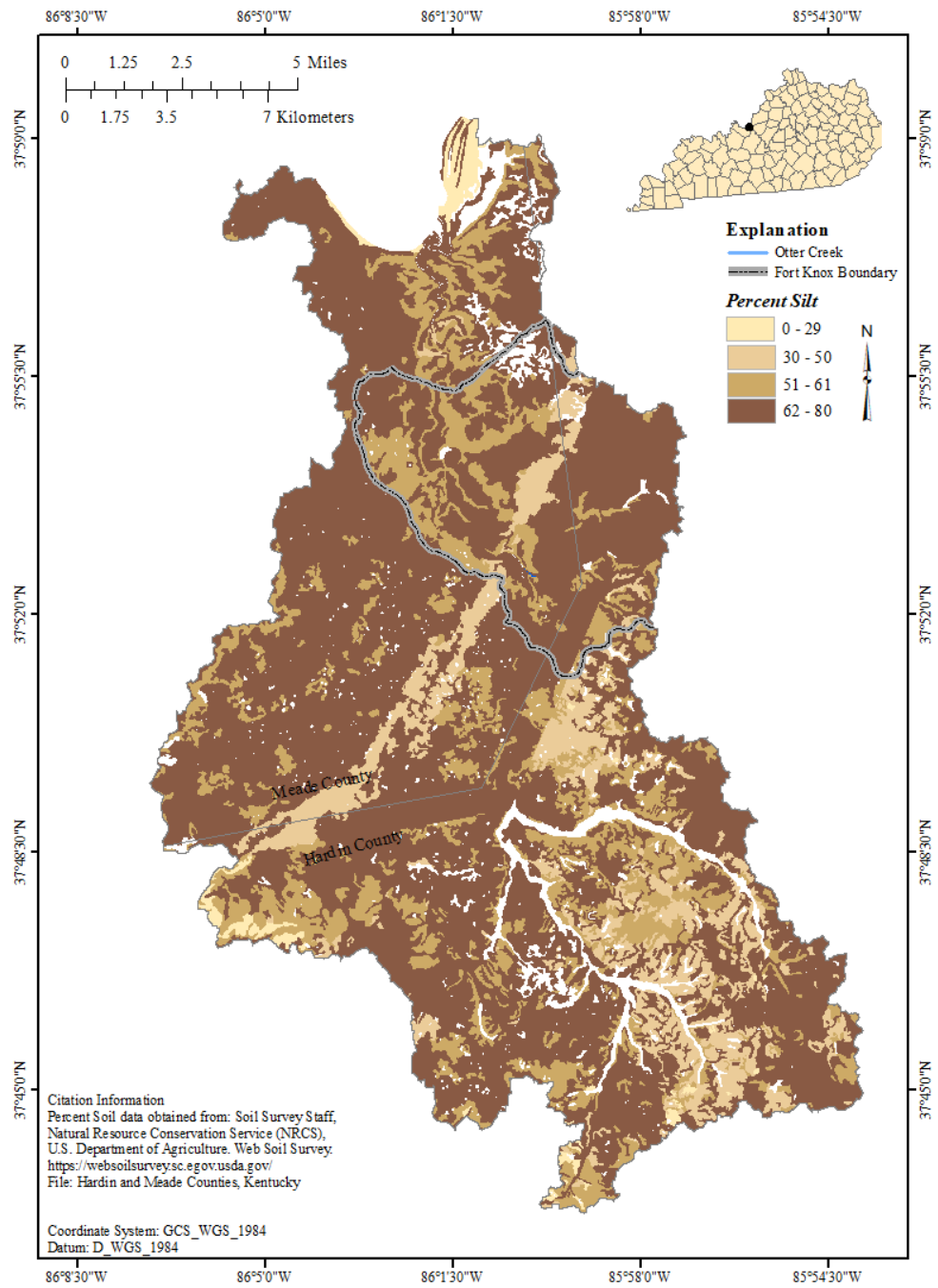


Figure 2.10 Percent silt in the study area, Hardin and Meade counties, Kentucky.

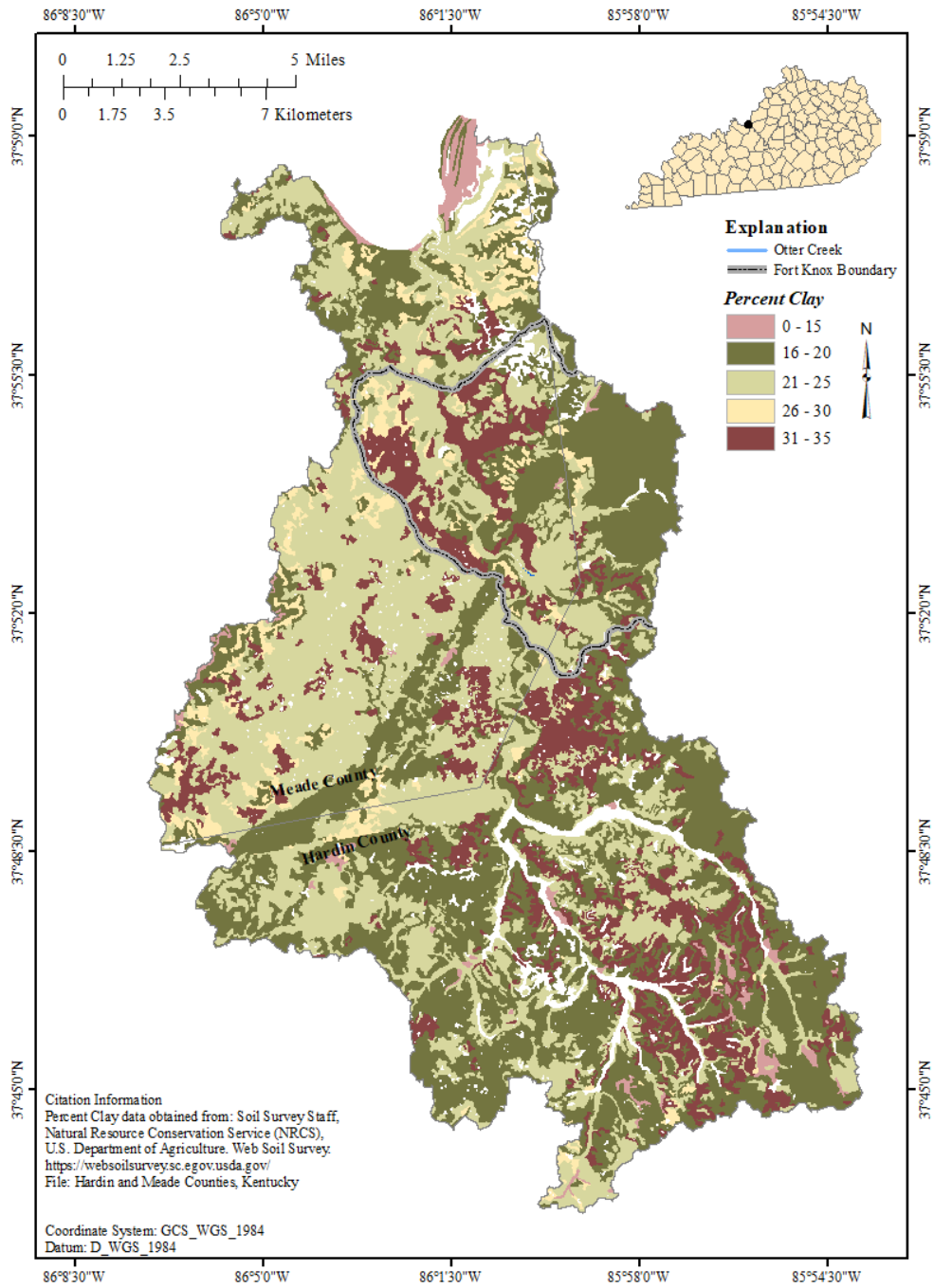


Figure 2.11 Percent clay in the study area, Hardin and Meade counties, Kentucky.

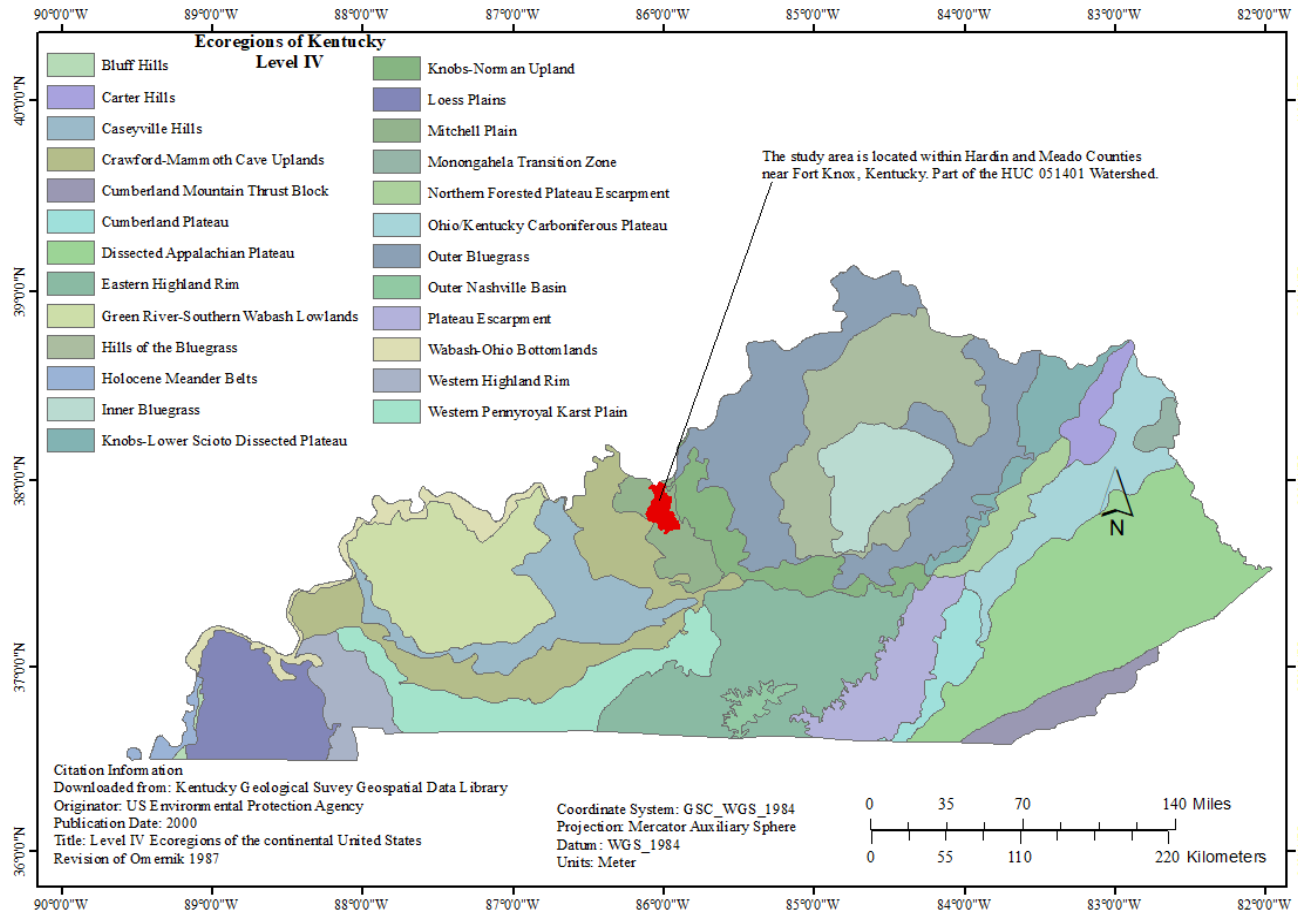


Figure 2.12 Ecoregions of Kentucky; location of the study area is in red.

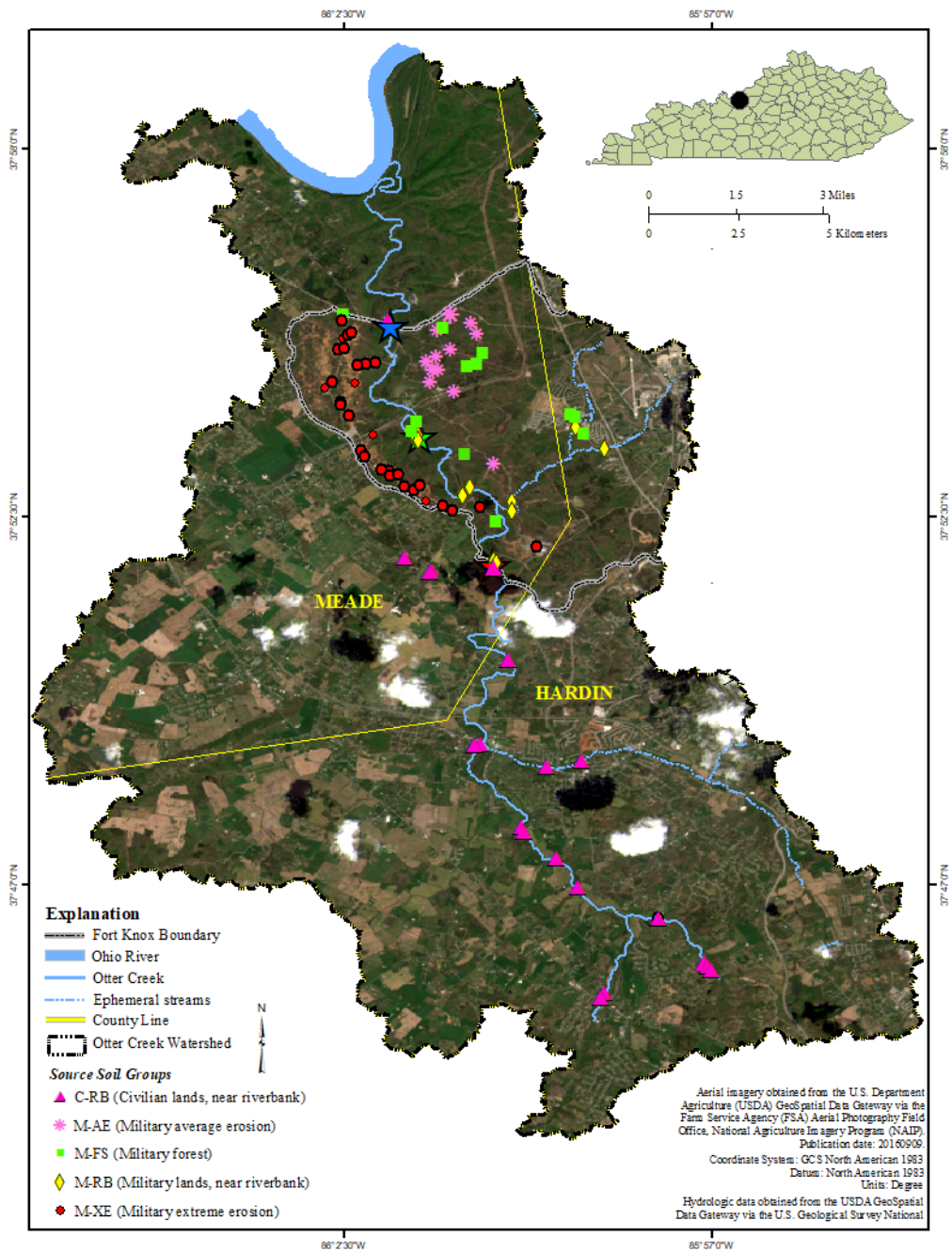


Figure 2.13 Source soil sampling locations, Hardin and Meade counties, Kentucky.

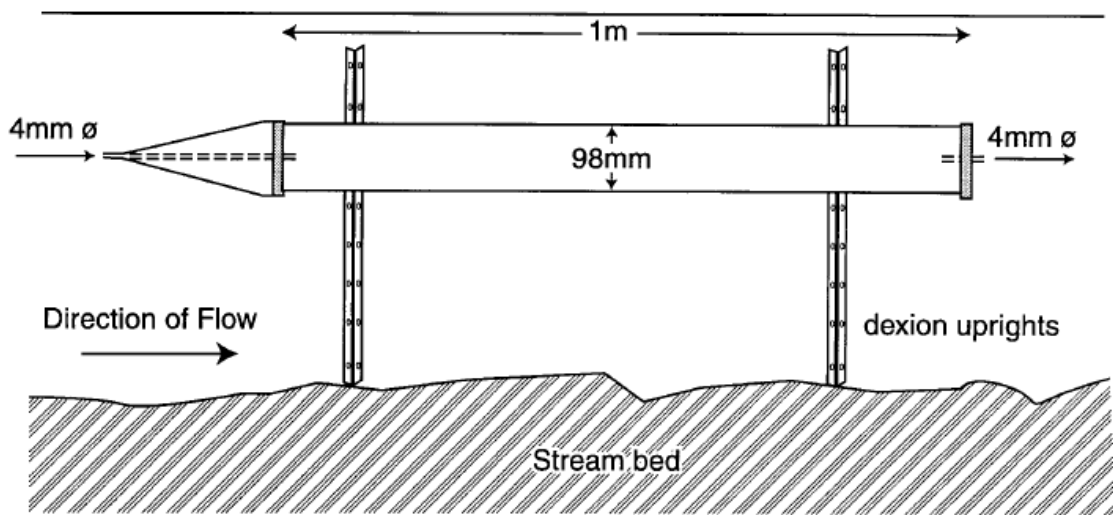


Figure 2.14 Cross-section of time-integrated suspended sediment samplers. Image taken from Phillips et al. (2000).



Figure 2.15 Pictures of the time-integrated sediment samplers in situ at site 1. Images taken by C. Peterman, October 2015.

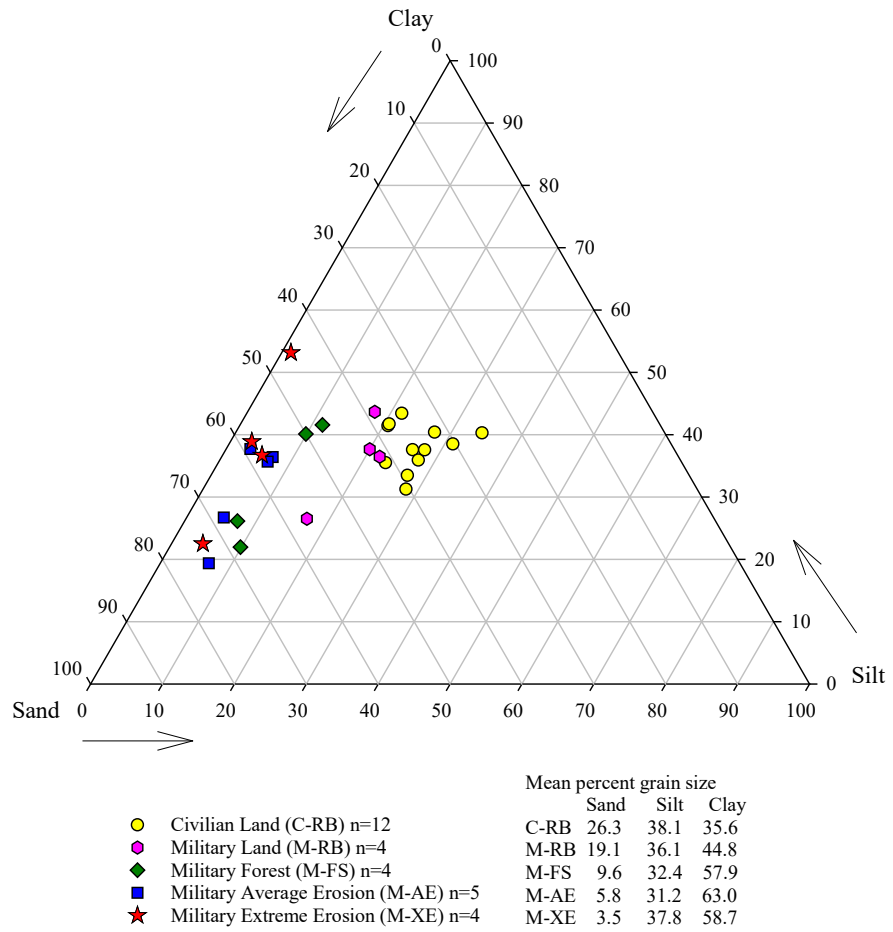


Figure 2.16 Ternary diagram for selected source soils, Hardin and Meade counties, Kentucky.

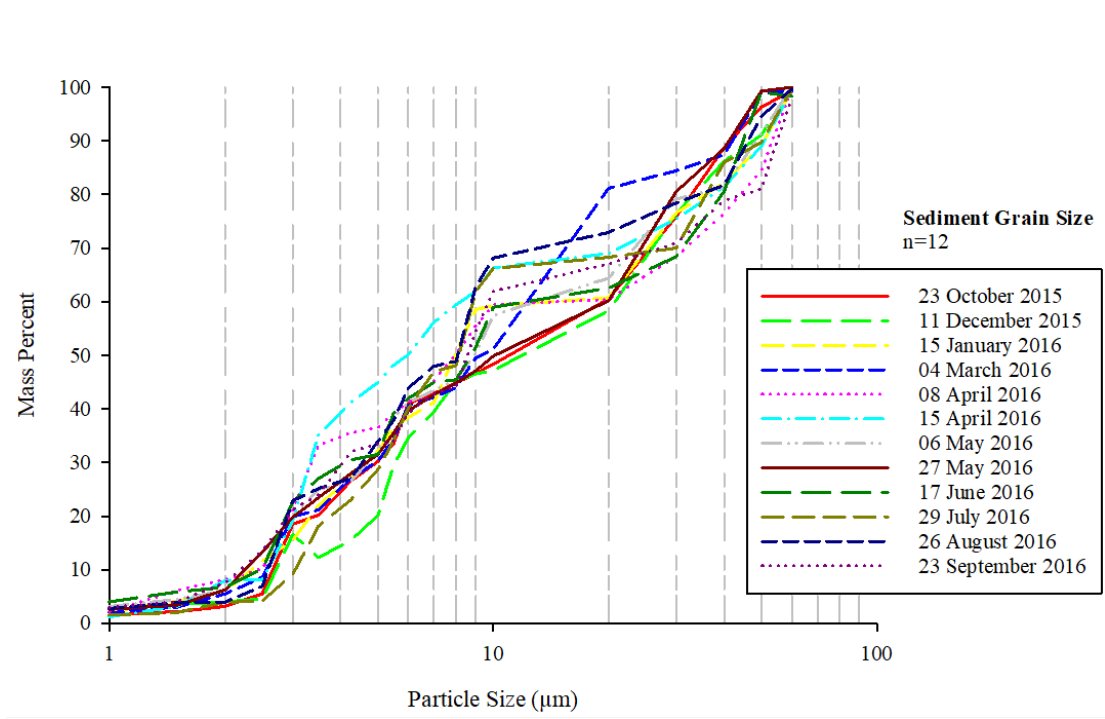


Figure 2.17 Fines analysis of selected target sediment samples collected from Otter Creek, Hardin and Meade counties, Kentucky.

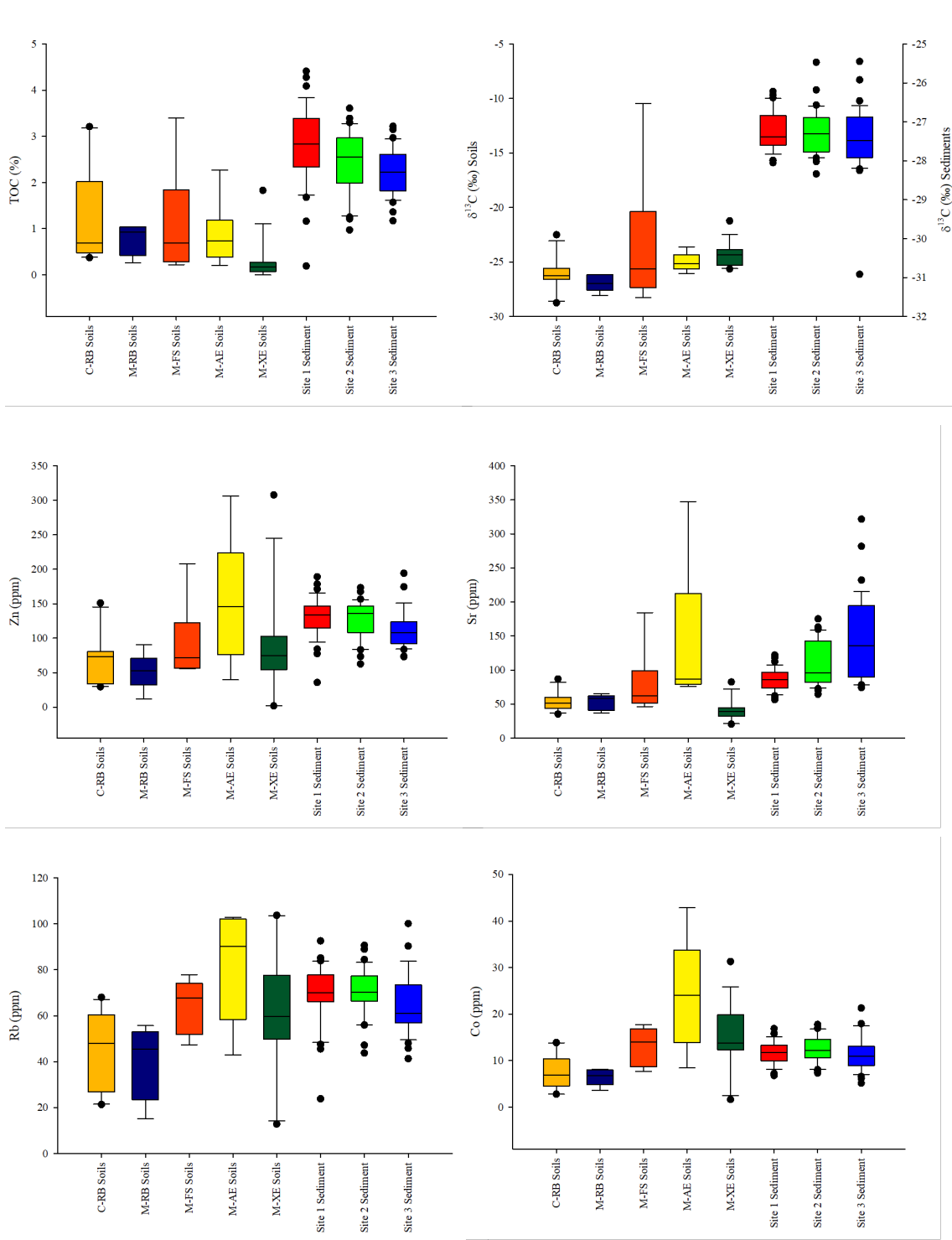


Figure 2.18 Box and whisker plots with error bars representing the 10th and 90th percentiles and outliers for source soil groups and sediment sampling locations by tracer. Tracers: TOC, $\delta^{13}\text{C}$, Zn, Sr, Rb and Co.

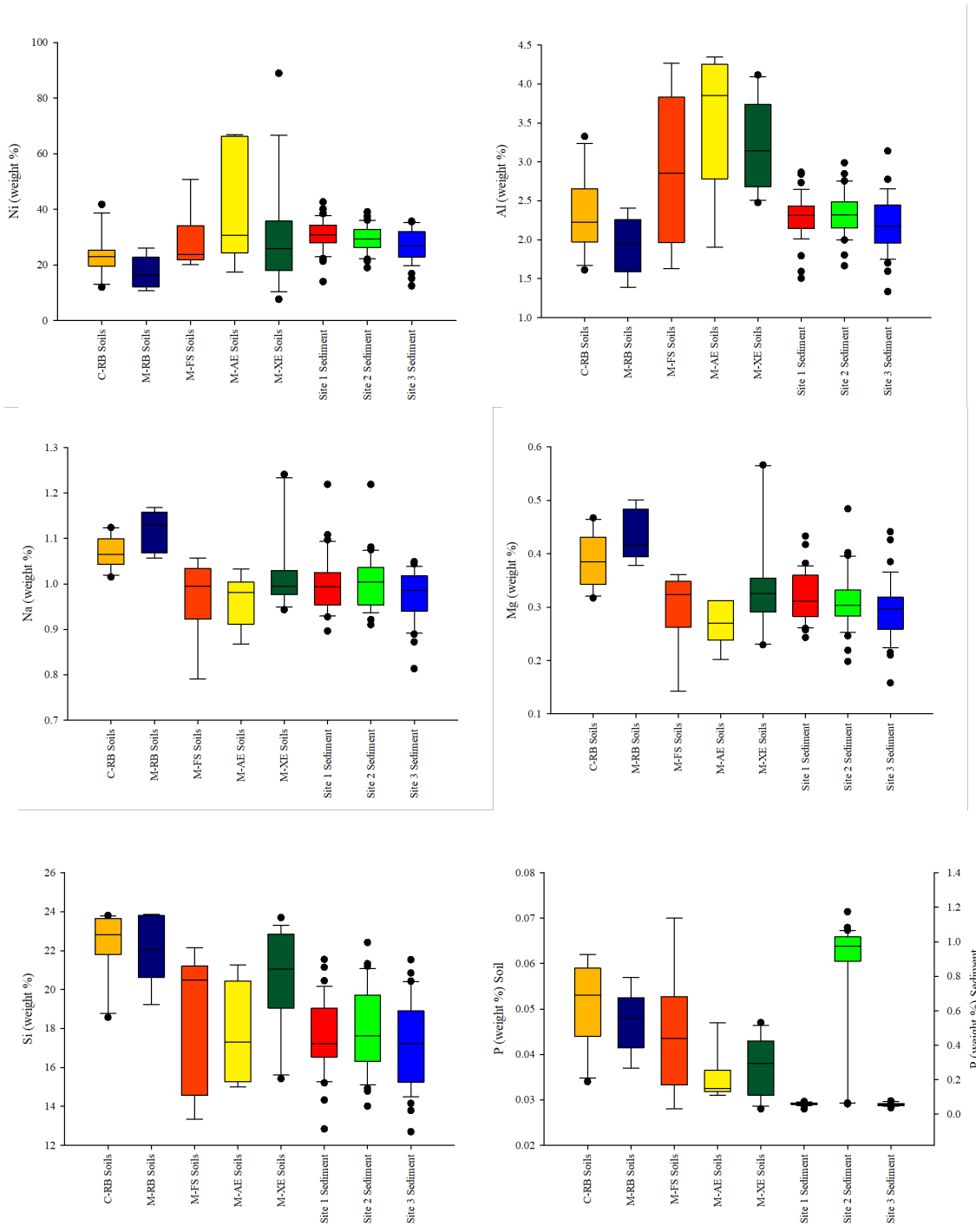


Figure 2.19 Box and whisker plots with error bars representing the 10th and 90th percentiles and outliers for source soil groups and sediment sampling locations by tracer. Tracers: Ni, Al, Na, Mg, Si and P.

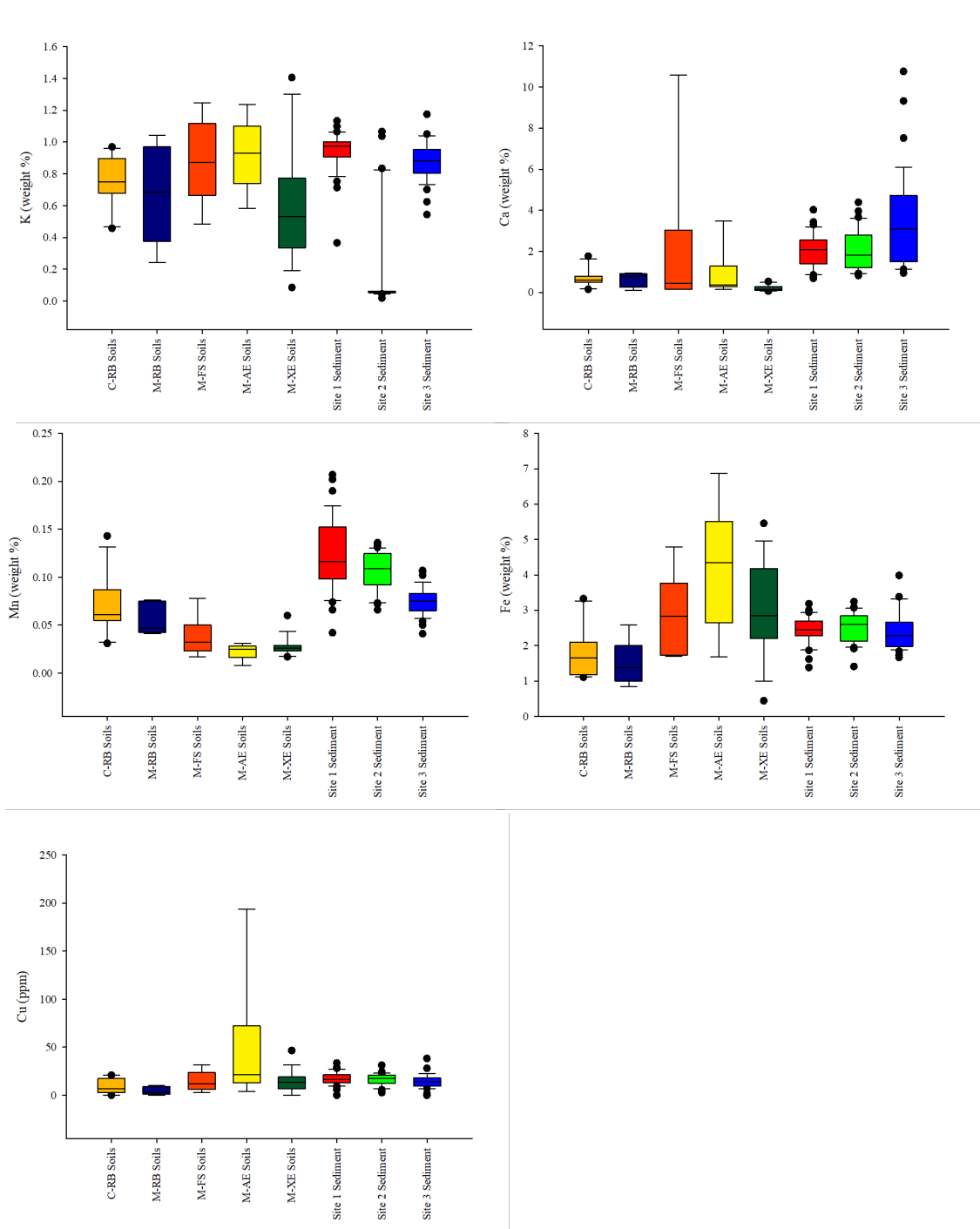


Figure 2.20 Box and whisker plots with error bars representing the 10th and 90th percentiles and outliers for source soil groups and sediment sampling locations by tracer. Tracers: K, Ca, Mn, Fe and Cu.

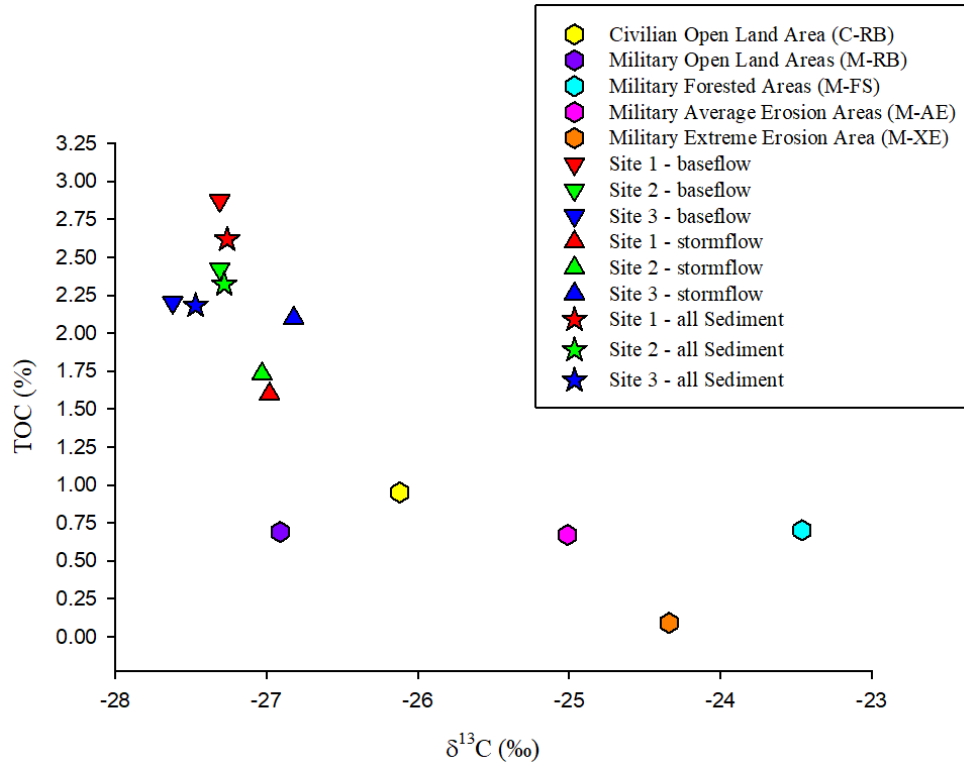


Figure 2.21 δ¹³C and TOC for all source soil groups, all target sediment and base- and stormflow by monitoring location along Otter Creek.

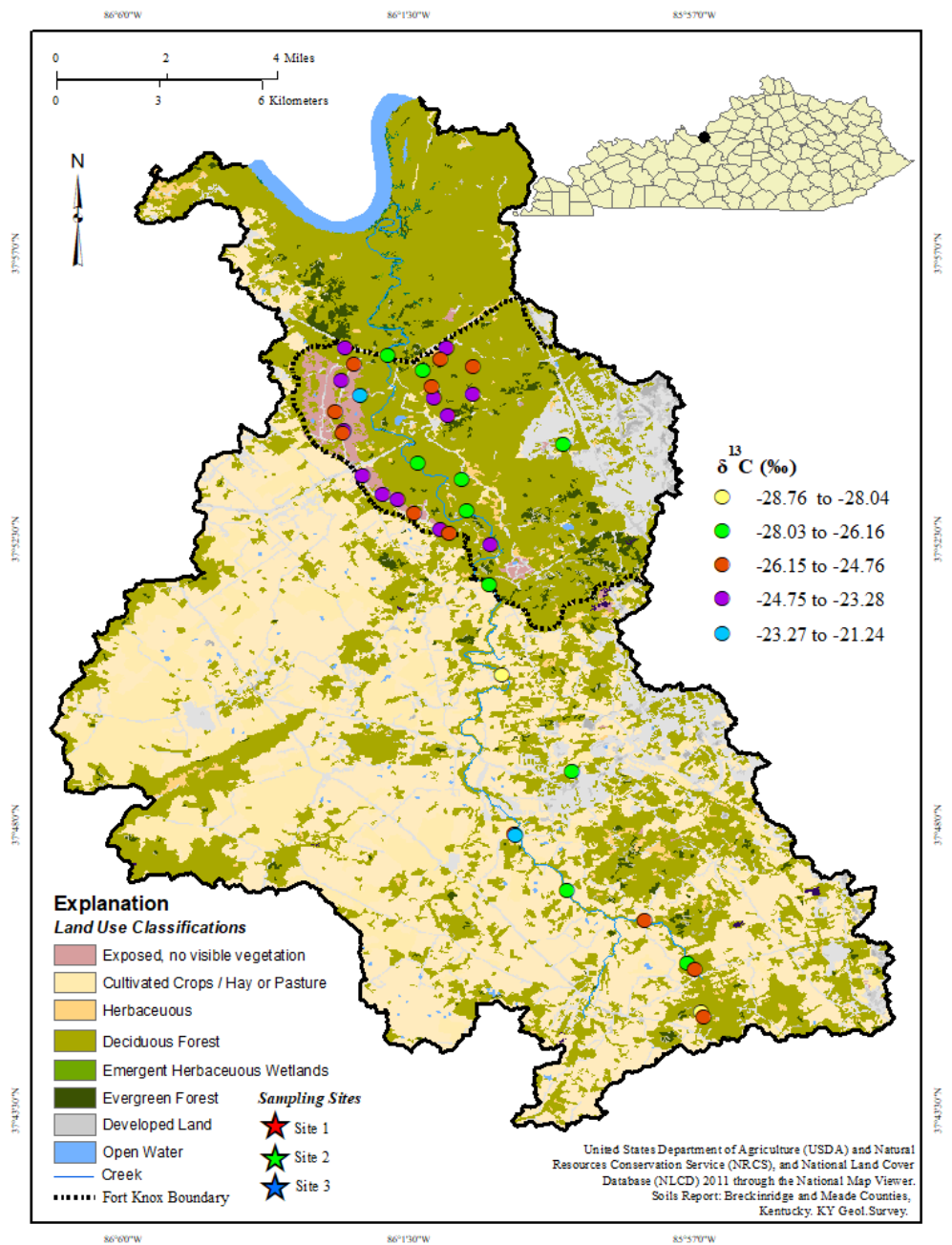


Figure 2.22 Source soil $\delta^{13}\text{C}$ (‰) values overlaid onto the LU/LC map, Hardin and Meade counties, Kentucky.

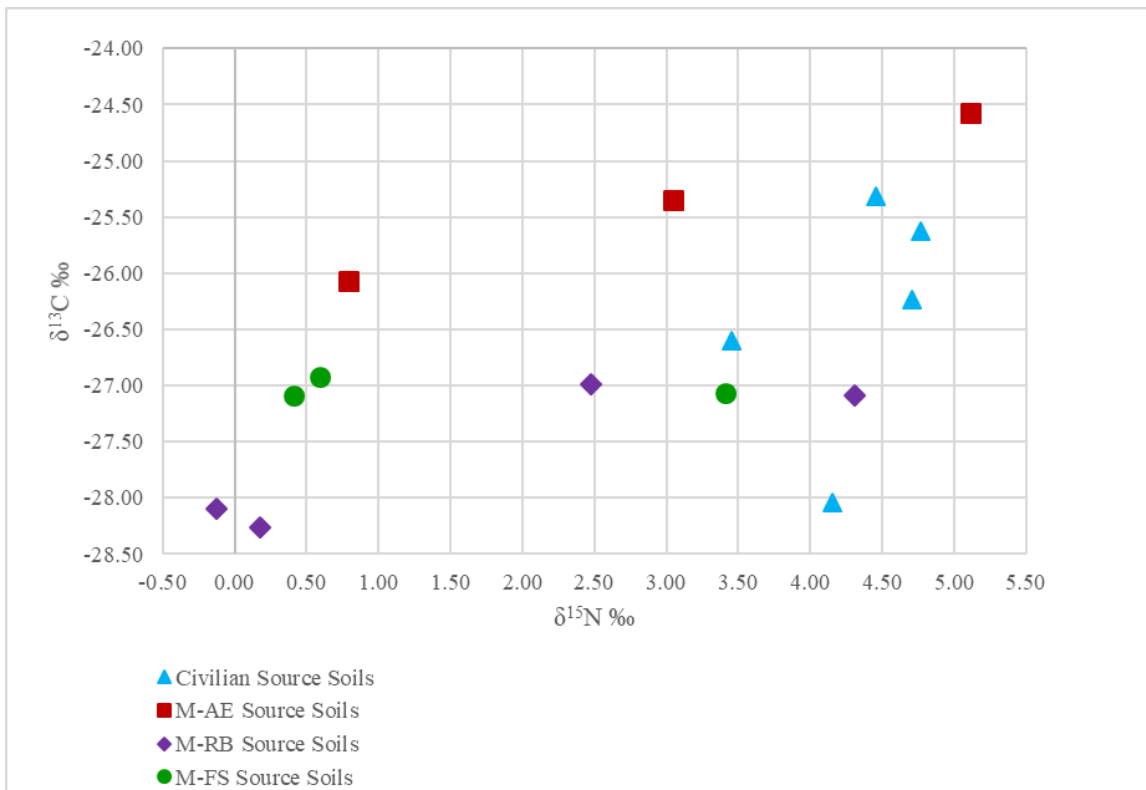


Figure 2.23 Source soil $\delta^{15}\text{N}$ versus $\delta^{13}\text{C}$ (‰) for civilian and three military source soil groups.

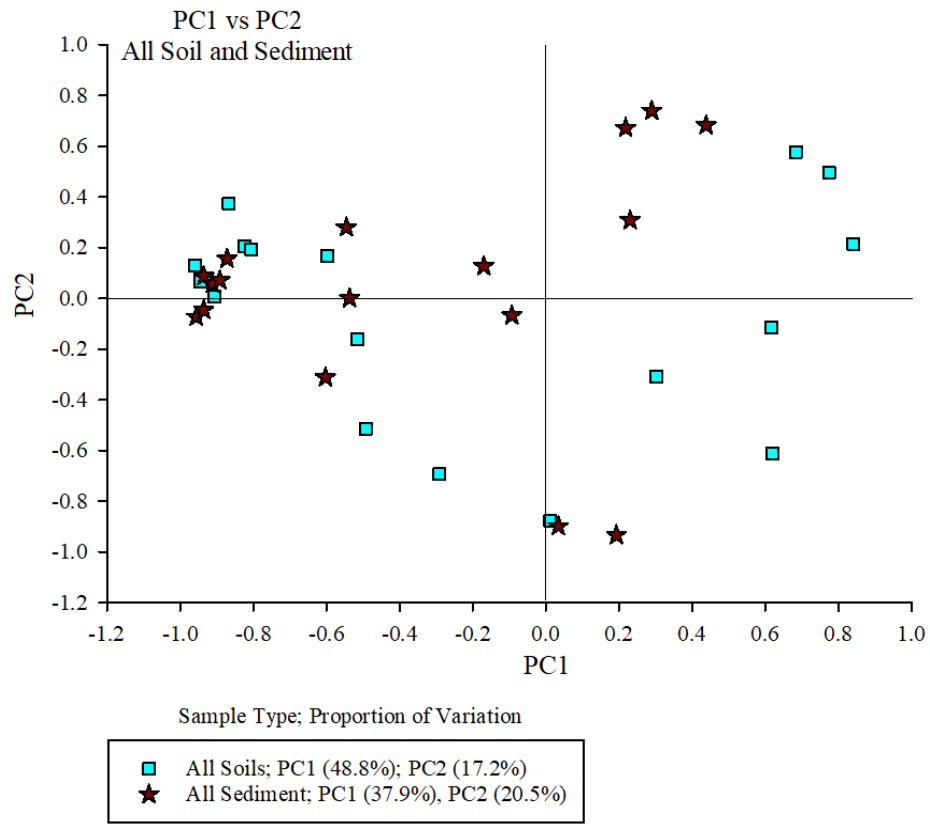


Figure 2.24 Plot of second versus first principal factor loadings and proportion of variation for all source soils and target sediments.

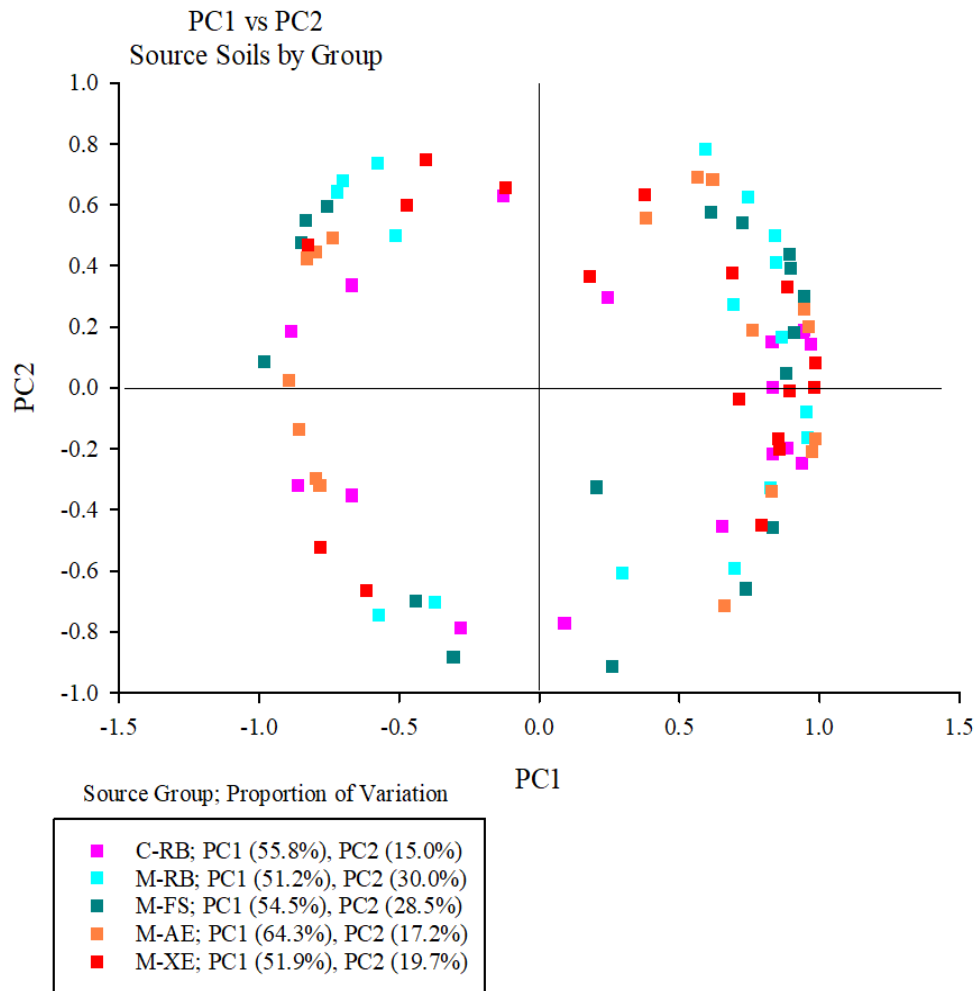


Figure 2.25 Plot of second versus first principal factor loadings and proportion of variance for each of the five source soil categories.

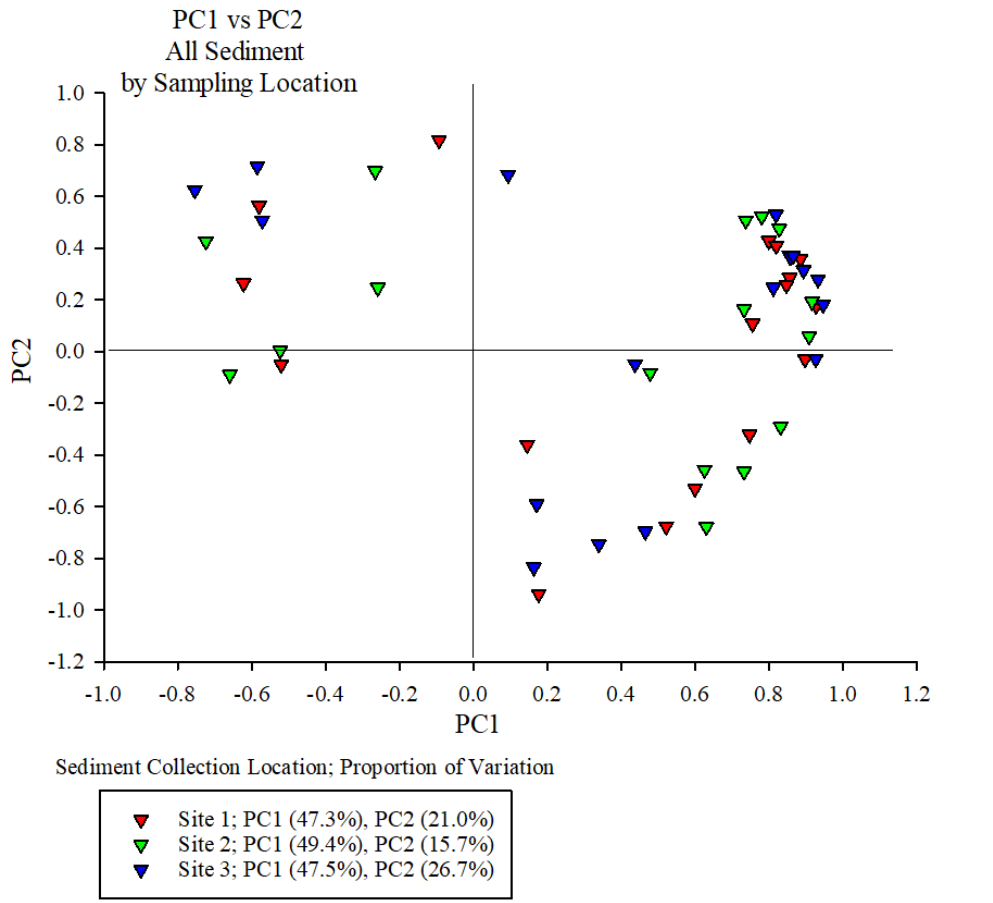
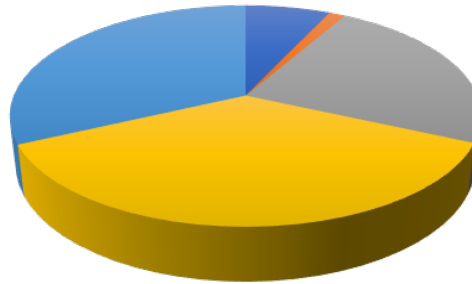


Figure 2.26 Plot of second versus first principal factor loadings and proportion of variation for all target sediments.

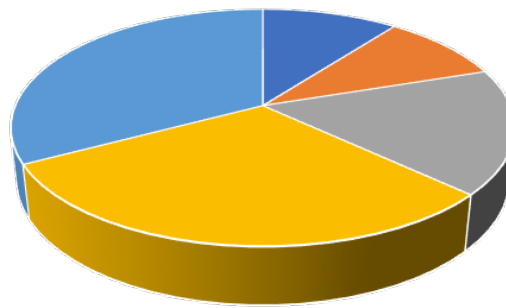
- C-RB
- M-RB
- M-FS
- M-AE
- M-XE

Site 1 - Baseflow Sediment



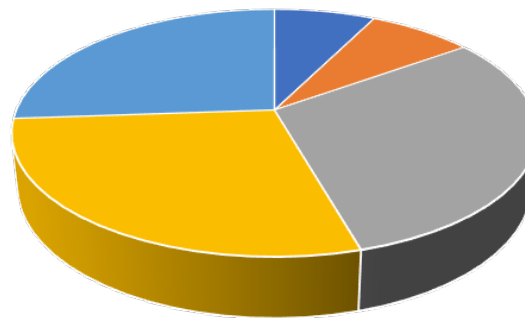
C-RB	6.95%
M-RB	1.33%
M-FS	23.46%
M-AE	36.29%
M-XE	31.97%

Site 2 - Baseflow Sediment



C-RB	10.41%
M-RB	9.51%
M-FS	17.00%
M-AE	30.30%
M-XE	32.78%

Site 3 - Baseflow Sediment



C-RB	7.42%
M-RB	7.69%
M-FS	30.45%
M-AE	28.32%
M-XE	26.12%

Figure 2.27 Percentages of target sediment apportioned to source soil groups by Sed_SAT for baseflow at each of the sediment sampling sites.

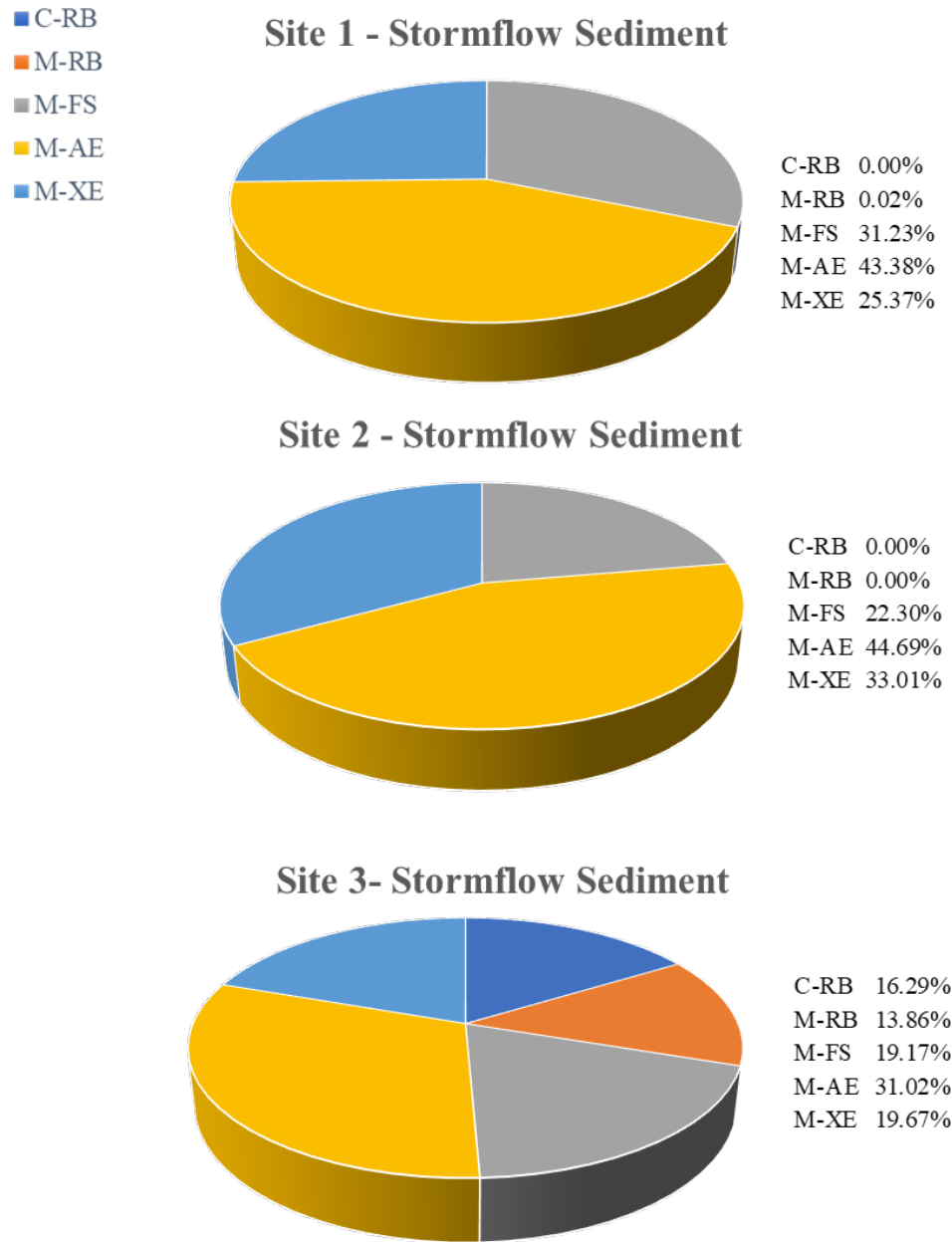


Figure 2.28 Percentages of target sediment apportioned to source soil groups by Sed_SAT for stormflow at each of the sediment sampling sites.

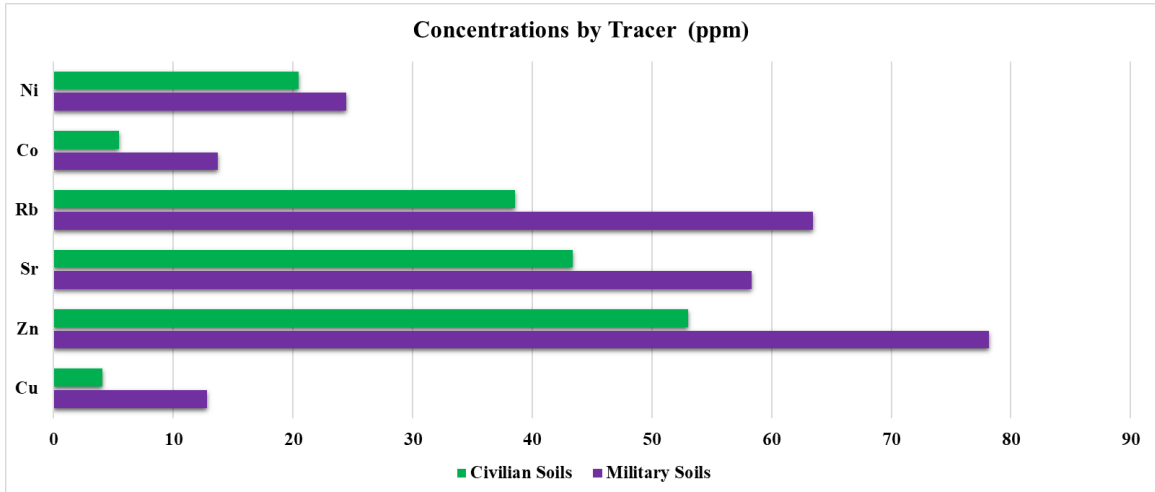


Figure 2.29 Tukey test on XRF data (post-hoc analysis completed after ANOVA) showing that mean concentrations of Ni, Co, Rb, Sr, Zn and Cu were statistically significant ($p < 0.0001$) in differentiating civilian from military source soils, Hardin and Meade counties, Kentucky.

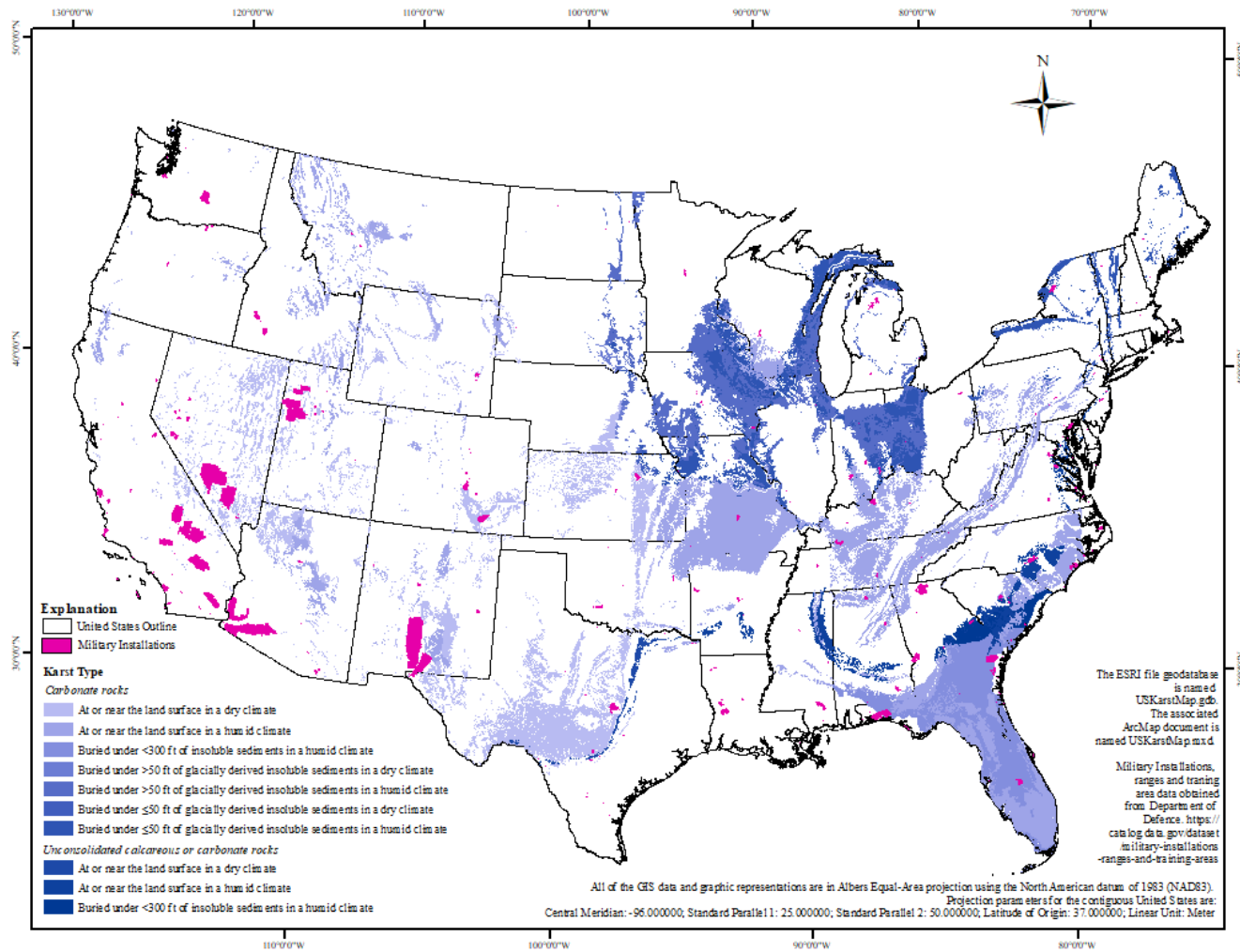


Figure 2.30 Conterminous United States karst map, with different types of karst formations and identified military installations. Data obtained from ERSI and the Department of Defense.

CHAPTER 3. SPATIAL AND TEMPORAL VARIABILITY IN STREAM WATER QUALITY IN A MIXED LAND-USE WATERSHED: OTTER CREEK, KENTUCKY

Peterman, C.^{a *}, A. Fryar^a, D. Edwards^b, K. Murray^c, H. Young^a

^a University of Kentucky, Department of Earth and Environmental Sciences, 121 Washington Avenue, 101 Slone Research Building, Lexington, KY 40506

^b University of Kentucky, Department of Biosystems and Agricultural Engineering, 128 C.E. Barnhart Building, Lexington, KY 40546

^c University of Michigan–Dearborn, Department of Natural Sciences, 4901 Evergreen Rd, Dearborn, MI 48128

* Corresponding author

Email address: cara.peterman@uky.edu; (859) 257-3758; ORCID No.: 0000-0003-1822-2552

Keywords: water quality, anions, sediment, erosion, civilian, military

Abstract

Understanding the influence of multiple land uses and land covers on a watershed can be difficult when trying to outline best-management practices. In this study we examined spatial and temporal variability in water quality along Otter Creek, which drains a 203-km² basin containing farmland, forested areas, and military tracked-vehicle training areas in Hardin and Meade counties, Kentucky (USA). Base- and stormflow were distinguished using an operational definition of baseflow as less than 3 cm of precipitation within a 72-hour period. Field parameters and solute data were obtained at three monitoring sites along Otter Creek. Field parameters, which included water temperature, specific conductance (SC), dissolved oxygen (DO), and pH, were monitored weekly for 1 year (October 2015–October 2016). Water pressure, temperature, and electrical conductivity (EC) were continuously logged every 15 minutes at two sites. Samples were analyzed for anion concentrations from October 2015 to April 2016. Measurements of pH and EC showed downstream increases along Otter Creek, interpreted as resulting from dissolution of carbonate bedrock. During

high-flow events, discharge to the stream is likely to have occurred from runoff and from stormflow through karst conduits. During late winter, chloride concentrations showed peaks that are consistent with road deicer washing off pavement. Pearson correlation analysis indicated that chloride and sulfate may come from similar sources. Elevated sulfate concentrations may result from groundwater inputs along the stream. Elevated nitrate and phosphate concentrations may reflect discharge of treated municipal wastewater, septic-tank leachate, or agricultural runoff.

3.1 Introduction

Many anthropogenic activities can impact the quality of water, elevating concentrations of suspended sediment, nutrients and other non-point-source contaminants (Haag and Porter 1996; USGS 2000). The changes in water quality are associated not only with the temporal fluctuations of climate and streamflow, but also with changes in basin processes as a result of human-induced activities, including land-use practices (e.g. agriculture and forestry) and point-source loading rates (Fuhrer et al. 1996). According to KYEEC (2018), the top 10 categories of stream impairment in Kentucky are sedimentation/siltation, nutrient/eutrophication, specific conductance (SC), unknown causes (nonpoint), total dissolved solids (TDS), organic enrichment (sewage), iron, pH, dissolved oxygen (DO) and lead. These problems are frequently attributed to nonpoint-source pollution via runoff from urban areas and farmlands, as a result of row cropping and animal grazing (KYDOW 2014).

Changes in land use and/or land cover (LU/LC) without proper environmental management strategies can impact surface soils, resulting in an increase in erosion and delivery of excess sediment and nutrients to waterways. Activities that have been shown to

dramatically increase surface erosion include agriculture, off-road vehicles, construction, deforestation and any other activity that disturbs surface soils (NRCS 1995). In addition to the loss of fertile soil and nutrients from erosion, the excess sediment negatively effects aquatic organisms by reducing the ability of light to penetrate water, thereby degrading habitats and impeding respiration of fish and other aquatic organisms (Newcombe and MacDonald 1991; Shields et al. 1994; Newcombe and Jensen 1996; Wilson et al. 2014). Sediment-laden waters can shorten lifespans of reservoirs and hinder fresh water supplies (Owens et al. 2005) and excess nutrients eroded from agricultural fields and residential areas can cause eutrophication of downstream waters (Rabalais et al. 1991; Wilson et al. 2014).

The purpose of this research is to examine water-quality and associated parameters along a stream draining a mixed-use karst watershed during a 1-year period. The Otter Creek watershed in Hardin and Meade counties, Kentucky, drains farms, forests, residential areas, and the Fort Knox Army Installation (hereafter referred to as Fort Knox) (Figure 3.1). We investigate how selected parameters varied seasonally and during base- and stormflow conditions, and we compare values to water-quality standards where appropriate. We relate results to other basins with similar lithology, LU/LC, climate and topographic relief. Lastly, we compare results to historical data obtained from the U.S. Geological Survey (USGS) along Otter Creek and data obtained from the National Oceanic and Atmospheric Administration (NOAA) to examine how the catchment has changed over time.

3.2 Regional Setting

Otter Creek originates from a karst spring within a forest in Hardin County (Figure 3.2), then flows north through rural residential and agricultural (pasture and cropland) areas before entering Fort Knox and ultimately draining to the Ohio River. At baseflow, the stream

disappears into a karst conduit, reemerging from fractured bedrock ~ 1.6 km (1.2 mi) downstream (Figure 3.3). Connair and Murray (2002) performed dye tracing on Fort Knox and noted that two spring basins draining to Otter Creek (Sycamore Spring and Dry Branch; Figure 3.2) account for almost 80% of measured sitewide groundwater discharge.

Weather in the study area can be highly variable given its mid-latitude position on the continent; prevailing surface winds are southerly and light, while upper-level westerly winds steer frontal systems across the state (KYCC 2017). Weather data was collected from two NOAA weather stations: USC00152510 (Elizabethtown, Kentucky, ~ 18 km south of Fort Knox) and USC00150955 (near Brandenburg, Kentucky, ~ 26 km west of Fort Knox). In addition, the U.S. Department of Agriculture (USDA) National Agricultural Statistics Service (NASS) agricultural report for Kentucky provides monthly and annual climate summaries. Figure 3.4 shows minimum and maximum air temperatures and precipitation for October 2015 through September 2016 (NASS 2017).

The watershed lies on the eastern side of the Western Pennyroyal Plateau (KGS 2012), which is underlain by St. Louis and St. Genevieve limestones of Mississippian age (Connair and Murray 2002). These thick limestones form a broad, gently-dipping plateau marked by karst features, including sinkholes and sinking streams (Kepferle 1967; Kepferle and Sable 1977; KGS n.d.). A narrow, linear sandstone body (Figure 3.5) within the Mooretown Formation (Grabowski 2001), part of the Bethel paleochannel (Potter et al. 1958), is oriented southwest–northeast through part of the study area, clipping the northwestern corner of the Fort Knox cantonment area. Soils within the watershed (Figure 3.6) consist predominantly of silt loams with patches of silty clay loam. In particular, soils within the Fort Knox training areas consist mostly of silt loams and large swaths of gravelly

clay with 6-20% exposed slopes, which can be easily eroded (NRCS 2019). Steep rocky outcrops become more prevalent along the creek between the northern boundary of Fort Knox and the Ohio River.

Land use in the study area is predominantly row-crop farming and pastures, but it also includes the City of Vine Grove (population 4,250; 2010 U.S. Census) as well as Fort Knox. Civilian lands make up 81.6% (165.7 km²) of the watershed while military lands are the remaining 18.4% (37.3 km²) (Figure 3.1). According to NASS (2017), the predominant crops grown in Hardin and Meade counties (Table 3.1) were soybeans, hay, corn, winter wheat, and tobacco. There were approximately 47,500 head of cattle in the two counties in 2017 (NASS 2017). Row-crop farmers in the area use two predominant types of N-based fertilizer, urea and anhydrous ammonia.

The military portion of the watershed consists of training lands that have forested areas, large tracts of land with minimal vegetation, and some land that is heavily eroded with little to no vegetation present. Tracked-vehicle training maneuvers were conducted at Fort Knox for more than 40 years. As a result of Base Realignment and Closure (BRAC), a congressionally authorized process that restructured and reorganized military forces as of November 2005 (USDOA 2005), the Armor Center and School, which included heavy tracked vehicles such as tanks, relocated to Fort Benning, Georgia (US Army 2018). Consequently, some heavily disturbed areas at Fort Knox experienced vegetation regrowth and restoration. Despite efforts to restore heavily eroded lands by planting native vegetation, installing erosion barriers in areas where gully erosion is present, and rotating training activities, large swaths of exposed land in the former tracked-vehicle training areas (TAs) are still prevalent. The former TAs lie in Meade County and feature karst uplands (with more

than 20 sinkholes in each training area), steep hills, and flood plains downstream to the confluence with the Ohio River (Crim et al. 2011).

Otter Creek's primary pollutant contributions are listed as municipal point-source discharges, livestock (grazing and feeding operations), and unspecified urban stormwater and landfills (KYEEC 2018). The Vine Grove sewage treatment plant (STP) discharges to an outfall on Otter Creek upstream of the monitoring sites in this study. Vine Grove STP influent is passed through screens for the removal of solids, then sequentially into an aeration tank, to secondary clarifiers, to a chlorine contact basin for disinfection, and through post-aeration steps before discharge (Vine Grove 2019). This STP was constructed in 1989 and has a design capacity of 0.710 million gallons per day (MGD), which is equivalent to 2.71 million liters per day (MLD). The recorded average is 0.370 MGD (1.40 MLD, or 0.0162 m³/s) and a recorded maximum daily average was 2.89 MGD (10.9 MLD, or 0.13 m³/s) (KIA 2017). Under the National Pollutant Discharge Elimination System (NPDES) (USEPA 2010, 2018a), the Vine Grove STP reported less than the maximum amount allowed for all parameters where limitations were specified. The EPA ECHO website showed two effluent permit limit exceedances reported in 2015 (for total suspended solids [TSS] and the fecal bacterial indicator *Escherichia coli*, both in March) and one in 2016 (for TSS in December). Maximum allowed effluent amounts, known as mass-based permit limitations, are listed in Appendix 3.1.

3.3 *Materials and Methods*

In this study, the site 1 sampling location was immediately upstream of Fort Knox where LU/LC is predominantly agricultural, with some military forest just to the east (Figure 3.1). Site 2 was located about halfway through the training areas; land cover consists of

forest and open land with minimal grass cover. Between sites 2 and 3, land use is predominantly military training that involves vehicles and foot maneuvers, ranging from areas with tree canopy, to minor areas with some vegetative cover but no tree canopy, to areas with no vegetative cover and extreme rills and gullies present.

At each site, a stilling well was installed (Figure 3.7), consisting of a 2.5-m metal rod pounded roughly 0.9-1.2 m into the streambed and attached to a 10-cm diameter polyvinyl chloride (PVC) pipe with several 5-cm holes drilled into the sides to allow water to pass through. The stilling well was secured to the metal rod using stainless-steel washers. A Forestry Suppliers WaterMark® Style “C” staff gage graduated in 0.01-ft (3-mm) increments was attached to the rod with zip ties and used for manual stage measurements. Inside the PVC pipe a non-vented In-Situ® Aqua Troll 200 datalogger was housed. The datalogger was scheduled to take readings at 15-minute intervals for EC (electrical conductivity, $\mu\text{S}/\text{cm}$), temperature ($^{\circ}\text{C}$) and pressure (kPa) from 13 November 2015 to 14 October 2016. The dataloggers consisted of a 1.8-cm diameter titanium housing with titanium electrodes (In-Situ 2019). Every 2 to 4 weeks, data were downloaded and sensors were cleaned; once a month the sensors were calibrated to ensure the dataloggers were staying within the manufacturer’s specified range. Due to a programming error no data were logged from 15 January 2016 to 5 February 2016. The stilling well and staff gage at site 3 were lost in a storm event shortly after installation. Forty-one manual stream-stage measurements were collected weekly at sites 1 and 2 from 13 November 2015 to 14 October 2016. There were eight instances when no trip was made to field sites to collect samples and no manual stream-stage measurement was taken: 4 December 2015, 8 January 2016, 22 January 2016, 12 February 2016, 25 March 2016, 29 April 2016, 22 July 2016 and 7 October 2016.

From October 2015 to September 2016, weekly water-quality monitoring was conducted at the three sampling locations using a YSI (Xylem Inc.) 556 multiparameter (MPS) instrument measuring water temperature, DO, specific conductance (SC; temperature-compensated EC), and pH. Calibrations were performed weekly for DO, SC, and pH following the YSI operating manual guidelines (YSI 2009). From 2 October 2015 to 22 April 2016, 20 sets of samples for anion analyses were taken using a depth-integrated sampler (DH-48) (USGS n.d.) at each site, although samples for sites 2 and 3 on 27 November 2015 were lost. The sampler was slowly moved ~ 0.5 m/sec from the bottom of the streambed to the water surface while the sample was being taken following USGS guidelines (Edwards and Glysson 1999). On 18 July 2016, stream profiles and discharge were measured at the three sampling locations along Otter Creek using a YSI SonTek (Xylem Inc.) Flow-Tracker Acoustic Doppler Velocimeter (ADV). The ADV uses an acoustic signal to measure the velocity and direction of flowing water and calculates discharge using established USGS methods (SonTek 2007).

Samples were collected in clean 250-mL HDPE bottles, placed in a cooler to keep water temperature at $\sim 4^{\circ}\text{C}$, and immediately refrigerated upon arrival (the same day) in the laboratory at the University of Kentucky. Water samples were filtered using a $0.45\text{-}\mu\text{m}$ Millipore filter and then split; one set (for anions other than sulfate) was preserved with 4.5 N sulfuric acid (H_2SO_4) to a pH of 2. USEPA (1994) mandates a holding time of 28 days prior to analysis. Given that this threshold could not be met (the holding time was ~ 6 months), all samples were stored in a freezer at -80°C to inhibit chemical transformations, following common practice (Klingaman and Nelson 1976; USEPA 1979; Florence and Batley 1980; Motter and Jones 2015).

Anions were analyzed at the University of Michigan–Dearborn using a Dionex (ThermoFisher Scientific) ICS-3000 ion chromatograph with an IonPac AS22 Fast Analytical Column with Guard Column attachment, following Pfaff et al. (1997). Random duplicate samples, method blanks, and spiked blanks were run for quality control. Eluent solution was made fresh for each run and a seven-anion calibration standard (for bromide, chloride, fluoride, nitrate, nitrite, phosphate, and sulfate) was analyzed before and after each run to ensure accuracy and to check for drift in the instrument. Concentrations of bromide, fluoride and nitrite were below detection limits for all samples.

3.4 Results

3.4.1 Stage and Discharge

During and immediately following a precipitation event, stream stage and flow increase with runoff, especially where soils are saturated or compacted or where there are artificially created impervious surfaces (Rasmussen 1988). Figure 3.8 shows fluctuations in water pressure, which is related to stream stage, at sites 1 and 2 relative to precipitation. Seasonality in precipitation is discernable: 51.5% of the total rainfall occurred during spring and summer (March–September), whereas 48.5% occurred during fall and winter (October–February). Monthly rainfall totals for the entire study period (25 September 2015 to 14 October 2016; Figure 3.9) were mostly above the 30-year monthly averages, particularly in December 2015 and February 2016 (NOAA City ID US210005; Menne et al. 2012a, 2012b). Fluctuations in manually measured stream stage can be seen at both sites, but more so at site 1 than at site 2 (Figure 3.10). Conversely, site 2 exhibited a gradual decline in both pressure and stream stage from March through September.

Stream gaging at baseflow conditions on 18 July 2016 indicated that Otter Creek was relatively wide and shallow, with width ranging from 7 m at site 1 to 20 m at site 3 (Figures 3.11 a–c). Total discharge was 0.44 m³/s at site 1, 0.77 m³/s at site 2 and 0.74 m³/s at site 3, whereas mean velocity was 0.36 m/s at site 1, 0.25 m/s at site 2 and 0.54 m/s at site 3. The discharge at site 3 was lower than the median historical (1999-2010) value for the same date and approximate time (18 July at 1200 hr) at USGS gaging station #03302110, which had been located near site 3 (Figure 3.12).

3.4.2 *Field Parameters*

Seasonality can be observed in both continuous and manual water temperature readings at sites 1 and 2 (Figure 3.13), with an overall cooling trend from October through February and an overall warming trend from March through September. Manual water temperature readings varied by as much as 12.4°C on June 17, 2016 from continuous readings, with the greatest discrepancies occurring from April through August. The discrepancies between continuous and manual readings could be due to differences in where the readings were taken or to radiant heating or cooling of the stilling well. Manual readings were taken at the same location near the sediment traps every sampling period, whereas the stilling well was located downstream near the east bank.

In contrast to water temperature, continuous EC readings at sites 1 and 2 showed less clear seasonality, but still varied with precipitation (Figure 3.14). Throughout the study period, site 1 EC readings tended to be markedly lower than site 2 readings. Exceptions occurred in May and June, when EC readings at both sites tended to track together, and on 23 September 2016) when site 2 EC readings fell below those at site 1. Manually measured SC values (Figure 3.15) were highest on 23 October 2015 at site 1 (598 µS/cm) and on 9

October 2015 at sites 2 and 3 (797 $\mu\text{S}/\text{cm}$ and 732 $\mu\text{S}/\text{cm}$, respectively). SC values were lowest on 11 March 2016 at site 1 (279 $\mu\text{S}/\text{cm}$), site 2 (313 $\mu\text{S}/\text{cm}$) and site 3 (360 $\mu\text{S}/\text{cm}$). Throughout the study period, SC values were lowest at site 1, and they were highest at site 2 except in four instances: 27 November 2015 (site 2, 432 $\mu\text{S}/\text{cm}$; site 3, 574 $\mu\text{S}/\text{cm}$); 11 March 2016 (site 2, 313 $\mu\text{S}/\text{cm}$; site 3, 360 $\mu\text{S}/\text{cm}$); 24 June 2016 (site 2, 499 $\mu\text{S}/\text{cm}$; site 3, 575 $\mu\text{S}/\text{cm}$); and 5 August 2016 (site 2, 398 $\mu\text{S}/\text{cm}$; site 3, 481 $\mu\text{S}/\text{cm}$). Overall, EC and SC demonstrated similar trend but on 20 May 2016 there were large differences at site 1 (EC 337 $\mu\text{S}/\text{cm}$, SC 442 $\mu\text{S}/\text{cm}$) and site 2 (EC 335 $\mu\text{S}/\text{cm}$, SC 460 $\mu\text{S}/\text{cm}$). The discrepancies could be due to where the readings were taken. SC was measured at the sediment traps in the main flow of the stream, closer to the bridge and adjoining agricultural fields on the west bank, whereas EC was measured at the stilling well on the bank adjoining forested areas.

At all three sites DO concentrations were lower in summer and higher in winter (Figure 3.16). DO concentrations ranged from 6.02 mg/L on 6 November 2015 to 11.72 mg/L on 18 December 2015 at site 1, from 8.46 mg/L on 12 August 2016 to 11.53 mg/L on 29 January 2016 at site 2, and from 8.21 mg/L on 12 August 2016 to 11.91 mg/L on 29 January 2016 at site 3. All three sites met Kentucky's water-quality requirements for DO, which state that warm-water aquatic habitats shall be maintained at a 24-hour-average minimum of 5.0 mg/L, with an instantaneous minimum of at least 4.0 mg/L (KYEEC 2019). Values of pH (Figure 3.17) were lowest on 29 January 2016 at site 1 (6.55), on 15 January at site 2 (6.24), and on 29 January at site 3 (6.55). Values of pH were highest on 9 October 2015 at site 1 (8.57), on 8 July 2016 at site 2 (8.19), and on 9 October 2015 at site 3 (8.57).

3.4.3 *Solutes*

Results of solute analyses for sites 1, 2 and 3 can be found in Appendices 3.2, 3.3 and 3.4, respectively. Chloride concentrations ranged from 105.29 mg/L on 13 November 2015 to 743.89 mg/L on 19 February 2016 at site 1; from 89.61 mg/L on 6 November 2015 to 835.63 mg/L on 19 February 2016 at site 2; and from 26.49 mg/L on 16 October 2015 to 723.67 mg/L on 29 January 2016 at site 3 (Figure 3.18). Chloride increased from site 1 to site 2 in 14 of 19 instances where both sites were sampled. Chloride is regulated as a secondary drinking-water constituent with a maximum concentration of 250 mg/L (KYEEC 2019). This standard was exceeded in seven instances at site 1, 12 instances at site 2, and seven instances at site 3. In the absence of other standards, using drinking-water standards is a conservative approach to assess water quality in Otter Creek.

Maximum SO_4^{2-} concentrations were 564.82 mg/L on 18 March 2016 at site 1, 940.61 mg/L on 22 April 2016 at site 2, and 880.21 mg/L on 22 April 2016 at site 3 (Figure 3.19). Sulfate concentrations increased from site 1 to site 2 in 18 of 19 instances. Sulfate concentrations at sites 2 and 3 were relatively similar throughout the study period except for 16 October, when site 2 was 553.10 mg/L and site 3 was 76.63 mg/L. The Kentucky regulatory limit for in-stream SO_4^{2-} (250 mg/L; KYEEC 2019) was exceeded in nine instances at site 1, 17 instances at site 2, and 12 instances at site 3.

The highest NO_3^- concentrations along Otter Creek were on 8 April 2016 at site 1 (127.67 mg/L), 6 November 2015 at site 2 (165.22 mg/L), and 4 March 2016 at site 3 (113.70 mg/L) (Figure 3.19). Nitrate concentrations were greatest at site 1 in 11 of 19 instances. Nitrate concentrations exceeded the Kentucky drinking-water standard of 10 mg/L

as NO₃-N (44.3 mg/L as NO₃) (KYEEC 2019) for at least one site on all but one sampling date.

The highest PO₄³⁻ concentrations along Otter Creek were 78.13 mg/L at site 1 on 2 October 2015, 76.16 mg/L at site 2 on 15 April 2016, and 84.39 mg/L at site 3 on 15 April 2016 (Figure 3.19). Phosphate concentrations were highest at site 1 for eight of 19 instances, particularly in October and in late February to mid-March, and at site 2 for seven instances. Kentucky has not developed water-quality criteria for PO₄³⁻, but West Virginia stipulates maximum total P of 0.03 mg/L for cool-water lakes and 0.04 mg/L for warm-water lakes (USEPA 2018b). By comparison with these values, PO₄³⁻ concentrations at each site along Otter Creek were markedly elevated.

3.5 Discussion

3.5.1 Streamflow and Field Parameters

Streams that have received minimal precipitation over an extended period of time (e.g., several days or longer) and are sustained by groundwater discharge are considered to be at baseflow (Rasmussen 1998). The hydrologic baseflow index (BFI) is calculated as the ratio of baseflow to total streamflow for a given period of time. Munn et al. (2018) created a BFI map for the conterminous United States using over 19,000 measurements from USGS historical data obtained from the streamgauge network. The interpolated raster data map obtained from Munn et al. (2018) for Kentucky (Figure 3.20) shows that baseflow in the Otter Creek basin is mostly estimated to be between 24 to 30 percent of the total streamflow. This BFI range is broadly comparable to those seen in the Ozark Plateau of north-central Arkansas and south-central Missouri and the White and Miami valleys of southern Indiana

and southwest Ohio. These areas, like much of Kentucky, are marked by tile-drained croplands and/or karst terrain (Munn et al. 2018).

The USEPA (40 CFR 122.21(g)(7)(ii)) qualifies a storm event as any rainfall greater than 0.25 cm within the last 72 hours (USEPA 2020). Studies by Ward et al. (2009) and Reed et al. (2011) in two small karst basins in central Kentucky (areas of ~ 2.6 and 8.0 km²) identified wet days as those with ≥ 0.5 cm of precipitation within the preceding 72 hours. For this study, wet days (stormflow conditions) were defined as those with rainfall > 3 cm within the preceding 72 hours. During the 55-week study, 7 weekly measurements were classified as stormflow, and no samples were collected during 8 other weeks because of difficulty accessing sampling sites, adverse weather, or logistical issues. The remaining 40 monitoring dates were classified as baseflow.

Continuous monitoring at sites 1 and 2 showed pressure, water temperature, and EC responses that slightly lagged precipitation. Site 1, which drains 59.4% of the monitored basin area, tended to be flashier than site 2, which drains an additional 32.9% of the area. The less flashy response at site 2 could be a consequence of the larger overall drainage area, but could also result from attenuation of stormflow peaks by subsurface drainage through the karst conduit network between sites 1 and 2. Higher pressure peaks were observed from December through mid-May (Figure 3.8), corresponding to when most precipitation is received in the study area (UKAG 2017). These results are consistent with hydrographs at USGS gaging station #03302110 during 1999–2010, which showed a tendency for streamflow to decrease from late spring to early fall (Figure 3.21).

Median water temperatures were higher during baseflow than during stormflow. Median baseflow temperature was highest at site 3 (15.33 °C) and lowest at site 2 (14.20 °C),

whereas median stormflow temperature was highest at site 2 (12.59 °C) and lowest at site 1 (10.78 °C). The relatively small difference between median baseflow and stormflow temperatures for site 2 may reflect buffering by groundwater discharge downstream of site 1. The tendency for EC values at both sites to decrease following precipitation reflects dilution of TDS in baseflow by runoff. Median SC values were highest during baseflow than stormflow. The highest median SC values during baseflow was site 2 (587 $\mu\text{S}/\text{cm}$) and site 3 (446 $\mu\text{S}/\text{cm}$), whereas site 1 had the lowest median SC during base and stormflow (474 and 388 $\mu\text{S}/\text{cm}$, respectively). The tendency for EC and SC to increase from site 1 to site 2 is consistent with groundwater discharge. The greater residence time of groundwater relative to stream water results in greater solute concentrations from dissolution of minerals, particularly carbonates in limestone. Moore et al. (2009) found that during low-flow conditions the allogenic (point-source) runoff and groundwater in the karstic Upper Floridan aquifer had a different composition than water entering the Santa Fe River during high flow.

3.5.2 *Solutes*

Chloride is a conservative solute that can have both natural and anthropogenic sources (Hem 1985; Sherwood 1989; Wanty et al. 2004). Median base- and stormflow concentrations were higher at site 2 for Cl^- (332.91 and 283.13 mg/L, respectively) than at the other two sites. Anthropogenic Cl^- inputs could be attributed to septic-tank leachate, STP effluent, agricultural runoff (Yanze-Kontchou and Gschwind 1994; Hale and Groffman 2006; Annable et al. 2007; Hunt et al. 2012), or application of highway deicers during winter (Evans and Frick 2001; Hunt et al. 2012). No wastewater is discharged to Otter Creek downstream of Vine Grove, which is upstream of site 1. Elevated Cl^- concentrations on 29 January and 19 February may reflect delayed runoff of road salt following 10.1 cm of snow

that fell 22-23 January and 6.3 cm of rain that fell within 72 hours of 5 February. There was minimal precipitation between 12 February (0.4 cm) and 19 February (1.1 cm). Air temperatures were 18.6°C on 29 January and 18.1°C on 19 February. Road salt from surface runoff enters waterways (Corsi et al. 2010) as well as by entering shallow aquifers, from which it discharges slowly (Ledford et al. 2016; Stets et al. 2018).

Like Cl^- , SO_4^{2-} can have both natural and anthropogenic sources (Hem 1985). For site 2, both base- and stormflow SO_4^{2-} concentrations were higher (637.18 and 409.24 mg/L, respectively) than at the other two sites. Sulfur is naturally occurring in the environment in a reduced form in sedimentary rocks and when oxidized becomes sulfate (Crain and Martin 2009). Water in the basal, gypsiferous part of the St. Louis Limestone is likely to have SO_4^{2-} concentrations in excess of 250 mg/L (Lambert 1979), so elevated SO_4^{2-} may reflect groundwater discharge from springs along the stream.

During baseflow, sites 1 and 2 had comparable median NO_3^- concentrations (74.46 and 74.36 mg/L, respectively) and were only marginally lower than observed stormflow concentrations (76.14 and 76.46 mg/L, respectively). In contrast, concentrations at site 3 were markedly higher during stormflow (70.99 mg/L) than during baseflow (51.61 mg/L). During baseflow, concentrations of NO_3^- decreased slowly from site 1 to site 3, while during stormflow minimal increases were seen moving downstream. In aerated soils, nitrification transforms ammonium to NO_3^- , which is readily leached (Wells 1996). Because Kentucky soils are usually not frozen throughout the winter, but remain relatively wet, the residual NO_3^- remaining after harvest is lost either by leaching or back to the atmosphere through denitrification (UKAG 2011). A study of predominantly agricultural watersheds in karst terrains in eight Kentucky counties found that NO_3^- in streams was primarily contributed by

groundwater discharge (Taraba et al. 1997). Those authors noted that denitrification within the stream and the riparian zone can significantly affect the mean NO_3^- concentrations of water discharging from a watershed. Agricultural land uses and nonpoint source contributions to surface waters can effectively undermine the ecological balance and in-stream nutrient processes of freshwater systems (Carey and Migliaccio 2009).

Median concentrations for PO_4^{3-} during baseflow were similar at sites 1 and 2 (55.85 mg/L and 55.25 mg/L, respectively) and lowest at site 3 (49.05 mg/L). Baseflow solute values were marginally higher than stormflow. For stormflow, sites 1 and 3 had higher median PO_4^{3-} concentrations (53.94 and 52.28 mg/L, respectively) than site 2 (47.79 mg/L). Phosphorus can be contributed to streams by mineral weathering, fertilizer runoff, and sewage (Hem 1985). Adsorption and coprecipitation on minerals and uptake by aquatic vegetation limit PO_4^{3-} concentrations in natural waters (Hem 1985; Daniel et al. 1998; Withers and Jarvie 2008). When applied to soils, PO_4^{3-} reacts rapidly to form compounds that are less soluble than the form in which the fertilizer was added, which is in large part due to the iron and aluminum oxides found in Kentucky soils (Wells 1996). Consequently, some of the PO_4^{3-} measured in stream-water samples, particularly during stormflow, may be particulate (e.g., colloidal).

3.5.3 *Statistical Analyses*

Relationships among variables were tested using a Pearson correlation coefficient (Table 3.2) with statistical significance at a p-value of 0.05. A significant negative relationship was observed between water temperature and DO, which is expected based on solubility constraints (Appendix 3.5). For sites 1 and 2, the significant positive relationship between SC and pH could reflect solute loading from carbonate dissolution (via groundwater

discharge) as well as from the Vine Grove STP. At all three sites, there was a significant positive relationship between Cl^- and SO_4^{2-} , which suggests common sources for both anions, such as effluent from individual septic systems, STP discharge, and/or fertilizer runoff.

Principal component analysis (PCA) was conducted to analyze spatial patterns of water-quality variables. The first two factor loadings (F_1 and F_2) and proportion of variance are displayed in Table 3.3. For site 1, the proportions of variances were 52.7% for F_1 and 28.2% for F_2 , with F_1 having high correlations ($p > 0.4$) for Cl^- , SO_4^{2-} , and NO_3^- , while F_2 was only highly correlated with SO_4^{2-} and PO_4^{3-} . The first two factor loadings for site 2 had relatively close proportions of variance (39.3% and 32.1%, respectively), with F_1 being positively correlated with Cl^- and SO_4^{2-} and F_2 with SO_4^{2-} and PO_4^{3-} . For site 3, F_1 had a proportion of variance of 50.2% and was highly correlated with Cl^- , SO_4^{2-} , and NO_3^- , while F_2 had a proportion of variance of 27.2% and was highly correlated with SO_4^{2-} and PO_4^{3-} . Sites 1 and 3 had relatively similar proportions of variance for F_1 and F_2 and had the same positive correlations with Cl^- , SO_4^{2-} , NO_3^- and PO_4^{3-} , indicating that water chemistry at sites 1 and 3 was similar.

3.5.4 Comparisons with Historical Data

Historical (1994-98) water-quality data from USGS gaging station #03302110 show several significant differences relative to data from site 3 during the study period. Monthly measurements of water temperature, SC, DO, and pH were recorded during most months (36 of 47) from October 1994 through August 1998 (Table 3.4). For water temperature, the blue number indicates the coldest value for each month and red indicates the warmest value, while for SC, DO, and pH, the red numbers indicate the highest value for that month. A Kruskal-Wallis H-test (Table 3.5) indicates that median DO for 1994-98 (10.9 mg/L) was

significantly higher than for weekly 2015-16 monitoring (9.73 mg/L; $p = 0.0002$), although there was not a significant difference in water temperature (medians 12.5 °C for 1994-98 and 14.89 °C for 2015-16; $p = 0.054$). Conversely, 1994-98 SC was significantly lower than 2015-16 SC (median 433 versus 547.5 $\mu\text{S}/\text{cm}$, respectively; $p = 2.3 \times 10^{-7}$). There was a marginally significant difference between 1994-98 and 2015-16 median pH values (7.95 versus 8.12, respectively; $p = 0.047$).

Historical data indicate that mean annual discharge (in m^3/s) along Otter Creek increased in years with elevated precipitation (in cm). These included 1996 (6.2 m^3/s , 149.1 cm), 1997 (6.6 m^3/s , 140.8 cm), 2002 (6.0 m^3/s , 157.6 cm), 2003 (5.1 m^3/s , 154.1 cm), 2006 (5.3 m^3/s , 139.3 cm), and 2008 (7.2 m^3/s , 139.3 cm). The NOAA Earth System Research Laboratory has identified 1994-95, 1997-98, 2002-03, 2006-07 and 2014-15 as El Niño events (NOAA 2019). For the current study period, there were 6 months of above normal precipitation with a warmer-than-average winter (NASS 2017), which corresponded with an El Niño year. For such conditions, rates of weathering and solute fluxes would be expected to increase (Eimers and Dillon 2002).

Differences between historical values of field parameters along Otter Creek and values in this study could reflect LU/LC changes in the watershed. Using historical LU/LC imagery from the National Land Cover Database with the Spatial Analyst extension in ArcGIS 10.6, LU/LC for civilian and military lands in the Otter Creek watershed was compared for 1992 and 2011 (Table 3.6). In 1992, civilian lands were composed of 66.4% farmland (including crop and pasture), 21.1% forest (trees, shrubs, herbaceous), 11.6% developed, and 1.0% other. In 2011, civilian lands were composed of 57.1% farmland, 29.6% forest, 12.2% developed, and 1.1% other. Figure 3.1 provides a detailed image of

2011 LU/LC distributions for the study area. The resolution of aerial imagery has improved since 1992, which could lead to some uncertainty in calculating changes in different LU/LC types. However, general trends are evident (a decrease in cropland and an increase in forest cover). The increase in civilian developed lands is consistent with population growth. Between 1990 and 2010, the population of each county grew by 18.3% (by 16,303 persons for Hardin County and by 4,432 persons for Meade County) (U.S. Census Bureau 1990, 2010). Military lands were composed of 34.9% forest, 57.8% developed, and 7.3% other in 1992, versus 63.6% forest, 23.8% developed and 12.3% other in 2011. The training lands are part of the forested area and there was notable increase in forest cover from 1992 to 2011.

3.5.5 *Limitations of Results*

Data gaps in this study include loss of the datalogger at site 3 during a storm event shortly after installation; missing measurements from the dataloggers at sites 1 and 2 between 15 January and 5 February 2016; the 8 weeks during which manual measurements were not taken; the abbreviated period of solute monitoring; and the loss of anion samples for sites 2 and 3 on 27 November 2015. In addition, fluid pressure readings have not been corrected for barometric pressure fluctuations because the Solinst Barologger deployed at site 3 failed shortly after installation. Although a positive relationship between measured fluid pressure and stream stage was observed as expected at sites 1 and 2, the correlation coefficient for the linear regression was weaker at site 1 ($R^2 = 0.49$; Figure 3.22) than at site 2 ($R^2 = 0.80$; Figure 3.23). We speculate that the staff gage at site 1 may not have been as well secured as at site 2. Differences between manually measured and continuously monitored water temperature values may reflect radiant heating of the datalogger inside the stilling well, as inferred by Fryar et al. (2000) based on observations of a streambank

monitoring well in western Kentucky. Consequently, we have focused on qualitative trends in fluid pressure, stream stage, and logged water temperature at sites 1 and 2, rather than absolute values of those parameters. The combination of weekly field parameter readings and continuous monitoring provided cross-validation of results.

3.6 *Conclusions*

This study has documented temporal and spatial trends in water quality along Otter Creek, which drains a patchwork of LU/LC (farms, residential areas, forests, and military training lands) in karst terrain in north-central Kentucky. During a 1-year period (October 2015–October 2016), field parameters were monitored weekly at three sites. Water pressure, temperature and EC were continuously recorded at the two upstream sites (November 2015–October 2016) and solutes (Cl^- , SO_4^{2-} , NO_3^- and PO_4^{3-}) were monitored weekly at all three sites (October 2015–April 2016). An operational definition of baseflow as < 3 cm of rainfall within 72 hours of manual monitoring provided a distinction between high- and low-flow events.

As a result of storms, fluid pressure temporarily increased (consistent with stage rises), EC temporarily decreased (as a result of dilution by runoff), and water temperature fluctuated at sites 1 and 2, as observed by Reed et al. (2011) and Fryar et al. (2017) for a mixed-LU/LC karst basin in central Kentucky. From December through mid-May, higher pressure responses were seen, whereas during drier months (summer and late fall) pressure tended to be lower. The relatively small difference between median baseflow and stormflow temperatures for site 2 and the tendency for EC and SC to increase from site 1 to site 2 is consistent with groundwater discharge along that reach of the stream.

A significant negative relationship was observed between water temperature and DO, which is expected based on solubility constraints. Dissolved oxygen varies seasonally with water temperature, but groundwater discharge and forest cover along the stream network are likely to modulate water temperature and DO fluctuations. A significant positive relationship between Cl^- and SO_4^{2-} at all three sites suggests common sources of both anions, such as septic systems, the Vine Grove STP, and/or surface runoff from fertilized agricultural lands. In addition, elevated Cl^- values in January and February 2016 could have resulted from road-salt runoff, as inferred for streams in northern Kentucky (Crain and Martin 2009). Dissolution of gypsum by groundwater in the St. Louis Limestone is a plausible source of SO_4^{2-} in Otter Creek. Covariance with Cl^- suggests that SO_4^{2-} is conservative in this system. Nitrate concentrations, particularly at site 3 (the farthest downstream), tended to increase from late autumn through winter, which may reflect slow nitrification and leaching from soils following higher-than-average precipitation. The origins of nonpoint-source nitrate within the watershed are not easily identified due to mixing of different sources and the spatial variability of inputs and transformation across the variable hydrologic conditions (Kaushal et al. 2011).

Differences between historical and present-day hydrochemical data can be examined in the context of LU/LC changes. Notwithstanding the increase in population in Hardin and Meade counties, the percentage of developed civilian land increased only slightly ($\sim 1 \text{ km}^2$) between 1992 and 2011. The percentages of forested civilian and military lands increased, whereas the percentages of civilian farmland and military training land decreased. Between 1994-98 and 2015-16, there was a significant increase in SC, a significant decrease in DO, and a marginally significant increase in pH at the farthest downstream monitoring site. An

increase in TDS, as indicated by SC, would seem to be inconsistent with increasing forest cover in the watershed because of concomitant decreases in application of agrichemicals and in erosion of bare soil (Wolter et al. 2006). However, the available data does not allow us to apportion solute loads to different LU/LC settings.

The results of this study indicate that water quality in Otter Creek has been impacted by nutrients and other non-point-source pollutants. Water-quality standards were met for DO but not for various solutes. In addition, karst terrains are sensitive to contamination because of the direct and rapid connection that exists between the land surface, groundwater, and streams via sinkholes, conduits, and springs (Dressing et al. 2016). To assess the impacts of various land-use activities on water quality and aquatic health in Otter Creek, including recreational exposure of visitors to Otter Creek Park, continued monitoring of stream flow, field parameters, nutrients, and other water-quality parameters (including suspended sediment and fecal indicators) is recommended.

Acknowledgements

The authors gratefully acknowledge support from the Fort Knox Environmental Management Division, Natural Resource Division and Range Control for providing access to training lands. Funding for this project was provided by U.S. Geological Survey grant G16AP00055 through the Kentucky Water Resources Research Institute; by a Casner Fellowship from the University of Kentucky (UK) Tracy Farmer Institute for Sustainability and the Environment; and by the University of Kentucky's Department of Earth and Environmental Sciences (UKEES) Ferm Research Support Fund. We thank the Kentucky Geological Survey and UKEES Pioneer Lab for laboratory support.

Table 3.1 Predominant crops grown in Hardin and Meade Counties, Kentucky.

Crop	Acres	Hectare
Soybeans	66,900	27,074
Hay	52,800	21,367
Corn	39,300	15,904
Winter Wheat	7,600	3,076
Tobacco	980	397

Table 3.2 Pearson correlation between water quality parameters. For pairs where there is a negative correlation coefficient (R) and p-values ≤ 0.05 , one variable tends to decrease while the other increases. For p-values greater than 0.05 there is no significant relationship between the two variables.

Site 1	DO (mg/L)	SC ($\mu\text{S/cm}$)	pH	Cl (mg/L)	SO ₄ ²⁻ (mg/L)	NO ₃ ⁻ (mg/L)	PO ₄ ³⁻ (mg/L)
Water Temp (°C)	R = -0.551	0.300	0.097	-0.275	-0.035	-0.482	0.331
	p = 0.000	0.067	0.546	0.286	0.895	0.050	0.195
DO (mg/L)		-0.090	-0.084	0.236	0.027	0.393	-0.083
		0.563	0.585	0.316	0.909	0.0867	0.727
SC ($\mu\text{S/cm}$)			0.315	0.078	0.455	-0.241	0.439
			0.037	0.751	0.051	0.320	0.060
pH				-0.107	0.136	-0.450	0.492
				0.653	0.568	0.046	0.0274
Cl (mg/L)					0.668	0.250	-0.544
					0.001	0.288	0.013
SO ₄ ²⁻ (mg/L)						0.055	-0.153
						0.819	0.521
NO ₃ ⁻ (mg/L)							-0.450
							0.046
							20
Site 2	DO (mg/L)	SC ($\mu\text{S/cm}$)	pH	Cl (mg/L)	SO ₄ ²⁻ (mg/L)	NO ₃ ⁻ (mg/L)	PO ₄ ³⁻ (mg/L)
Water Temp (°C)	R = -0.623	0.387	0.432	-0.541	-0.071	-0.178	0.293
	p = 0.000	0.014	0.005	0.030	0.794	0.510	0.271
DO (mg/L)		-0.197	-0.487	0.329	-0.421	-0.041	-0.554
		0.189	0.001	0.169	0.073	0.867	0.014
SC ($\mu\text{S/cm}$)			0.340	0.046	0.524	-0.204	0.150
			0.022	0.858	0.026	0.418	0.552
pH				0.191	0.236	0.094	0.102
				0.434	0.331	0.701	0.679
Cl (mg/L)					0.515	0.204	-0.483
					0.024	0.402	0.036
SO ₄ ²⁻ (mg/L)						-0.051	0.142
						0.837	0.561
NO ₃ ⁻ (mg/L)							-0.102
							0.678
							19
Site 3	DO (mg/L)	SC ($\mu\text{S/cm}$)	pH	Cl (mg/L)	SO ₄ ²⁻ (mg/L)	NO ₃ ⁻ (mg/L)	PO ₄ ³⁻ (mg/L)
Water Temp (°C)	R = -0.593	0.426	0.158	-0.423	-0.033	-0.613	0.033
	p = 0.000	0.006	0.324	0.102	0.905	0.012	0.905
DO (mg/L)		-0.167	-0.141	0.332	-0.364	0.364	-0.111
		0.267	0.344	0.165	0.126	0.126	0.650
SC ($\mu\text{S/cm}$)			0.250	0.043	0.267	-0.268	0.104
			0.094	0.866	0.284	0.282	0.682
pH				-0.335	-0.061	-0.099	0.060
				0.161	0.803	0.687	0.807
Cl (mg/L)					0.559	0.503	-0.208
					0.013	0.028	0.392
SO ₄ ²⁻ (mg/L)						0.238	-0.058
						0.326	0.815
NO ₃ ⁻ (mg/L)							-0.443
							0.057
							19

Table 3.3 Principal component analysis for solutes with first and second factor loadings, proportion of variance and variables.

	F ₁	F ₂
Site 1	52.7%	28.2%
Cl ⁻	0.895	0.275
SO ₄ ²⁻	0.670	0.648
NO ₃ ⁻	0.541	-0.673
PO ₄ ³⁻	-0.752	0.422
Site 2	39.3%	32.1%
Cl ⁻	0.954	0.074
SO ₄ ²⁻	0.512	0.820
NO ₃ ⁻	0.283	-0.395
PO ₄ ³⁻	-0.566	0.670
Site 3	50.2%	27.2%
Cl ⁻	0.834	0.293
SO ₄ ²⁻	0.640	0.618
NO ₃ ⁻	0.786	-0.331
PO ₄ ³⁻	-0.532	0.714

Table 3.4 Historical water-quality data from the U.S. Geological Survey. Red numbers for SC, pH and DO indicate highest value seen between years for that month. For WT the blue numbers indicate the coldest value seen between the years for that month while the red numbers indicate warmest.

	Specific Conductivity ($\mu\text{S}/\text{cm}$)						pH							
	1994	1995	1996	1997	1998	2015	2016	1994	1995	1996	1997	1998	2015	2016
January		353	367		410		552		7.20	7.50		8.10		8.28
February		267	496	442	432		485		6.50	8.20	8.20	8.50		8.03
March		434	349	314	381		455		6.30	7.60	7.10	8.30		7.57
April		472	419	435	409		471		7.10	8.10	7.70	8.00		7.44
May		386	440	396	420		439		7.00	8.20	7.90	8.10		8.23
June					309		544					7.90		8.25
July		464	391	490	479		566		8.20	8.30	8.00	8.20		7.89
August				453	505		521				8.00	8.10		8.02
September		446	497				577			7.70				7.89
October	550	513	518			688	665	7.40	7.90	7.80			8.37	7.69
November	483	351				511		7.30	7.80				8.11	
December	428		445	424		483		7.60	8.00	8.00	8.40		8.03	

	Dissolved Oxygen (mg/L)						Water Temperature ($^{\circ}\text{C}$)							
	1994	1995	1996	1997	1998	2015	2016	1994	1995	1996	1997	1998	2015	2016
January		16.0	10.4		10.9		11.2		0.00	12.00		9.80		12.81
February		16.2	12.2	11.5	14.1		10.9		1.20	5.50	9.00	10.10		11.02
March		11.3	10.2	11.3	12.3		10.4		10.70	13.00	10.50	6.80		8.79
April		11.5	12.0	10.8	10.8		9.4		11.80	11.50	12.00	13.70		12.13
May		9.3	9.9	11.0	12.5		9.6		18.50	19.00	14.50	17.60		14.73
June					8.9		8.8					18.00		14.92
July		7.8	9.0	9.8	9.8		8.8		21.50	19.50	23.00	22.10		16.09
August				9.7	9.6		8.6				19.50	22.40		20.11
September		10.1	8.2				8.9		15.70	20.50				21.10
October	9.4	13.5	10.0			9.8	10.4	14.80	11.50	13.50			16.00	21.72
November	11.0					10.3		13.10	9.90				14.53	
December	11.4		11.6	13.4		10.8		5.80		9.00	3.80		12.37	

Table 3.5 Kruskal-Wallis H-test, historical versus study period parameters. Otter Creek, Hardin and Meade counties, Kentucky.

	Adj H	p-value	Significant
SC	26.99	2.3×10^{-7}	Yes
pH	3.94	0.0470	No
DO	13.79	0.0002	Yes
WT	3.72	0.0540	No

p-value < 0.05 = Statistically Significant

Table 3.6 Percent land use / land cover for 1992 and 2011, Hardin and Meade counties, Kentucky.

	1992		2011		Percent Change	
	Civilian	Military	Civilian	Military	Civilian	Military
Forest	21.1	34.9	29.6	63.6	8.5	28.7
Cropland	66.4	0.0	57.1	0.0	-9.3	0.0
Other	1.0	7.3	1.1	12.3	0.1	5.0
Developed	11.6	57.8	12.2	23.8	0.6	-34.0

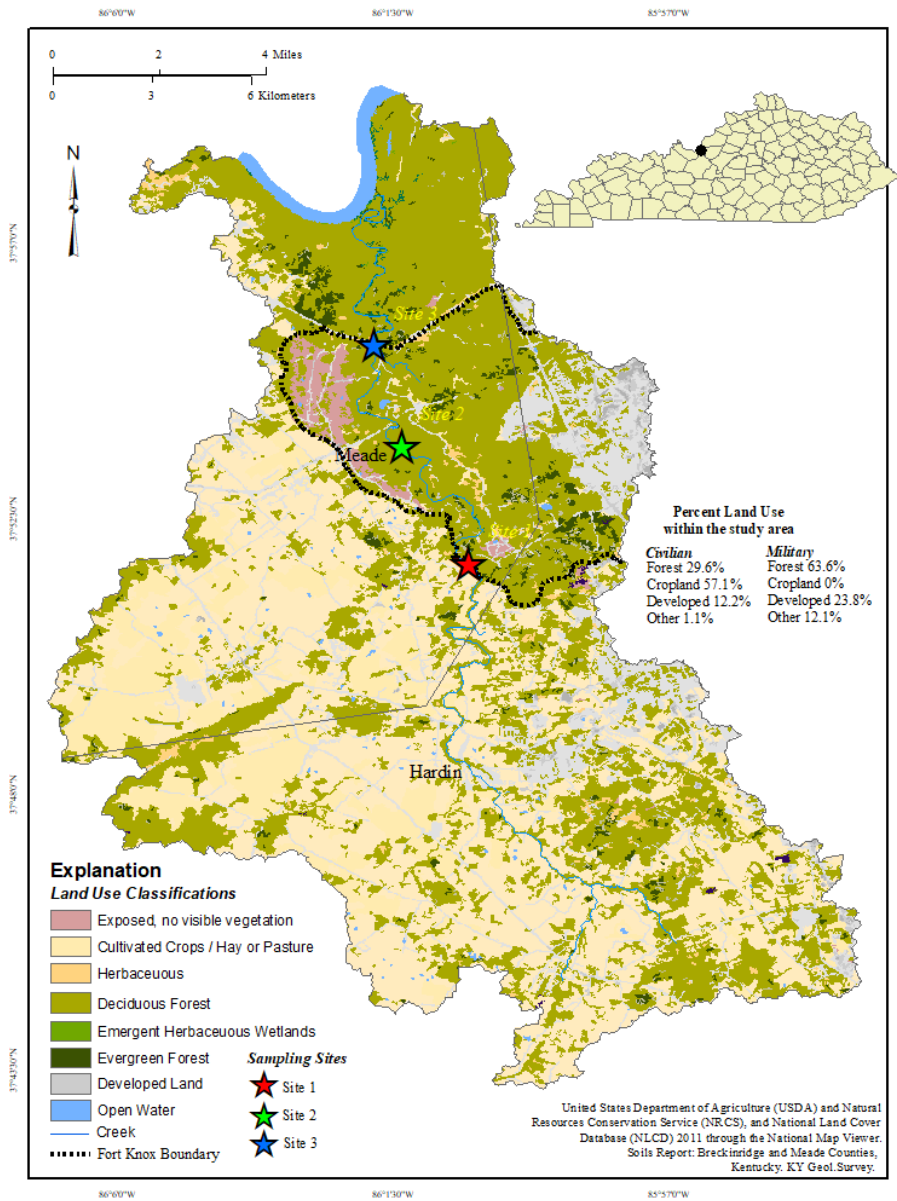


Figure 3.1 Land use and land cover for Hardin and Meade counties, Kentucky.

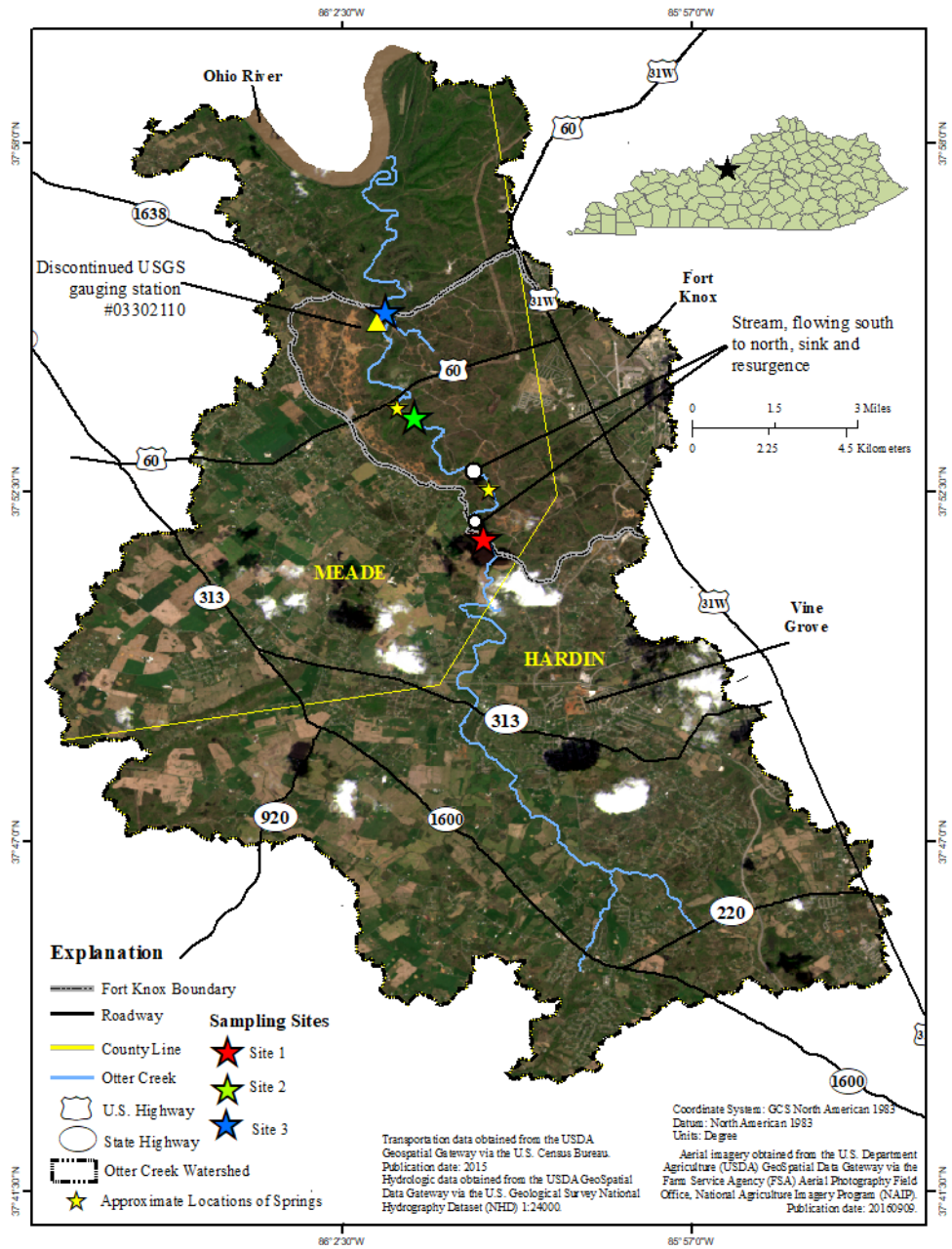


Figure 3.2 Study area, Hardin and Meade counties, Kentucky.



Figure 3.3 Otter Creek disappearing into karst conduit. (right) and reappearing out of fractured limestone bedrock on left.

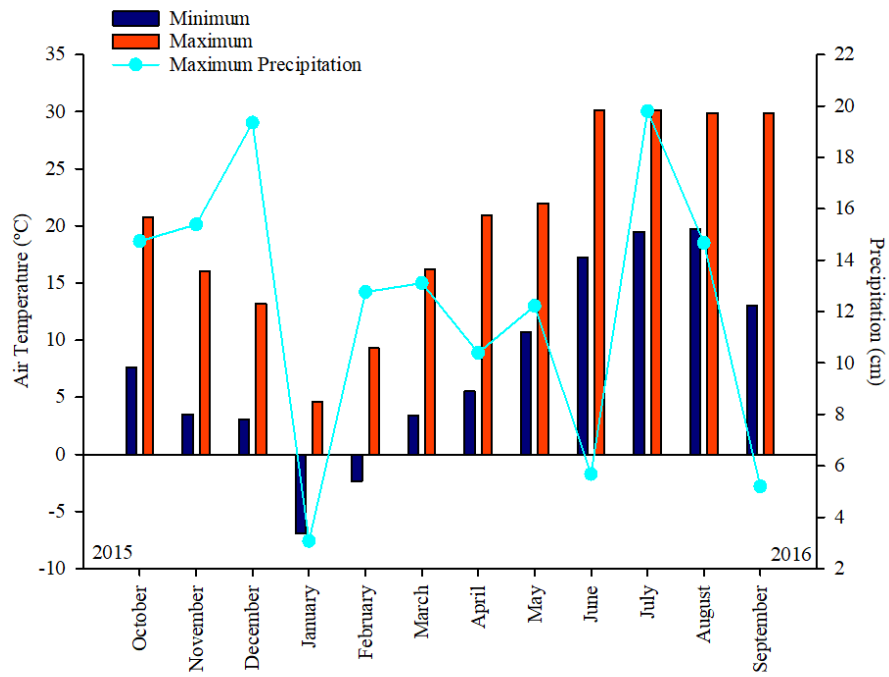


Figure 3.4 Minimum and maximum air temperature and precipitation throughout the study period, Hardin and Meade counties, Kentucky.

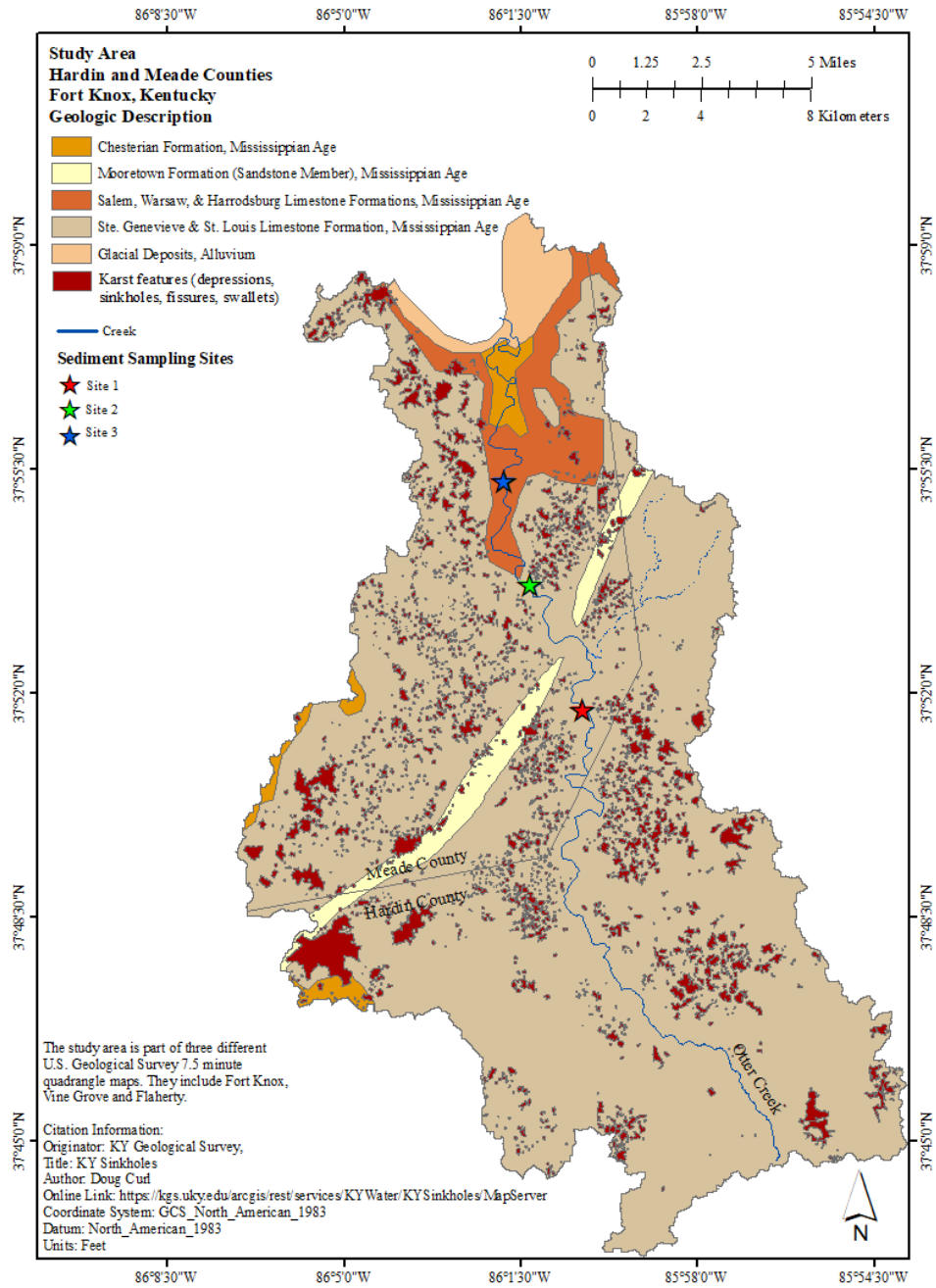


Figure 3.5 Kentucky geology with karst overlay within Hardin and Meade counties, Kentucky.

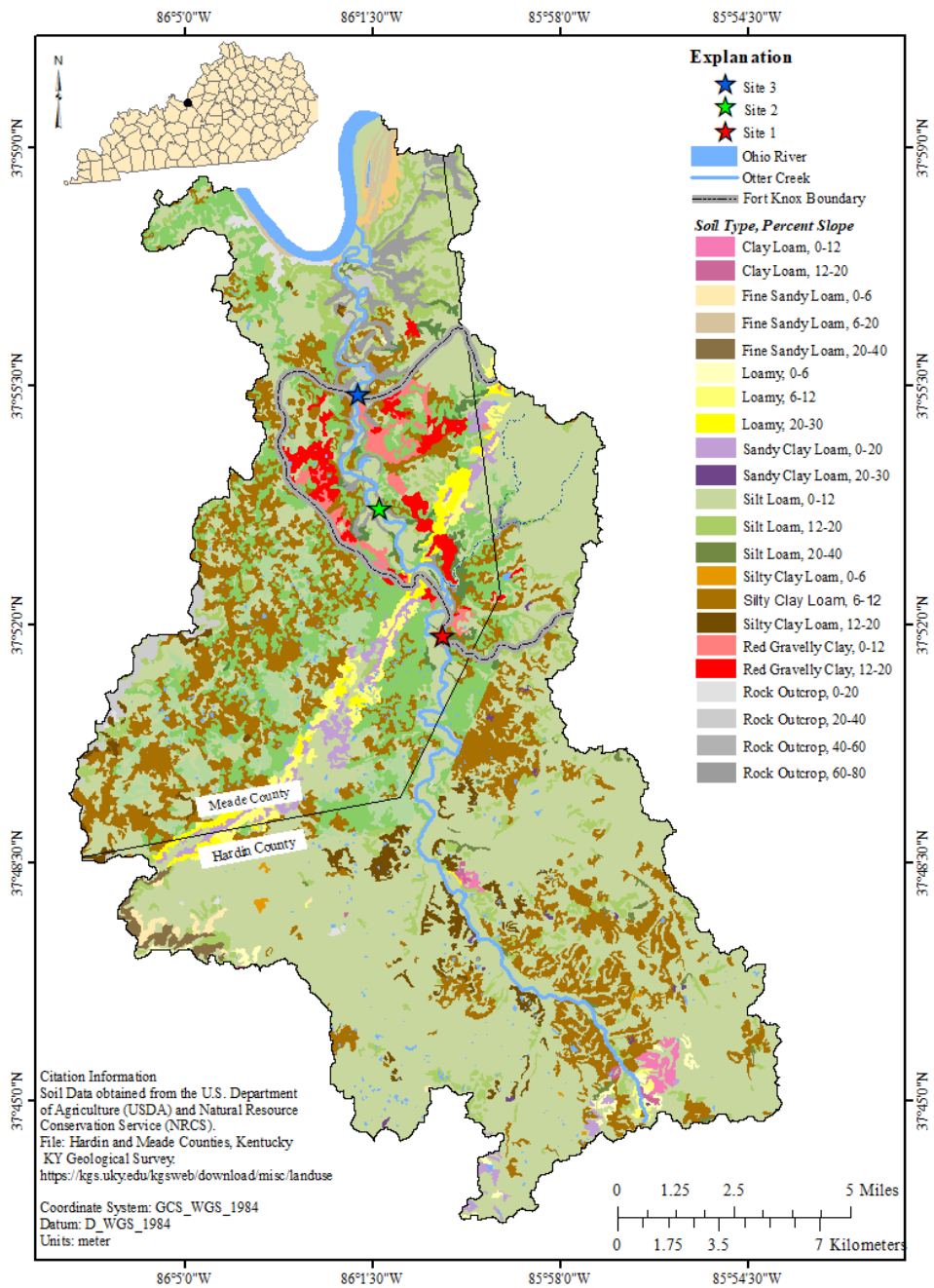


Figure 3.6 Soils and percent slope within Hardin and Meade counties, Kentucky.



Figure 3.7 Image to far right is Xylem YSI InSitu® datalogger and still well at site 2. Middle and far right image is of stage-gage at site 2. Pictures taken by C. Peterman, dates vary.

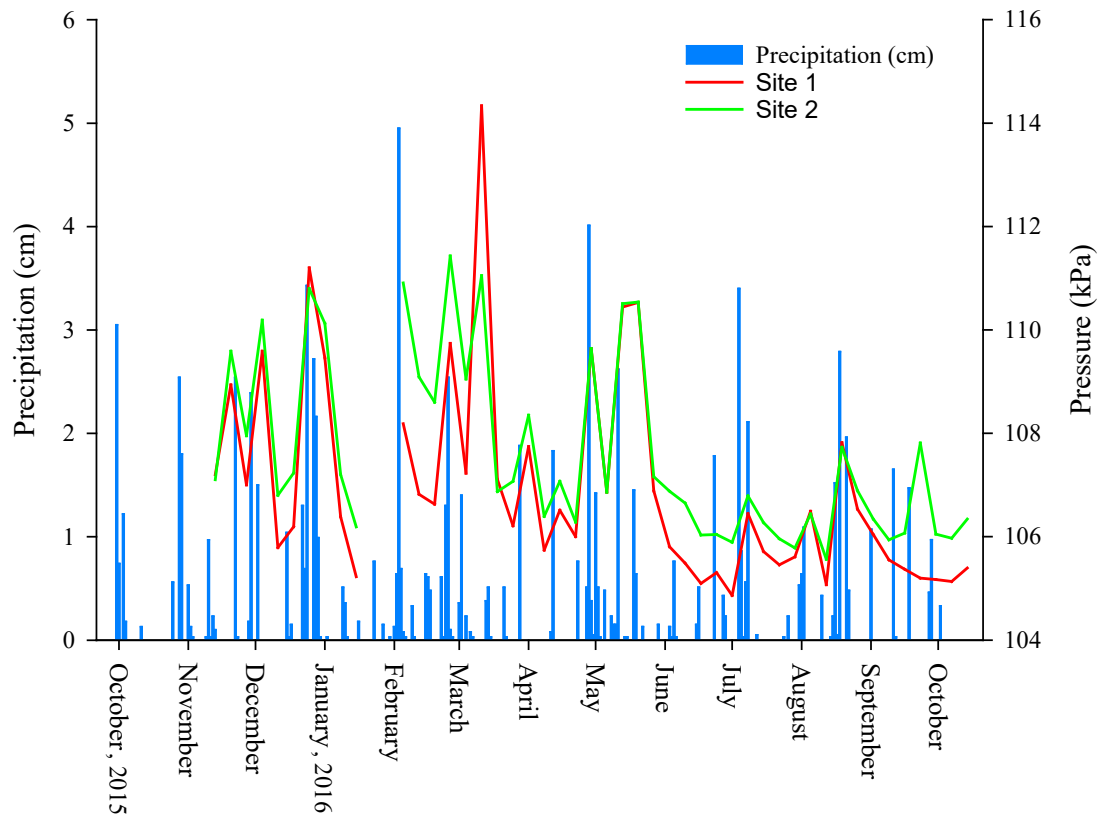


Figure 3.8 Precipitation (cm) obtained from NOAA for October 2015 through October 2016. Site 1 and 2 pressure (kPa) obtained from InSitu continuous dataloggers on Otter Creek, Kentucky from 13 November 2015 through 14 October 2016.

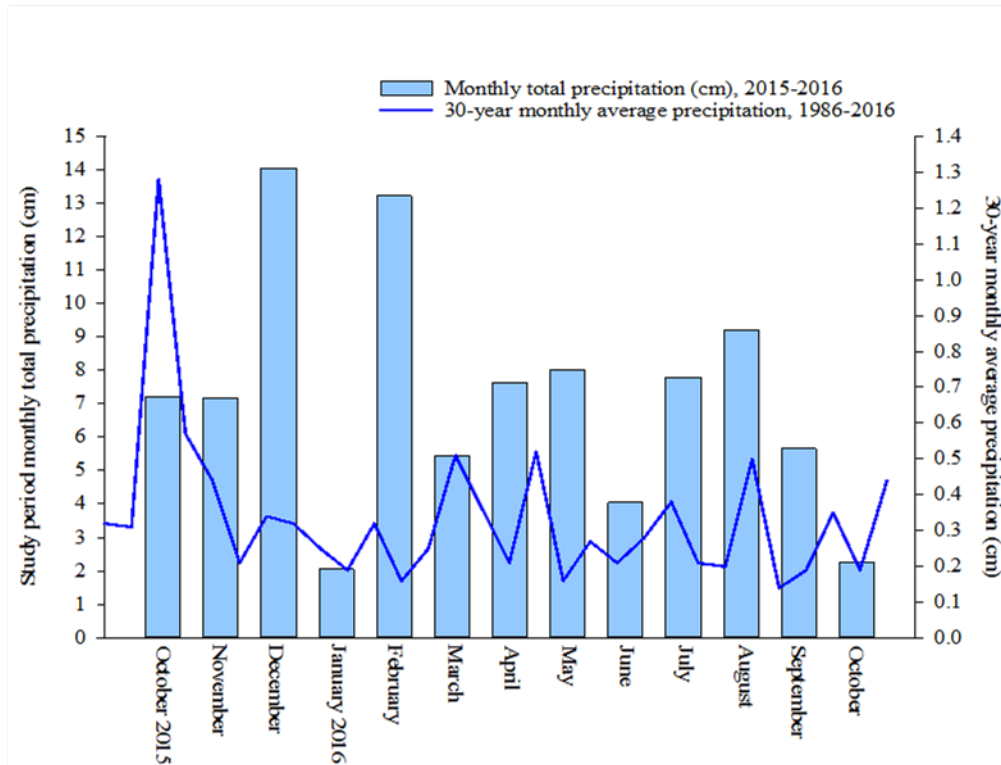


Figure 3.9 Comparison of the study period monthly total precipitation from October 2015 through October 2016 with average monthly precipitation for 1986 through 2016, Otter Creek, Kentucky (NOAA, Fort Knox City ID US210005).

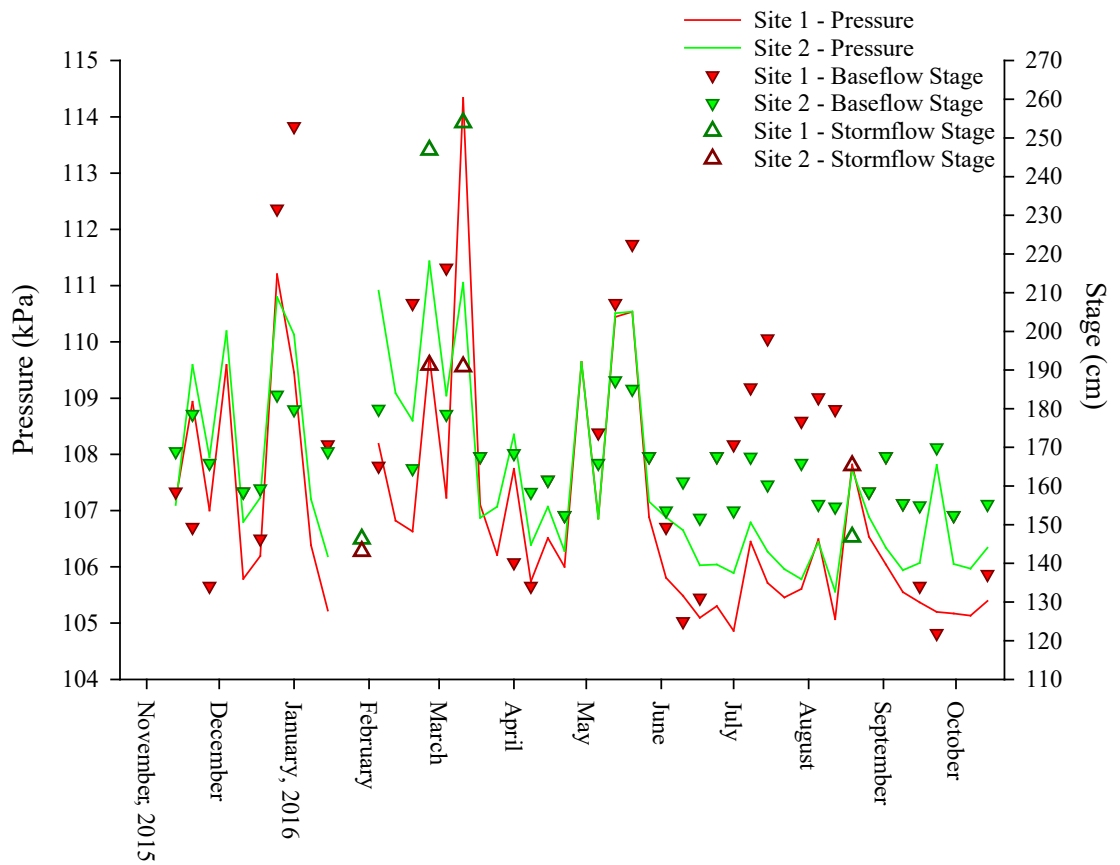


Figure 3.10 Pressure (kPa) and stage (cm) obtained from InSitu continuous dataloggers located at sites 1 and 2, Otter Creek, Kentucky from 13 November 2015 through 14 October 2016. Operational definition of baseflow was < 3 cm of precipitation 72 hours prior.

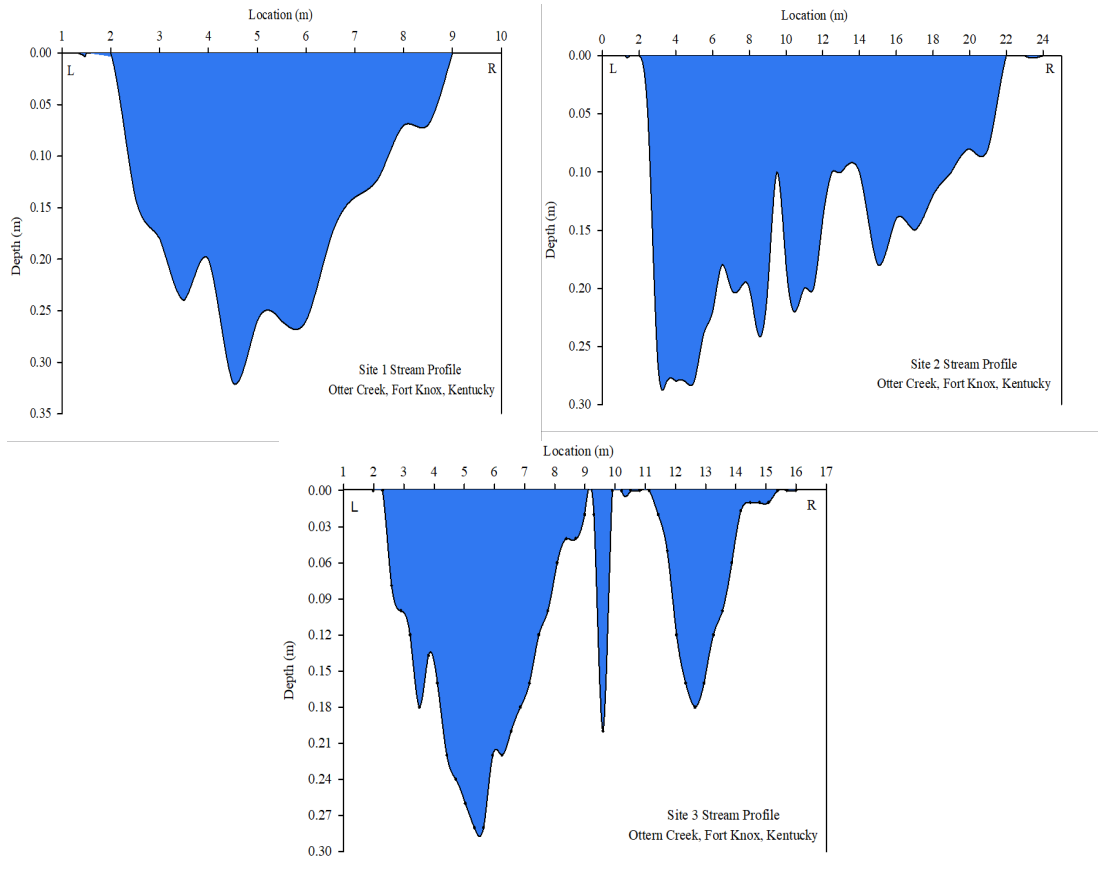


Figure 3.11 Stream profiles completed on July 18, 2016 for each sampling location along Otter Creek, Kentucky. a) site 1, b) site 2 and c) site 3.

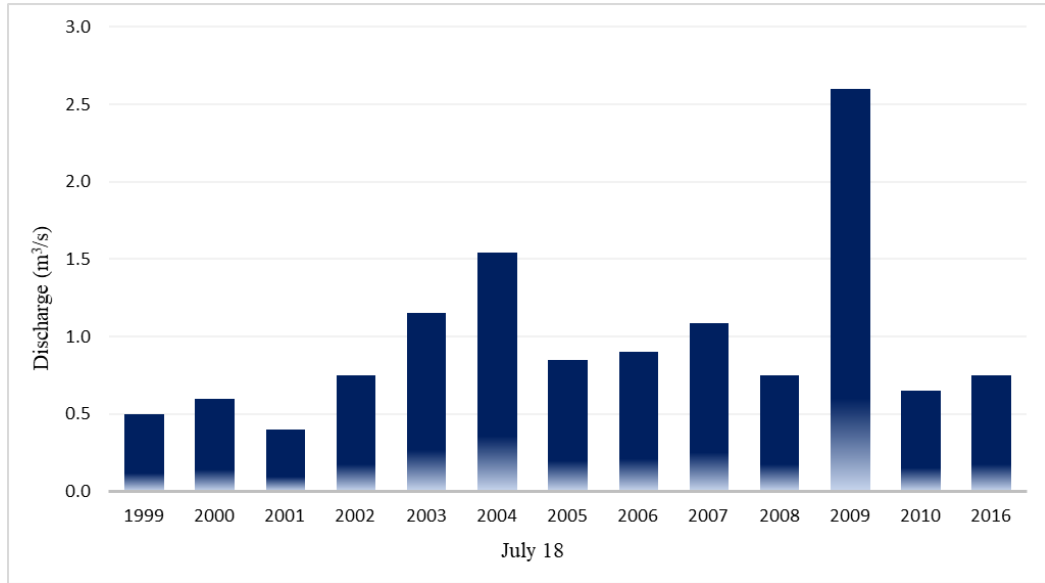


Figure 3.12 Measured discharge on July 18 at ~ 1200 hr from 1999 to 2010, and 2016, Otter Creek, Kentucky.

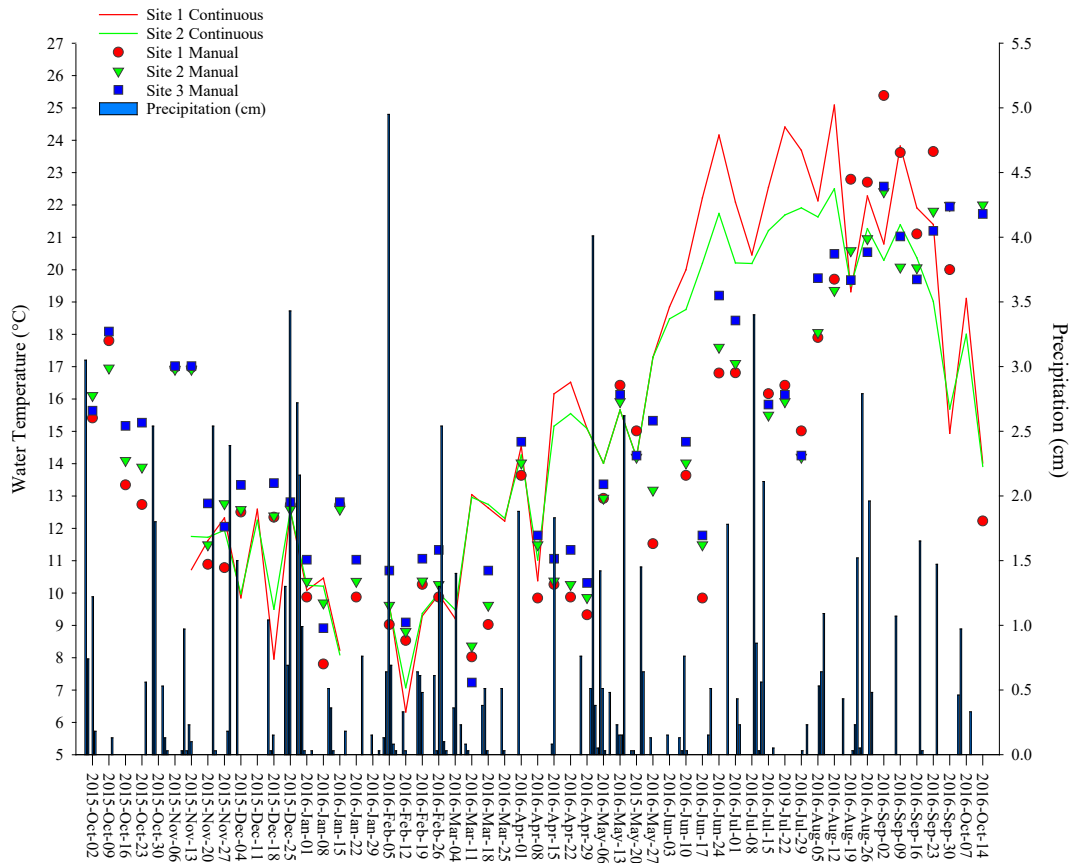


Figure 3.13 Water temperature data obtained from InSitu continuous dataloggers located at site 1 and 2 from 13 November 2015 through 14 October 2016. Weekly manual water temperature readings for sites 1, 2 and 3 from 2 October 2015 through 14 October 2016, Otter Creek, Kentucky. Precipitation (cm) obtained from NOAA for October 2015 through October 2016.

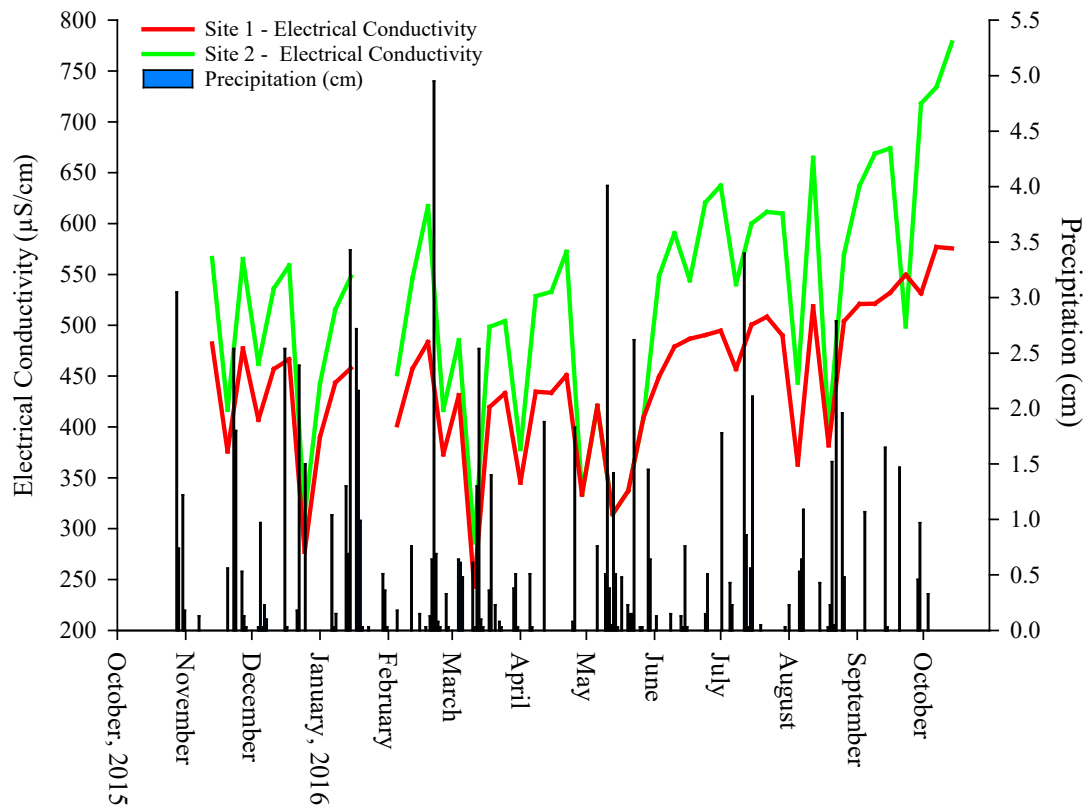


Figure 3.14 Continuous water-quality monitoring of electrical conductivity ($\mu\text{S}/\text{cm}$) from 13 November 2015 through 14 October 2016, Otter Creek, Kentucky. Precipitation (cm) obtained from NOAA for October 2015 through October 2016.

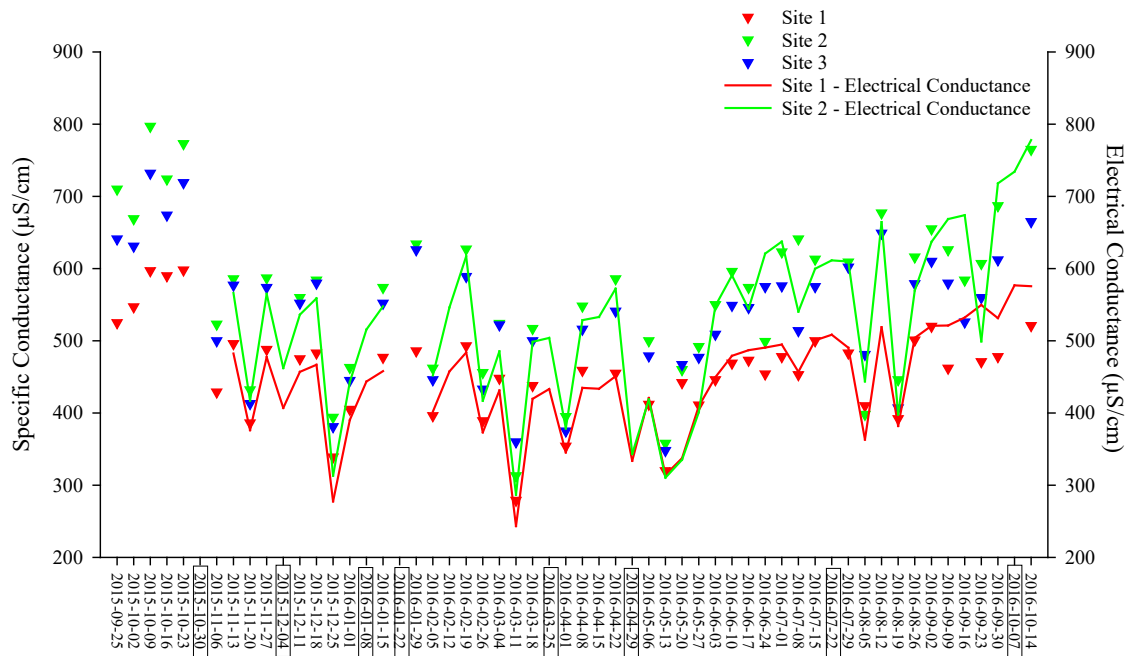


Figure 3.15 Weekly manual readings of specific conductivity ($\mu\text{S}/\text{cm}$) for all three sampling sites, continuous water-quality monitoring of electrical conductivity ($\mu\text{S}/\text{cm}$) using InSitu continuous datalogger located at sites 1 and 2 from 13 November 2015 through 14 October 2016, Otter Creek, Kentucky. Dates that are bracketed indicate that no reading was taken that day.

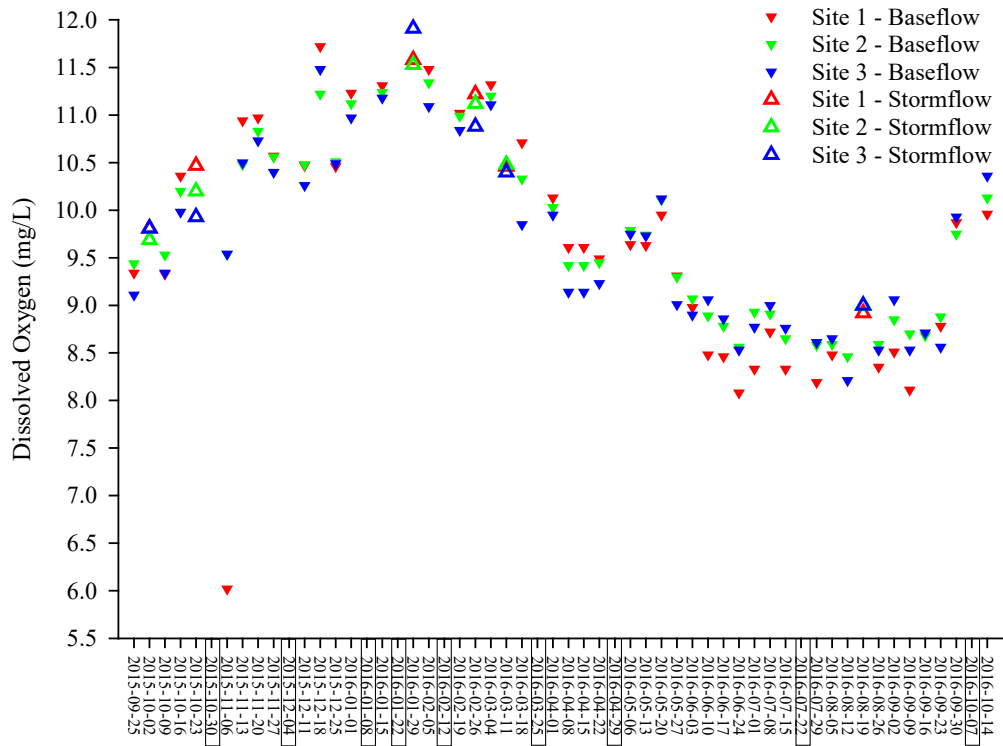


Figure 3.16 Weekly manual readings of dissolved oxygen (mg/L) for all three sampling sites, Otter Creek, Kentucky. Dates that are bracketed indicate that no reading was taken that day.

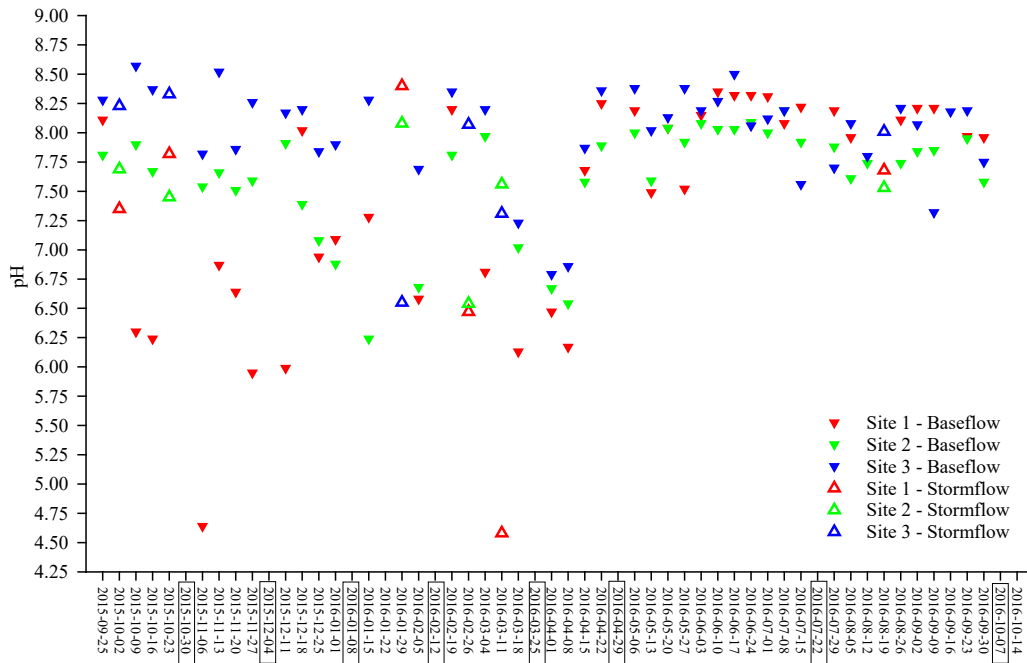


Figure 3.17 Weekly manual readings for pH for all three sampling sites, Otter Creek, Kentucky. Dates that are bracketed indicate that no reading was taken that day.

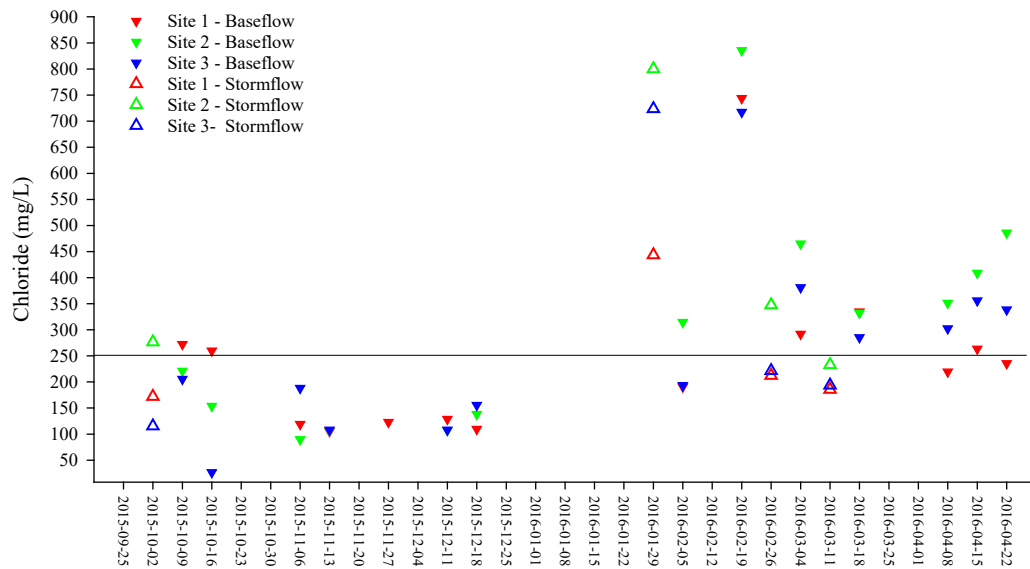


Figure 3.18 Weekly water samples for chloride (mg/L) for all three sampling sites, Otter Creek, Kentucky. Horizontal line represents the USEPA SMCL for chloride (250 mg/L).

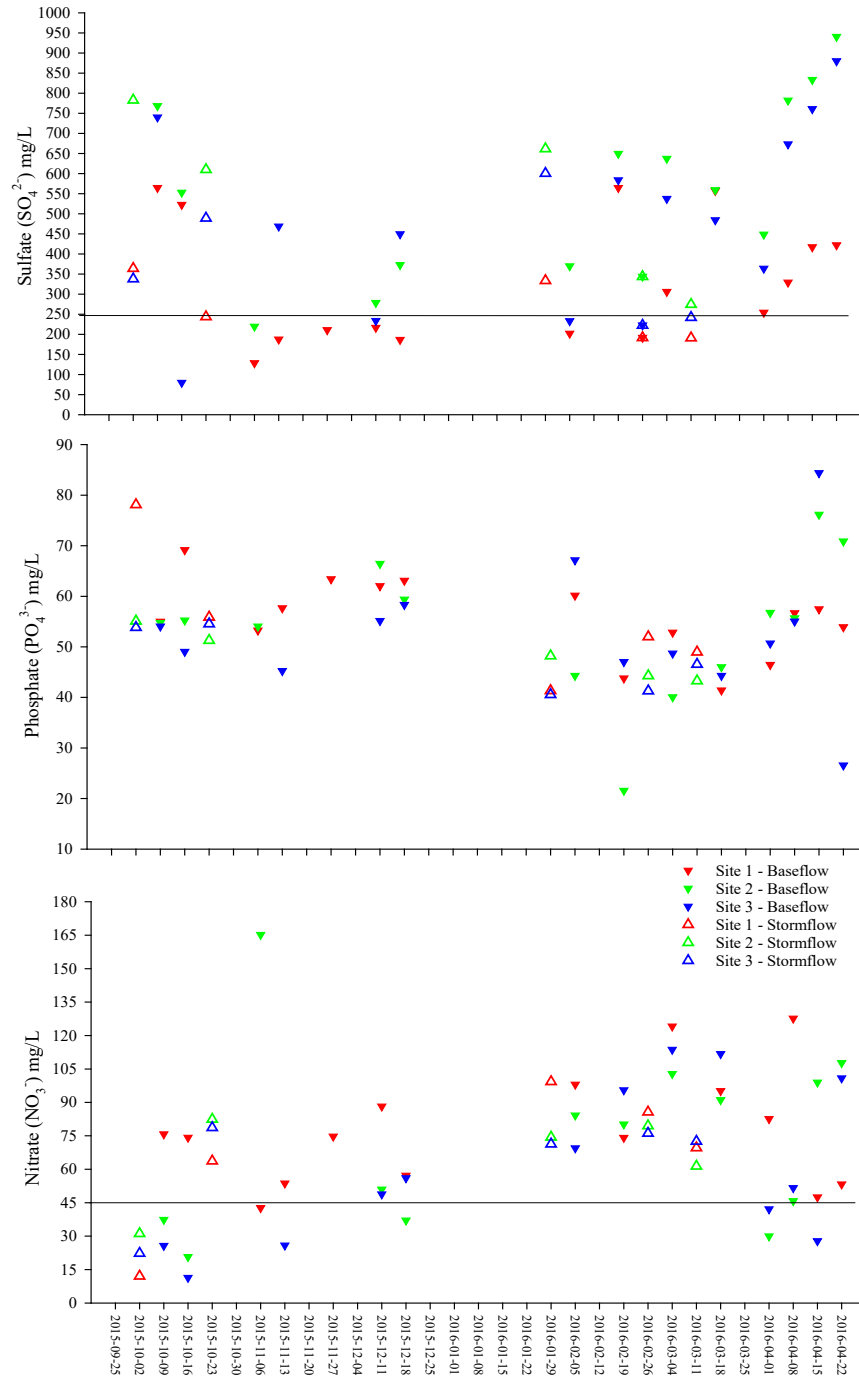


Figure 3.19 Weekly water samples for sulfate, phosphate and nitrate (mg/L) for all three sampling sites, Otter Creek, Kentucky. Horizontal lines represent water-quality standards noted in the text. No water quality guidelines for phosphate.

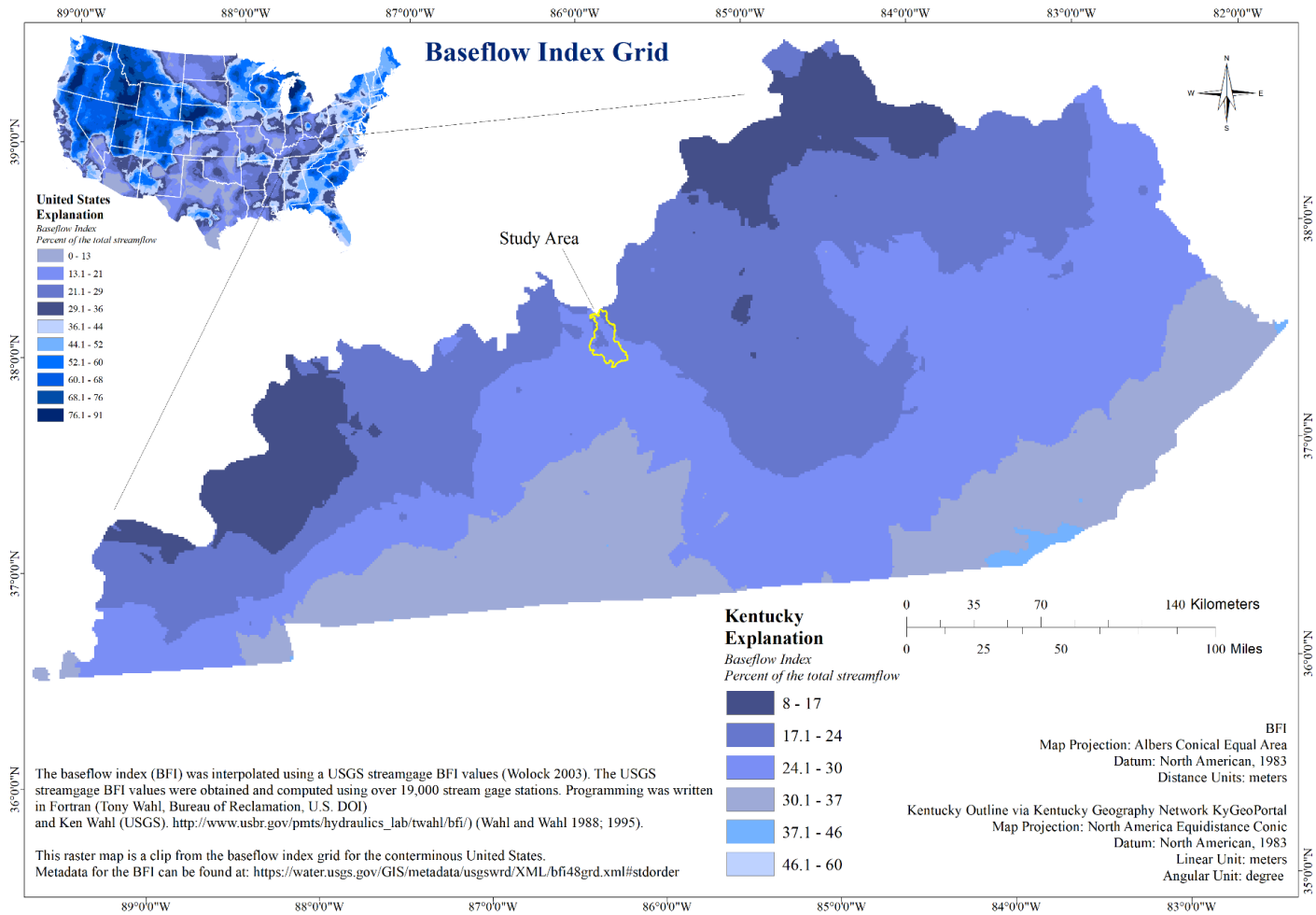


Figure 3.20 Baseflow index for the Commonwealth of Kentucky. Study area highlighted in yellow.

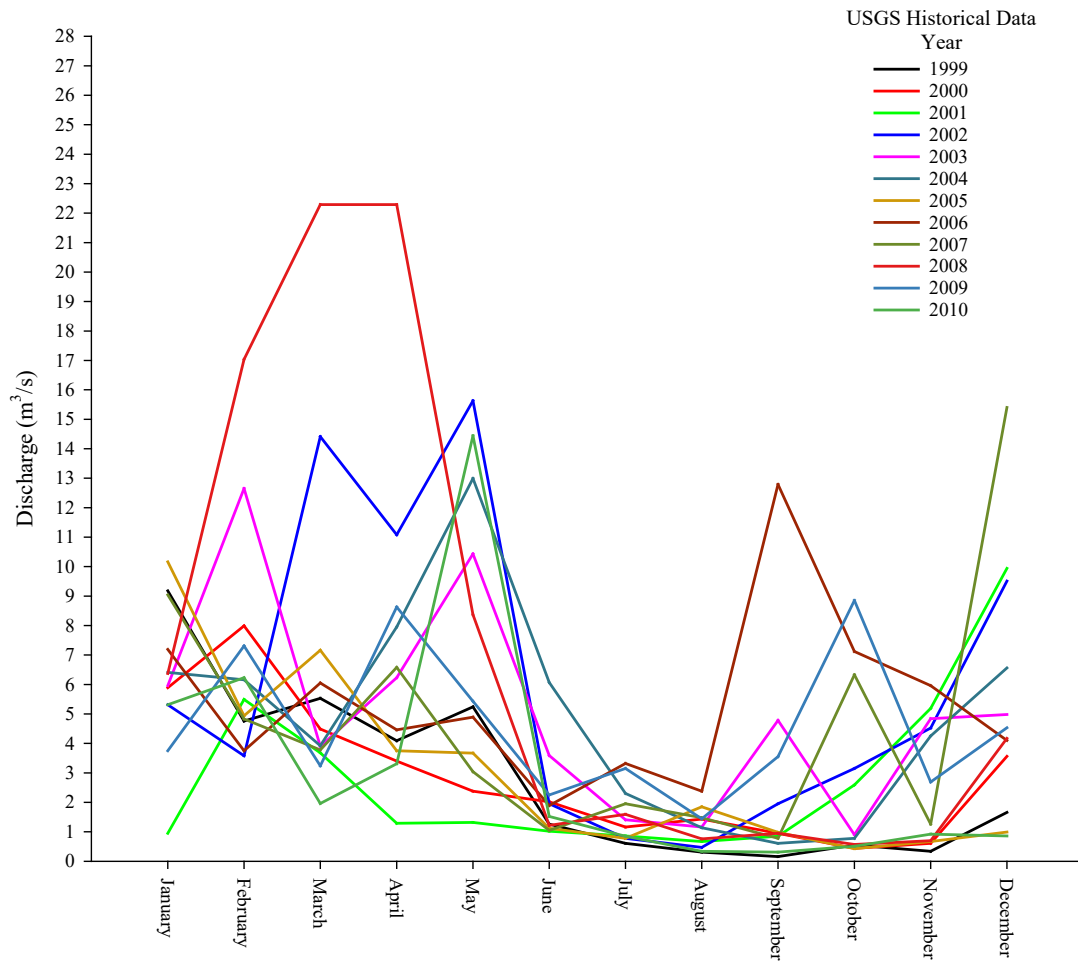


Figure 3.21 Historical discharge for Otter Creek from the discontinued USGS gaging station (03302110) from 1999 through 2010.

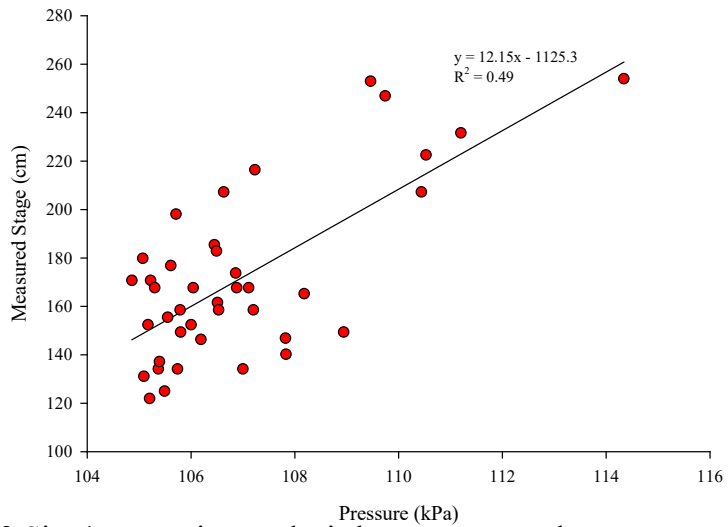


Figure 3.22 Site 1 regression analysis between manual stage measurements and InSitu datalogger continuous monitoring of pressure, Otter Creek, Kentucky.

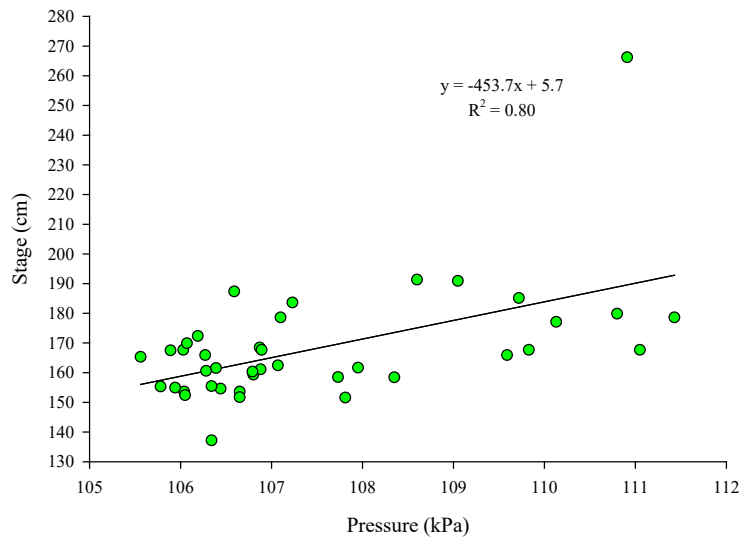


Figure 3.23 Site 2 regression analysis between manual stage measurements and InSitu datalogger continuous monitoring of pressure, Otter Creek, Kentucky.

CHAPTER 4. CONCLUSIONS

4.1 Purpose and Objectives

The purpose of this study was to identify major sediment source contributions and explain spatial and temporal variability in water quality along Otter Creek, a perennial stream draining karst terrain with mixed agricultural, military, and residential land uses in north-central Kentucky. Previous studies of erosion and water quality at the catchment scale have variously included urban, rural, industrial and agricultural land use/land cover (LU/LC), but few (if any) have included catchments where military training has occurred. Sediment fingerprinting objectives were:

- 1) to identify and differentiate unique characteristics of civilian and military source soils transported to Otter Creek;
- 2) to collect sediment at different locations along Otter Creek and apportion it to different source-soil categories.

Water-quality analysis objectives were:

- 1) to draw inferences about spatial and temporal controls on water chemistry in Otter Creek, based on monitoring field parameters, anions, fluid pressure, and stream stage at different locations;
- 2) to compare measurements conducted during this study to historical data obtained from the U.S. Geological Survey (USGS) and the National Oceanic and Atmospheric Administration (NOAA).

4.2 *Major Findings*

4.2.1 *Sediment Fingerprinting*

Differences were observed in sediment yield and composition between summer (March–September) and winter (October–February) and between baseflow and stormflow. At each sampling location, sediment yields were greater during summer than winter and during stormflow than baseflow. Sampling site 3, which was farthest downstream, had the greatest sediment yield among the three sites for summer, winter, baseflow and stormflow. Of the civilian lands, which occupy 81.6% of the study area, the main LU/LC (57.1%) is cropland, with the remainder being forest (29.6%), developed (12.2%) and other (1.1%). Military lands, which occupy 18.4% of the study area, have forest as the predominant LU/LC (63.6%), no cropland, 23.8% developed area and 12.1% as other. Subcatchment 3, which had the greatest proportion of military lands, had the greatest amount of LU/LC in forest (74.5%) and the least amount in cropland (5.3%).

The Sed_SAT program identified Cu, Zn, Co, Ni, Al and Mg as conservative tracers that could distinguish between source-soil groups during the unmixing model process. Sed_SAT allocated target sediment to five source-soil groups: civilian and military near-stream (C-RB and M-RB), military forest (M-FS), and military average and extreme erosion (M-AE and M-XE). Independent of Sed_SAT, additional statistical tests were run to assess the capability of individual tracers to provide further insight beyond the unmixing model results. A Tukey test showed that tracers were able to distinguish between civilian and military source soils. Principal component analysis was used to reduce dimensionality and assist in identifying tracers that might influence source discrimination.

Considering all sediments combined, there was not a statistically significant correlation between the sediment sampling sites at base- or stormflow for TOC or $\delta^{13}\text{C}$. The greatest proportion of sediment in summer was attributed to M-XE at sites 1 and 2 and M-FS at site 3, whereas the greatest proportion of sediment in winter was attributed to M-AE at all three sites. Source-soil group C-RB consistently reported very low contributions. For baseflow, the greatest proportion of sediment was attributed to M-RB at all sites, whereas for stormflow, the greatest proportion of sediment was attributed to M-RB at site 1 and M-XE at sites 2 and 3.

The higher contributions of M-AE and M-XE observed during summer could be related to an increase in intensive vehicular training activities in those areas, but it was not possible to document the timing, nature, and location of training. We suspect that the sinkholes prevalent in the study area could be storing sediment that is transported during rainfall events, which subsequently could skew sediment source allocation to source-soil groups. Elemental analysis indicated that military soils had statistically higher tracer concentrations than civilian soils, which might reflect wear of metal parts on military vehicles during training.

There were geochemical similarities among source-soil groups C-RB, M-RB and M-FS, which may have affected sediment apportionment by misclassification of source soils. Consequently, we combined soil groups into simplified categories in an effort to distinguish where primary contributions were originating: streambank/forest (STR-FS = C-RB + M-RB + M-FS) and military erosion (MIL-E = M-AE + M-XE) in one scenario; streambank (STR = C-RB + M-RB) and military upland (MIL-U = M-FS + M-AE + M-XE) in a second scenario. At all three sediment sampling sites, sediment contributions were dominated by STR-FS

(63.39–68.66%) in scenario one and by MIL-U (57.01–65.58%) in scenario two. We compared these results with a watershed in Iowa on similar soils, but with crop- and grassland as primary LU/LC. Results suggest that sediment contributions from tracked-vehicle military training areas are broadly analogous to those from tilled cropland.

4.2.2 *Stream-Water Quality*

Continuous monitoring during storm events showed temporary EC decreases in response to dilution from runoff and corresponding increases in fluid pressure, which is consistent with rises in stage at sites 1 and 2. Higher-pressure responses were observed from December through mid-May, when precipitation was increased, and subsequent lower-pressure responses during the drier months of mid-May through November. Site 2 had small differences between median base- and stormflow temperatures and EC and SC saw increases from site 1 to 2, which is consistent with contributions of groundwater discharge along that reach of the stream.

A comparison of historical water quality data (1994-98) to the study period (2015-16) shows there was a significant increase in SC, a significant decrease in DO, and a marginally significant increase in pH at site 3. Those differences might reflect LU/LC changes, such as the partial revegetation of military training land and conversion of farmland to forest. However, decreases in agricultural land use and a subsequent decrease in agrichemical loading is inconsistent with an increase in TDS, as indicated by SC. The available data do not allow us to apportion solute loads to different LU/LC settings. The study took place during a NOAA-documented El Niño, which could have influenced results due to increased precipitation during the beginning of the study period in fall 2015 and the drier conditions seen during summer 2016.

With respect to solute concentrations, Cl^- and SO_4^{2-} demonstrated a significant positive relationship at all three sites, which suggests a common source for both anions, such as septic systems, the Vine Grove sewage treatment plant and/or agricultural contributions from runoff. During winter, elevated concentrations of Cl^- could be attributed to road-salt runoff. Sulfate could be contributed by the dissolution of gypsum by groundwater in the St. Louis Limestone. From late fall through winter months, NO_3^- concentrations increased, which may be a result of higher-than-average precipitation and slow nitrification and leaching from soils. However, it is difficult to identify the origins of the non-point source contributions of nitrate due to spatial variability of inputs and geochemical transformations across the variable hydrologic conditions.

Continuous monitoring during storm events showed temporary EC decreases in response to dilution from runoff and corresponding increases in fluid pressure, which is consistent with rises in stage at sites 1 and 2. Higher-pressure responses were observed from December through mid-May, when precipitation was increased, and subsequent lower-pressure responses during the drier months of mid-May through November. Site 2 had small differences between median base- and stormflow temperatures and EC and SC saw increases from site 1 to 2, which is consistent with contributions of groundwater discharge along that reach of the stream.

A comparison of historical water quality data (1994-98) to the study period (2015-16) shows there was a significant increase in SC, a significant decrease in DO, and a marginally significant increase in pH at site 3. Those differences might reflect LU/LC changes, such as the partial revegetation of military training land and conversion of farmland to forest.

However, decreases in agricultural land use and a subsequent decrease in agrichemical loading is inconsistent with an increase in TDS, as indicated by SC. The available data do not allow us to apportion solute loads to different LU/LC settings. The study took place during a NOAA-documented El Niño, which could have influenced results due to increased precipitation during the beginning of the study period in fall 2015 and the drier conditions seen during summer 2016.

With respect to solute concentrations, Cl^- and SO_4^{2-} demonstrated a significant positive relationship at all three sites, which suggests a common source for both anions, such as septic systems, the Vine Grove sewage treatment plant and/or agricultural contributions from runoff. During winter, elevated concentrations of Cl^- could be attributed to road-salt runoff. Sulfate could be contributed by the dissolution of gypsum by groundwater in the St. Louis Limestone. From late fall through winter months, NO_3^- concentrations increased, which may be a result of higher-than-average precipitation and slow nitrification and leaching from soils. However, it is difficult to identify the origins of the non-point source contributions of nitrate due to spatial variability of inputs and geochemical transformations across the variable hydrologic conditions.

4.3 Study Limitations and Recommendations for Future Research

Limitations in this study for sediment fingerprinting included the sampling device, source sampling design and tracers. The sediment trap devices used in this study are non-isokinetic with a fixed 4-mm opening; the velocity of water flowing into the device is not the same as the water flowing outside. The physics of the device is biased in favor of coarse-grained sediment because of its higher settling velocity, specifically during storm flow

events. Suspended sediment at high-flow velocities may not all settle within the device. Source sampling was performed after reviewing aerial photography of the study area and mapping the different land uses within it. Channel-bank sediments were not collected because channel bank slopes along the study reach were mild relative to those farther downstream and therefore judged unlikely to be significant sources of sediment in comparison to upland sediment contributions. Even so, collection of channel bank samples would have enabled an evaluation of the contribution of that source to total sediment loads, thus providing additional perspective on the results. Because biogeochemical properties can change between source-soil and sediment sampling locations, the selected tracers may not have been conservative. For example, some of the tracers identified by Sed_SAT may have been prone to sorption onto soil or sediment.

Limitations of the water-quality study include the number of samples collected for anion analysis, their holding times, the small number of discharge measurements, and the loss of the datalogger and barometric pressure logger at site 3. Anion samples were collected only over a 6-month period and were not collected each week of that period. Although samples were frozen for storage, holding times exceeded EPA's recommended limits. Simultaneous discharge measurements at each site during each sampling period would have enabled estimates of net inflow and solute fluxes along the stream. Barometric pressure corrections would have enabled quantitative analyses of stream-stage measurements.

To refine discrimination of sediment sources and apportion sediment loads to different LU/LC categories, additional research would be required to determine: 1) the duration of sediment storage within sinkholes and connected karst conduits; 2) the rainfall threshold for sediment remobilization from sinkholes and connected karst conduits to Otter

Creek; and 3) the ultimate sinks of sediment derived from areas of extreme erosion on Fort Knox. For determining storage and transit times, sediment data are needed. In addition to using carbon and nitrogen isotopes as ambient tracers, artificial sediment tracers could be introduced. An effective artificial tracer would need to be quantifiable, not normally present within the study area, detectable at very low concentrations, conservative, and non-toxic (Wagner et al. 2006).

In order to better assess the water quality and aquatic health of Otter Creek, regular sampling for major solutes, metals, and nutrients and monitoring of field parameters should be continued, in addition to adding sampling for fecal coliform, suspended sediment, and chlorophyll-a and monitoring of discharge. Deployment of logging sensors for stage, water temperature, SC, and turbidity would provide information on event-scale variability in those parameters and enable development of a stage-discharge rating curve. Such a curve, along with correlations between SC and total dissolved solids and between turbidity and total suspended solids, would permit estimates of total dissolved and suspended mass fluxes.

APPENDICES

APPENDIX 2.1 Site 1 Percent Sediment Classified Correctly Sed_SAT.

Site 1		Percent Classified Correctly					Sed Amt	Sample Info
Sample Date	C-RB	M-RB	M-FS	M-AE	M-XE			
2015-Oct-02	0.00	0.00	0.00	56.55	43.45	1.23	BS	
2015-Oct-09	0.00	0.00	0.00	83.21	16.79	12.20	SF	
2015-Oct-16						0.22	NES	
2015-Oct-23	0.00	0.00	0.00	67.30	32.70	0.85		
2015-Oct-30						0.28	NES-BS	
2015-Nov-06	0.00	0.00	0.00	42.07	57.93	84.30	SF	
2015-Nov-13							SLT	
2015-Nov-20	0.00	0.00	0.00	51.22	48.78	1.57		
2015-Nov-27	0.00	0.00	37.76	45.26	16.98	39.56	SF	
2015-Dec-04							NSC	
2015-Dec-11	0.00	0.00	14.81	62.98	22.21	1.90		
2015-Dec-18	0.00	0.00	0.00	68.28	31.72	1.34		
2015-Dec-25						0.38	NES-BS	
2016-Jan-01	0.00	0.00	0.00	51.22	48.78	31.90	SF	
2016-Jan-08							NSC	
2016-Jan-15	0.00	0.00	41.57	28.87	29.56	2.41		
2016-Jan-22							NSC	
2016-Jan-29	0.00	0.00	66.49	33.51	0.00	1.13		
2016-Feb-05						4.31	SF	
2016-Feb-12							NSC	
2016-Feb-19	45.70	5.37	0.00	48.93	0.00	1.53	BS	
2016-Feb-26	0.00	0.08	69.62	23.67	6.63	56.77	SF	
2016-Mar-04						0.39	NES	
2016-Mar-11							SLT	
2016-Mar-18	0	0	0	39	61	130.27	SF	
2016-Mar-25							NSC	
2016-Apr-01	0	0	0	37	63	24.56	SF	
2016-Apr-08	52.89	11.97	18.05	17.09	0.00	56.48	SF	
2016-Apr-15	0.00	0.00	56.53	15.39	28.08	2.66		
2016-Apr-22	21.63	3.62	60.29	14.46	0.00	1.11		
2016-Apr-29							NSC	
2016-May-06	0.00	0.00	35.19	33.31	31.51	155.42	SF	
2016-May-13	84.03	15.97	0.00	0.00	0.00	1.57	BS	

2015-May-20	0.00	0.00	47.71	30.84	21.44	1.45	BS
2016-May-27	0.00	0.00	59.41	18.70	21.89	105.84	SF
2016-Jun-03	0.00	0.00	4.90	41.90	53.20	4.89	
2016-Jun-10	0.00	0.00	19.46	44.60	35.95	2.46	
2016-Jun-17	0.00	0.00	40.18	59.82	0.00	1.31	
2016-Jun-24	0.00	0.00	60.19	39.81	0.00	3.47	
2016-Jul-01	0.00	0.00	80.48	0.00	19.52	3.57	
2016-Jul-08	0.00	0.00	20.41	30.13	49.46	17.06	
2016-Jul-15	0.00	0.00	25.94	23.51	50.55	3.72	
2019-Jul-22							NSC
2016-Jul-29	0.00	0.00	0.00	20.79	79.21	57.95	
2016-Aug-05	0.00	0.00	0.00	36.72	63.28	18.09	
2016-Aug-12	0.00	0.00	24.50	24.81	50.69	1.31	
2016-Aug-19	0.00	0.00	20.04	35.87	44.09	38.00	
2016-Aug-26	0.00	0.00	0.00	39.88	60.12	17.49	
2016-Sep-02						0.22	NES
2016-Sep-09	0.00	0.00	30.43	43.25	26.33	4.09	
2016-Sep-16						0.31	NES
2016-Sep-23	0.00	0.00	0.00	44.25	55.75	3.65	
2016-Sep-30	25.15	6.92	49.64	18.29	0.00	0.82	
2016-Oct-07							NSC
2016-Oct-14	0.00	0.00	46.57	41.69	11.73	1.30	

Explanation

NES = Not enough sample

NSC = No sample taken

SWP = Sampler wiped out by high flow event

SLT = Sample lost

BS = Bucket sample

SF = Stormflow

APPENDIX 2.2 Site 2 Percent Sediment Classified Correctly Sed_SAT.

Site 2		Percent Classified Correctly					Sed Amt	Sample Info
Sample Date	C-RB	M-RB	M-FS	M-AE	M-XE			
2015-Oct-02						0.17	NES-BS	
2015-Oct-09	0.00	0.00	7.43	52.65	39.92	22.36	SF	
2015-Oct-16						0.21	NES	
2015-Oct-23	0.00	0.00	0.00	78.68	21.32	0.99		
2015-Oct-30						0.33	NES-BS	
2015-Nov-06	0.00	0.00	0.00	34.33	65.67	55.80	SF	
2015-Nov-13	0.00	0.00	0.00	47.72	52.28	3.46		
2015-Nov-20	0.00	0.00	0.00	31.79	68.21	1.13		
2015-Nov-27	0.00	3.43	72.53	21.78	2.26	41.05	SF	
2015-Dec-04							NSC	
2015-Dec-11	0.00	4.12	10.46	65.11	20.32	1.77		
2015-Dec-18							SWO	
2015-Dec-25						0.08	NES-BS	
2016-Jan-01	0.00	0.00	0.00	31.82	68.18	43.30	SF	
2016-Jan-08							NSC	
2016-Jan-15	0.00	0.00	75.02	22.37	2.61	2.17		
2016-Jan-22							NSC	
2016-Jan-29	0.00	0.00	48.13	24.70	27.17	1.77		
2016-Feb-05						3.54	SF	
2016-Feb-12							NSC	
2016-Feb-19	0.00	100.00	0.00	0.00	0.00	6.94	BS	
2016-Feb-26	0.00	0.00	41.06	28.99	29.95	46.31	SF	
2016-Mar-04						0.28	NES	
2016-Mar-11							SLT	
2016-Mar-18	0.00	0.00	9.49	20.26	70.25	13.41	SF	
2016-Mar-25							NSC	
2016-Apr-01	0.00	100.00	0.00	0.00	0.00	13.38	SF	
2016-Apr-08	39.14	32.92	27.94	0.00	0.00	62.87	SF	
2016-Apr-15						0.60	NES	
2016-Apr-22	61.53	0.00	17.70	20.77	0.00	0.83		
2016-Apr-29							NSC	
2016-May-06	0.00	0.00	46.92	32.60	20.48	139.98	SF	
2016-May-13						0.60	NES-BS	
2015-May-20	85.94	8.99	0.00	5.07	0.00	1.98	BS	
2016-May-27	50.81	0.00	30.86	18.32	0.00	150.38	SF	

2016-Jun-03	0.00	0.00	10.57	36.73	52.70	1.93	
2016-Jun-10	66.03	33.97	0.00	0.00	0.00	2.90	
2016-Jun-17	0.00	0.00	0.00	60.94	39.06	10.86	
2016-Jun-24	8.92	1.84	60.13	29.10	0.00	0.64	
2016-Jul-01	0.00	0.00	36.82	42.68	20.49	1.40	
2016-Jul-08	0.00	0.00	6.14	53.84	40.01	25.57	
2016-Jul-15							SLT
2019-Jul-22							NSC
2016-Jul-29	0.00	0.00	0.00	18.91	81.09	22.13	
2016-Aug-05	0.00	0.00	4.40	38.85	56.75	31.84	
2016-Aug-12	0.00	0.00	0.00	45.47	54.53	5.22	
2016-Aug-19	0.00	0.00	0.00	46.40	53.60	62.87	
2016-Aug-26	0.00	0.00	0.00	37.06	62.94	10.49	
2016-Sep-02						0.38	NES
2016-Sep-09	0.00	0.00	39.93	20.37	39.70	2.34	
2016-Sep-16						0.27	NES
2016-Sep-23	0.00	0.00	23.96	44.40	31.64	0.96	
2016-Sep-30	0.00	0.00	29.71	35.44	34.86	0.62	
2016-Oct-07							NSC
2016-Oct-14	0.00	0.00	0.00	40.53	59.47	2.92	

Explanation

NES = Not enough sample

NSC = No sample taken

SWP = Sampler wiped out by high flow event

SLT = Sample lost

BS = Bucket sample

SF = Stormflow

APPENDIX 2.3 Site 3 Percent Sediment Classified Correctly Sed_SAT.

Site 3		Percent Classified Correctly					Sed Amt	Sample Info
Sample Date	C-RB	M-RB	M-FS	M-AE	M-XE			
2015-Oct-02						0.19	NES-BS	
2015-Oct-09	0.00	0.00	42.30	14.38	43.32	42.00	SF	
2015-Oct-16						0.17	NES	
2015-Oct-23	0.00	55.44	26.41	18.14	0.00	0.87		
2015-Oct-30						0.48	NES-BS	
2015-Nov-06	0	0	0	41.86	58.14	129.40	SF	
2015-Nov-13	0.00	0.00	0.00	42.27	57.73	7.93		
2015-Nov-20	0.00	0.00	0.00	21.16	78.84	3.97		
2015-Nov-27	0.00	20.29	42.09	37.62	0.00	62.54	SF	
2015-Dec-04							NSC	
2015-Dec-11							SWO	
2015-Dec-18	0.00	0.00	44.13	54.25	1.62	1.77		
2015-Dec-25						0.33	NES-BS	
2016-Jan-01	0	0	38.06	33.82	28.12	3.51	SF	
2016-Jan-08							NSC	
2016-Jan-15	13.89	19.02	29.67	37.41	0.00	1.79		
2016-Jan-22							NSC	
2016-Jan-29	49.75	0.00	50.25	0.00	0.00	1.98		
2016-Feb-05						5.95	SF	
2016-Feb-12							NSC	
2016-Feb-19	49.52	14.21	19.82	16.44	0	2.29	BS	
2016-Feb-26	15.41	0.00	0.00	63.05	21.54	76.31	SF	
2016-Mar-04	4.07	17.47	55.11	23.35	0	2.09		
2016-Mar-11							SLT	
2016-Mar-18	24.92	3.18	65.45	6.45	0.00	28.41	SF	
2016-Mar-25							NSC	
2016-Apr-01	0	0	0	21.16	78.84	23.27	SF	
2016-Apr-08	0.00	0.00	0.00	21.16	78.84	87.33	SF	
2016-Apr-15	0.00	0.00	19.95	33.02	47.04	1.11		
2016-Apr-22	0.00	100.00	0.00	0.00	0.00	3.09		
2016-Apr-29							NSC	
2016-May-06	0.00	0.00	41.96	22.94	35.10	187.20	SF	
2016-May-13	0	0	0	53.03	46.97	1.35	BS	
2015-May-20	51.13	10.9	34.7	3.27	0	2.23	BS	
2016-May-27	0.00	6.41	90.43	3.16	0.00	174.08	SF	

2016-Jun-03	0.00	0.00	0.00	59.94	40.06	2.70	
2016-Jun-10	56.51	0.00	27.96	15.52	0.00	6.19	
2016-Jun-17	0.00	0.00	54.58	42.58	2.85	3.28	
2016-Jun-24	44.75	27.08	23.20	4.97	0.00	1.98	
2016-Jul-01	0.00	0.00	17.30	45.64	37.05	3.25	
2016-Jul-08	0.00	0.00	0.00	33.01	66.99	19.65	
2016-Jul-15	0.00	6.56	63.91	29.52	0.00	6.47	
2019-Jul-22							NSC
2016-Jul-29	0.00	0.00	0.00	11.26	88.74	27.22	
2016-Aug-05	0.00	0.00	36.40	30.85	32.75	11.76	
2016-Aug-12	0.00	2.07	46.07	44.63	7.23	12.89	
2016-Aug-19	0.00	0.00	0.00	42.88	57.12	99.08	
2016-Aug-26	0.00	0.00	32.47	35.95	31.58	8.42	
2016-Sep-02						0.29	NES
2016-Sep-09	0.00	0.00	61.45	38.55	0.00	1.56	
2016-Sep-16						0.38	NES
2016-Sep-23	0.00	5.03	58.31	36.66	0.00	1.63	
2016-Sep-30						0.37	NES
2016-Oct-07							NSC
2016-Oct-14	0.00	21.60	59.62	18.78	0.00	1.09	

Explanation

NES = Not enough sample

NSC = No sample taken

SWP = Sampler wiped out by high flow event

SLT = Sample lost

BS = Bucket sample

SF = Stormflow

APPENDIX 2.4 Source Soil Geochemical Data.

SampleName	SourceType	TOC	Copper	Zinc	Strontium	Rubidium	Cobalt	Nickel	Aluminum	Sodium	Magnesium	Silica	Phosphorus	Potassium	Calcium	Manganese	Iron	$\delta^{13}\text{C}$	$\delta^{15}\text{N}$
C_12	C-RB	0.65	0.00	29.19	50.84	22.56	4.56	11.96	1.611	1.124	0.422	22.877	0.059	0.457	1.763	0.061	1.173	-26.50	
C_132	C-RB	0.37	7.08	74.13	60.05	54.92	10.37	25.35	2.654	1.053	0.385	22.196	0.054	0.897	0.683	0.056	1.914	-22.51	
C_134	C-RB	2.02	20.43	123.30	51.23	60.39	8.94	22.38	2.225	1.015	0.343	23.273	0.062	0.766	0.230	0.078	1.713	-26.60	3.45
C_74	C-RB	0.48	20.88	150.96	62.83	63.65	13.40	41.69	3.326	1.046	0.333	19.623	0.034	0.679	0.677	0.038	3.324	-25.58	
C_76	C-RB	0.92	17.36	73.84	86.71	67.97	13.85	25.17	2.870	1.036	0.317	18.570	0.038	0.969	1.087	0.031	2.998	-26.36	
C_78	C-RB	0.42	1.64	49.00	46.21	45.70	5.48	22.94	2.094	1.043	0.431	23.801	0.044	0.749	0.148	0.087	1.102	-25.76	
C_89	C-RB	0.69	2.96	33.42	43.03	26.73	2.78	17.22	1.907	1.065	0.415	23.660	0.062	0.689	0.795	0.087	1.278	-28.76	
C_90	C-RB	3.21	10.35	80.48	59.88	55.44	7.71	24.43	2.241	1.078	0.376	21.805	0.050	0.921	0.611	0.143	2.097	-25.63	4.77
C_93	C-RB	1.70	4.09	45.39	43.37	40.00	5.85	20.05	1.972	1.121	0.453	22.827	0.047	0.702	0.506	0.057	1.446	-26.24	4.71
C_95	C-RB	0.52	2.64	33.29	35.30	21.30	2.95	19.61	1.999	1.099	0.467	23.681	0.054	0.502	0.571	0.055	1.158	-25.32	4.46
C_98	C-RB	3.07	9.86	73.03	54.97	47.88	6.86	26.33	2.248	1.074	0.358	22.059	0.053	0.844	0.536	0.080	1.659	-28.04	4.15
M_18	M-AE	0.82	193.78	306.16	80.00	96.67	30.68	66.87	4.020	0.926	0.250	15.360	0.033	0.854	0.378	0.019	5.064	-24.57	5.11
M_23	M-AE	0.67	16.99	88.02	75.81	63.48	15.67	26.77	3.075	1.033	0.312	21.277	0.032	0.793	0.347	0.027	2.957	-24.95	
M_26	M-AE	0.44	31.65	196.09	167.83	102.88	28.37	66.05	4.348	0.969	0.257	16.198	0.032	1.237	0.552	0.027	4.752	-25.35	3.05
M_29	M-AE	0.21	15.87	118.34	347.56	101.86	42.86	28.19	4.222	0.867	0.202	14.987	0.031	1.054	0.146	0.008	6.874	-23.61	
M_30	M-AE	0.80	26.43	173.07	81.83	83.93	19.61	32.93	3.685	0.993	0.312	18.372	0.033	1.003	0.323	0.023	3.942	-25.51	
M_38	M-AE	2.27	3.99	39.53	92.33	42.98	8.41	17.35	1.902	0.994	0.283	20.168	0.047	0.583	3.470	0.031	1.680	-26.07	0.79
M_17	M-FS	0.22	20.91	93.70	46.29	72.29	17.72	28.62	3.685	0.967	0.302	20.263	0.035	0.485	0.165	0.025	3.429	-24.35	
M_20	M-FS	0.36	14.00	79.94	68.36	77.89	14.73	20.08	3.051	1.022	0.344	20.721	0.043	1.248	0.151	0.038	3.057	-23.68	
M_33	M-FS	1.33	9.78	63.75	70.84	63.23	13.34	23.91	2.660	1.057	0.361	20.894	0.044	1.072	0.367	0.041	2.604	-26.92	0.59
M_67	M-FS	0.31	31.89	208.14	53.16	72.84	16.49	50.69	4.265	1.026	0.316	14.985	0.028	0.925	0.522	0.017	4.792	-27.07	
M_88	M-FS	3.40	7.14	55.38	55.68	53.32	9.01	22.44	2.073	0.966	0.331	22.144	0.047	0.821	0.528	0.078	1.737	-28.26	0.18
M_15	M-RB	0.26	0.00	11.88	36.79	15.05	3.65	10.66	1.386	1.168	0.501	23.860	0.048	0.241	0.882	0.044	0.835	-26.16	
M_2	M-RB	1.03	2.51	49.39	45.01	31.69	7.85	16.21	1.793	1.129	0.410	22.031	0.057	0.510	0.946	0.076	1.436	-27.09	4.31
M_66	M-RB	1.02	2.83	56.71	184.38	47.31	7.71	23.56	1.628	0.791	0.143	13.339	0.070	0.723	10.574	0.027	1.704	-27.09	0.41
M_72	M-RB	0.93	2.66	38.63	58.20	50.19	6.80	13.62	2.105	1.081	0.417	23.761	0.048	1.043	0.110	0.047	1.145	-26.99	2.48

M_83	M-RB	1.04	10.29	64.69	65.16	55.70	5.96	19.48	1.950	1.057	0.378	22.031	0.046	0.898	0.392	0.074	1.368	-28.10	-0.13
M_85	M-RB	0.58	8.10	90.31	58.33	45.47	8.09	25.96	2.406	1.148	0.465	19.227	0.037	0.685	0.775	0.041	2.583	-26.19	
M_41	M-XE	0.00	5.90	45.27	41.43	49.71	12.81	18.00	2.754	1.003	0.329	22.923	0.047	0.398	0.101	0.024	2.479	-21.24	3.41
M_43	M-XE	0.10	17.16	74.38	82.34	75.35	17.34	18.06	3.273	0.982	0.311	20.067	0.041	1.230	0.228	0.024	3.760	-23.28	
M_45	M-XE	0.30	15.34	65.04	60.62	103.39	22.23	35.72	3.877	0.943	0.232	17.171	0.029	1.405	0.450	0.020	4.325	-24.37	
M_48	M-XE	0.17	10.04	65.66	33.08	56.54	15.39	25.77	3.161	0.995	0.310	21.053	0.035	0.335	0.161	0.023	3.127	-25.30	
M_49	M-XE	0.63	6.72	54.25	65.47	50.87	12.33	20.50	2.475	1.000	0.291	22.824	0.040	0.772	0.280	0.033	2.207	-25.56	
M_50	M-XE	0.09	9.08	90.65	31.51	46.93	13.68	28.11	2.683	0.953	0.329	23.056	0.043	0.264	0.058	0.024	2.755	-23.93	
M_51	M-XE	0.27	11.02	82.94	39.65	54.63	12.32	20.94	2.736	0.996	0.334	21.907	0.040	0.444	0.360	0.026	2.629	-25.59	
M_53	M-XE	1.83	13.34	61.36	44.75	68.10	10.07	22.95	2.582	0.993	0.354	23.693	0.046	0.697	0.086	0.060	1.963	-24.07	
M_56	M-XE	0.10	19.05	74.39	38.82	70.11	13.80	26.19	3.140	0.977	0.322	21.498	0.038	0.531	0.097	0.032	2.873	-24.00	
M_58	M-XE	0.18	17.10	102.79	37.92	59.70	13.80	36.85	3.043	1.030	0.326	20.779	0.046	0.511	0.215	0.027	2.844	-24.48	
M_60	M-XE	0.21	46.50	307.65	42.16	92.07	31.26	88.90	4.115	0.969	0.229	15.723	0.028	0.751	0.527	0.018	5.455	-24.76	
M_62	M-XE	0.00	21.73	203.14	32.16	77.69	20.19	51.82	4.083	1.057	0.364	15.419	0.029	0.773	0.144	0.017	4.637	-23.66	
M_63	M-XE	0.07	0.00	2.37	22.03	12.76	3.07	12.01	3.458	1.228	0.564	20.257	0.031	0.084	0.072	0.027	1.353	-25.30	
M_65	M-XE	0.23	21.13	150.40	36.80	103.73	19.82	34.34	3.736	0.987	0.249	19.048	0.033	1.108	0.225	0.026	4.174	-23.89	
M_71	M-XE	0.00	0.00	1.66	20.38	15.12	1.63	7.63	2.527	1.241	0.566	22.858	0.031	0.266	0.138	0.029	0.437	-25.65	
	n (Row)	43	n (Col)	17															
	Min	0.00	0.00	1.66	20.38	12.76	1.63	7.63	1.39	0.79	0.14	13.34	0.03	0.08	0.06	0.01	0.44	-28.76	-0.13
	Max	3.40	193.78	307.65	347.56	103.73	42.86	88.90	4.35	1.24	0.57	23.86	0.07	1.40	10.57	0.14	6.87	-21.24	5.11
	Mean	0.36	4.65	64.78	55.27	52.54	10.48	24.64	2.70	1.03	0.34	20.30	0.04	0.67	0.36	0.04	2.30	-25.45	2.78
	Median	0.48	10.29	73.84	53.16	55.70	12.33	23.91	2.68	1.03	0.33	21.28	0.04	0.75	0.37	0.03	2.58	-25.56	3.41
	Std Dev	0.86	29.07	68.40	53.45	24.01	8.46	15.78	0.82	0.08	0.09	2.87	0.01	0.30	1.62	0.03	1.41	1.56	1.84
	Var	0.74	845.06	4677.93	2857.25	576.66	71.49	249.09	0.67	0.01	0.01	8.23	0.00	0.09	2.63	0.00	1.99	2.44	3.38
	SE	0.06	0.71	9.88	8.43	8.01	1.60	3.76	0.41	0.16	0.05	3.09	0.01	0.10	0.05	0.01	0.35	-3.88	0.42

APPENDIX 2.5 Target Sediment Geochemical Data.

Sample Date	Source Type	TOC	Copper	Zinc	Strontium	Rubidium	Cobalt	Nickel	Aluminum	Sodium	Magnesium	Silica	Phosphorus	Potassium	Calcium	Manganese	Iron	$\delta^{13}\text{C}$	$\delta^{15}\text{N}$
SIBF_20151002	SIBF	4.09	24.22	188.90	112.23	76.87	12.97	35.52	2.329	1.021	0.283	15.200	0.055	0.925	2.965	0.159	2.717	-27.78	6.61
SIBF_20151016	SIBF	3.58	25.26	147.90	93.64	60.48	10.36	23.41	2.055	0.991	0.273	16.606	0.070	0.882	2.859	0.202	2.278	-28.00	6.63
SIBF_20151030	SIBF	3.71	24.82	141.44	92.31	73.50	10.83	33.50	2.270	0.954	0.306	17.195	0.060	0.934	2.093	0.129	2.448	-27.35	6.70
SIBF_20151113	SIBF	4.28	28.13	164.69	94.08	75.12	13.11	29.95	2.635	0.990	0.341	16.435	0.061	0.974	2.194	0.096	2.927	-27.78	6.06
SIBF_20151127	SIBF	2.78	17.05	115.90	79.45	68.43	9.91	32.89	2.245	1.041	0.373	18.588	0.062	0.923	1.478	0.111	2.339	-27.55	10.67
SIBF_20151211	SIBF	2.90	20.47	123.73	73.80	68.82	9.41	29.66	2.326	0.958	0.348	19.326	0.069	0.988	1.137	0.131	2.256	-26.65	6.06
SIBF_20151218	SIBF	3.69	33.46	133.80	86.50	68.88	11.64	31.49	2.321	0.996	0.314	18.000	0.073	0.974	2.042	0.173	2.345	-28.05	3.18
SIBF_20160115	SIBF	2.61	14.99	128.35	71.20	73.69	11.54	30.09	2.293	1.022	0.417	18.670	0.056	1.002	0.861	0.113	2.458	-26.54	3.52
SIBF_20160129	SIBF	2.50	13.40	112.13	67.47	67.90	9.66	28.06	2.279	0.971	0.305	19.739	0.062	1.000	0.847	0.112	2.305	-26.40	4.63
SIBF_20160304	SIBF	2.06	12.26	105.51	68.40	66.07	10.43	29.51	2.291	0.979	0.302	20.133	0.056	0.949	0.966	0.099	2.179	-26.78	4.04
SIBF_20160311	SIBF	2.28	26.00	171.13	60.06	85.10	16.87	38.41	2.608	1.027	0.294	17.149	0.046	1.099	0.736	0.101	2.943	-26.38	2.95
SIBF_20160415	SIBF	2.73	12.30	126.66	75.64	70.49	12.48	27.97	2.378	0.940	0.316	19.006	0.065	0.981	1.491	0.086	2.446	-27.36	4.57
SIBF_20160422	SIBF	1.74	10.03	117.78	63.48	45.49	8.71	29.10	2.058	1.108	0.375	17.225	0.063	0.791	1.987	0.074	2.180	-27.55	4.43
SIBF_20160506	SIBF	2.29	15.80	120.00	75.90	75.26	11.54	29.89	2.299	1.017	0.366	19.130	0.053	1.000	1.084	0.112	2.308	-26.83	4.54
SIBF_20160527	SIBF	1.68	12.50	99.91	61.95	67.71	11.78	28.00	2.271	1.021	0.364	21.141	0.050	0.948	0.683	0.088	2.130	-26.22	4.75
SIBF_20160603	SIBF	3.23	19.11	131.22	82.07	70.62	11.97	35.08	2.429	0.957	0.346	18.421	0.061	1.028	2.180	0.142	2.443	-27.42	4.99
SIBF_20160610	SIBF	2.57	18.01	138.52	85.19	66.24	11.24	32.94	2.364	0.977	0.293	17.127	0.071	0.980	2.659	0.151	2.457	-27.67	4.44
SIBF_20160617	SIBF	3.81	19.05	162.38	84.87	67.31	12.01	32.48	1.591	1.219	0.433	12.835	0.030	0.713	2.480	0.150	2.385	-27.42	4.98
SIBF_20160624	SIBF	3.21	14.71	128.82	98.03	62.71	9.89	28.94	2.036	1.093	0.352	15.622	0.050	0.815	3.172	0.144	2.276	-27.43	5.30
SIBF_20160701	SIBF	3.39	9.29	133.64	118.18	69.49	13.21	32.09	2.370	0.941	0.261	16.389	0.071	0.937	4.017	0.207	2.327	-27.59	5.13
SIBF_20160708	SIBF	3.08	16.51	144.63	91.11	82.39	12.92	30.22	2.389	1.030	0.358	16.705	0.055	0.983	2.368	0.129	2.684	-27.33	5.00
SIBF_20160715	SIBF	3.26	15.45	145.29	105.23	71.56	13.65	37.73	2.401	0.896	0.286	16.698	0.070	0.993	3.137	0.160	2.623	-27.60	5.50
SIBF_20160729	SIBF	2.33	17.21	126.17	91.03	81.99	14.53	35.59	2.732	0.929	0.305	18.920	0.050	1.031	1.703	0.110	2.768	-26.95	5.20
SIBF_20160805	SIBF	2.66	23.62	155.15	97.19	83.92	15.82	36.60	2.551	1.012	0.338	16.561	0.053	0.979	1.978	0.118	2.905	-27.28	5.20
SIBF_20160812	SIBF	2.63	15.36	146.07	91.09	83.64	14.06	33.69	2.448	0.934	0.257	17.018	0.061	1.029	2.092	0.115	2.872	-27.59	5.04
SIBF_20160819	SIBF	2.34	16.82	110.03	121.95	69.38	12.39	31.53	2.389	0.929	0.281	18.708	0.056	0.990	2.421	0.084	2.600	-27.60	4.64
SIBF_20160826	SIBF	3.01	20.13	139.57	83.59	81.43	13.53	40.07	2.434	0.945	0.308	18.550	0.057	1.061	1.562	0.129	2.514	-27.34	5.11
SIBF_20160902	SIBF	2.69	14.24	135.01	99.24	72.33	12.31	27.22	2.251	0.954	0.267	16.760	0.059	0.976	2.528	0.156	2.439	-27.57	5.24
SIBF_20160909	SIBF	3.19	17.17	138.48	106.64	77.10	11.74	34.00	2.174	0.996	0.277	15.824	0.058	0.938	2.950	0.168	2.453	-27.54	5.69
SIBF_20160923	SIBF	2.99	20.39	160.41	97.96	79.49	14.85	32.57	2.508	0.983	0.243	15.263	0.055	1.016	2.310	0.190	2.853	-27.07	6.29
SIBF_20160930	SIBF	3.29	10.09	105.95	95.12	47.47	8.24	24.57	2.149	0.979	0.295	15.333	0.068	0.852	3.428	0.173	2.294	-27.81	5.26
SIBF_20161014	SIBF	3.56	15.57	146.64	95.94	69.49	11.10	27.75	2.136	1.001	0.277	14.320	0.071	0.916	3.295	0.102	2.673	-27.57	6.64
S2BF_20151023	S2BF	2.94	31.22	131.26	147.41	56.47	11.56	26.12	2.144	0.910	0.270	15.658	0.925	0.080	3.951	0.136	2.623	-28.34	6.11
S2BF_20151030	S2BF	3.02	19.46	130.11	110.27	69.88	11.24	26.68	2.364	0.962	0.325	18.082	0.974	0.071	2.203	0.116	2.450	-27.69	6.01

S2BF_20151113	S2BF	3.20	24.38	153.86	122.20	79.63	14.62	33.25	2.722	0.936	0.246	16.770	1.059	0.064	2.500	0.117	2.851	-28.02	5.62
S2BF_20151211	S2BF	2.56	20.49	108.46	92.49	66.71	9.49	29.72	2.165	1.039	0.329	19.693	0.983	0.060	1.296	0.123	2.032	-26.67	4.20
S2BF_20160115	S2BF	2.25	11.81	107.87	81.50	66.35	10.48	27.63	2.217	1.023	0.337	19.731	0.966	0.059	1.126	0.096	2.115	-26.76	3.03
S2BF_20160304	S2BF	2.07	11.42	98.37	81.88	67.50	10.72	27.80	2.176	0.936	0.284	21.203	0.918	0.063	1.122	0.088	2.004	-26.97	3.88
S2BF_20160411	S2BF	2.42	23.21	173.16	69.90	88.88	16.36	35.76	2.988	0.951	0.270	17.650	1.174	0.051	0.924	0.115	3.081	-26.57	2.76
S2BF_20160418	S2BF	1.46	10.97	85.26	72.55	56.20	8.03	22.82	2.093	1.075	0.397	20.822	0.871	0.053	0.938	0.089	2.029	-26.90	3.88
S2BF_20160506	S2BF	1.96	14.36	103.05	85.10	68.50	11.05	26.13	2.363	0.965	0.291	21.326	1.012	0.058	1.410	0.100	2.132	-26.99	4.17
S2BF_20160527	S2BF	1.63	10.57	83.12	64.25	55.92	9.47	21.38	2.011	1.081	0.402	20.247	0.876	0.052	0.918	0.066	1.913	-26.18	4.03
S2BF_20160603	S2BF	2.98	17.97	116.95	86.33	66.50	12.09	30.95	2.444	0.999	0.393	18.960	1.004	0.057	1.579	0.103	2.516	-27.91	4.81
S2BF_20160610	S2BF	3.12	5.05	93.74	76.78	43.66	7.84	22.02	1.995	1.026	0.376	18.431	0.825	0.050	1.797	0.072	1.945	-27.64	4.03
S2BF_20160617	S2BF	1.36	22.33	142.75	78.88	69.20	12.62	27.46	2.130	1.071	0.337	17.872	0.919	0.043	0.815	0.108	2.635	-27.11	2.30
S2BF_20160624	S2BF	2.84	12.12	138.42	84.02	61.48	9.57	24.41	1.663	1.219	0.484	14.007	0.639	0.018	1.839	0.092	2.420	-27.79	4.69
S2BF_20160701	S2BF	3.30	16.24	133.10	150.06	66.61	10.81	27.58	2.302	0.948	0.283	16.909	0.987	0.063	3.508	0.134	2.466	-27.77	4.86
S2BF_20160708	S2BF	1.70	19.41	110.60	102.82	71.21	12.19	27.18	2.259	1.054	0.269	19.350	0.973	0.055	1.842	0.085	2.375	-27.19	4.23
S2BF_20160715	S2BF	2.91	13.92	143.15	122.14	67.79	12.61	30.13	2.248	1.021	0.300	16.454	0.979	0.056	2.802	0.122	2.737	-27.37	4.98
S2BF_20160729	S2BF	2.17	20.09	140.01	121.96	90.59	17.76	39.04	2.846	0.964	0.314	17.579	1.050	0.044	1.687	0.098	3.238	-26.89	5.17
S2BF_20160805	S2BF	1.25	18.45	125.61	99.89	71.92	14.11	29.33	2.320	1.049	0.319	20.480	0.972	0.049	1.192	0.092	2.387	-27.34	4.18
S2BF_20160812	S2BF	2.34	21.36	156.66	150.47	84.42	14.79	36.06	2.753	1.013	0.219	16.239	1.067	0.052	2.532	0.120	3.016	-27.72	5.53
S2BF_20160819	S2BF	2.19	20.75	117.43	89.75	73.42	13.85	30.28	2.375	0.990	0.292	20.103	1.030	0.052	1.421	0.109	2.586	-27.12	4.69
S2BF_20160826	S2BF	3.39	20.55	144.50	93.96	80.41	16.94	35.61	2.384	1.022	0.293	16.786	1.028	0.054	1.717	0.109	2.844	-27.22	5.07
S2BF_20160902	S2BF	2.82	14.64	140.69	142.74	76.42	11.30	29.93	2.502	1.024	0.286	17.453	1.032	0.059	2.785	0.125	2.665	-27.76	5.06
S2BF_20160909	S2BF	2.66	13.96	143.10	163.04	77.17	12.96	30.85	2.420	1.003	0.292	16.261	0.992	0.056	3.194	0.131	2.704	-27.90	5.60
S2BF_20160916	S2BF	2.55	16.24	151.37	159.73	80.59	16.96	37.46	2.426	0.941	0.281	16.212	1.056	0.058	2.913	0.125	3.063	-25.47	5.56
S2BF_20160923	S2BF	3.24	16.75	146.57	175.16	74.56	14.58	35.46	2.250	0.921	0.198	14.778	0.972	0.061	4.383	0.127	2.802	-27.61	6.60
S2BF_20160930	S2BF	3.61	16.32	146.79	155.40	70.47	12.03	30.65	2.311	0.977	0.307	14.926	0.953	0.052	3.660	0.128	2.793	-27.90	6.54
S2BF_20161014	S2BF	2.41	21.59	167.51	142.87	72.59	14.46	29.47	2.603	0.985	0.312	15.471	1.082	0.059	2.794	0.129	3.036	-27.93	6.06
S3BF_20151016	S3BF	2.01	12.86	118.59	232.04	72.26	14.83	32.76	2.502	0.952	0.226	14.782	0.063	0.833	5.632	0.050	2.833	-28.18	6.69
S3BF_20151023	S3BF	2.94	6.76	90.13	321.50	45.75	6.57	16.85	1.593	0.813	0.158	12.692	0.070	0.624	10.754	0.058	1.838	-28.25	6.48
S3BF_20151030	S3BF	2.42	15.46	107.85	201.09	67.46	11.33	31.16	2.318	0.889	0.299	17.220	0.073	0.917	4.129	0.089	2.264	-28.16	5.92
S3BF_20151113	S3BF	2.78	18.59	145.04	195.61	73.66	15.29	35.24	2.491	0.892	0.215	16.343	0.060	0.956	4.342	0.092	2.749	-28.11	5.51
S3BF_20151127	S3BF	2.21	12.65	95.38	185.76	58.66	8.68	26.34	1.961	0.919	0.270	17.539	0.066	0.807	4.746	0.082	1.892	-27.94	4.58
S3BF_20151218	S3BF	3.15	16.57	116.97	153.26	57.35	10.59	24.95	2.026	0.929	0.244	17.557	0.072	0.880	4.151	0.102	2.220	-28.10	2.55
S3BF_20160115	S3BF	1.63	12.90	85.50	90.33	61.03	8.14	26.72	2.193	1.038	0.300	20.844	0.049	0.949	1.118	0.088	2.001	-26.61	3.06
S3BF_20160129	S3BF	1.75	7.28	84.42	84.51	56.70	11.02	21.59	2.231	1.047	0.426	20.430	0.055	0.984	1.155	0.080	2.199	-27.41	3.05
S3BF_20160304	S3BF	1.96	10.67	92.71	88.98	59.79	8.72	26.88	2.241	0.986	0.283	19.667	0.050	0.941	1.282	0.079	2.295	-26.73	3.59
S3BF_20160318	S3BF	2.01	8.89	92.33	78.45	59.93	9.80	28.13	2.092	1.049	0.385	19.333	0.049	0.862	1.239	0.083	2.075	-26.67	4.29

APPENDIX 3.1 Basic Statistics for Solutes and Field Parameters.

	Season	NPDES Permitted Discharge			**Maximum Allowed Permitted Per Year							
		Minimum Daily Concentration (mg/L)	Average Monthly Concentration (mg/L)	Maximum Daily Concentration (mg/L)	2015 Maximum Allowed (lb/yr)	2016 Maximum Allowed (lb/yr)	2015 Total (lb/yr)	2016 Total (lb/yr)	2015 Maximum Allowed (kg/yr)	2016 Maximum Allowed (kg/yr)	2015 Total (kg/yr)	2016 Total (kg/yr)
		Ammonia as N	Summer		4	6						
Ammonia as N	Winter		10	15	15,167	15,167	1,085	453	6,790	6,880	492	205
BOD carb (5-day, 20°C) % removal			20	30								
BOD carb (5-day, 20°C)					43,435	43,435	6,489	6,760	19,702	19,702	2,943	3,066
*Total Coliform (MF, mTEC)			130	240								
Nitrogen			monitoring only	monitoring only	None Listed	None Listed	20,132	17,522	None Listed	None Listed	9,132	7,948
§Inorganic Nitrogen			monitoring only	monitoring only		None Listed		352		None Listed		160
§Oil and grease			monitoring only	monitoring only		None Listed		7,043		None Listed		3,195
Oxygen		7										
Phosphorus			monitoring only	monitoring only	None Listed	None Listed	3,618	3,978	None Listed	None Listed	1,641	1,804
*§Total Kjeldahl Nitrogen			monitoring only	monitoring only		None Listed		11,973		None Listed		5,431
Solids, suspended % removal		85										
Solids, total dissolved			monitoring only	monitoring only		None Listed		612,737		None Listed		277,933
Solids, total suspended			30	45	65,335	65,335	10,205	11,521	29,635	29,635	4,629	5,226
§Temperature (°F)			monitoring only	monitoring only								
Total Residual Chlorine			0.019	0.019	29	22	15	14	13	10	7	6
pH		6		9								

APPENDIX 3.2 Site 1 Water Quality Results and Field Parameter Readings.

Site 1	Cl⁻	SO₄²⁻	NO₃⁻	PO₄³⁻	WT	DO	SC	pH
		(mg/L)			(°C)	(mg/L)	(µS/cm)	
2015-Oct-02	171.93	363.88	12.04	78.13	15.41	9.81	547	7.35
2015-Oct-09	272.07	564.69	75.73	55.01	17.80	9.33	597	6.30
2015-Oct-16	259.61	522.81	74.2	69.16	13.34	10.36	590	6.24
2015-Oct-30	151.81	243.45	63.72	55.89				
2015-Nov-06	119.02	128.35	42.67	53.26	16.97	6.02	429	4.64
2015-Nov-13	105.29	187.19	53.68	57.67	10.78	10.94	496	6.87
2015-Nov-27	122.72	210.60	74.72	63.41	12.50	10.57	488	5.95
2015-Dec-11	128.80	216.45	88.2	62.03	12.34	10.47	475	5.99
2015-Dec-18	109.56	186.54	57.14	63.1	7.80	11.72	483	8.08
2016-Jan-29	443.75	333.58	99.31	41.33	8.02	11.58	486	8.40
2016-Feb-05	190.50	201.80	98.07	60.15	9.02	11.48	396	6.58
2016-Feb-19	743.89	564.82	74.12	43.77	10.26	11.48	396	8.20
2016-Feb-26	212.32	191.47	85.68	51.99	9.87	11.22	389	6.47
2016-Mar-04	291.90	305.76	124.13	52.84	9.32	11.32	448	6.81
2016-Mar-11	185.59	190.87	69.63	48.98	12.92	10.46	279	4.58
2016-Mar-18	334.52	557.34	95.15	41.39	11.52	10.71	438	6.13
2016-Apr-01	214.40	254.27	82.64	46.47	13.63	10.13	354	6.47
2016-Apr-08	219.51	329.14	127.67	56.68	9.87	9.61	459	6.17
2016-Apr-15	263.16	416.99	47.46	57.46	16.80	9.61	0	7.68
2016-Apr-22	235.39	421.88	53.26	53.91	16.81	9.49	455	8.25

Cl⁻ (Chloride); SO₄²⁻ (Sulfate); NO₃⁻ (Nitrate); PO₄³⁻ (Phosphate); WT (Water Temperature); DO (Dissolved Oxygen); SC (Specific Conductivity); pH

APPENDIX 3.3 Site 2 Water Quality Results and Field Parameter Readings.

Site 2	Cl ⁻	SO ₄ ²⁻ (mg/L)	NO ₃ ⁻	PO ₄ ³⁻	WT (°C)	DO (mg/L)	SC (µS/cm)	pH
2015-Oct-02	276.41	783.018	31.15	55.1	16.11	9.69	669	7.69
2015-Oct-09	221.04	768.54	37.36	54.77	16.96	9.53	797	7.9
2015-Oct-16	153.61	553.096	20.7	55.25	14.1	10.2	724	7.67
2015-Oct-30	252.02	610.009	82.49	51.28				
2015-Nov-06	89.61	219.179	165.22	54.05	16.92	9.54	523	7.54
2015-Nov-13	107.01	278.339	50.92	66.45	12.76	10.48	586	7.66
2015-Nov-27					12.58	10.56	587	7.59
2015-Dec-11	107.01	278.339	50.92	66.45	12.38	10.48	560	7.91
2015-Dec-18	138.1	372.824	37.07	59.39	9.69	11.22	584	7.39
2016-Jan-29	800.2	661.813	74.39	48.22	8.36	11.53	634	8.08
2016-Feb-05	314.43	369.679	84.21	44.28	9.62	11.34	462	6.68
2016-Feb-19	835.63	649.646	80.21	21.55	10.37	10.99	627	7.81
2016-Feb-26	347.69	343.439	79.53	44.29	10.26	11.12	456	6.54
2016-Mar-04	465.08	637.183	102.84	40.04	9.86	11.2	524	7.97
2016-Mar-11	233.03	274.426	61.39	43.26	12.93	10.48	313	7.56
2016-Mar-18	332.91	559.401	91.1	46.01	13.18	10.33	517	7.02
2016-Apr-01	289.82	448.796	29.95	56.76	14.02	10.03	395	6.67
2016-Apr-08	351.15	782.067	45.77	55.69	11.49	9.42	548	6.54
2016-Apr-15	409.12	833.712	98.97	76.16	17.6	9.42	0	7.58
2016-Apr-22	486.02	940.614	107.71	70.88	17.1	9.45	586	7.89

Cl⁻ (Chloride); SO₄²⁻ (Sulfate); NO₃⁻ (Nitrate); PO₄³⁻ (Phosphate); WT (Water Temperature); DO (Dissolved Oxygen); SC (Specific Conductivity); pH

APPENDIX 3.4 Site 3 Water Quality Results and Field Parameter Readings.

Site 3	Cl ⁻	SO ₄ ²⁻ (mg/L)	NO ₃ ⁻	PO ₄ ³⁻	WT (°C)	DO (mg/L)	SC (µS/cm)	pH
2015-Oct-02	115.53	337.726	22.31	53.86	15.64	9.81	631	8.23
2015-Oct-09	205.41	740.148	25.7	54.06	18.09	9.34	732	8.57
2015-Oct-16	26.49	79.629	11.35	49.05	15.17	9.98	674	8.37
2015-Oct-30	211.45	489.157	78.71	54.56			0	
2015-Nov-06	188.16	468.732	25.83	45.26	17.02	9.54	500	7.82
2015-Nov-13	108.02	233.464	48.76	55.16	12.77	10.5	577	8.52
2015-Nov-27					13.34	10.4	574	8.26
2015-Dec-11	108.02	233.464	48.76	55.16	13.4	10.26	552	8.17
2015-Dec-18	155.52	449.481	56.04	58.34	8.91	11.48	580	8.2
2016-Jan-29	723.67	600.824	71.33	40.54	7.23	11.91	626	6.55
2016-Feb-05	193.3	232.885	69.44	67.16	10.69	11.09	446	7.69
2016-Feb-19	717.34	583.92	95.55	47.04	11.06	10.84	589	8.35
2016-Feb-26	221.57	222.523	76.13	41.28	11.33	10.88	433	8.07
2016-Mar-04	381.02	537.522	113.7	48.7	10.31	11.11	522	8.2
2016-Mar-11	193.66	241.955	72.54	46.56	13.36	10.4	360	7.31
2016-Mar-18	285.1	484.435	111.76	44.28	15.33	9.85	500	7.23
2016-Apr-01	220.68	363.443	42.08	50.69	14.68	9.95	375	6.79
2016-Apr-08	302.36	673.35	51.61	55.05	11.78	9.14	516	6.86
2016-Apr-15	355.66	760.987	27.78	84.39	19.2	9.14	0	7.87
2016-Apr-22	338.49	880.207	100.86	26.55	18.43	9.23	541	8.36

Cl⁻ (Chloride); SO₄²⁻ (Sulfate); NO₃⁻ (Nitrate); PO₄³⁻ (Phosphate); WT (Water Temperature); DO (Dissolved Oxygen); SC (Specific Conductivity); pH

APPENDIX 3.5 Basic Statistics for Solutes and Field Parameters.

Baseflow (< 3cm of Precipitation within 72 hours)												
Site 1				Site 2				Site 3				
	Min	Median	Max	SE	Min	Median	Max	SE	Min	Median	Max	SE
Chloride <i>mg/L</i>	105.29	247.50	743.89	45.66	89.61	332.91	835.63	69.79	26.49	285.10	723.67	56.69
Sulfate <i>mg/L</i>	128.35	331.36	564.82	41.73	219.18	637.18	940.61	64.17	79.63	537.52	880.21	63.93
Nitrate <i>mg/L</i>	42.67	74.46	127.67	7.15	20.70	74.39	165.22	10.93	11.35	51.61	113.70	9.71
T. Phosphorus <i>mg/L</i>	41.33	55.85	69.16	2.24	21.55	55.25	76.16	3.96	26.55	49.05	84.39	3.62
Water Temperature <i>°C</i>	7.80	15.01	25.38	0.82	8.81	14.20	22.41	0.66	8.91	15.33	22.57	0.63
Dissolved Oxygen <i>mg/L</i>	6.02	9.49	11.72	0.21	846.00	9.44	11.56	0.15	8.21	9.14	11.91	0.15
Specific Conductance <i>µS/cm</i>	320	474	598	9	358	587	797	16	348	556	732	14
pH	4.64	7.97	8.40	0.15	6.24	7.81	8.19	0.07	6.55	8.17	8.57	0.07
Stormflow (≥ 3cm of Precipitation within 72 hours)												
Site 1				Site 2				Site 3				
	Min	Median	Max	SE	Min	Median	Max	SE	Min	Median	Max	SE
Chloride <i>mg/L</i>	151.81	188.05	214.40	9.78	233.03	283.12	347.69	17.01	115.53	202.56	221.57	16.28
Sulfate <i>mg/L</i>	190.87	222.62	363.88	26.95	274.43	409.24	783.02	77.96	222.52	289.84	489.16	42.36
Nitrate <i>mg/L</i>	12.04	76.14	98.07	12.36	29.95	70.46	84.21	10.32	22.31	70.99	78.71	9.31
T. Phosphorus <i>mg/L</i>	46.47	53.94	78.13	4.68	43.26	47.79	56.76	2.45	41.28	52.28	67.16	3.58
Water Temperature <i>°C</i>	8.02	10.78	15.41	0.91	8.36	12.59	16.11	0.86	7.23	11.33	15.64	0.87
Dissolved Oxygen <i>mg/L</i>	9.81	10.46	11.48	0.22	9.69	10.50	11.34	0.20	9.81	10.40	11.09	0.17
Specific Conductance <i>µS/cm</i>	279	388	547	28	313	444	669	36	360	446	631	33
pH	4.58	6.61	8.04	0.34	6.54	7.30	8.04	0.20	6.79	7.99	8.26	0.18

REFERENCES

- Abban, B., Papanicolaou, A. N., Cowles, M. K., Wilson, C. G., Abaci, O., Wacha, K., Schilling, K. and Schnoebelen, D., 2016, An enhanced Bayesian fingerprinting framework for studying sediment source dynamics in intensively managed landscapes, *Water Resour Res* 52: 4646-4673.
- Albertson, P. E., 2001, Sustainability of military lands: Historic erosion trends at Fort Leonard Wood, Missouri, *The Environmental Legacy of Military Operations: Geo Soc Am Rev Eng Geol* 14:151-162.
- Altman, D. G. and Bland, J. M., 1995. Statistics notes: the normal distribution. *Bmj*.310(6975): 298p.
- Anderson, A. B., Palazzo, A. J., Ayers, P.D., Fehmi, J. S., Shoop, S. and Sullivan, P., 2005, Assessing the impacts of military vehicle traffic on natural areas, Introduction to the special issue and review of the relevant military impact literature, *J. of Terramchanics* 42:143-158.
- Anderson, C. and Lockaby, B., 2011, Research gaps related to forest management and stream sediment in the United States, *Env Mgmt* 47: 303-313.
- Annabel, W. K., Frape, S. K., Shouakar-Stash, O., Shanoff, T., Drimmie, R. J. and Harvey, F. E., 2007, ³⁷Cl, ¹⁵N, ¹³C isotopic analysis of common agro-chemicals for identifying non-point source agricultural contaminants, *Appl Geochem* 22(7):1530-1536.
- Anning, D. W. and Flynn, M. E., 2014, Dissolved-solids sources, loads, yields, and concentrations in streams of the conterminous United States, U.S. Geological Survey *Sci Inv Rep* 2014-5012:101p.
- Arriaga, F. J. and Lowery, B., 2003, Soil physical properties and crop productivity of an eroded soil amended with cattle manure, *Soil Sci*, 168 (12): 888-899.
- Belmont, P., Willenbring, J. K., Schottler, S. P., Marquard, J., Kumarasamy, K. and Hemmis, J. M., 2014, Toward generalizable sediment fingerprinting with tracers that are conservative and nonconservative over sediment routing timescales, *J. of Soils Sediment* 14 (8):1479-1492.
- Benson, P. E., Nokes, W. A., Cramer, R. L., O'Conner, J. and Lindeman, W., 1986, Air-quality and noise issues in environmental planning: Washington, D.C., *Transportation Res B, Natl Res Council Tech Rep*:72p.
- Blake, W. H., Taylor, K. J., Russell, M. A. and Walling, D. E., 2012, Tracing crop-specific sediment sources in agricultural catchments, *Geomorph*,139: 322-329.
- Braun, E., 1950, *Deciduous forests of eastern North America*, The Blakiston Co., Philadelphia, Pennsylvania:596p.

- Brown, A. G., 1985, The potential use of pollen in the identification of suspended sediment sources, *Earth Surf Proc Land*, 10(1): 27-32.
- Bruker, (n.d), Bruker Elemental Tracer Series User Guide, Bruker Products, Accessed April 2, 2018.
- Bruker, 2015, Tracer XRF Spectrometer, Bruker Products, Accessed April 2, 2018.
- Bryant, W. L. and Carlisle, D. M., 2012, The relative importance of physiochemical factors to stream biological condition in urbanizing basins: Evidence from multimodel inference, *J Freshwater Sci*, 31(1):154-166.
- Caitcheon, G G., 1993, Applying environmental magnetism to sediment tracing, *Tracers in Hydro: P Yokohama Symp*, IAHS Publ. No. 215:285-292.
- Carey, R. O. and Migliaccio, K. W., 2009, Contribution of wastewater treatment plant effluents to nutrient dynamics in aquatic systems: A Review, *Env Mgmt*, 44:205-217.
- Carter, J., Owens, P. N., Walling, D. E. and Leeks, G. L. L., 2003, Fingerprinting suspended sediment sources in a large urban river system, *Sci Total Environ*, 314-316: 513-534.
- Cashman, M. J., Gellis, A. C., Gorman Sanisaca L., Noe, G. B., Cogliandro, V. and Baker, A., 2018, Bank-derived material dominates fluvial sediment in a suburban Chesapeake Bay watershed, *River Res Applic*, John Wiley & Sons, Ltd. 1-13.
- Charlesworth, S. M. and Lees, J. A., 2001, The application of some mineral magnetic measurements and heavy metal analysis for characterizing find sediments in urban catchment, Coventry, UK. *J. of Appl Geophy*, 48 (2): 113-125.
- Charlesworth, S., Miguel, E. D. and Ordóñez, A., 2011, A review of distribution of particulate trace elements in urban terrestrial environments and its application to considerations of risk. *Env. Geochem. Health*, 33 (2): 103-123.
- Charlesworth, S. M., Ormerod, L. M. and Lees, J. A., 2000, Tracing sediments within urban catchments using heavy metal, mineral magnetic and radionuclide signatures. *Tracers in Geomorph*, 345-368.
- Chen, F., Taylor, W. D., Anderson, W. B. and Huck, P. M., 2013, Application of fingerprint-based multivariate statistical analyses in source characterization and tracking of contaminated sediment migration in surface water, *Env Poll*, 179:224-231.
- Collins, A. L., Walling, D. E. and Leeks, G. J. L., 1996, Source type ascription for fluvial suspended sediment based on quantitative composite fingerprinting technique, *Catena* 29: 1-27.
- Collins, A. L., Walling, D. E. and Leeks, G. J. L., 1998, Use of composite fingerprints to determine the provenance of the contemporary suspended sediment load transported by river, *Earth Surf Proc Land*, 23:31-52.

- Collins, A. L., Walling, D. E. and Leeks, G. J. L., 1997, Use of the geochemical record preserved in floodplain deposits to reconstruct recent changes in river basin sediment sources, *Geomorph*, 9(1-2):151-167.
- Collins, A. L. and Walling, D. E., 2002, Selecting fingerprint properties for discriminating potential suspended sediment sources in river basins, *J. Hydrol* 261 (1-4): 218-244.
- Collins, A. L., Zhang, Y., Walling, D. E. and Black, K., 2010a, Apportioning sediment sources in a grassland dominated agricultural catchment in the UK using a new tracing framework. In: *Sediment Dynamics for a Changing Future*, IAHS 337: 68-75.
- Collins, A. L., Walling, D. E., Stroud, R. W., Robson, M. and Peet, L. M., 2010b, Assessing damaged roads verges as suspected sediment source in the Hampshire Avon catchment southern United Kingdom, *Hydrol. Process* 1106-1122.
- Collins, A. L., Walling, D. E., Webb, L. and King, P., 2010c, Apportioning catchment scale sediment sources using a modified composite fingerprinting technique incorporating property weightings and prior information, *Geoderm* 155(3-4): 249-263.
- Collins, A. L., Zhang Y., Walling, D.E., Grenfell, S.E. and Smith, P., 2010, Tracing sediment loss from eroding farm tracks using a geochemical fingerprinting procedure combining local and genetic algorithm optimization, *Sci Total Env* 408 (22): 5461-5471.
- Collins, A. L., Pulley, S., Foster, I. D. L., Gellis, A., Porto, P. and Horowitz, A. J., 2017, Sediment source fingerprinting as an aid to catchment management: A review of the current state of knowledge and methodological decision-tree for end-users, *J Env Mgmt*, (194): 86-108.
- Connair, D. P. and Murray, B. S., 2002, Karst groundwater basin delineation, Fort Knox, Kentucky, *Eng. Geol.* 65:125-131.
- Coplen, T. B., Brand, W. A., Gehre, M., Groning, M., Meijer, H. A. J., Toman, B., Verkouteren, R. M., 2006, New guidelines for $\delta^{13}\text{C}$ measurements, *Analyt Chem*, 78: 2439-2441.
- Corsi, S. R., Graczyk, D. J., Geis, S. W., Booth, N. L. and Richards, K. D., 2010, A fresh look at road salt: aquatic toxicity and water-quality impacts on local, regional, and national scales, *Env Sci Tech*, 44(19):7374-7382.
- Crain, A. S. and Martin, G. R., 2009, Trends in surface-water quality at selected ambient-network stations in Kentucky, 1979-2004. U.S. Geological Survey Sci Inv Rep 2009-5027, 61p.
- Cranfill, R., 1991, Flora of Hardin County, Kentucky, *Castanea* 56.4:228-267.
- Crim, J. F., Schoonover, J. E., Willard, K. W. J., Groninger, J. W., Zaczek, J. J. and Ruffner, C. M., 2011, Evaluation of erosion and sedimentation associated with tracked vehicle training, *Proc Central Hardwood Forest Conf*, 375-388.

- Curtis, W. R., 1978, Sediment yield from strip-mined watersheds in Eastern Kentucky. Amer Astronautical Soc, Sci Technol Series 88-100.
- d'Oleire-Oltmanns, S., Marzloff, I., Peter, K. D. and Ries, J. B., 2012, Unmanned aerial vehicle (UAV) for monitoring soil erosion in Morocco. *Remote Sens.* 4:3390-3416.
- Dale, V. H., Beyeler, S. C. and Jackson, B., 2002, Understory vegetation indicators of anthropogenic disturbance in longleaf pine forests at Fort Benning, Georgia, USA, *Ecol Indic*, 1: 155-170.
- Daniel, T. C., Sharpley, A. N. and Lemunyon, J. L., 1998, Agricultural phosphorus and eutrophication: A symposium overview, *J Env Qual*, 27(2):251-257.
- Davis, C. M. and Fox, J. F., 2009, Sediment fingerprinting: review of the method and future improvements for allocating nonpoint source pollution, *J Env Eng*, (135): 490-504.
- Davies, W. E. and LeGrand, H. E., 1972, Karst of the United States. In: Herak M, Stringfield VT (eds.) *Karst: important karst regions of the northern hemisphere*, Elsevier, New York: 467-505.
- Deacon, J. R., Soule, S. A. and Smith, T. E., 2005, Effects of urbanization on stream quality at selected sites in the seacoast region in New Hampshire, 2001-03, U.S. Geological Survey Sci Inv Report 2005-5103:18p.
- Dogwiler, T. and Wicks, C. M., 2004, Sediment entrainment and transport in fluvio karst systems, *J. Hydrol*, 295:163-172.
- Dressing, S. A., Meals, D. W., Harcum, J. B., Spooner, J., Stribling, J. B., Richards, R. P., Millard, C. J., Lanberg, S. A. and O'Donnell, J. G., 2016, Monitoring and evaluating nonpoint source watershed projects. U.S. Environmental Protection Agency, Nonpoint Source Control Branch, EPA841-R-16-010.
- Driscoll, P., Lecky, F. and Crosby, M., 2000, An introduction to everyday statistics-1, *J Accid Emerg Med*, 17(3):205-11.
- Earle, S., 2015, *Physical Geology*, BCcampus Open Textbook. Accessed January 12, 2019.
- Eberl, D. D., 2004, Quantitative mineralogy of the Yukon River system: changes with reach and season, and determining sediment provenance, *Am Min*, 89:1784-1794.
- Edwards, T. K. and Glysson, G. D., 1999, Chapter C2, Field Methods for Measurements of Fluvial Sediment; Techniques of water-resources investigations of the U.S. Geological Survey, Book 3, Applications of Hydraulics. Revision of Guy, H. P. and Norman, V. W., 1970. U.S. Geological Survey.
- Eimers, M. C. and Dillon, P. J., 2002, Climate effects on sulphate flux from forested catchments in south-central Ontario, *Biogeochem*, 61:337-335.

- Evrard, O., Navratil, O., Ayrault, S., Ahmadi, M., Nemery, J., Legout, C., Lefevre, I., Poirel, A., Bonte, P. and Esteves, M., 2011, Combining suspended sediment monitoring and fingerprinting to determine the spatial origin of fine sediment in a mountainous river catchment, *Earth Surf Proc Land*, 1072-1089.
- Evans, M., and Frick, C., 2001, The effects of road salts on aquatic ecosystems. NWRI Contribution Series No. 02:308, National Water Research Institute and University of Saskatchewan, Saskatoon, SK, Canada. Accessed April 1, 2019.
- Falcone, J. A., Murphy, J. C. and Sprague, L. A., 2018, Regional patterns of anthropogenic influences on streams and rivers in the conterminous United States, from the early 1970s to 2012, *J Land Use Sci*, 13(6):585-514.
- Ffolliott, P. F., Brooks, K. N., Neary, D. G., Tapia, R. P. and Garcia-Chevesich, P., 2013, Soil erosion and sediment production on watershed landscapes: processes, prevention and control, International Hydrology Programme for Latin America and the Caribbean, PHI-VII. United Nations Educational, Scientific and Cultural Organizations, ISBN978-92-9089-190-1
- Field, A., 2009, *Discovering statistics using SPSS*, 3ed. London: SAGE publications Ltd, p.822.
- Florence, T. M. and Batley, G. E., 1980, Chemical speciation in natural waters. *CRC Critical Review in Analyt Chem*, 9:219-296.
- Fort Knox, 2019, Army technology, history Fort Knox Army Base, Kentucky. <https://home.army.mil/knox/index.php/about/history>, Website last updated: 2019, Accessed April 15, 2019.
- Forstner, U. and Salomans, W., 1980, Trace metal analysis on polluted sediments. Part I: assessment of source and intensities, *Env Technol Lett*, 1:494-505.
- Foster, I. D. L. and Charlesworth, S, 1996, Heavy metals in the hydrological cycle: trends and explanation, *Hydrol Processes*, 10:227-261.
- Foster, I. D. L., Grew, R. and Dearing, J. A., 1990, Magnitude and frequency of sediment transport in agricultural catchments: a paired lake-catchment study in Midland England, *Soil Erosion and Agricultural Land*, Proceedings of a workshop sponsored by the British Geomorphological Research Group, Coventry, UK, John Wiley & Sons Ltd:153-171.
- Foster, I. D. L. and Lees, J. A., 2000, Tracers in geomorphology: theory and applications in tracing fine particulate sediments, In: Foster, I.D.L. (Ed.), *Tracers in Geomorph*: 3-20.
- Foucher, A., Laceby, P. J., Salvador-Blanes, S., Evrard, O., Le Gall, M., Lefèvre, I., Cerdan, O., Rajkumar, V. and Desmet, M., 2015, Quantifying the dominant sources of sediment in a drained lowland agricultural catchment: The application of a thorium-based particle size correction in sediment fingerprinting. *Geomorph*, 250: 271-281.

- Fox, J. F., 2005, Fingerprinting using biogeochemical tracers to investigate watershed processes. Ph.D Thesis, University of Iowa, Iowa City.
- Fox, J. F., 2009, Identification of sediment sources in forested watersheds with surface coal mining disturbance using carbon and nitrogen isotopes, *J Amer Wtr Res As*, 45(5):1273-1289.
- Fox, J. F. and Martin, D. K., 2015, Sediment fingerprinting for calibrating a soil erosion and sediment-yield model in mixed land-use watersheds, *ASCE J. Hydrol Eng*, 20: C4014002.1-11.
- Fox, J. F. and Papanicolaou, A. N., 2007, The use of carbon and nitrogen isotopes to study watershed erosion processes, *JAWRA*, 43(4):1047-1064.
- Fox, J. F. and Papanicolaou, A. N., 2008, An un-mixing model to study watershed erosion processes, *Adv Water Resour As*, 31:96-108.
- Fryar, A. E., Ward, J. W., Howell, B. A., Reed, T. M., 2017, Responses of karst springs to precipitation reflect land use, lithology, and climate, National Ground Water Association Groundwater Summit, <https://ngwa.confex.com/ngwa/2017gws/webprogram/meeting.html>
- Fryar, A. E., Wallin, E. J., Brown, D. L., 2000, Spatial and temporal variability in seepage between a contaminated aquifer and tributaries to the Ohio River, *Groundwater Monitor Remed* 20:129-146.
- Fuchs, E. H., Wood, K. M., Jones, T. L. and Racher, B., 2003, Impacts of tracked vehicles on sediment from a desert soil, *J. Range Mgmt* 56: 342-352.
- Fuhrer, G. J., Tanner, D. Q., Morace, J. L., McKenzie, S. W. and Skach, K. A., 1996, Water Quality of the Lower Columbia River Basin: Analysis of Current and Historical Water-Quality Data through 1994, U.S. Geological Survey, Water-Resour Inv Report 95-4294.
- Gale, S J., 1984, The hydraulics of conduit flow in carbonate aquifers. *J Hydrol*, 70:309-327.
- Garcia, A. M., Alexander, R. B., Arnold, J. G., Norfleet, L., White, M., Roberston, D. M. and Schwarz, G., 2016, Regional effects of agricultural conservation practices on nutrient transport in the upper Mississippi River basin, *Env Sci Tech*, 50:6991-7000.
- Gellis, A. C., Fitzpatrick, F. and Schubauer-Berigan, J., 2016, A manual to identify sources of fluvial sediment, U.S. Environmental Protection Agency, EPA/600/R-16/210.
- Gellis, A. C., Fuller, C. C., Van Metre, P., Filstrup, C. T., Tomer, M. D., Cole, K. J. and Sabitov, T. Y., 2019, Combining sediment fingerprinting with age-dating sediment using fallout radionuclides for an agricultural stream, Walnut Creek, Iowa, USA, *J Soils Sed*, 19:3374-3396.

- Gellis, A. C. and Gorman Sanisaca, L., 2018, Sediment fingerprinting to delineate sources of sediment in the agricultural and forested Smith Creek Watershed, Virginia, USA, *JAWRA*, 54(6):1197-1221
- Gellis, A. C. and Noe, G. B., 2013, Sediment source analysis in the Linganore Creek Watershed, Maryland, USA, using the sediment fingerprinting approach: 2008 to 2010. *Watershed Sediment Source Identification: Tools, Approaches, and Case Studies*, edited by R. Mukundan and A.C. Gellis, *J Soils Sed*,13(10):1735-53.
- Gellis, A. C., Noe, G. B., Clume, J. W., Myers, M. K., Hupp, C. R., Schenk, E. R. and Schwarz, G. E., 2014, Sources of fine-grained sediment in the Linganore Creek watershed, Frederick and Carroll Counties, Maryland 2008-10, U.S. Geological Survey Sci Inv Rep, 2014-5147:56p.
- Gellis, A. C. and Walling, D. E., 2011, Sediment source fingerprinting (tracing) and sediment budgets as tools in targeting river and watershed restoration programs. *Stream restoration in dynamic fluvial systems: scientific approaches, analyses, and tools*, 194:263-291.
- George, M. R., Larsen, R. E., McDougald, N. K., Tate, K. W., Gerlach, Jr., J. D. and Fulgham, K. O., 2004, Cattle grazing has varying impacts on stream-channel erosion in oak woodlands, *California Agriculture*, July-September:38-143.
- Ghasemi, A. and Zahediasl, S., 2012, Normality tests for statistical analysis: A guide for non-statisticians, *Int J Endocrtnol Metab*, 10(2):486-9.
- Gibbs, R. J., Matthews, M. D. and Link, D. A., 1971, The relationship between sphere size and settling velocity, *J of Sed Petrology*, 41(1):7-18.
- Gingele, F. X. and De Deckker, P., 2005, Clay mineral, geochemical and Sr-Nd isotopic fingerprinting of sediments in the Murray-Darling fluvial system, southeast Australia, *Aust J Earth Sci*, 52:965-974.
- Glymph, M. L., 1957, Importance of sheet erosion as a source of sediment, *Eos Transactions Am Geophy Union*, 38.6:903-907.
- Goldberg, E. D., 1954, Marine Geochemistry 1: Chemical scavengers of the sea, *J Geol*, 62(3): 249-265.
- Goldberg, E. D. and Arrhenius, G. O. S., 1958, Chemistry of Pacific pelagic sediments, *Geo. et Cosmochimica*, 12(2-3):153-198.
- Gorman Sanisaca, L. E., Gellis, A. C. and Lorenz, D. J., 2017, Determining the sources of fine-grained sediment using the Sediment Source Assessment Tool (Sed_SAT), U.S. Geological Survey Open File Report 2017-1062:104p.
- Grabowski, Jr., G. J., 2001, Mississippian system, contribution to the geology of Kentucky, U.S. Geological Survey Professional Paper 1151-H, updated 2019.
- Gruszowski, K. E., Foster, I. D. L., Lees, J. A. and Charlesworth, S., 2003, Sediment sources and transport pathways in a rural catchment, Herefordshire, UK. *Hydrol Processes*, 17:2665-2681.

- Guzman, G., Quinton, J. N., Nearing, M. A., Mabit, L. and Gomez, J. A., 2013, Sediment tracers in water erosion studies: Current approaches and challenges. *J. Soil Sed*, 13(4):816-833.
- Haag, K. H. and Porter, S. D., 1996, Water quality assessment of the Kentucky River Basin, Kentucky: nutrients, sediments and pesticides in streams, 1987-90. U.S. Geological Survey, Water Resour Inv Rep, 94.4227:144p.
- Haddadchi, A. S., Ryder, D., Evrard, O. and Olley, J., 2013, Sediment fingerprinting in fluvial systems: review of tracers, sediment sources and mixing models, *Intl J Sed Research*, 28(4): 560-578.
- Hale, R. L. and Groffman, P. M., 2006, Chloride effects on nitrogen dynamics in forested and suburban stream debris dams, *J Env Qual*, 35:2425-2432.
- Hancock, G. J. and Revill, T. A., 2013, Erosion source discrimination in a rural Australian catchment using compound-specific isotopes analysis (CSIA), *Hydrol Processes*, 27(6):923-932.
- Hardin County Water District No.1., 2018, Water Quality Reports CCR, <https://hcwd.com/water-quality-reports>, Accessed August 1, 2019.
- Harrel, R. C. and Dorris, T. C., 1968, Stream order, morphometry, physico-chemical conditions, and community structure of benthic macroinvertebrates in an intermittent stream system, *Am Midland Naturalist*, 220-251.
- Hem, J. D., 1985, Study and interpretation of the chemical characteristics of natural water, Vol. 2254, Department of the Interior, US Geological Survey.
- Hill, S. M., 1981, Fort Knox-Army Armor Center Ongoing Mission: Environmental Impact Statement, Fort Knox, KY.NEPA Collection, 130p.
- Homoya, M. D., Abrell, D., Aldrich, J. and Post, T., 1985, The natural regions of Indiana, *Proceedings Indiana Acad Sci*, 94:245-268.
- Horowitz, A., 1991, A primer on sediment-trace metal chemistry, Chelsea, CO: Lewis Publishing.
- Horowitz, A. and Elrick, K., 1987, The relation of stream sediment surface area, grain size and composition to trace element chemistry, *Appl Geochem*, 2:437-51.
- Hribar, C., 2010, Understanding concentrated animal feeding operations and their impact on communities, National Assoc Local Boards of Health, Bowling Green, Ohio. www.nalboh.org.
- Hunt, M., Herron, E. and Green, L., 2012, Chlorides in fresh water, Univ of Rhode Island. URIWW. www.uri.edu/ce/wq/ww. Accessed April 1, 2019.
- Hynes, H. B. N., 1960, The biology of polluted waters, No. 574.52632, Liverpool University Press, Liverpool.

- Imes, J. L., Schumacher, J. G. and Kleeschulte, M. J., 1996, Geohydrologic and water-quality assessment of the Fort Leonard Wood Military Reservation, Missouri, 1994-95, 96(4270), US Department of the Interior, US Geological Survey.
- IMCOM Fort Knox, 2016, Fort Knox Army Defense Environmental Restoration Program Installation Action Plan, FY2016.
- IMCOM Fort Campbell, 2016, Fort Campbell Army Defense Environmental Restoration Program Installation Action Plan, FY2016.
- InSitu, 2019, Operator's manual, Level TROLL, 400, 500, 700, 700H instruments, v0052212, updated May 6, 2019, <https://www.in-situ.com>.
- Johnson, M. L., Richards, C., Host, G. E. and Arthur, J. W., 1997, Landscape influences on water chemistry in Midwestern stream ecosystems, *Freshwater Biol*, 37(1):193-208.
- Jones, B. and Bowser, C., 1978, The mineralogy and related chemistry of lake sediments, In: Lerman A. (eds) *Lakes*. New York, NY, Springer.
- Jones, J. I., Collins, A. L., Sear, D. A. and Naden, P. S., 2012, The impact of fine sediment on macro-invertebrates, *River Res Appl*, 28:1055-1071.
- Karathanasis, A. D. and USDA Natural Resources and Conservation Service, 2018, Kentucky Soil Atlas, Plant and Soil Sciences Faculty Book Gallery 4. https://uknowledge.uky.edu/pas_book/4.
- Kaushal, S. S., Groffman, P. M., Band, L. W., Elliot, E. M., Shields, C. A. and Kendall C., 2011, Tracking nonpoint source nitrogen pollution in human-impacted watersheds. *Env Sci Technol*, 42:8225-8232.
- KEEC, 2018, Kentucky Energy and Environment Cabinet. Integrated Report to Congress on the Condition of Water Resources in Kentucky, 2016, Dept of Env Protection, Division of Water, Water Quality Branch, Accessed October 1, 2018.
- Kemp, P., Sear, D., Collins, A., Naden, P. and Jones, I., 2011, The impacts of fine sediment on riverine fish, *Hydrol Processes*, 25:1800-1821.
- Kepferle, R. C., 1967, Geologic map of the Vine Grove Quadrangle, Hardin and Meade Counties, Kentucky, U.S. Geological Survey Geologic Quadrangle Map GQ-645.
- Kepferle, R. C. and Sable, E. G., 1977, Geologic map of the Fort Knox quadrangle, north-central Kentucky, U.S. Geological Survey Geologic Quadrangle Map GQ-1375.
- KGS, (n.d), Kentucky Geologic Map Information Service, <https://kgs.uky.edu/kgsweb/main.asp>, Accessed June 15, 2017,
- KGS, 2012, The Mississippian Plateau or Pennyroyal Region, Kentucky. Kentucky Geological Survey, www.uky.edu/KGS/geoky/regionPennyroyal.html, Accessed June 15, 2017.

- KIA, 2017, Kentucky Infrastructure Authority. Internet mapping of wastewater infrastructure and water infrastructure, <https://kia.ky.gov/WRIS/Pages/Internet-Mapping.aspx>. Accessed June 19, 2019.
- Klages, M. G. and Hsieh, Y. P., 1975, Suspended solids carried by the Gallatin River of Southwestern Montana: using mineralogy for inferring sources, *J Env Qual*, 4(1):68-73.
- Klingaman, E. D. and Nelson, D. W., 1976, Evaluation of methods for preserving the levels of soluble inorganic phosphorus and nitrogen in unfiltered water samples, *J Env Qual*, 5:42-46.
- Kononova, M.M, 1966, *Soil Organic Matter*, (Translators by T.Z. Nowakowski and A.C.D. Newman), 2nd Edition, Pergamon Press, 1966.
- Kottek, M., Grieser, J., Beck, C., Rudolf, B. and Rubel, F., 2006, World map of the Köppen-Geiger climate classification updated, *Meteorologische Zeitschrift*, 15(3): 259-263.
- Krein, A., Petticrew, W. and Udelhoven, T., 2003, The use of fine sediment fractal dimensions and colour to determine sediment sources in a small watershed, *Catena* 53:165-179.
- Kuehne, R. A., 1962, A classification of streams illustrated by fish distribution in an eastern Kentucky creek, *Ecology*, 43(4):608-614.
- Kuehne, R. A., 1966, Depauperate fish faunas of sinking creeks near Mammoth Cave, Kentucky, *Copeia*, 306-311p.
- KYCC, 2017, Kentucky Climate Center. <http://www.kyclimate.org/>. Accessed December 12, 2018
- KYDOW, 2014, Kentucky Division of Water, Kentucky Nutrient Management Strategy, Kentucky Energy and Environment Cabinet, <http://water.ky.gov/Documents/NRS%20draft%203-20.pdf>, Accessed December, 03 2016.
- KYEEC, 2018, by Kentucky Energy and Environment Cabinet, Department of Environmental Protection, Integrated Report to Congress on the Condition of Water Resources in Kentucky, Water Quality Branch, Accessed October 1, 2018.
- KYEEC, 2019, 401 KAR 10:031 Surface water standards, Edited by Kentucky Energy and Environment Cabinet, Department of Environmental Protection, <http://water.ky.gov/waterquality/Pages/WaterQualityStandards.aspx>, Accessed October 18, 2018.
- KYFB, 2015, Kentucky Agriculture Facts, Second Edition, Kentucky Farm Bureau, <https://www.kyfb.com/federation/commodities/kentucky-ag-facts-book/>, Accessed May 25, 2019.

- Lacey, J. P., Evrard, O., Smith, H. G., Blake, W. H., Olley, J. M., Minella, J. P. G. and Owens, P. N., 2017, The challenges and opportunities of addressing particle size effects in sediment source fingerprinting: A Review, *Earth Sci Reviews*, 169:85-103.
- Lamba, J. and Thompson, K. A. M., 2015, Apportionment of suspended sediment sources in an agricultural watershed using sediment fingerprinting. *Geoderma*, 239: 25-33.
- Lambert, T. W., 1979, Water in the Elizabethtown Area – A study of limestone terrane in North-Central, Kentucky, U.S. Geological Survey Water Res Inv No. 79-53.
- LECO Corp, 2008, SC-144DR Sulfur/Carbon Determination Specification Sheet, www.LECO.com. Accessed January 13, 2017.
- Ledford, S. H., Lautz, L. K. and Stella, J. C., 2016, Hydrogeologic processes impacting storage, fate and transport of chloride from road salt in urban riparian aquifers. *Environ Sci Technol*, 50(10):4979-4988.
- Livingstone, D. A., 1963, Chemical composition of rivers and lakes. U.S. Government Printing Office, Vol 440, Accessed April 2, 2019.
- Lund, J. W. G., 1950, Studies on *Asterionella formosa hass* II, Nutrient depletion and the spring maximum. *J Ecol*, 38:1-35.
- Lutgens, F. K. and Tarbuck, E. J., 1995, *The Atmosphere: An Introduction to Meteorology*, 6th Edition, Prentice-Hall, Englewood Cliffs. NJ. 462p.
- Macdonald, J. S., Beaudry, P. G., MacIsaac, E. A. and Herunter, H. E., 2003, The effects of forest harvesting and best management practices on streamflow and suspended sediment concentrations during snowmelt in headwater streams in sub-boreal forests of British Columbia, Canada, *Canada J Forest Research*, 33.8:1397-1407.
- Maloney, K. O., Mulholland, P. J. and Feminella, J. W., 2005, Influence of catchment-scale military land use on stream physical and organic matter variables in small southeastern plains catchments (USA), *Env Mgmt*, 35(5):677-691.
- Mardia, K. V., Kent, J. T. and Bibby, J. M., 1979, *Multivariate Analysis (Probability and Mathematical Statistics)*, 1st Ed. London, United Kingdom: Academic Press. ISBN 0-12-471250-9.
- Marshall, J. D., Brooks, J. R. and Lajtha, K., 2007, Sources of variation in the stable isotopic composition of plants, Chapter 2, *Stable isotopes in ecology and environmental science*, 2:22-60.
- Martínez-Carreras, N., Krein, A., Udelhoven, T., Gallart, F., Iffly, J. F., Hoffmann, L., Pfister, L. and Walling, D. E., 2010, A rapid spectra-reflectance-based fingerprinting approach for documenting suspended sediment sources during storm runoff events, *J Soils Sed*, 10:400-413.
- Megahan, W. F. and King, J. G., 2004, Erosion, sedimentation, and cumulative effects in the northern Rocky Mountains, In: Ice GG, Stednick D (eds) *A century of forest and Wildland Watershed Lessons*, Bethesda Maryland, Soc Am Foresters, 201-222p.

- Menne, M. J., Durre, I., Korzeniewski, B., McNeal, S., Thomas, K., Yin, X., Anthony, A., Ray, R., Vose, R. S., Gleason, B. E., and Houston, T. G., 2012a, Global Historical Climatology Network - Daily (GHCN-Daily), Version 3. NOAA National Climatic Data Center. Accessed February 4, 2020.
- Menne, M. J., Durre, I., Vose, R. S., Gleason, B. E., Houston, T. G., 2012b, An overview of the global historical climatology network-daily database, *J Atmos Oceanic Technol*, 29:897-910.
- Meyer, J. L., McDowell, W. H., Bott, T. L., Elwood, J.R., Ishizaki, C., Melack, J. M., Peckarsky, B. L., Peterson, B. J. and Rublee, P. A., 1988, Elemental dynamics in streams, *J N.Am Benthological Soc*, 7:410-432.
- Miguel, E. D., Charlesworth, S., Ordóñez, A. and Seijas, E., 2005, Geochemical fingerprints and controls in the sediment of an urban river: River Manzanares, Madrid (Spain), *Sci Total Env*, 340(1-3):137-148.
- Miller, J., Mackin, G. and Miller, S.M.O., 2015, Application of geochemical tracers to fluvial sediment, 142p, Dordrecht, The Netherlands, Springer International Publishing.
- Minella, J. P. G., Walling, D. E. and Merten, G. H., 2008, Combining sediment source tracing techniques with traditional monitoring to assess the impact of improved land management on catchment sediment yields, *J Hydrol*, 348:546-563.
- Moore, P. J., Martin, J. B. and Sreaton, E. J., 2009, Geochemical and statistical evidence of recharge, mixing, and controls on spring discharge in an eogenetic karst aquifer, *J Hydrol*, 376:443-455.
- Mohamed, E. A., El-Kammar, A. M., Yehia, M. M. and Salem, H. S. A., 2015, Hydrogeochemical evolution of inland lakes' water: A study of major element geochemistry in the Wadi El Raiyan depression, Egypt, *J Adv Research*, 6(6):1031-1044.
- Morgan, M. D. and Good, R. E., 1988, Stream chemistry in the New Jersey Pinelands: the influence of precipitation and watershed disturbance. *Water Resour Research*, 24:1091-1100.
- Motha, J. A., Wallbrink, P. H., Hairsine, P. B. and Grayson, R. B., 2003, Determining the sources of suspended sediment in a forested catchment in southeastern Australia. *Water Resour Research* 39(3):1056
- Motter, K. and Jones, C., 2015, Standard operating procedure for the analysis of chloride, bromide and sulfate in fresh waters by Ion Chromatography. CCAL 50B.2. Cooperative Chemical Analytical Lab, College of Forestry, Oregon State Univ.
- Muldraugh, 2018, Muldraugh Water Department Water Quality Report. <http://www.krwa.org/2018ccr/muldraugh.pdf>. Accessed July 1, 2019.

- Munn, M. D., Frey, J. W., Tesoriero, A. J., Black, R. W., Duff, J. H., Lee, K., Maret, T. R., Mebane, C. A., Waite, I. R. and Zelt, R. B., 2018, Understanding the influence of nutrients on stream ecosystems in agricultural landscapes: U.S. Geological Survey Circular 1437:80 p.
- NASS, 2017, National agricultural statistics service, Kentucky Field Office, Kentucky County Estimates. https://www.nass.usda.gov/Statistics_by_State/Kentucky/Publications/County_Estimates/coest/2017/index.php, Accessed February 10, 2019.
- Navratil, O., Evrard, O., Esteves, M., Legout, C., Ayrault, S., Némery, J., Mate-Marin, A., Ahmadi, A., Lefèvre, I., Poirel, A. and Bonté, P., 2012, Temporal variability of suspended sediment sources in an alpine catchment combining river/rainfall monitoring and sediment fingerprinting, *Earth Surf Processes Land*, 38(8):828-846.
- Nelson, E. J. and Booth, D. B., 2002, Sediment sources in an urbanizing, mixed land-use watershed, *J Hydrol*, 264(1-4):51-68.
- Neugirg, F., Kaiser, A., Schmidt, J., Becht, M. and Haas, F., 2015, Quantification, analysis and modelling of soil erosion on steep slopes using LiDAR and UAV photographs. *Sediment Dynamics from the Summit to the Sea. Proceedings of a symposium in New Orleans, LA USA. IAHD Publ. 367.*
- Newcombe, C. P. and Jensen, J. O. T., 1996, Channel suspended sediment and fisheries: a synthesis for quantitative assessment of risk and impact. *N.Am J Fisheries Mgmt*, 16(4):693-727.
- Newcombe, C. P. and MacDonald, D. D., 1991, Effects of suspended sediments on aquatic ecosystems, *N.Am J Fisheries Mgmt*, 11:78-82.
- NLCD, 2011, National Land Cover Database 2011, Multi Resolution Land Characteristics Consortium, <https://data.nal.usda.gov/dataset/national-land-cover-database-2011-nlcd-2011/resource/6439be43-ac42-4510-82af-d942ca9e2c73>, Accessed March 3, 2017.
- NOAA, (n.d), Climate Graphs for Louisville International. KGSs. https://www.weather.gov/lmk/climate_graphs, Accessed January 25, 2020.
- NOAA, 2019, El Niño & La Niña (El Niño-Southern Oscillation), <https://www.climate.gov/enso>, Accessed July 1, 2019.
- Nosrati, K., Govers, G., Ahmadi, H., Sharifi, F., Ammozegar, M. A., Merckx, R. and Vanmaercke, M., 2011, An exploratory study on the use of enzyme activities as sediment tracers: biochemical fingerprints, *Int J Sed Res*, 26(2):136-151.
- NRCS, 1995, Effects of sediment on the aquatic environment: Potential NRCS actions to improve aquatic habitat – working paper no. 6. U.S. Department of Agriculture, Natural Resources Conservation Service. https://www.nrcs.usda.gov/wps/portal/nrcs/detail/national/technical/?cid=nrcs143_01420, Accessed January 27, 2020.

- NRCS, (n.d.), Cover crops and soil health. U.D. Department of Agriculture, Natural Resources Conservation Service.
<https://www.nrcs.usda.gov/wps/portal/nrcs/detail/national/climatechange/?cid=stelprdb1077238>, Accessed January 25, 2020.
- NRCS, 2019, Natural Resources Conservation Service (NRCS) Web Soil Survey, U.S. Department of Agriculture, <https://websoilsurvey.sc.egov.usda.gov>, Accessed June 17, 2019.
- Oelbermann, M. and Voroney, R. P., 2007, Carbon and nitrogen in a temperate agroforestry system: Using stable isotopes as a tool to understand soil dynamics. *Ecol Eng*, 26:342-349.
- Oldfield, F., Rummery, T. A., Thompson, R. and Walling, D. E., 1979, Identification of suspended sediment sources by means of magnetic measurements; some preliminary results, *Water Resour Research*, 15(2):211-218.
- O'Leary, M. H., 1981, Carbon isotope fractionations in plants, *Phytochemistry*, 20:553-567.
- Olley, J., Burton, J., Smolders, K., Pantus, F. and Pietsch, T., 2013, The application of fallout radionuclides to determine the dominant erosion process in water supply catchments of subtropical South-east Queensland, Australia., *Hydrol Processes*, 27(6):885-895.
- Owens, P. N., Walling, D. E. and Leeks, G. J. L., 1999, Use of floodplain sediment cores to investigate recent historical changes in overbank sedimentation rates and sediment sources in the catchment of the River Ouse, Yorkshire, UK, *Catena*, 36(1-2):21-47.
- Owens, P. N., Walling, D. E. and Leeks, G. J. L., 2000, Tracing fluvial suspended sediment sources in the catchment of the River Tweed, Scotland, using composite fingerprints and a numerical mixing model. I.D.L. Foster (Ed.), *Tracers in Geomorph*, 291-308p.
- Owens, P. N., Batalla, R. J., Collins, A. J., Gomez, B., Hicks, D. M., Horowitz, A. J., Kondolf, G. M., 2005, Fine-grained sediment in river systems: Environmental significance and management issues, *River Research Applic*, 21:396-717.
- Oztuna, D., Elhan, A. H. and Tuccar, E., 2006, Investigation of four different normality tests in terms of type 1 error rate and power under different distributions. *Turkish J of Med Sci*, 36(3):171-6.
- Pallant, J., 2007, *SPSS survival manual, a step-by-step guide to data analysis using SPSS for windows*, 3rd Edition. Sydney: McGraw Hill: 179-200p.
- Papanicolaou, T. and Fox, J. 2004, Tracing sediment sources by using stable carbon and nitrogen isotopes: an exploratory research. IIHR Tech Report No. 437. Hydro Science and Engineering, College of Engineering, The University of Iowa City, Iowa, 52242-1585.

- Patault, E., Alary, C., Franke, C. and Abriak, N., 2019, Quantification of tributaries contributions using a confluence-based sediment fingerprinting approach in the Canche river watershed (France), *Sci Total Env*, 668:457-469.
- Peart, M. R. and Walling, D. E., 1986, Fingerprinting sediment sources: the example of a drainage basin in Devon, UK. In: Hadley, R.F. (Ed.), *Drainage Basin Sediment Delivery*, IAHS 41-55.
- Peart, M. R. and Walling, D. E., 1988, Techniques for establishing suspended sediment sources in two drainage basins in Devon, UK: a comparative assessment, in Bordas, M.P. and Walling D.E. (Eds), *Sediment Budgets*, IAHS Publication No. 174, IAHS Press, Wallingford, 269-279.
- Peter, K. D., d'Oleire-Oltmanns, S., Ries, J. B., Marzolff, I. and Ait Hssaine, A., 2014, Soil erosion in gully catchments affected by land-levelling measured in the Souss Basin, Morocco, analyzed by rainfall simulation and UAV remote sensing data, *Catena*, 113:24-40.
- Peterson, E. W. and Wicks, C. M., 2003, Characterization of the physical and hydraulic properties of the sediment in karst aquifers of the Springfield Plateau, Central Missouri, USA. *Hydrogeol*, 11:357-367.
- Phillips, J. M., Russell, M. A. and Walling, D. E., 2000, Time-integrated sampling of fluvial suspended sediment: a simple methodology for small catchments. *Hydrol Processes*, 14:2589-2602.
- Phillips, J. D. and Walls, M. D., 2004, Flow partitioning and unstable divergence in fluviokarst evolution in central Kentucky, *Nonlinear Processes Geophys*, 11:371-381.
- Pfaff, J. D., Hautman, D. P. and Munch, D. J., 1997, EPA Method 300.1, Revision 1.0. Determination of Inorganic Anions in Drinking Water by Ion Chromatography, U.S. Environmental Protection Agency, NERL, ORD, Cincinnati, Ohio.
- Potter, P. E., Nosow, E., Smith, N. M., Swann, D. H. and Walker, F. H., 1958, Chester cross-bedding and sandstone trends in Illinois basin, *AAPG Bulletin*, 42(5):1013-1046.
- Porto, P., Walling, D. E. and Callegari, G., 2005, Investigating sediment sources within a small catchment in southern Italy, *IAHS-AISH*, 291:113-122.
- Poulenard, K., Perrette, Y., Fanget, B., Quetin, P., Trevisan, D. and Dorioz, J. M., 2009, Infrared spectroscopy tracing of sediment sources in a small rural watershed, French Alps, *Sci Total Env*, 407:2808-2819.
- Pulley, S., Foster, I. and Collins, A. L., 2017, The impact of catchment source group classification on the accuracy of sediment fingerprinting outputs, *J Env Mgt*, 194: 16-26.
- Quinn, D., Poffenbarger, H. and Lee, C., 2019, Cover crop benefits and challenges in Kentucky, AGR-240, University of Kentucky College of Agriculture, Food and Env, Issue August 2019.

- Rabalais, N. N., Turner, R. E., Wiseman, Jr., W. J. and Boesch, D. F., 1991, A brief summary of hypoxia on the northern Gulf of Mexico continental shelf: 1985-1988, In *Modern and Ancient Continental Shelf Anoxia*, eds. R.V. Tyson, T.H. Pearson. Geol Soc Special Publication 58.0
- Rasmussen, P. P., 1998, Concentrations, loads and yields of selected water-quality constituents during low flow and storm runoff from three watersheds at Fort Leavenworth, Kansas, May 1994 through September 1996, U.S. Geological Survey, Water Resour Inv Rep, 98-4001p.
- Rawson, J., 2008, Fort Knox, Kentucky. Joint Land Use Study. Lincoln Trail Area Development District. <https://www.ltadd.org/cgi-bin/filelibraries/ltadd-filelibrary>. Accessed June 20, 2015.
- Reed, T. M., Fryar, A. E., Brion, G. M. and Ward, J. W., 2011, Differences in pathogen indicators between proximal urban and rural karst springs, Central Kentucky, USA. *Env Earth Sci*, 64(1):47-55.
- Rex, R. and Goldberg, E., 1958, Quartz contents of pelagic sediments of the Pacific Ocean. *Tellus*, 10(1):153-159.
- Retta, A., Wagner, L. E. and Tatarko, J., 2014, Military vehicle trafficking impacts on vegetation and soil bulk density at Fort Benning, Georgia, *Amer Soc Ag Biol Eng*, 57(4):1043-1055.
- Richards, J. M., Rylund, P. H. and Barr, M. N., 2012, Hydrologic and sediment data collected from selected basins at the Fort Leonard Wood Military Reservation, Missouri – 2010-11, U.S. Geological Sci Inv Rep, 2012-5268.23p.
- Rodríguez-Eugenio, N., McLaughlin, M. and Pennock, D., 2018, Soil Pollution: a hidden reality, FAO, 142p.
- Royston, P., 1991, Estimating departure from normality, *Stat Med*, 10(8):1283-93.
- Russ, E., Palinkas, C. and Cornwell, J., 2020, Evaluating estuarine sediment provenance from geochemical patterns in upper Chesapeake Bay, *Chem Geol*, 533,119404.
- Russell, M. A., Walling, D. E. and Hodgkinson, R. A., 2001, Suspended sediment sources in two small lowland agricultural catchments in the UK, *J Hydrol*, 252(1-4): 1-24.
- Ryan, M. and Meiman, J., 1996, An examination of short-term variations in water quality in a karst spring in Kentucky, *Ground Water*, 34(1):23-30.
- Ryberg, K. R. and Gilliom, R. J., 2015, Trends in pesticide concentrations and use for major rivers of the United States, *Sci Total. Env*, 538:431-444.
- Ryberg, K. R., Blomquist, J. D., Sprague, L. A., Sekellick, A. J. and Keisman, J., 2017, Modeling drivers of phosphorus loads in Chesapeake Bay tributaries and inferences about long-term change, *Sci Total Env*, 616-617:1423-1430.

- Salmon, Y., Barnard, R. L. and Buchmann, N., 2011, Ontogeny and leaf gas exchange mediate the carbon isotopic signature of herbaceous plants, *Plant Cel Env*, 34:465-479.
- Schoonover, J. E., Crim, J. F., Williard, K. W. J., Groninger, J. W., Zaczek, J. J. and Pattumma, K., 2015, Sediment dynamics within buffer zone and sinkhole splay areas under extreme soil disturbance conditions, *Env Mgmt* 56:618-629.
- Sherwood, W. C., 1989, Chloride loading in the south fork of the Shenandoah River, Virginia, USA, *Env Geol Water Sci*, 14(2):99-106.
- Shields, F. D., Knight, Jr., S. S. and Cooper, C. M., 1994, Effects of channel incision on base flow stream habitats and fishes. *Env Mgmt*, 18(1):43-57.
- Shoda, M. E., Stone, W. W. and Nowell, L. H., 2016, Prediction of pesticide toxicity in Midwest streams, *J Env Qaul*, 45:1856-1864.
- Slattery, J. and Burt, T. P., 2000, Use of mineral magnetic measurements to fingerprint suspended sediment sources: results from a linear mixing model, *Geomorph*, 309-322.
- Smith, H. G. and Blake, W. H., 2014, Sediment fingerprinting in agricultural catchments: A critical re-examination of source discrimination and data corrections, *Geomorph*, 204:177-191.
- Smith, S. R., Lacefield, G. and Keene, T., 2009, Native warm-season perennial grasses for forage in Kentucky. Cooperative Extension Service, University of Kentucky College of Agriculture. AGR-145.
- SonTek, 2007, FlowTracker Handheld ADV Technical manual. Firmware Version 3.3, Software Version 2.20, P/N 6054-60050-C.
- Sprandel, G., 1999, Description of Level III and Level IV Ecoregions of Kentucky, Department of Fish and Wildlife, Commonwealth of Kentucky. <https://fw.ky.gov/WAP/documents/1.11%20Ecoregions%20of%20Kentucky.pdf>, Accessed August 2, 2019.
- Stets, E. G., Lee, C. J., Lytle, D. A. and Schock, M. R., 2017. Increasing chloride in rivers of the conterminous U.S. and linkages to potential corrosivity and lead action level exceedances in drinking water, *Sci Total Env* 613-614:1498-1509.
- Stone, W. W., Gilliom, R. J. and Ryberg, K. R., 2014, Pesticides in U.S. streams and rivers: Occurrence and trends during 1992-2011. *Env Sci Tech*. 48(19):11025-11030.
- Sudduth, E., 2018, Kentucky Crop Timeline. Kentucky Department of Education. Commonwealth of Kentucky, <https://education.ky.gov/federal/progs/tic/Documents/KY%20Crop%20Time-line.pdf>, Accessed January 26, 2020.
- Sullivan, D. J., Vecchia, A. V., Lorenz, D. L., Gilliom, R. J. and Martin, J. D., 2009, Trends in pesticide concentrations in corn-belt streams: 1996-2002, U.S. Geological Survey *Sci Inv Rep* 2009-5132.

- Taraba, J. L., Dinger, J. S., Sendlein, L. V. A. and Felton, G. K., 1997, Land use impacts on water quality in small Karst Agricultural watersheds, Karst-Water Environment Symposium Proceedings. Virginia Water Resources Research Center. 127-140.
- Tong, S.T.Y. and Chen, W., 2002, Modeling the relationship between land use and surface water quality, *J Env Mgmt*, 66:377-393.
- UIC, 2017, Carbon Dioxide Coulometer, <http://www.uicinc.com/carbon-dioxide-coulometer>, Accessed February 16, 2017.
- UKAG, 2011, 1990-2007 Description of Soil Test Summaries, College of Agriculture, Division of Regulatory Services, University of Kentucky, http://soils.rs.uky.edu/technical_Info/soil_Test_Summaries/summary/DescriptionOfSoilTestSummaries.php, Accessed June 2, 2019.
- UKAG, 2017, Distribution of Fertilizer Sales in Kentucky, Fertilizer Year 2017, July 2016 through June 2017, https://www.rs.uky.edu/regulatory/fertilizer/tonnage/tonnage_reports/FY2017/2017DistributionYearlyReport.pdf. Accessed July 10, 2019.
- USARMY, 2018, History of Fort Knox, section 2005 BRAC announcement sets stage for Fort Knox Transition, <https://www.knox.army.mil/about/history.aspx>. Accessed May 24, 2019.
- University of Kentucky. 2018. University of Kentucky Dissertation Template. UKnowledge Documents and Forms. 11. https://uknowledge.uky.edu/uknowledge_docs/11
- U.S. Census Bureau, 1990, 1990 Census of population and housing unit counts, Kentucky, CPH-2-19, Issued Sept 1992, U.S. Department of Commerce, Economic and Statistics Administration, Bureau of the Census, <https://www.census.gov>, Accessed July 1, 2019.
- U.S. Census Bureau, 2010, 2010 Census of population and housing, Kentucky, CPH-1-19, Issued Nov. 2012, U.S. Department of Commerce, Economic and Statistics Administration. Bureau of the Census, <https://www.census.gov>, Accessed July 1, 2019.
- USDOA, 2005, Base Realignment and Closure (BRAC), Office of the Under Secretary of Defense for Acquisition, Technology and Logistics, <https://www.acq.osd.mil/brac/>. Accessed May 24, 2019.
- USEPA, 1997, Method 300.1 Determination of inorganic anions in drinking water by ion chromatography. 1-40, <https://www.epa.gov/sites/production/files/2015-06/documents/epa-300.1.pdf>. Accessed July 11, 2019.
- USEPA, 1979, Methods for chemical analysis of water and wastes, U.S. Environmental Protection Agency, Cincinnati: EPA-600/4-79-020, Accessed July 11, 2019.

- USEPA, 1994, Determination of Inorganic Anions by Ion Chromatography, Method 300.1: 9056, SW-846, US Environmental Protection Agency, Office of Solid Water and Emergency Response, Washington, DC, Accessed July 11, 2019.
- USEPA, 1999, Protocol for Developing Sediment TMDL's. Vers. First Edition. U.S. Environmental Protection Agency, October, Accessed July 11, 2019.
- USEPA, 2010, National Pollutant Discharge Elimination System (NPDES) Chapter 5: Technology-Based Effluent Limitations, U.S. Environmental Protection Agency, Office of Water Enforcement and Permits. Washington DC, Accessed July 11, 2019.
- USEPA, 2012, Overview of impaired waters and total maximum daily loads program, U.S. Environmental Protection Agency.
<http://water.epa.gov/lawsregs/lawsguidance/cwa/tmdl/intro.cfm>, Accessed October 11, 2017.
- USEPA, 2016, A Manual to Identify Sources of Fluvial Sediment, U.S. Environmental Protection Agency. Edited by J.P. Schubauer-Berigan. September, Accessed March 30, 2018.
- USEPA, 2018a, Environmental Protection Agency, National Pollutant Discharge Elimination System (NPDES) Stormwater Program,
<https://www.epa.gov/npdes/npdes-stormwater-program>, Accessed January 14, 2019.
- USEPA, 2018b, State progress toward developing numeric nutrient water quality criteria for Nitrogen and Phosphorus, <https://www.epa.gov/nutrient-policy>, Accessed October 15, 2019.
- USEPA, 2020, Electronic code of federal regulations, Title 40, Chapter 1, Subchapter D, Part 122, EPA Administered permit programs: The National Pollutant Discharge Elimination System, <https://www.ecfr.gov>. Accessed January 20, 2020.
- USDOA, 2005, Base Realignment and Closure (BRAC), Office of the Under Secretary of Defense for Acquisition, Technology and Logistics, <https://www.acq.osd.mil/brac/>. Accessed May 24, 2019.
- USGS, (n.d.), Sampling with the US DH-48 Depth-Integrating Suspended-Sediment Sampler, Federal Interagency Sedimentation Project.
https://water.usgs.gov/fisp/docs/Instructions_US_DH-48_001010.pdf
- USGS, 2000, Effects of human activities on the interaction of ground water and surface water, U.S. Geological Survey, 22. Accessed December 9, 2018.
- van der Waal, B., Rowntree, K. and Pulley, S.. 2015, Flood bench chronology and sediment source tracing in the upper Thina catchment, South Africa: the role of transformed landscape connectivity, *J Soil Sed*, 15(2):2398-2411.
- Verado, D. J., Froelich, P. N. and McIntyre, A., 1990, Determination of organic-carbon and nitrogen in marine-sediments using the Carlo-Erba-NA-1500 Analyzer, *Deep-Sea Research Part A, Oceanographic Research Papers*, (37):157-165.

- Vesper, D. J., 2008, Karst resources and other applied issues. *Frontiers of karst research. Special Publication*, 13:1-9.
- Vesper, D. J. and White, W. B., 2003, Metal transport to karst springs during storm flow: an example from Fort Campbell, Kentucky/Tennessee, USA, *J Hydrol*, 276(1-4):20-36.
- Vine Grove, 2019, City of Vine Grove, Kentucky. Wastewater Department. <http://www.vinegrove.org/wastewater.shtml>. Accessed January 3, 2020.
- Wagner, R. J., Bougler, R. W., Oblinger, C. J. and Smith, B. A., 2006, Guidelines and standard procedures for continuous water-quality monitors – Station operation, record computation, and data reporting: U.S. Geological Survey Tech and Methods, 1-D3:51p.
- Wall, G. J. and Wilding, L. P., 1976, Mineralogy and Related Parameters of Fluvial Suspended Sediments in Northwestern Ohio, *J Env Qual*, 5(2):168-173.
- Walling, D. E., Peart, M. R., Oldfield, F. and Thompson, R., 1979, Suspended sediment sources identified by magnetic measurements, *Nature*, 28 (5727):110p
- Walling, D. E., Nicholas, A. P. and Woodward, J. C., 1993, A multi-parameter approach to fingerprinting suspended -sediment sources. In: Peters, N.E., Hoehn, E. Leibundgut., Tase, N., Wallings, D.E. (Eds.), *Tracers in Hydrol*, IAHS (215):329-338.
- Walling, D. E. and Woodward, J. C., 1995, Tracing sources of suspended sediment in river basins: A case study of the River Culm, Devon, UK, *Mar. Freshwater Res*: 327-336.
- Walling, D. E. and Amos, A. M., 1999, Source, Storage, and Mobilization of Fine Sediment in a Chalk Stream, *Hydrol Processes*, 13(3):323-340.
- Walling, D. E., Collins, A. L., Jones, P. A., Leeks, G. J. L. and Old, G., 2006, Establishing Fine-Grained Sediment Budgets for the Pang and Lambourn LOCAR Catchments, UK, *J Hydrol*, 330 (1-2): 126-141.
- Walling, D. E., Collins, A. L. and Stroud, R. W., 2008, Tracing suspended sediment and particulate phosphorus sources in catchments, *J Hydrol* 350(3-4): 274-289
- Walling, D. E. and Moorehead, P. W., 1989, The particle size characteristics of fluvial suspended sediment: an overview, In *Sed Water Interactions*, Springer, Dordrecht: 125-149.
- Wanty, R. B., Verplanck, P. L., Tuttle, M. L., Runkel, R. L., Berger, B. R. and Kimball, B. A., 2004, Resolving natural and anthropogenic sources of solutes to a watershed from historic mining, In *Proceedings of the Eleventh International Symposium on Water–Rock Interaction*, WRI-11 (27):1659-1663.
- Ward, J. W., Reed, T. M., Fryar, A. E. and Brion, G. M., 2009, Using the AC/TC ratio to evaluate fecal inputs in a karst groundwater basin, *Env Eng Geosci*, XV(2): 57-65.

- Warren, S. D., Diersing, V. E., Thompson, P. J. and Goran, W. D., 1989, An Erosion-Based Land Classification System for Military Installations, *Environmental Management*, 13(2):251-257.
- Wells, K., 1996, When to apply lime and fertilizer, AGR-5, College of Agriculture. Univ.KY. 5(72).
- White, W. B., 1988, *Geomorphology and hydrology of karst terrains*, No. 5441.447 W4, Oxford University Press, New York.
- White, D. and Palmer-Ball, Jr., B., 1994, An endangered species survey of Fort Knox Military Reservation, Kentucky, United States Army Armor Center Fort Knox, Kentucky Technical Report.
- Williamson, J. E., Haj, A. E., Stamm, Jr., J. F. and Prautzch, V. L., 2014, Fluvial sediment fingerprinting - Literature review and annotated bibliography. No. 2014-1216, U.S. Geological Survey Open-File Report.
- Wilson, C. G., Kuhnle, R. A., Dabney, S. M., Lerch, R. B., Huang, C. H., King, K. W. and Livingston, S. J., 2014, Fine sediment sources in conservation effects assessment project watershed, *J Soil Water Conser*, 69(5):402-413.
- Wirtz, S., Iserloh, T., Rock, G., Hansen, R., Marzen, M., Seeger, M., Betz, S., Remke, A., Wengel, R., Butzen, V. and Ries, J. B., 2012, Soil Erosion on Abandoned Land in Andalusia: A Comparison of Interrill and Rill Erosion Rates, *ISRN Soil Science*.
- Withers, P. J. A., and Jarvie, H. P., 2008, Delivery and cycling of phosphorus in rivers: a review, *Sci Total Env*, 400(1-3):379-395.
- Wolter, P. T., Johnston, C. A. and Niemi, G. J., 2006, Land Use Land Cover Change in the U.S. Great Lakes Basin 1992 to 2001, *J Great Lakes Research*, 32:607-628.
- Yanze-Kontchou, C. and Gschwind, N., 1994, Mineralization of the herbicide Atrazine as a carbon source by a *pseudomonas* strain, *Applied and Env Microb*, 60(12):4297-4302.
- YSI, 2009, YSI 556 Multi Probe System Operational Manual, Item No. 655279, Rev D. YSI Environmental. <https://www.yei.com>. Accessed September 15, 2015.
- Zampella, R. A., Procopio, N. A., Lathrop, R. G. and Dow, C. L., 2007, Relationship of land-use/land-cover patterns and surface-water quality in the Mullica River Basin, *J AmerWater Resour As*, 43(3):594-604.
- Zhu, C. and Schwartz, F. W., 2010, Hydrogeochemical processes and controls on water quality and water management, *Elements*, 7:169-174.

VITA

Cara Leigh Peterman

Education

2013 M.S.- Environmental Science (Chemistry, Geology, Ecology) University of Michigan-Dearborn

2011 B.S.- Earth Science, Minor Geology, Univ. of Michigan

2007 A.S.- Chemistry, Monroe County Community College, Michigan

Professional positions held

U.S. Geological Survey, Kansas Water Science Center:

Nov 2018 - Present

Lawrence, Kansas

Commonwealth of Kentucky, Division of Water, Wastewater Infrastructure Branch:

August 2018 – October 2018

Frankfort, KY

University of Kentucky, Dept. Earth and Environmental Sciences (Geology)

August 2013 – May 2018

Lexington, KY

University of Michigan-Dearborn, Dept. of Natural Sciences

August 2011 – May 2013

Dearborn, Michigan

University of Michigan-Dearborn, Dept. of Natural Sciences

August 2008 – May 2011

Dearborn, Michigan

Henry Ford College, Math and Science Division

January 2011- June 2013

Dearborn, Michigan